

amdg

**Potentially fluorescent ligands based on the *N,N*-dialkyl-*N'*-
aroylthiourea motif and their Pt(II) and Pd(II) complexes.**

Jocelyn Bruce

A thesis submitted to the
University of Stellenbosch
in fulfillment of the requirements for the degree of
Master of Science

Professor Klaus Koch

April 2005

I, the undersigned, hereby declare that the work contained in this thesis is my own original work and that I have not previously in its entirety or in part submitted it at any university for a degree.

Signature.....

Date.....

Abstract

The successful synthesis of fluorescent *N,N*-dialkyl-*N'*-aroylthiourea ligands and their Pt(II) and Pd(II) complexes is described.

Two methods of ligand synthesis were investigated, the Douglass and Dains procedure and that of Dixon and Taylor. The high yielding synthesis of a series of *N,N*-dialkyl-*N'*-9-anthracoylthiourea and *N,N*-dialkyl-*N'*-pivaloylthiourea ligands using the Douglass and Dains procedure is described. Crystal structure determinations of *N,N*-diethyl-*N'*-9-anthracoylthiourea (HL¹), *N*-morpholine-*N'*-9-anthracoylthiourea (HL²), *N,N*-di(2-hydroxyethyl)-*N'*-9-anthracoylthiourea (HL³) and *N,N*-di(2-hydroxyethyl)-*N'*-pivaloylthiourea (HL⁶) were carried out and various inter- and intramolecular interactions which occur in these compounds are described. In particular HL³ and HL⁶ exhibit similar and extensive inter- and intramolecular hydrogen bonding and HL² is the only ligand in its series to exhibit intermolecular π - π interactions between the anthracene residues.

A description of the Dixon and Taylor method used in the synthesis of *N,N*-diethyl-*N'*-[4-(pyrene-1-yl)butanoyl]thiourea (HL⁷), *N*-morpholine-*N'*-[4-(pyrene-1-yl)butanoyl]thiourea (HL⁸) and *N,N*-diethyl-*N'*-[pyrene-1-ylacetyl]thiourea (HL¹⁰) is given. Crystal structure determinations of HL⁷ and HL⁸ were performed, these being to our knowledge, the first of their kind; prevalent inter- and intramolecular interactions are illustrated.

The complexing behaviour of the *N,N*-dialkyl-*N'*-9-anthracoylthioureas, *N,N*-dialkyl-*N'*-[4-(pyrene-1-yl)butanoyl]thioureas and *N,N*-diethyl-*N'*-[pyrene-1-ylacetyl]thioureas was investigated with both platinum (II) and palladium (II). Metal complexes of all these derivatives were successfully synthesised and their detailed characterisation is reported. The crystal structures of the novel *cis*-bis(*N,N*-diethyl-*N'*-9-anthracoylthioureato)platinum(II) (*cis*-[Pt(L¹-S,O)₂]) and *cis*-bis(*N,N*-diethyl-*N'*-9-anthracoylthioureato)palladium(II) (*cis*-[Pd(L¹-S,O)₂]) were determined. Detailed NMR studies making use of two-dimensional techniques were carried out on all potentially fluorescent compounds, and enabled full assignment of the peaks in the aromatic regions of these compounds. NMR investigations also indicated the formation of *cis* isomers in all cases and this was confirmed with ¹⁹⁵Pt NMR and crystal structure determinations where possible.

A description of the fluorescent properties of the *N,N*-dialkyl-*N'*-9-anthracoylthiourea and *N,N*-dialkyl-*N'*-[4-(pyrene-1-yl)butanoyl]thiourea derivatives is given. A reduction in the quantum efficiency of the fluorophores (anthracene and pyrene) was observed upon introduction of the acylthiourea moiety and possible reasons for this phenomenon are discussed. Introduction of a metal ion in both the *N,N*-dialkyl-*N'*-9-anthracoylthiourea and *N,N*-dialkyl-*N'*-[4-(pyrene-1-yl)butanoyl]thiourea derivatives resulted in a further reduction of the quantum efficiency of these compounds and possible explanations for these observations are suggested. At certain concentrations an increase in the emission intensity of *cis*-[Pd(L⁷-S,O)₂] and *cis*-[Pt(L⁷-S,O)₂] was evident and the implications of this on the applicability of these fluorescent complexes is discussed.

Opsomming

Die suksesvolle sintese van fluoresserende *N,N*-dialkiel-*N'*-aroieltioüreum ligande en hulle Pt(II)- en Pd(II)- komplekse word beskryf.

Twee metodes van ligandsintese is ondersoek, dié van Douglass en Dains en dié van Dixon en Taylor. Die hoë-opbrengs sintese van 'n reeks *N,N*-dialkiel-*N'*-9-antrasoieltioüreum en *N,N*-dialkiel-*N'*-pivaloieltioüreum ligande deur gebruik te maak van die Douglass en Dains prosedure word beskryf. Die kristalstrukture van *N,N*-diëtiel-*N'*-9-antrasoieltioüreum (HL¹), *N*-morfolien-*N'*-9-antrasoieltioüreum (HL²), *N,N*-di(2-hidroksiëtiel)-*N'*-9-antrasoieltioüreum (HL³) en *N,N*-di(2-hidroksiëtiel)-*N'*-pivaloieltioüreum (HL⁶) is bepaal, en verskeie intra- en intermolekulêre interaksies word uitgelig. Veral van belang is die uitgebreide inter- en intramolekulêre waterstofbindings wat in die struktuur van beide HL³ en HL⁶ voorkom. HL² is die enigste ligand in die *N,N*-dialkiel-*N'*-9-antrasoieltioüreum reeks waar π - π interaksies tussen die antraseengroepe waargeneem word.

'n Beskrywing van die Dixon en Taylor metode wat gebruik is in die bereiding van *N,N*-diëtiel-*N'*-[4-(pireen-1-iel)butanoïel]tioüreum (HL⁷), *N*-morfolien-*N'*-[4-(pireen-1-iel)butanoïel]tioüreum (HL⁸) en *N,N*-diëtiel-*N'*-[pireen-1-ielasetiel]tioüreum (HL¹⁰) word gegee. Kristalstruktuurbepalings van HL⁷ en HL⁸ is uitgevoer, na ons kennis die eerste van hulle soort, en die verskeie inter- en intramolekulêre interaksies wat waargeneem is, word beskryf.

Die koördinasie van die *N,N*-dialkiel-*N'*-9-antrasoieltioüreum, *N,N*-dialkiel-*N'*-[4-(pireen-1-iel)butanoïel]tioüreum en *N,N*-diëtiel-*N'*-[pireen-1-ielasetiel]tioüreum met Pt(II) en Pd(II) is ondersoek. Die metaalkomplekse van al hierdie ligande is suksesvol berei en die volledige karakterisering van die verbindings word beskryf. Die kristalstrukture van *cis*-bis(*N,N*-diëtiel-*N'*-9-antrasoieltioüreato)-platinum(II) (*cis*-[Pt(L¹-S,O)₂]) and *cis*-bis(*N,N*-diëtiel-*N'*-9-antrasoieltioüreato)palladium(II) (*cis*-[Pd(L¹-S,O)₂]) is bepaal en is die eerste van hulle soort wat beskryf word.

KMR-spektroskopie is gebruik in die karakterisering van al die moontlike fluoresserende verbindings, en 'n volledige analise van die pieke in die aromatiese gebiede van die verbindings is uitgevoer deur gebruik te maak van twee-dimensionele KMR-tegnieke. Die ¹H- en ¹³C- KMR-spektra het aangedui dat die komplekse wat gevorm word die *cis* isomere is; dit is waar moontlik bevestig met ¹⁹⁵Pt- KMR-studies en kristalanalises.

Die fluoresserende eienskappe van die *N,N*-dialkiel-*N'*-9-antrasoieltioüreum en *N,N*-dialkiel-*N'*-[4-(pireen-1-iel)butanoïel]tioüreum derivate word beskryf. 'n Vermindering in die kwantumopbrengs is waargeneem met die binding van die fluorofoor aan 'n asieltioüreumgroep; moontlike redes vir hierdie waarneming word bespreek. Die kwantumopbrengs van die metaal komplekse is ook laer as vir die vry ligande, en 'n moontlike verklaring daarvoor word aangevoer. By sekere konsentrasies is die uitstraling van *cis*-[Pd(L⁷-S,O)₂] en *cis*-[Pt(L⁷-S,O)₂] waarneembaar, en die implikasie van hierdie waarneming op die toepaslikheid van hierdie verbindings word bespreek.

I will light in your heart the lamp of understanding, which shall not be put out until what you are about to write is finished.

II Esdras (ch. XIV, v. 25)

Acknowledgements:

Gratias tibi ago, Domine, qui mihi dedisti facultatem copiamque me hunc opusculum conficere

I would sincerely like to thank:

- My promoter, Professor Klaus Koch for his continual support, enthusiastic guidance and encouragement throughout this project
- Dr Dave Robinson for his continual interest and valued advice
- Ms Jean McKenzie and Elsa Malherbe for their cheerful and helpful NMR analysis and to Jean for proof reading parts of this thesis
- Dr C. Esterhuysen for her crystallographic assistance
- The members of the PGM Research Group for creating a pleasant working environment as well as their continual interest and advice
- All the staff and students in the Department of Chemistry
- My parents Len and Poppy as well as Hugh and John for their interest in my “glow in the dark molecules!”
- Mr G. Murray for his encouragement, good advice and valued friendship
- Mr A Westra for his invaluable assistance in the laboratory, particularly in the early stages of this project and for his continual interest and good advice in later stages
- The University of Stellenbosch, AngloPlatinum, the NRF and the H. B. Thom Trust for financial assistance

Different sections of this work have been presented in the form of:

- A talk presented by the author at the SACI young chemists meeting, October 2003, at Palmiet Pumped Storage Hydro-Electricity Station, Grabouw, South Africa.

- A poster presented at the Cape Organometallic Symposium, October 2003, Morgenhof Wine Estate, Stellenbosch, South Africa.

- A poster presented at the XXXVIth International Conference on Coordination Chemistry, 18-23 July 2004, Merida, Yucatan, Mexico.

- A poster presented at the Cape Organometallic Symposium, October 2004, Breakwater Lodge, Cape Town, South Africa.

Table of Contents

Abstract	iii
Opsomming	iv
Acknowledgements	vi
Table of contents	viii
List of equations, figures, tables and schemes	xii
Chapter 1. Introduction	
1.1 Platinum Overview	1
1.2 Acylthioureas	4
1.3 Fluorescence	6
1.4 Objectives	9
References	11
Chapter 2. Synthesis and detailed characterisation of potentially fluorescent ligands	
2.1 Conversion of aroyl acids to their acid chlorides	14
2.1.1 Introduction	14
2.1.2 Review of literature methods	15
2.1.3 Conversion of 9-anthracenecarboxylic acid to 9-anthracoyl chloride	16
2.1.4 Conversion of 1-pyrenebutyric acid and 1-pyreneacetic acid to their corresponding chlorides	19
2.2 Synthesis of <i>N,N</i> -dialkyl- <i>N'</i> -aroylthiourea ligands	21
2.2.1 Introduction	21
2.2.1.1 Douglass and Dains methods	21
2.2.1.2 Dixon and Taylor method	22
2.2.2 Results and Discussion	25
2.2.2.1 Douglass and Dains method	25
2.2.2.2 Synthesis of <i>N</i> -substituted thioureas	27
2.2.2.3 “Modified” Douglass and Dains method and Dixon and Taylor method	29
2.2.2.4 Nature of competing electrophilic centres	32
2.2.2.5 Nature of the nucleophilic amine	35
2.2.3 Characterisation of potentially fluorescent ligands by means of ¹ H and ¹³ C NMR spectroscopy	37
2.2.3.1 ¹ H and ¹³ C NMR spectra of <i>N,N</i> -dialkyl- <i>N'</i> -9-anthracoylthiourea derivatives	37
2.2.3.2 ¹ H and ¹³ C NMR spectra of <i>N,N</i> -dialkyl- <i>N'</i> -[4-(pyrene-1-yl)butanoyl]thiourea derivatives	48

2.2.3.3	^1H and ^{13}C NMR spectra of <i>N,N</i> -dialkyl- <i>N'</i> -[pyrene-1-ylacetyl]thiourea derivatives	60
2.2.4	Single Crystal X-Ray Diffraction analysis	64
2.2.4.1	Crystal and molecular structure of <i>N,N</i> -diethyl- <i>N'</i> -9-anthracoylthiourea (HL ¹)	64
2.2.4.2	Crystal and molecular structure of <i>N</i> -morpholine- <i>N'</i> -9-anthracoylthiourea (HL ²)	65
2.2.4.3	Crystal and molecular structure of <i>N,N</i> -di(2-hydroxyethyl)- <i>N'</i> -9-anthracoylthiourea (HL ³)	67
2.2.4.4	Crystal and molecular structure of <i>N,N</i> -di(2-hydroxyethyl)- <i>N'</i> -pivaloylthiourea (HL ⁶)	69
2.2.4.5	Discussion of the <i>N,N</i> -dialkyl- <i>N'</i> -9-anthracoylthiourea and <i>N,N</i> -dialkyl- <i>N'</i> -pivaloylthiourea derivatives	69
2.2.4.6	Crystal and molecular structure of <i>N,N</i> -diethyl- <i>N'</i> -[4-(pyrene-1-yl)butanoyl]thiourea (HL ⁷)	71
2.2.4.7	Crystal and molecular structure of <i>N</i> -morpholine- <i>N'</i> -[4-(pyrene-1-yl)butanoyl]thiourea (HL ⁸)	73
2.2.5	Conclusion	76
	References	84
Chapter 3.	Synthesis and detailed characterisation of Pt(II) and Pd(II) complexes	
3.1	Synthesis of Pt(II) and Pd(II) complexes	86
3.1.1	Introduction	86
3.1.2	Synthesis of Platinum complexes	90
3.1.3	Synthesis of Palladium complexes	92
3.1.4	Discussion of complex formation	93
3.2	Characterisation of Pt(II) and Pd(II) complexes	94
3.2.1	Characterisation of potentially fluorescent complexes by means of ^1H and ^{13}C NMR spectroscopy	94
3.2.1.1	^1H and ^{13}C NMR spectra of <i>N,N</i> -diethyl- <i>N'</i> -9-anthracoylthiourea derivatives	94
3.2.1.2	^1H and ^{13}C NMR spectra of <i>N,N</i> -diethyl- <i>N'</i> -[4-(pyrene-1-yl)butanoyl]thiourea and <i>N,N</i> -diethyl- <i>N'</i> -[pyrene-1-ylacetyl]thiourea derivatives	99
3.2.1.3	^{195}Pt NMR of potentially fluorescent complexes	109
3.2.2	Characterisation of potentially fluorescent complexes by means of Infra-Red Spectroscopy	110
3.2.3	Single Crystal X-Ray Diffraction Analysis	112

	3.2.3.1 Crystal and molecular structure of <i>cis</i> -bis(<i>N,N</i> -diethyl- <i>N'</i> -9-anthracoylthioureato)palladium(II).	112
	3.2.3.2 Crystal and molecular structure of <i>cis</i> -bis(<i>N,N</i> -diethyl- <i>N'</i> -9-anthracoylthioureato)platinum(II).	114
3.3	Conclusions	117
	References	120
Chapter 4.	Fluorescent properties of synthesised ligands and Pt(II) and Pd(II) complexes	
4.1	Principles of Luminescence	121
4.1.1	Electronic excitation processes	121
4.1.2	Electronic de-excitation processes	122
4.1.3	Rayleigh and Raman Scatter	126
4.1.4	Fluorescence Quenching	127
4.1.5	Instrumentation and practical considerations in fluorimetry	128
4.1.6	Difference between absorption and fluorescence spectroscopy	130
4.1.7	The “inner filter” effect	131
4.1.8	Spectral correction and quantum efficiency	132
4.1.9	Practical methods of spectral correction	133
4.2	Fluorescence as a means of detection	134
	4.2.1 Measurement of quantum yield of the anthracoylthiourea and pyrenebutanoylthiourea derivatives	138
4.3	Experimental	139
4.4	Results	140
	4.4.1 UV Spectra of <i>N,N</i> -diethyl- <i>N'</i> -9-anthracoylthiourea and its metal complexes	140
	4.4.2 Emission spectra of <i>N,N</i> -diethyl- <i>N'</i> -9-anthracoylthiourea and its metal complexes	142
	4.4.2.1 Emission spectra of <i>N,N</i> -diethyl- <i>N'</i> -9- anthracoylthiourea in dichloromethane	147
	4.4.2.2 Emission spectra of <i>cis</i> -[Pd(L ¹ - <i>S,O</i>) ₂] in dichloromethane	149
	4.4.3 Discussion of the photophysical properties of the anthracoyl derivatives	150
	4.4.3.1 Orientation of the carboxyl group	150
	4.4.4 UV/Visible Spectra of pyrenebutanoylthiourea derivatives	153
	4.4.5 Emission Spectra of the pyrenebutanoylthiourea derivatives	155
	4.4.6 Quantum yield determination of pyrenebutanoylthiourea derivatives	160
	4.4.6.1 Results and Discussion	161
4.5	Conclusions	165
	References	166
Chapter 5.	Experimental procedures and instrumentation	

5.1	Conversion of aroyl acids to their acid chlorides	169
5.1.1	Conversion of 9-anthracenecarboxylic acid	169
5.1.2	Conversion of 1-pyrenebutyric acid	170
5.1.3	Conversion of 1-pyreneacetic acid	171
5.1.4	Characterisation of aroyl chlorides	171
5.2	Synthesis of the <i>N,N</i> -dialkyl- <i>N'</i> -aroylthiourea ligands	172
5.2.1	Douglass and Dains method for ligand synthesis	172
5.2.2	“Modified” Douglass and Dains method for ligand synthesis	173
5.2.3	Dixon and Taylor method for ligand synthesis	173
5.2.4	Characterisation of pivaloylthiourea derivatives	174
5.2.5	Characterisation of <i>N</i> -substituted thioureas	174
5.2.6	Characterisation of anthracoylthiourea derivatives	175
5.2.7	Characterisation of pyreneacetylthiourea and pyrenebutanoylthiourea derivatives	176
5.3	Complex synthesis	177
5.3.1	Synthesis of platinum complexes	177
5.3.2	Synthesis of palladium complexes	178
5.3.3	Characterisation of platinum complexes	179
5.3.4	Characterisation of palladium complexes	179
5.4	Instrumentation	180
5.4.1	NMR Analysis	180
5.4.2	X-Ray Analysis	181
5.4.3	Elemental Analysis	181
5.4.4	Melting point determination	181
5.4.5	Infra-Red Spectroscopy	181
5.4.6	UV/Visible Absorption spectroscopy	181
5.4.7	Fluorescence spectroscopy	182
5.4.8	High Performance Liquid Chromatographic separations	182
	References	182
	Conclusions and future recommendations	183

List of Equations, Figures, Tables and Schemes.

Equations

Equation 1	Dixon and Taylor synthesis of acylthioureas	22
Equation 2	Quantum yield of a fluorophore	126
Equation 3	Stern-Volmer Equation	127
Equation 4	Fluorescence intensity	132
Equation 5	Fluorescence intensity for dilute solutions	132
Equation 6	Determination of quantum yield (Russo)	138
Equation 7	Determination of quantum yield (Hrdlovic)	160

Figures

Figure 1	Global Platinum production	1
Figure 2	Supply and Demand of Platinum	1
Figure 3	Demand by application of platinum and palladium	2
Figure 4	Averaged monthly prices for platinum and palladium	2
Figure 5	Overview of Mining Operations	3
Figure 6	General structure of an <i>N,N</i> -dialkyl- <i>N'</i> -aroyl(acyl)thiourea	4
Figure 7	Crystal structure of <i>cis</i> -bis(<i>N,N</i> -diethyl- <i>N'</i> -benzoylthioureato)Pt(II) illustrating the <i>cis</i> square planar coordination of the acylthioureas	4
Figure 8	Pt(II) 3:3 metallamacrocycle with 3,3,3',3'-tetra(<i>n</i> -butyl)-1,1'-terephthaloylbis(thiourea)	5
Figure 9	RP-HPLC chromatogram of <i>cis</i> -[Pt(L- <i>S,O</i>) ₂], <i>cis</i> -[Pd(L- <i>S,O</i>) ₂], and <i>fac</i> -[Rh(L- <i>S,O</i>) ₃], in 90:10 (%v/v) acetonitrile:0.1M sodium acetate buffer (pH6). λ detection at 254 nm	6
Figure 10	Keto-enol tautomerism exhibited by acetone	19
Figure 11	Two electrophilic centers of isothiocyanate intermediate	31
Figure 12	Space filled model of selected isothiocyanates	34
Figure 13	Numbering scheme used for <i>N,N</i> -dialkyl- <i>N'</i> -9-anthracoylthiourea derivatives	37
Figure 14	Illustration of ² J _{C-H} and ³ J _{C-H} couplings in aromatic systems	40
Figure 15	GHMQC 2D spectrum of 9-anthracenecarboxylic acid, showing multiple bond ¹³ C- ¹ H correlations and unexpected correlations (25°C, CDCl ₃)	42
Figure 16	¹ H NMR spectrum of <i>N,N</i> -di(2-hydroxyethyl)- <i>N'</i> -9-anthracoylthiourea (25°C, DMSO- <i>d</i> ₆)	47
Figure 17	Numbering scheme for <i>N,N</i> -dialkyl- <i>N'</i> -[4-(pyrene-1-yl)butanoyl]thiourea derivatives	48
Figure 18	COSY spectrum of <i>N,N</i> -diethyl- <i>N'</i> -[4-(pyrene-1-yl)butanoyl]thiourea showing ¹ H- ¹ H correlations (25°C, CDCl ₃)	51

Figure 19	^{13}C NMR spectrum of <i>N,N</i> -diethyl- <i>N'</i> -[4-(pyrene-1-yl)butanoyl]thiourea (25°C, CDCl_3)	52
Figure 20	GHSQC spectrum of <i>N,N</i> -dialkyl- <i>N'</i> -[4-(pyrene-1-yl)butanoyl]thiourea showing single bond ^{13}C - ^1H correlations (25°C, CDCl_3)	57
Figure 21	GHMQC spectrum of <i>N,N</i> -dialkyl- <i>N'</i> -[4-(pyrene-1-yl)butanoyl]thiourea showing multiple bond ^{13}C - ^1H correlations (25°C, CDCl_3)	58
Figure 22	GHMQC spectrum of <i>N,N</i> -dialkyl- <i>N'</i> -[4-(pyrene-1-yl)butanoyl]thiourea showing multiple bond ^{13}C - ^1H correlations (25°C, CDCl_3)	59
Figure 23	Numbering scheme for <i>N,N</i> -dialkyl- <i>N'</i> -[pyrene-1-ylacetyl]thiourea derivatives	60
Figure 24	Molecular structure of <i>N,N</i> -diethyl- <i>N'</i> -9-anthracoylthiourea (HL^1)	64
Figure 25	Intermolecular hydrogen bonding ($\text{N(H)}\dots\text{S} = 2.62(3) \text{ \AA}$) leading to dimerisation of HL^1 (A) and face to edge interactions ($\text{H4}\dots\text{C8} = 2.767 \text{ \AA}$) in <i>N,N</i> -diethyl- <i>N'</i> -9-anthracoylthiourea (B)	65
Figure 26	Molecular structure of <i>N</i> -morpholine- <i>N'</i> -9-anthracoylthiourea (HL^2)	66
Figure 27	π - π Interactions between anthracene moieties and hydrogen bonding between $\text{N(H)}\dots\text{O2}$ of an adjacent molecule (symmetry operator 1+X, Y, Z) in <i>N</i> -morpholine- <i>N'</i> -9-anthracoylthiourea	66
Figure 28	Molecular structure of <i>N,N</i> -di(2-hydroxyethyl)- <i>N'</i> -9-anthracoylthiourea (HL^3)	67
Figure 29	Intramolecular and intermolecular hydrogen bonding exhibited by <i>N,N</i> -di(2-hydroxyethyl)- <i>N'</i> -9-anthracoylthiourea (HL^3)	68
Figure 30	Molecular packing of <i>N,N</i> -di(2-hydroxyethyl)- <i>N'</i> -9-anthracoylthiourea (HL^3)	68
Figure 31	Molecular structure of <i>N,N</i> -di(2-hydroxyethyl)- <i>N'</i> -pivaloylthiourea (HL^6)	69
Figure 32	Molecular structure of <i>N,N</i> -diethyl- <i>N'</i> -[4-(pyrene-1-yl)butanoyl]thiourea (HL^7)	71
Figure 33	Intermolecular hydrogen bonding ($\text{N(H)}\dots\text{S} = 2.59(8) \text{ \AA}$) leading to dimerisation of HL^7 (A) and offset π - π overlap (B)	72
Figure 34	Molecular packing of <i>N,N</i> -diethyl- <i>N'</i> -[4-(pyrene-1-yl)butanoyl]thiourea (HL^7)	72
Figure 35	Molecular structure of <i>N</i> -morpholine- <i>N'</i> -[4-(pyrene-1-yl)butanoyl]thiourea	73
Figure 36	Offset π overlap between pyrene moieties (A) and intramolecular hydrogen bond $\text{N(H)-O1} = 2.59(8) \text{ \AA}$ with T shaped contact between aromatic moieties of HL^8 (B)	74
Figure 37	Molecular packing of <i>N</i> -morpholine- <i>N'</i> -[4-(pyrene-1-yl)butanoyl]thiourea (HL^8)	74
Figure 38	Molecular structure of <i>S</i> -(9-anthryl)- <i>N,N</i> -tetramethylene isothiuronium perchlorate	87
Figure 39	Numbering scheme for <i>N,N</i> -dialkyl- <i>N'</i> -9-anthracoylthiourea derivatives	94
Figure 40	Restricted rotation about partial double bond in the <i>N,N</i> -dialkyl- <i>N'</i> -aroylthiourea ligands	96
Figure 41	^1H NMR spectrum of <i>N,N</i> -diethyl- <i>N'</i> -9-anthracoylthiourea and <i>cis</i> -bis(<i>N,N</i> -diethyl- <i>N'</i> -9-anthracoylthioureato)palladium(II) (25°C, CDCl_3)	97

Figure 42	Numbering scheme for pyrenebutanoylthiourea derivatives	99
Figure 43	Numbering scheme for pyreneacetylthiourea derivatives	99
Figure 44	^{13}C NMR spectra of <i>N,N</i> -diethyl- <i>N'</i> -9-anthracoylthiourea and <i>cis</i> -bis(<i>N,N</i> -diethyl- <i>N'</i> -9-anthracoylthioureato)palladium(II) (25°C, CDCl_3)	108
Figure 45	IR spectrum of <i>N,N</i> -diethyl- <i>N'</i> -[4-(pyrene-1-yl)butanoyl]thiourea	111
Figure 46	IR spectrum of <i>cis</i> -bis(<i>N,N</i> -diethyl- <i>N'</i> -[4-(pyrene-1-acetyl)butanoyl]thioureato)palladium(II)	111
Figure 47	Molecular structure of <i>cis</i> -bis(<i>N,N</i> -diethyl- <i>N'</i> -9-anthracoylthioureato)palladium(II)	112
Figure 48	Offset π overlap between adjacent molecules (A) and crystal packing of <i>cis</i> -[Pd(L^1 - <i>S,O</i>) $_2$] (B)	113
Figure 49	Buckled coordination sphere of <i>cis</i> -[Pd(L^1 - <i>S,O</i>) $_2$] illustrating the deviation of the sulphur atom from the coordination plane	114
Figure 50	Molecular structure of <i>cis</i> -bis(<i>N,N</i> -diethyl- <i>N'</i> -anthracoylthioureato)Pt(II) <i>cis</i> -[Pt(L^1 - <i>S,O</i>) $_2$]	114
Figure 51	Coordination sphere of <i>cis</i> -[Pt(L^1 - <i>S,O</i>) $_2$]	115
Figure 52	Jablonski diagram	121
Figure 53	Mirror image rule and Franck-Condon principle	125
Figure 54	Outline of the processes of Rayleigh and Raman Scattering	127
Figure 55	Major components of a fluorimeter	129
Figure 56	Graphical depiction of the inner filter effect	131
Figure 57	Chemosensor based on the binding site-signaling subunit approach	134
Figure 58	PET process with participation from the HOMO, LUMO and an external molecular orbital	135
Figure 59	PET process with participation from the HOMO, LUMO and an empty external molecular orbital	136
Figure 60	EET process with participation of the HOMO and LUMO of the fluorophore and an external molecular orbital	136
Figure 61	Fluor-receptor configurations potentially applicable to the studied systems	137
Figure 62	UV/Visible spectra of anthracene, <i>N,N</i> -diethyl- <i>N'</i> -9-anthracoylthiourea and <i>cis</i> -bis(<i>N,N</i> -diethyl- <i>N'</i> -anthracoylthioureato)palladium(II) in dichloromethane at $1 \times 10^{-4}\text{M}$	140
Figure 63	UV/Visible spectrum of <i>cis</i> -bis(<i>N,N</i> -diethyl- <i>N'</i> -benzoylthioureato)platinum(II)	142
Figure 64	Emission spectrum of anthracene. $\lambda_{\text{EX}} = 320\text{nm}$ at $1 \times 10^{-6}\text{M}$ in ethanol	143
Figure 65	Graph depicting linear correlation between fluorescence intensity and anthracene concentration (mol dm^{-3}). $\lambda_{\text{EX}} = 320\text{ nm}$.	144

Figure 66	Graph depicting limited linear correlation between fluorescence intensity and concentration of <i>N,N</i> -diethyl- <i>N'</i> -anthracoylthiourea in ethanol. $\lambda_{\text{Ex}} = 320\text{nm}$	145
Figure 67	Emission spectra of anthracene, 9-anthracenecarboxylic acid and <i>N,N</i> -diethyl- <i>N'</i> -anthracoylthiourea illustrating quenching	146
Figure 68	Possible tautomeric forms of <i>N,N</i> -dialkyl- <i>N'</i> -aroylthiourea in solution.	146
Figure 69	Influence of solvent on emission spectra of anthracene	147
Figure 70	Emission spectra of <i>N,N</i> -diethyl- <i>N'</i> -anthracoylthiourea at varying concentrations in dichloromethane	148
Figure 71	Graph depicting limited linear correlation between fluorescence intensity of emission maxima at 413 nm and concentration of <i>N,N</i> -diethyl- <i>N'</i> -anthracoylthiourea in dichloromethane	148
Figure 72	Emission spectra of of <i>N,N</i> -diethyl- <i>N'</i> -anthracoylthiourea and <i>cis</i> -[Pd(L ¹ - <i>S,O</i>) ₂] in dichloromethane	149
Figure 73	Coplanar orientation of the carboxyl group stabilised via hydrogen bonding with the <i>peri</i> hydrogens	150
Figure 74	Resonance structure of 9-[(Methyl-amino)thiocarbonyl]anthracene	151
Figure 75	Structure of <i>N</i> -methyl- <i>N</i> -9-(methylantracene)- <i>N'</i> -benzoylthiourea	152
Figure 76	UV spectra of pyrene, <i>N,N</i> -diethyl- <i>N'</i> -[4-(pyrene-1-yl)butanoyl]thiourea, <i>cis</i> -bis(<i>N,N</i> -diethyl- <i>N'</i> -[4-(pyrene-1-yl)butanoyl]thioureato)palladium(II) and <i>cis</i> -bis(<i>N,N</i> -diethyl- <i>N'</i> -[4-(pyrene-1-yl)butanoyl]thioureato)platinum(II) in dichloromethane at $1 \times 10^{-5}\text{M}$	154
Figure 77	Emission spectrum of pyrene determined in dichloromethane Conc = $6 \times 10^{-7}\text{M}$ and $\lambda_{\text{Ex}} = 340\text{nm}$	155
Figure 78	Graph depicting limited linear correlation between fluorescence intensity and concentration for pyrene. $\lambda_{\text{Ex}} = 340\text{nm}$	156
Figure 79	Emission spectrum of <i>N,N</i> -diethyl- <i>N'</i> -[4-(pyrene-1-yl)butanoyl]thiourea in dichloromethane. Conc = $2.5 \times 10^{-6}\text{M}$ and $\lambda_{\text{Ex}} = 340\text{nm}$	157
Figure 80	Graph depicting limited linear correlation between fluorescence intensity and concentration of <i>N,N</i> -diethyl- <i>N'</i> -[4-(pyrene-1-yl)butanoyl]thiourea, $\lambda_{\text{Ex}} = 340\text{nm}$	157
Figure 81	Emission spectrum of <i>N,N</i> -diethyl- <i>N'</i> -[4-(pyrene-1-yl)butanoyl]thiourea, and the platinum and palladium complexes in dichloromethane. Conc = $1.0 \times 10^{-6}\text{M}$ and $\lambda_{\text{Ex}} = 344\text{nm}$	158
Figure 82	Emission spectra reported by Schuster where DEPyBuT refers to <i>N,N</i> -diethyl- <i>N'</i> -[4-(pyrene-1-yl)butanoyl]thiourea, DEPyT to <i>N,N</i> -diethyl- <i>N'</i> -pyrenoylthiourea and Pt(DEPyBuT) ₂ to the platinum complex of <i>N,N</i> -diethyl- <i>N'</i> -[4-(pyrene-1-yl)butanoyl]thiourea,	159

Figure 83	Emission spectra of <i>N,N</i> -diethyl- <i>N'</i> -[4-(pyrene-1-yl)butanoyl]thiourea, and the platinum and palladium complexes in dichloromethane. Conc = 1×10^{-4} M and $\lambda_{\text{Ex}} = 344$ nm	159
Figure 84	UV Spectra of pyrene in ethanol and dichloromethane at conc. = 1×10^{-5} M.	161
Figure 85	Emission spectra of pyrene in ethanol and dichloromethane and <i>N,N</i> -diethyl- <i>N'</i> -[4-(pyrene-1-yl)butanoyl]thiourea, in dichloromethane. Conc = 1×10^{-6} M and $\lambda_{\text{Ex}} = 313$ nm	162
Figure 86	Emission spectra of <i>N,N</i> -diethyl- <i>N'</i> -[4-(pyrene-1-yl)butanoyl]thiourea, <i>cis</i> -bis(<i>N,N</i> -diethyl- <i>N'</i> -[4-(pyrene-1-yl)butanoyl]thioureato)palladium(II) and <i>cis</i> -bis(<i>N,N</i> -diethyl- <i>N'</i> -[4-(pyrene-1-yl)butanoyl]thioureato)platinum(II) in dichloromethane. Conc = 1×10^{-6} M and $\lambda_{\text{Ex}} = 313$ nm	163

Tables

Table 1	Estimated yields of aroyl chlorides for each method used	20
Table 2	Compounds synthesised using Douglass and Dains method	26
Table 3	Yields of <i>N</i> -substituted thioureas	28
Table 4	Yields of pyrenebutanoylthiourea and pyreneacetylthiourea derivatives obtained using the “modified” Douglass and Dains, and Dixon and Taylor methods	30
Table 5	^1H NMR chemical shifts (in ppm) of <i>N,N</i> -dialkyl- <i>N'</i> -9-anthracoylthiourea derivatives (25°C, CDCl_3)	38
Table 6	^{13}C NMR chemical shifts (in ppm) of <i>N,N</i> -dialkyl- <i>N'</i> -9-anthracoylthiourea derivatives (25°C, CDCl_3)	39
Table 7	Difference in ^{13}C NMR chemical shifts (in ppm) of selected compounds relative to anthracene	44
Table 8	^1H NMR chemical shifts (in ppm) of <i>N,N</i> -dialkyl- <i>N'</i> -[4-(pyrene-1-yl)butanoyl]thiourea derivatives (25°C, CDCl_3)	49
Table 9	^{13}C NMR chemical shifts (in ppm) of <i>N,N</i> -dialkyl- <i>N'</i> -[4-(pyrene-1-yl)butanoyl]thiourea derivatives (25°C, CDCl_3)	53
Table 10	^1H NMR chemical shifts (in ppm) of <i>N,N</i> -dialkyl- <i>N'</i> -[pyrene-1-ylacetyl]thiourea derivatives (25°C, CDCl_3)	60
Table 11	^{13}C NMR chemical shifts (in ppm) of <i>N,N</i> -dialkyl- <i>N'</i> -[pyrene-1-ylacetyl]thiourea derivatives (25°C, CDCl_3)	62
Table 12	Bond lengths of selected <i>N,N</i> -dialkyl- <i>N'</i> -acylthiourea ligands (Å)	70
Table 13	Torsion angles of selected <i>N,N</i> -dialkyl- <i>N'</i> -acylthiourea derivatives	71
Table 14	Torsion angles of pyrenebutanoylthiourea derivatives illustrating the differing alkyl chain orientations	75

Table 15	Torsion angles of pyrenebutanoylthiourea derivatives	75
Table 16	Selected bond lengths of pyrenebutanoylthiourea derivatives (Å)	75
Table 17	Crystallographic data for <i>N,N</i> -diethyl- <i>N'</i> -9-anthracoylthiourea (HL ¹)	78
Table 18	Crystallographic data for <i>N</i> -morpholine- <i>N'</i> -9-anthracoylthiourea (HL ²)	79
Table 19	Crystallographic data for <i>N,N</i> -di(2-hydroxyethyl)- <i>N'</i> -9-anthracoylthiourea (HL ³)	80
Table 20	Crystallographic data for <i>N,N</i> -di(2-hydroxyethyl)- <i>N'</i> -pivaloylthiourea (HL ⁶)	81
Table 21	Crystallographic data for <i>N,N</i> -diethyl- <i>N'</i> -[4-(pyrene-1-yl)butanoyl]thiourea (HL ⁷)	82
Table 22	Crystallographic data for <i>N</i> -morpholine- <i>N'</i> -[4-(pyrene-1-yl)butanoyl]thiourea	83
Table 23	¹ H NMR chemical shifts (in ppm) of anthracene and <i>N,N</i> -diethyl- <i>N'</i> -9-anthracoylthiourea derivatives (25°C, CDCl ₃)	94
Table 24	¹³ C NMR chemical shifts (in ppm) of anthracene and <i>N,N</i> -diethyl- <i>N'</i> -9-anthracoylthiourea derivatives (25°C, CDCl ₃)	95
Table 25	Difference in ¹³ C NMR chemical shifts (in ppm) of selected compounds relative to anthracene	96
Table 26	¹ H NMR chemical shifts (in ppm) of <i>N,N</i> -diethyl- <i>N'</i> -[4-(pyrene-1-yl)butanoyl]thiourea derivatives (25°C, CDCl ₃)	100
Table 27	¹³ C NMR chemical shifts (in ppm) of pyrene and <i>N,N</i> -dialkyl- <i>N'</i> -[4-(pyrene-1-yl)butanoyl]thiourea derivatives (25°C, CDCl ₃)	101
Table 28	¹ H NMR chemical shifts (in ppm) of <i>N,N</i> -diethyl- <i>N'</i> -[pyrene-1-ylacetyl]thiourea derivatives (25°C, CDCl ₃)	103
Table 29	¹³ C NMR chemical shifts (in ppm) of pyrene and <i>N,N</i> -dialkyl- <i>N'</i> -[pyrene-1-ylacetyl]thiourea derivatives (25°C, CDCl ₃)	104
Table 30	Chemical shift displacements in selected complexes	107
Table 31	¹⁹⁵ δPt chemical shifts (in ppm) of complexes	109
Table 32	Bond distances and angles of selected complexes (Å)/(°)	116
Table 33	Relevant bond lengths of the chelate ring (Å)	117
Table 34	Crystallographic data for <i>cis</i> -bis(<i>N,N</i> -diethyl- <i>N'</i> -9-anthracoylthioureato)Pd(II)	118
Table 35	Crystallographic data for <i>cis</i> -bis(<i>N,N</i> -diethyl- <i>N'</i> -9-anthracoylthioureato)Pt(II)	119
Table 36	Molar absorptivities (cm.mol ⁻¹ .dm ³) of <i>N,N</i> -dialkyl- <i>N'</i> -9-anthracoylthiourea derivatives at selected wavelengths in dichloromethane	141
Table 37	Molar absorptivities (cm.mol ⁻¹ .dm ³) of pyrenebutanoylthiourea derivatives at selected wavelengths in dichloromethane	154
Table 38	Quantum yields of pyrenebutanoylthiourea derivatives in dichloromethane	162
Schemes		
Scheme 1	Reaction scheme of synthetic procedure described by Douglass and Dains	14
Scheme 2.	Mechanism of carboxylic acid conversion to yield an acid chloride	18

Scheme 3	Reaction mechanism of Dixon and Taylor method	23
Scheme 4	Dixon and Taylor method used for the synthesis of <i>N,N</i> -dialkyl- <i>N'</i> -[4-(pyrene-1-yl)butanoyl]thiourea and <i>N,N</i> -dialkyl- <i>N'</i> -[pyrene-1-ylacetyl]thiourea derivatives	24
Scheme 5	Acid hydrolysis of <i>N,N</i> -di(2-hydroxyethyl)thiourea resulting in the possible formation of an ionic liquid	29
Scheme 6	Nucleophilic attack at the carbonyl carbon leading to amide formation, <i>via</i> a tetrahedral intermediate	32
Scheme 7	Nucleophilic attack at the thiocarbonyl carbon leading to acylthioureas formation, <i>via</i> a trigonal zwitterionic intermediate	33
Scheme 8	Nucleophilic attack by an alcohol resulting in thiocarbamate formation	36
Scheme 9	Canonical forms of carboxylated <i>N,N</i> -dialkyl- <i>N'</i> -9-anthracoylthiourea derivatives	43
Scheme 10	Bidentate coordination of <i>N,N</i> -dialkyl- <i>N'</i> -acylthioureas to d^8 metal ions, resulting in square planar metal complexes	87
Scheme 11	Suggested two step oxidative mechanism for the rearrangement observed for <i>N,N</i> -tetramethylene- <i>N'</i> -anthracoylthiourea	88
Scheme 12	Representation of the effects of HCl addition to <i>cis</i> -[Pt(L-S,O) ₂] complexes	90

1.1 Platinum Overview

The earliest recordings of platinum are found in the writings of Julius Caesar Scaliger in 1557 and refer to a mysterious metal found in the alluvial deposits in Central America (between Panama and Mexico). It was however, first discovered by Antonio de Ulloa a Spanish astronomer in 1735 who called it “*platina del Pinto*” (“little silver of the Pinto river”)¹ and it was regarded as being an impurity in the mining of Colombian silver. Charles Wood independently isolated the metal in 1741 and Swedish Scheffer was the first to characterise it as the seventh element (known at that time), in 1751. Palladium was first isolated by W.H. Wollaston in 1803, whilst he was busy studying the aqua regia-soluble portion of platinum ores.² Platinum is found in economically viable concentrations in very few locations in the world. The largest of these is the South African Bushveld complex, the main ore body being the Merensky Reef, and the Noril’sk-Talnakh region in Northern Siberia; these two together making up close to 90% of the world supply of platinum. There are however deposits in North America, Colombia, Sudbury Canada, Gansu, China and the Great Dyke in Zimbabwe (Figure 1). Due to the increasing demand for platinum (Figure 2), it is estimated that if platinum production were to stop altogether the above ground reserves would last approximately one year. Russia is the only country thought to have significant stockpiles of platinum, however many of their reserves have been sold off over recent years. Interestingly, it is also one of the few deposits where the palladium concentration mined is higher than that of the platinum and both metals are a by-product of nickel production.² Due to platinum’s limited supply there are very few significant mining companies in the world and these include Anglo Platinum, Impala Platinum, Lonmin Platinum, Northam Platinum and Aquarius Platinum in South Africa, Norilsk Nickel in Russia, Stillwater Mining Company, North America Palladium Inc, and Inco in North America and Zimplats in Zimbabwe.

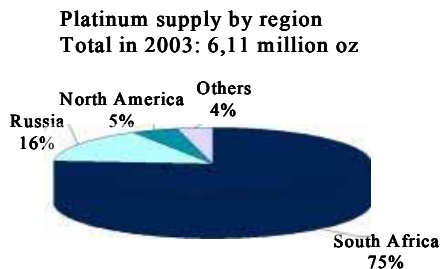


Figure 1 Global Platinum production.

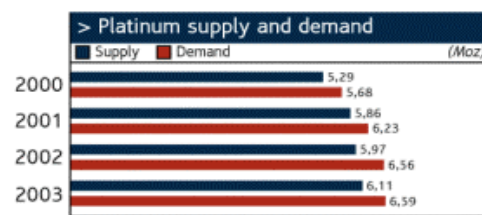


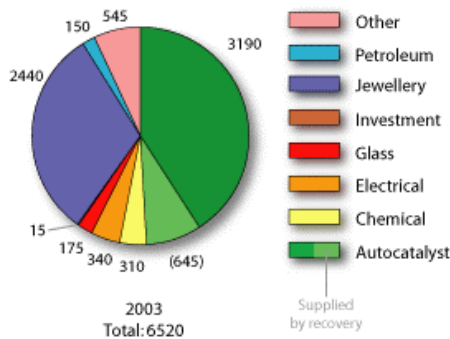
Figure 2 Supply and Demand of Platinum.³

It is estimated that one in every five goods manufactured is either produced using platinum, or contains it. The demand for the metal is therefore extremely high and its primary use is in the automotive industry in catalytic converters. Environmental concerns on the emission of greenhouse gases will no doubt serve to increase the demand for the metal in this sector, especially as America and the European Union have

introduced legislation to enforce more stringent emission standards, and it is expected that developing countries will follow suite.

Further industrial uses of platinum making use of its catalytic properties, include its incorporation in fuel cells, as well as the production of sulphuric and nitric acid. It is also employed in the reforming and isomerisation of petroleum as well as being used as a promoter in fluid catalytic cracking operations. Its electrical uses are in computer hard disks and thermocouples, and it is also used in liquid crystal displays (Figure 3). The discovery of cisplatin in 1965⁴ opened the way for its use in the drug market and other medical applications include its use (as an osmium alloy) in pacemakers and other surgical implants. A vast percentage of the market is in the jewellery industry and more recently platinum has been seen as a form of investment with the Chinese Panda, Australian Koala, Canadian Maple Leaf and Isle of Man Noble,⁵ all being 99.95% pure platinum coins. Palladium is also used in autocatalysts, electronics, *i.e.* multilayer ceramic capacitors for integrated circuits used in microcomputers, and palladium coated connectors, dental alloys as well as in the jewellery industry as an alloy with platinum, amongst other metals, in white gold.⁶

Platinum. Demand by Application ('000 oz)



Palladium. Demand by Application ('000 oz).

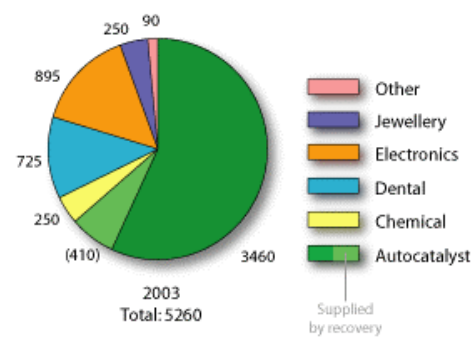


Figure 3 Demand by application of platinum and palladium.⁷

Revenue generated from the sale of PGM's contributes R35 billion to the South African economy (Figure 4).⁸

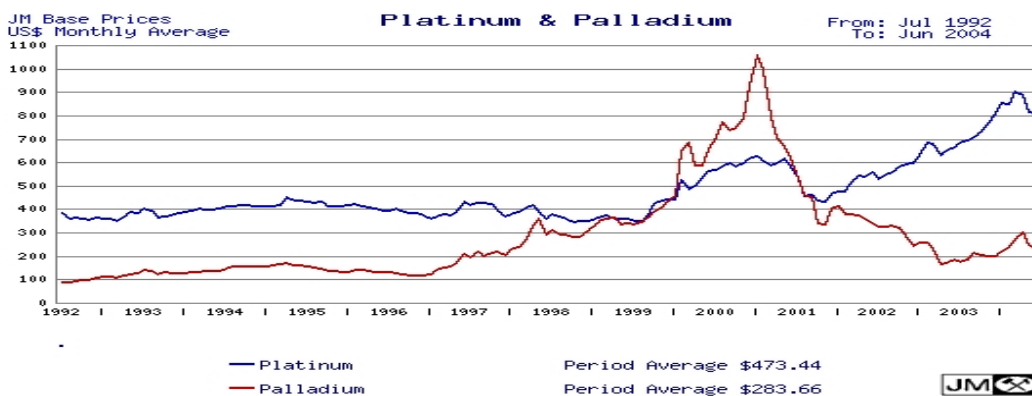


Figure 4 Averaged monthly prices for platinum and palladium.⁷

The production of platinum metal is however an expensive and complex process and approximately seven to twelve tonnes of ore need to be processed to produce an ounce of platinum. A brief outline of the processes involved is shown below in Figure 5.

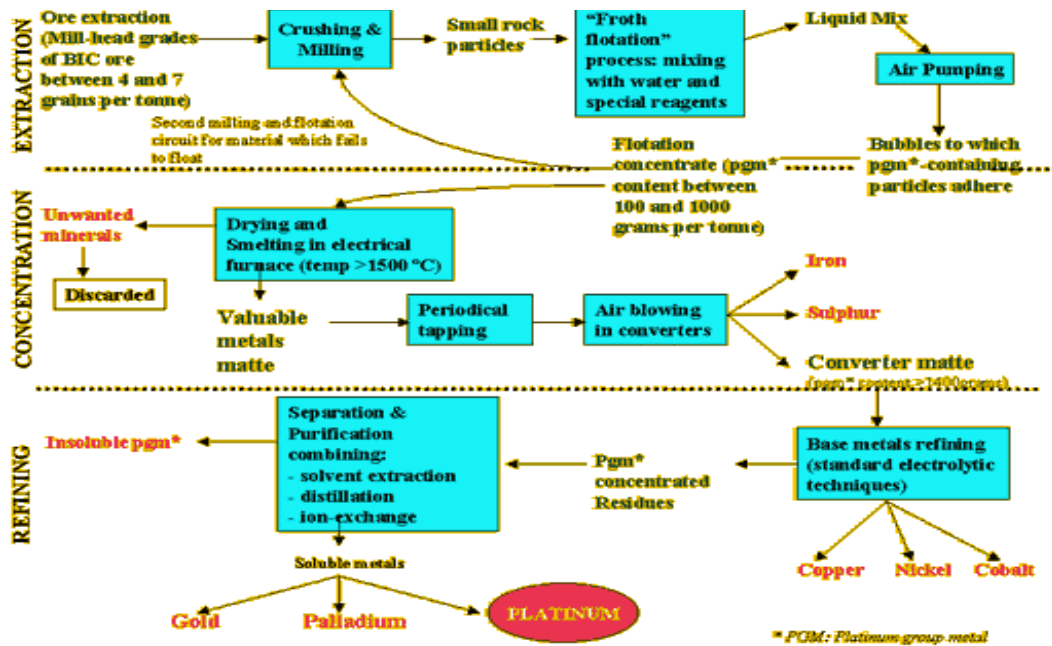


Figure 5 Overview of Mining Operations.⁹

The purification processes employed in precious metal refineries differ as well as the order in which the six main Platinum Group Metals (PGM's) are isolated. A comprehensive flowchart of the isolation of the PGM's can be found in Hartley,² however, in general, the refining process involves the conversion of the PGM ions to a charged, water soluble, chloro species *e.g.* PdCl_4^{2-} and PtCl_6^{2-} , which enables their separation. Processes employed in refineries include solvent extraction, the use of ion-exchangers and distillation. Following the pure metal recovery, a very small percentage of the PGM ions remain behind in the effluent stream as water soluble species and thus form part of a loss of revenue for the mining company as well as a potential environmental hazard as the effluent is usually stored in plastic lined dams (before being reintroduced into the process at the smelter for further recovery of PGM's) and leaks from these dams, although rare, are possible. Due to the water solubility of these species, their introduction into the surrounding environment could be facile and traces could be taken up by tree roots, crops and other vegetative matter and thus ingested by livestock.

There is therefore a need for a sensitive technique to determine low concentrations of PGM's. Current instrumental analytical methods include atomic absorption spectrometry, X-ray fluorescence spectrometry, neutron activation analysis, electrochemical methods,¹⁰ inductively coupled plasma mass spectrometry and ICP-Atomic Emission Spectrometry,¹¹ whilst chemical analyses include gravimetric, volumetric and UV/VIS spectrophotometric techniques.^{12,13}

1.2 *N,N*-dialkyl-*N'*-aroyl(acyl)thioureas

N,N-dialkyl-*N'*-acylthioureas have been known since 1873 and Douglass and Dains simplified the synthetic procedure in 1934.¹⁴ Sporadic interest was shown in these ligands^{15,16} until interest in them was rekindled by the work of Beyer and Hoyer.¹⁷

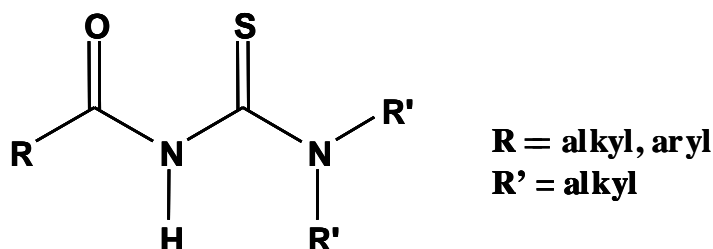


Figure 6 General structure of an *N,N*-dialkyl-*N'*-aroyl(acyl)thiourea.

Before the coordinating abilities of these ligands can be discussed further their differing nomenclature should briefly be addressed. The use of the term “acyl” in reference to these compounds conventionally refers to the use of an alkyl substituent attached to the carbonyl carbon of the molecule (*i.e.* R) and the use of the term “aroyl” in this context refers to the attachment of an aromatic moiety in this position. Conventionally however, when these compounds are discussed in a general context they are referred to as being *N,N*-dialkyl-*N'*-acylthioureas and this convention will be followed during the remainder of this report. The ability of the *N,N*-dialkyl-*N'*-acylthioureas to form metal chelates with various transition metals was reported, focusing on Ni(II), Cu(II), Pd(II) and Co(III) complexes,^{17,18,19} as well as Os(VIII).²⁰ The use of these ligands as a means of metal ion extraction with particular reference to Pb(II) was reported²¹ as well as the variation of the coordinating atoms to include selenium.^{22,23} As will be explained more fully in Chapter 3, metal coordination takes place through the oxygen and sulphur atoms following deprotonation of the central nitrogen atom (Figure 6) to yield primarily *cis* square planar complexes. The crystal structure of *cis*-bis(*N,N*-diethyl-*N'*-benzoylthioureato)platinum(II) illustrates this elegantly.

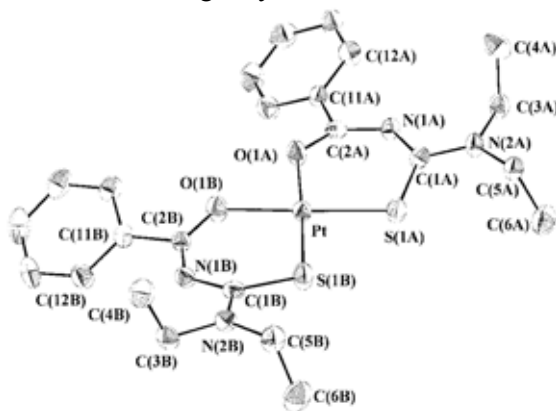


Figure 7 Crystal structure of *cis*-bis(*N,N*-diethyl-*N'*-benzoylthioureato)platinum(II) illustrating the *cis* square planar coordination of the *N,N*-dialkyl-*N'*-acylthioureas.²⁴

A potential industrial application of these ligands was reported when Schuster noted their selectivity towards the PGM ions and suggested their use in solvent extraction.^{25,26} The chromatographic separation of metal chelates formed part of his further work.^{27,28,29,30} The removal of a number of transition metal ions *via* precipitation with the *N,N*-dialkyl-*N'*-acylthioureas in aqueous solution was discussed³¹ as well as the preconcentration of some of the PGM ions in acidic media.³² The first silver complex was reported by Richter,³³ but Hg(II)³⁴ and Au(III)^{35,36} complexes are also known, and indeed these ligands have been used in the solvent extraction of Au(III)³⁷ and Pd(II).³⁸ Variation of the R groups, and more specifically the introduction of hydroxyl groups on the alkyl chains of the amine substituents (R' Figure 6), have led to more hydrophilic ligands and metal chelates.^{39,40} A particularly interesting elaboration of the complexing abilities of these ligands is the synthesis of bipodal derivatives⁴¹ and their self assembly with Pt(II), Pd(II) and Ni(II) to yield 2:2 and 3:3 metallamacrocycles.^{42,43} A crystal structure of the Pt(II) 3:3 metallamacrocycle 3,3,3',3'-tetra(*n*-butyl)-1,1'-terephthaloylbis(thiourea) is shown in Figure 8.

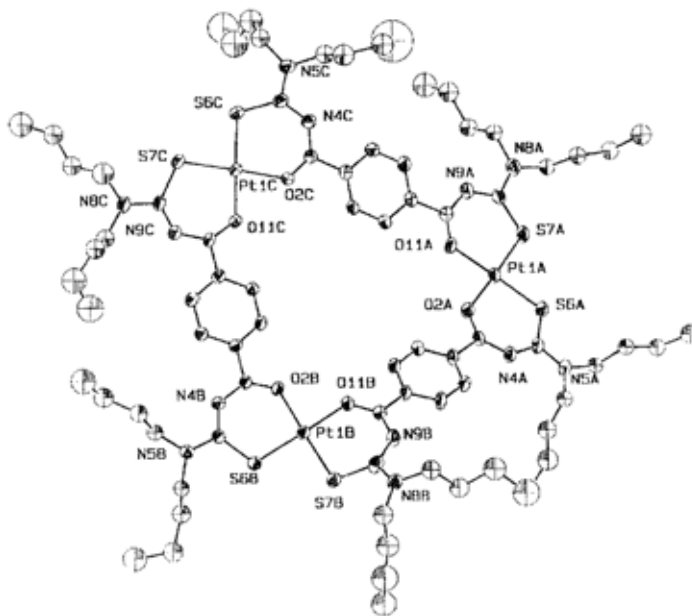


Figure 8 Pt(II) 3:3 metallamacrocycle with 3,3,3',3'-tetra(*n*-butyl)-1,1'-terephthaloylbis(thiourea).⁴²

Protonation studies have investigated the varying modes of coordination exhibited by these complexes,^{44,45} however this work will be discussed in more detail in Chapter 3. Recent work done by Koch *et al*⁴⁶ reported the reversed - phase HPLC separation of Pt(II), Pd(II) and Rh(III) complexes of the acylthioureas. Previous chromatographic work on these ligands and their complexes had mainly focused on *N,N*-dialkyl-*N'*-benzoylthioureas and normal-phase separations, however in this report more hydrophilic ligands were synthesised enabling the use of more polar solvents and C-18 columns during separation. As previously alluded to, coordination of the PGM's to these ligands is pH dependant, and as normal-phase systems frequently retain trace amounts of water and acids, irreversible retention of highly polar analytes as well as analyte decomposition are problematic in these systems. By employing the use of a reversed-phase separation

system, these complications are avoided as the pH of the mobile phase can be controlled. Figure 8 illustrates the elegant separation of the rhodium, palladium and platinum complexes of *N,N*-pyrrolidyl-*N'*-(2,2-dimethylpropanoyl)thiourea (L) in an acetonitrile solution with photometric detection at 254 nm.

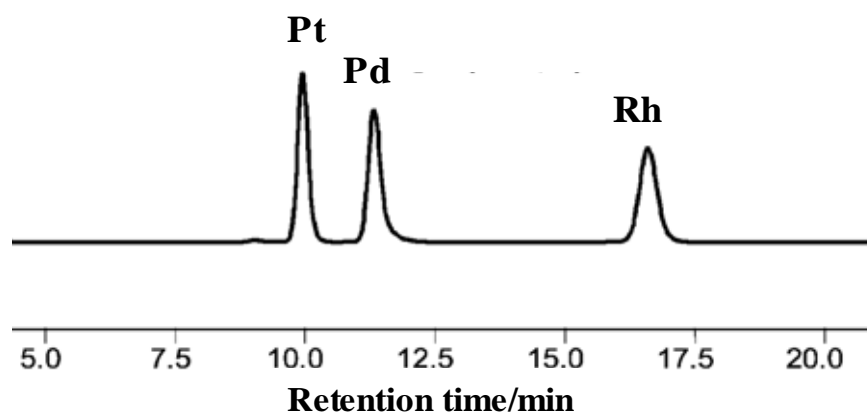


Figure 9 RP-HPLC chromatogram of *cis*-[Pt(L-S,O)₂], *cis*-[Pd(L-S,O)₂], and *fac*-[Rh(L-S,O)₃], in 90:10 (%v/v) acetonitrile:0.1M sodium acetate buffer (pH6). λ detection at 254 nm.⁴⁶

1.3 Fluorescence

Luminescence is the emission of light from any substance that occurs from an electronically excited state and can be divided into two broad categories, namely fluorescence and phosphorescence depending on the nature of the excited state.⁴⁷ Details on the principles of fluorescence as well as practical considerations in fluorimetry will be discussed in further detail in Chapter 4; this section merely serves as a review of recent fluorescence work.

A large number of fluorescent complexes with closed-shell metal ions such as Mg(II), Ca(II), Sr(II), Ba(II), Al(III),⁴⁸ Ga(III),⁴⁹ In(III), Ce(IV), Th(IV), Zn(II)⁵⁰ have been studied. More recently a selective and sensitive fluoroionophore for Hg(II), Ag(I) and Cu(II) ions was reported,⁵¹ as well as a fluorescent chemosensor for Pb(II) ions.⁵² Methods have been reported for the simultaneous detection of metal ions in solution and these make use of the differing fluorescent lifetimes exhibited by each of the metal ions.⁵³ However, until recently intensely fluorescent complexes from heavy metal ions with unfilled subshells, as is the case with most transition metal ions, were comparatively rare. The reason for this is most likely the strong fluorescent quenching caused by intramolecular charge transfer, magnetic interactions, and heavy atom effects, associated with these metal ions, despite the ligands themselves exhibiting considerable fluorescent quantum yields. However, in the past decade a number of fluorescent complexes with open-shell metal ions have been reported and of those, the complexes with the PGM's are of particular interest. Many of these involve Pt(II) and Pd(II) compounds, despite coordination to the metal ion usually leading to the quenching of the fluorescence exhibited by the ligands.

Several fluorescent ligands have been coordinated to platinum and the photophysics of the resulting complexes studied; the ligands include 2,2':6',2''-terpyridine,⁵⁴ diimine ligands,^{55,56,57} coumarin,⁵⁸ and dithiolate ligands.^{59,60} Seward *et al.* investigated star shaped luminescent platinum compounds based on 2,2'-dipyridylamino derivatised ligands.⁶¹ Luminescent metallamacrocycles were studied by Ballardini *et al.*⁶² and further research carried out by this group led to the development of a fluorescent sensor responsive to protons, however upon adduct formation with $\text{Pt}(\text{bpy})(\text{NH}_3)_2^{2+}$ the fluorescence of the free receptor was quenched.⁶³ Sautter *et al.* made use of a functional ditopic perylene ligand⁶⁴ to construct nanosized molecular squares with platinum(II) and palladium(II) phosphine corner units that exhibited a fluorescence quantum yield of almost unity.⁶⁵ The photo physical and photochemical properties of binuclear d^8-d^8 systems have been the focus of recent research and several luminescent binuclear platinum compounds have been reported.⁶⁶ The influence of pressure on luminescence was studied by measuring the effect that the Pt-Pt distance exhibited on the fluorescent properties of the binuclear molecule.⁶⁷ It was found that a decrease in the Pt-Pt distance gave rise to new visible absorption bands,⁶⁸ as well as shifting the emission maxima to lower energy values. The fluorescence intensity exhibited by certain metal ions in thin layer chromatography can be enhanced by making use of non-volatile reagents such as sodium dodecyl sulphate, liquid paraffin and Triton X-100. It is thought that the adsorption onto the silica gel plate provides additional nonradiative pathways for the loss of fluorescence excitation energy which are relieved by transfer of the adsorbed solvent to the liquid state when the plate is sprayed with a non-volatile liquid. However, in the liquid state, other fluorescent enhancing mechanisms may also be important.⁶⁹ The polarity and viscosity of the solvent chosen will also have an effect on the fluorescent intensity.⁷⁰

As is apparent from the above discussion, a variety of fluorescent tags are available, with condensed, aromatic, hydrocarbons being amongst those with the highest quantum efficiency. The use of three ring anthracene and four ring (pericondensed) pyrene was of particular interest in this work. The use of pyrene in a multifunctional probe in solution and in polymer matrices has been reported recently.^{71,72} Chae *et al.* developed a wholly aqueous fluorescence detection scheme with Hg(II) selectivity by making use of an anthracene moiety⁷³ and Sclafani followed the trend by developing a ratiometric fluorosensor for Zn(II) employing a bisanthracene host with a linear polyamine as coordinating moiety.⁷⁴ A Cu(II) chemosensor⁷⁵ and silver ion selective fluorophore⁷⁶ have also been reported, both making use of anthracene as fluorescing entity. An anthracene unit was attached to 2,2':6',2''-terpyridine and the luminescent properties of the resulting Zn(II), Ru(II) and Os(II) complexes was studied,⁷⁷ Michalec attached a pyrenyl unit to the same ligand and discussed the photo physical properties of the platinum complex.⁷⁸ Functionalisation of cyclopentadienyl with 9-methylanthracene enabled the study of Rh(I) and Ir(I) complexes as well as their luminescent properties⁷⁹ and this group went on to report their studies of homobimetallic anthracene bridged η^5 -cyclopentadienyl derivatives of Rh(I) complexes.⁸⁰

The combination of the *N,N*-dialkyl-*N'*-acylthioureas with a fluorescent tag gives rise to an elegant application of these ligands namely the fluorometric detection of heavy metal ions and the PGM's in particular.

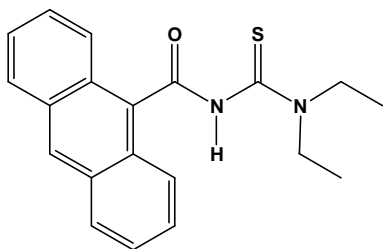
Relatively little has been reported in the literature in this field, however, several interesting complexes have been synthesised.⁸¹ Pakhomova *et al.* investigated the formation of Pt(II) and (IV) complexes with thiourea in HNO₃, HClO₄, H₂SO₄ and H₃PO₄ media. It was found that the nature of the anion and the acidity of the medium had substantial influence on the process of complex formation between the platinum and the thiourea as well as on the luminescent properties of the complex. The luminescent determination of platinum was performed at low temperatures (77 K) and the conditions optimised to yield a detection limit of 2 x 10⁻³ µg/ml. The incorporation of fluorophores, namely fluorescein and anthracene with thiourea to form Pt(II) complexes have been reported by Henderson *et al.*⁸² and were also studied by Grimmbacher,⁸³ however the emission spectra of the resulting platinum complexes were not reported. An interesting *N*-dansyl-*N'*-ethylthiourea ligand was complexed to a variety of heavy metal ions by Schuster *et al.*⁸⁴ Protonation of the basic N-atom contained in the fluorophore (dansyl group) was found to cause a strong quenching of the fluorescence and this was reflected in the metal chelates by a lack of fluorescence at very low pH values. Complexation with the heavy metal ions (in particular the PGM's and Hg(II)) caused quenching and a weak hypsochromic shift of the emission maxima in most cases. Another dansylthiourea complex namely *N*-butyl-*N'*-dansylthiourea was investigated by Konig *et al.*⁸⁵ and a similar moiety was exhibited in a sulfonamide derivative complexed with platinum.⁸⁶

Two particularly interesting studies were performed by Schuster and Unterreitmaier. They investigated the fluorescence of *N*-methyl-*N*-9-(methylanthracene)-*N'*-benzoylthiourea (MABT)⁸⁷ and in a second study, that of pyrene derivatised *N,N*-dialkyl-*N'*-acylthioureas.⁸⁸ Generally it has been found that the acylthiourea moiety strongly quenches the luminescence of most of the more common fluorescent labeling compounds. However this effect is weaker in aromatic hydrocarbons possessing a higher number of fused rings such as perylene or pyrene. An interesting and analytically useful effect observed, was the reduction of fluorescent quenching of the pyrene derivatised *N,N*-dialkyl-*N'*-acylthiourea ligand on complexation of heavy metal ions in particular Cu(II) and Co(II). It was also found that the presence of a -CH₂- spacer group in between the pyrene and actual acylthiourea moiety led to an increase in the fluorescence intensity yielding much lower detection limits of the metal ions in solution, approximately 10 times lower than that observed for the complex with the pyrene substituent directly attached to the carbonyl carbon of the acylthiourea moiety.⁸⁸ In this paper however, very little synthetic and fluorescent information is given, particularly the concentration ranges in which the represented data was obtained. Very little structural information is available in the literature⁸⁹ on these potentially fluorescent ligands as well as their platinum and palladium complexes.

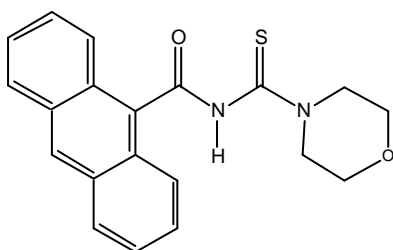
Due to the limited structural information available on fluorescent ligands derived from acylthioureas, it was of interest to synthesise and characterise a series of anthracoyl tagged ligands, and possibly their platinum and palladium complexes. It was also of interest to synthesise the ligands reported by Schuster *et al.*⁸⁸ using pyrene as a fluorescent tag, and to determine their structural characteristics as well as their emission spectra. As previously mentioned alteration of the R groups of the ligands can modify the properties (in particular solubility) of the ligands and resulting complexes and it was for this reason that the amine substituents (R' – Figure 6) were varied. The polarity of these substituents was increased with a view to increasing the water solubility of the ligands and complexes, thus increasing the potential industrial applicability of these compounds. Investigating the HPLC separation of the platinum and palladium complexes was also of interest as the detection limits of the metal ions could possibly be lowered, due to the sensitive nature of fluorescence spectroscopy as a means of detection. These objectives are summarised below.

1.4 Objectives

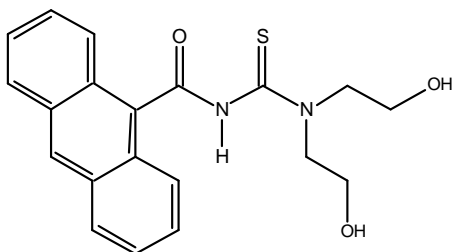
- Synthesis and characterisation of potentially fluorescent ligands such as those shown below.



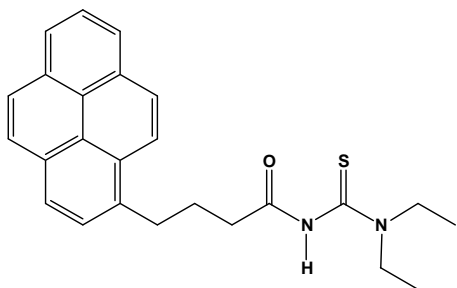
***N,N*-diethyl-*N'*-9-anthracoylthiourea**
3-9-anthracoyl-1,1-diethylthiourea



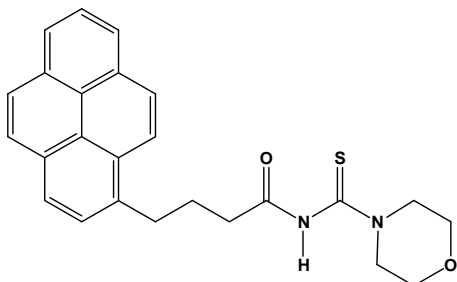
***N*-morpholine-*N'*-9-anthracoylthiourea**
3-9-anthracoyl-1,1-(3-oxapentane-1,5-diyl)thiourea



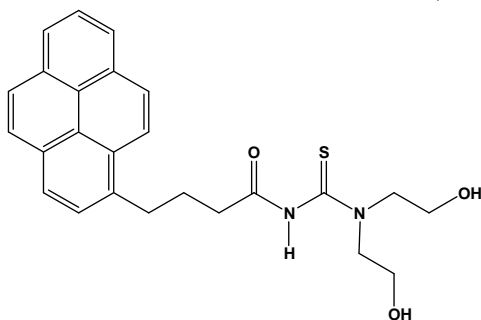
***N,N*-di(2-hydroxyethyl)-*N'*-9-anthracoylthiourea**
3-9-anthracoyl-1,1-di(2-hydroxyethyl)thiourea



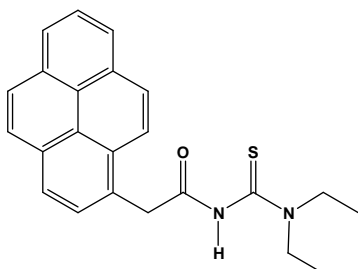
N,N-diethyl-N'-[4-(pyrene-1-yl)butanoyl]thiourea
*1,1-diethyl-3-[4-(pyrene-1-yl)butanoyl]thiourea**



N-morpholine-N'-[4-(pyrene-1-yl)butanoyl]thiourea
1,1-(3-oxapentane-1,5-diyl)-3-[4-(pyrene-1-yl)butanoyl]thiourea



N,N-di(2-hydroxyethyl)-N'-[4-(pyrene-1-yl)butanoyl]thiourea
1,1-di(2-hydroxyethyl)-3-[4-(pyrene-1-yl)butanoyl]thiourea



N,N-diethyl-N'-[pyrene-1-ylacetyl]thiourea
1,1-diethyl-3-[pyrene-1-ylacetyl]thiourea

- Synthesis and characterisation of Pt(II) and Pd(II) complexes using potentially fluorescent ligands.
- Determination of emission spectra of potentially fluorescent ligands as well as their Pt(II) and Pd(II) complexes.

* The compound names shown in italics are formulated according to IUPAC rules, however recent reports in the literature make use of “*N*” and “*N'*” to denote the positions of the thiourea substituents instead of “1” and “3” respectively. In general the “*N*” substituents are mentioned first followed by the “*N'*” substituents.⁹⁰ In keeping with the trends in the literature, the compound names given in bold will be used throughout this work. The use of the term “morpholine” denoting the “*N*” substituent in the applicable compounds, previously employed by Sacht *et al.*⁹¹ will be retained as opposed to 3-oxapentane-1,5-diyl.

- Preliminary investigation of the Reverse-phase High Performance Chromatography (RP-HPLC) separation of the platinum and palladium complexes of potentially fluorescent ligands.

References

1. S. A. Cotton, *Chemistry of Precious Metals*, Chapman and Hall, London, **1997**.
2. F. R. Hartley, *Chemistry of the Platinum Group Metals*, Elsevier, Amsterdam, **1991**.
3. Johnson Matthey, Interim Review, Platinum, **2003**.
4. E. Rosenberg, L. VanCamp, T. Krigas, *Nature*, **1965**, 205, 698-699.
5. Bullion Coin Collectors Site, <http://rscott.org/bullion/index.html>, last updated *March 30*, **2001**.
6. Anglo American Platinum Corporation Limited, Annual Report, **2002**, Volume 1: Business Report.
7. Johnson Matthey, <http://www.platinum.matthey.com/prices/chartintro.php>, **2004**.
8. Economic and Advisory unit of South African Chamber of Mines, **2003**.
9. Info comm, market information, <http://r0.unctad.org/infocomm/anglais/platinum/chain.htm>
10. R. Barefoot, J. Van Loon, *Talanta*, **1999**, 1-14.
11. P. Seeverens, E. Klaasen, F. Maessen, *Spectrochimica Acta*, **1983**, 5/6, 727-737.
12. R. Barefoot, *J. Anal. At. Spectrom.*, **1998**, 13, 1077-1084.
13. A. Douglas, F. Skoog, J. Holler, T. Nieman, *Principles of Instrumental Analysis*, 5th Edn, Saunders College Publishing, **1997**.
14. I. Douglass, F. Dains, *J. Am. Chem. Soc.*, **1934**, 56, 719-721.
15. N. Vijayakumaran, *J. Indian Chem. Soc.*, **1963**, 40, 953-6.
16. A. Polizu, C. Zahariadi, V. Bontea, C. Marches, E. Bucur, *Seria Botanica*, **1965**, 17, 93-100.
17. L. Beyer, E. Hoyer, H. Hennig, R. Kirmse, R. Hartmann, H. Liebscher, *J. fur Prakt. Chem.*, **1975**, 317, 829-39.
18. S. Behrendt, L. Beyer, F. Dietze, E. Hoyer, L. Eberhard, E. Uhlemann, *Inorg. Chim. Acta*, **1980**, 43, 141-4.
19. A. Mohamadou, I. Dechapms-Olivier, J. Barbier, *Polyhedron*, **1994**, 13, 1363-70.
20. S. Bhowal, *Indian J. Chem. Sect. A*, **1975**, 13, 92-4.
21. E. Uhlemann, W. Bechmann, E. Ludwig, *Anal. Chim. Acta*, **1978**, 100, 635-42.
22. L. Beyer, S. Behrendt, E. Kleinpeter, R. Borsdorf, E. Hoyer, *Z. Anorg. Allg. Chem.*, **1977**, 437, 282-8.
23. K. Koenig, H. Pletsch, M. Schuster, *Fresenius' J. Anal. Chem.*, **1986**, 325, 621-4.
24. C. Sacht, M. Datt, S. Otto, A. Roodt, *Dalton Trans*, **2000**, 727-733.
25. K. Koenig, M. Schuster, B. Steinbrech, G. Schneeweis, R. Schlodder, *Fresenius' J. Anal. Chem.*, **1985**, 321, 457-60.
26. P. Vest, M. Schuster, K. Koenig, *Fresenius' J. Anal. Chem.*, **1989**, 335, 759-763.
27. K. Koenig, M. Schuster, G. Schneeweis, B. Steinbrech, *Fresenius' J. Anal. Chem.*, **1984**, 319, 66-69.
28. M. Schuster, *Fresenius' J. Anal. Chem.*, **1986**, 324, 127-129.
29. M. Schuster, K. Koenig, *Fresenius' J. Anal. Chem.*, **1988**, 331, 383-386.

-
30. M. Schuster, B. Kugler, K. Koenig, *Fresenius' J. Anal. Chem.*, **1990**, 338, 717-720.
 31. S. Ringmann, M. Schuster, *Chem. Tech.*, **1997**, 49, 217-226.
 32. D. Handforth, K. Koch, *Precious Metals*, **1998**, 22, 29-45.
 33. R. Richter, F. Dietze, S. Schmidt, E. Hoyer, W. Poll, D. Mootz, *Z. Anorg. Allg. Chem.*, **1997**, 623, 135-140.
 34. R. Richter, J. Sieler, L. Beyer, O. Lindqvist, L. Andersen, *Z. Anorg. Allg. Chem.*, **1985**, 522, 171-183.
 35. W. Bensch, M. Schuster, *Z. Anorg. Allg. Chem.*, **1992**, 611, 95-98.
 36. S. Schmidt, F. Dietze, E. Hoyer, *Z. Anorg. Allg. Chem.*, **1991**, 603, 33-39.
 37. P. Vest, M. Schuster, K. Koenig, *Fresenius' J. Anal. Chem.*, **1991**, 341, 566-568.
 38. A. Domínduez, E. Antico, L. Beyer, A. Aguirre, S. Garcia-Granda, V. Salvado, *Polyhedron*, **2002**, 14-15, 1429-1437.
 39. F. Dietze, S. Schmidt, E. Hoyer, L. Beyer, *Z. Anorg. Allg. Chem.*, **1991**, 595, 35-43.
 40. K. Koch, C. Sacht, S. Bourne, *Inorg. Chim. Acta*, **1995**, 232, 109-115.
 41. R. Koehler, R. Kirmse, R. Richter, J. Sieler, E. Hoyer, L. Beyer, *Z. Anorg. Allg. Chem.*, **1986**, 537, 133-144.
 42. K. Koch, S. Bourne, A. Coetzee, J. Miller, *Dalton Trans*, **1999**, 3157-3161.
 43. K. Koch, O. Hallale, S. Bourne, J. Miller, J. Bacsá, *J. Mol. Struct.*, **2001**, 561, 185-196.
 44. A. Irving, K. Koch, M. Matoetoe, *Inorg. Chim. Acta*, **1993**, 206, 193-199.
 45. K. Koch, T. Grimmbacher, C. Sacht, *Polyhedron*, **1999**, 17, 267.
 46. A. Mautjana, J. Miller, A. Gie, S. Bourne, K. Koch, *Dalton Trans*, **2003**, 1952-1960.
 47. J. Lakowicz, *Principles of fluorescence Spectroscopy*, Kluwer Academic, London, **1999**.
 48. L. Saari, W. Seitz, *Anal. Chem.*, **1983**, 55, 667-670.
 49. M. Carroll, F. Bright, G. Hieftjie, *Anal. Chem.*, **1989**, 61, 1768-1772.
 50. K. Soroka, R. Vithanage, D. Phillips, B. Walker, P. Dasgupta, *Anal. Chem.*, **1987**, 59, 629-636.
 51. K. Rurack, M. Kollmannsberger, U. Resch-Genger, J. Daub, *J. Am. Chem. Soc.*, **2000**, 122, 968-969.
 52. C. Chen, W. Huang, *J. Am. Chem. Soc.*, **2002**, 124, 6246-6247.
 53. K. Hiraki, K. Morishige, Y. Nishikawa, *Anal. Chim. Acta*, **1978**, 97, 121-128.
 54. T. Aldridge, E. Stacy, D. McMillan, *Inorg. Chem.*, **1994**, 33, 722-727.
 55. V. Miskowski, V. Houlding, C. Che, Y. Wang, *Inorg. Chem.*, **1993**, 32, 2518-2524.
 56. W. Connick, H. Gray, *J. Am. Chem. Soc.*, **1997**, 119, 11620-11627.
 57. W. Connick, D. Geiger, R. Eisenberg, *Inorg. Chem.*, **1999**, 38, 3264-3265.
 58. K. Aye, R. Puddephatt, *Inorg. Chim. Acta*, **1995**, 235, 307-310.
 59. J. Bevilacqua, J. Zuleta, R. Eisenberg, *Inorg. Chem.*, **1993**, 32, 3689-3693.
 60. J. Bevilacqua, R. Eisenberg, *Inorg. Chem.*, **1994**, 33, 2913-2923.
 61. C. Seward, J. Pang, S. Wang, *Eur. J. Inorg. Chem.*, **2002**, 1390-1399.
 62. R. Ballardini, M. Gandolfi, L. Prodi, M. Ciano, V. Balzani, F. Kohnke, H. Shahriari-Zavareh, N. Spencer, J. Stoddart, *J. Am. Chem. Soc.*, **1989**, 111, 7072-7078.
 63. R. Ballardini, V. Balzani, A. Credi, M. Gandolfi, F. Kotzbyba-Hibert, J. Lehn, L. Prodi, *J. Am. Chem. Soc.*, **1994**, 116, 5741-5746.
 64. A. Sautter, D. Schmid, G. Jung, F. Wurthner, *J. Am. Chem. Soc.*, **2001**, 123, 5424-5430.

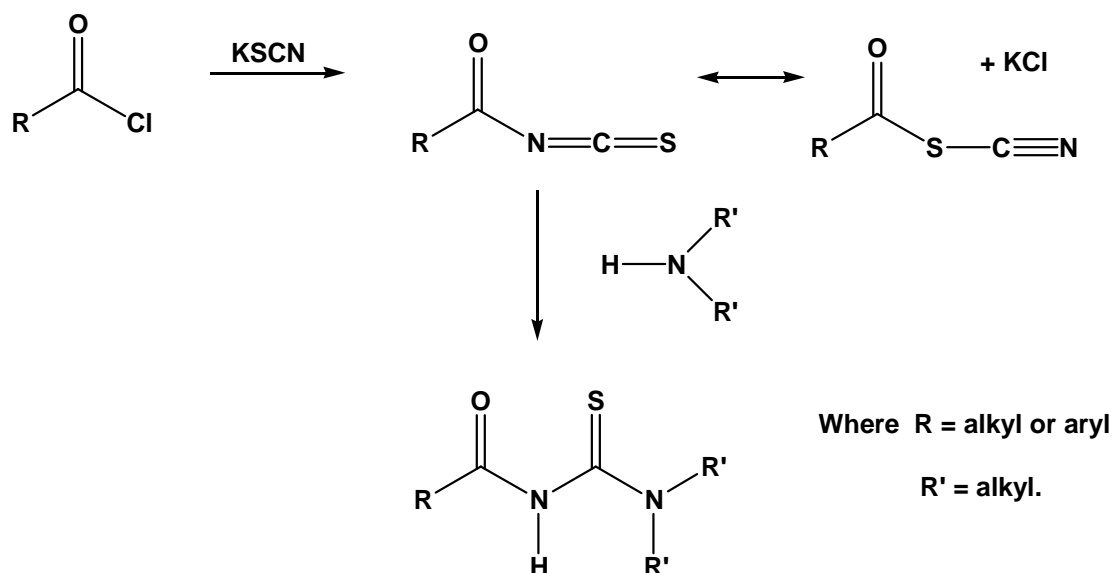
-
65. F. Wurther, A. Sautter, *Chem. Commun.*, **2000**, 445-446.
 66. H. Yip, Z. Zhou, T. Mak, *Chem. Commun.*, **1992**, 1369-1371.
 67. L. Bar, H. Englmeier, G. Gliemann, U. Klement, K. Range, *Inorg. Chem.*, **1990**, 29, 1162-1168.
 68. A. Bailey, V. Miskowski, H. Gray, *Inorg. Chem.*, **1993**, 32, 369-370.
 69. S. Ho, H. Butler, C. Poole, *J. Chromatogr.*, **1983**, 281, 330-339.
 70. S. Uchiyama, M. Uchiyama, *J. Chromatogr.*, **1978**, 153, 135-142.
 71. P. Hrdlovic, S. Chmela, *J. Photochem. Photobiol., A*, **1997**, 105, 83-88.
 72. L. Bucsiova, P. Hrdlovic, S. Chmela, *J. Photochem. Photobiol., A*, **2001**, 143, 59-68.
 73. M. Chae, A. Czarnik, *J. Am. Chem. Soc.*, **1992**, 114, 9704-9705.
 74. J. Sclafani, M. Maranto, T. Sisk, S. Van Arman, *Tetrahedron Lett.*, **1996**, 37, 2193-2196.
 75. M. Beltramello, M. Gatos, F. Mancin, P. Tecilla, U. Tonellato, *Tetrahedron Lett.*, **2001**, 42, 9143-9146.
 76. J. Ishikawa, H. Sakamoto, S. Nakao, H. Wada, *J. Org. Chem.*, **1999**, 64, 1913-1921.
 77. G. Albano, V. Balzani, E. Constable, M. Maestri, D. Smith, *Inorg. Chim. Acta*, **1998**, 225-231.
 78. J. Michalec, S. Bejune, D. Cuttell, G. Summerton, J. Gertenbach, J. Field, R. Haines, D. McMillin, *Inorg. Chem.*, **2001**, 40, 2193-2200.
 79. F. Cicogna, M. Colonna, J. Houben, G. Ingrosso, F. Marchetti, *J. Organomet. Chem.*, **2000**, 593, 251-266.
 80. M. Carano, M. Careri, F. Cicogna, I. D'Ambra, J. Houben, G. Ingrosso, M. Marcaccio, F. Paolucci, C. Pinzino, S. Roffia, *Organometallics*, **2001**, 20, 3478-3490.
 81. I. Pakhomova, N. Kuzyakova, V. Fadeeva, *Zh. Anal. Khim.*, **1988**, 43, 1472-1476.
 82. W. Henderson, B. Nicholson, C. Rickard, *Inorg. Chim. Acta*, **2001**, 320, 101-109.
 83. T. Grimmbacher, *PhD Thesis*, Univ Cape Town, **1995**.
 84. M. Schuster, M. Sandor, *Fresenius' J. Anal. Chem.*, **1996**, 356, 326-330.
 85. K. Koenig, J. Bosslet, C. Holzner, *Chem. Ber.*, **1989**, 122, 1, 59-61.
 86. W. Henderson, L. McCaffrey, M. Dinger, B. Nicholson, *Polyhedron*, **1998**, 18, 3137-3144.
 87. E. Unterreitmaier, M. Schuster, *Anal. Chim. Acta*, **1995**, 309, 339-344.
 88. M. Schuster, E. Unterreitmaier, *Fresenius' J. Anal. Chem.*, **1993**, 346, 630-633.
 89. J. Bricks, K. Rurack, R. Radeaglia, G. Reck, B. Schulz, H. Sonnenschein, U. Resch-Genger, *J. Chem. Soc., Perkin Trans. 2*, **2000**, 2, 1209-1214.
 90. C. Sacht, M. Datt, *Polyhedron*, **2000**, 1347-1354.
 91. C. Sacht, M. Datt, S. Otto, A. Roodt, *Dalton Trans.*, **2000**, 4579-4586.

2.1 Conversion of aroyl acids to their acid chlorides

2.1.1 Introduction

One of the primary objectives of this project was to synthesise a series of potentially fluorescent *N,N*-dialkyl-*N'*-aroyl(acyl)thiourea ligands. Traditionally ligands of this type have been synthesised according to the method described by Douglass and Dains.¹ While they were not the first to report the synthesis of these ligands, their simplified “one pot” procedure is widely regarded as being something of a milestone in the synthetic history of these molecules due to the relatively simple procedure and generally good yields obtained.

The method involves the addition of ammonium² or potassium thiocyanate to an acyl halide to form an isothiocyanate intermediate (Scheme 1). The isothiocyanate intermediate is in equilibrium with its thiocyanate isomer and there have been various discussions as to whether both or only one of the species undergo further reaction.³ However, later results which are now generally accepted have shown that whilst both species are present, it is only the isothiocyanate isomer that reacts further with a secondary (or primary) amine to yield the final *N,N*-dialkyl-*N'*-acylthiourea product.⁴ The procedure is carried out in dry acetone and under a N₂ atmosphere due to the hygroscopic nature of the potassium thiocyanate and the sensitivity to water of the isothiocyanate intermediate, as well as to avoid the potential side reaction of acyl halide hydrolysis.



Scheme 1 Reaction scheme of the synthetic procedure described by Douglass and Dains.¹

As can be seen from Scheme 1, in order to obtain the *N,N*-dialkyl-*N'*-aroylthiourea ligands the synthetic procedure called for the use of the corresponding acid chloride as one of the starting materials. Since 9-

anthracoyl chloride, 1-pyrenebutanoyl chloride and 1-pyreneacetyl chloride are not commercially available, all three of these compounds needed to be synthesised from their corresponding carboxylic acids. Various methods of converting carboxylic acids to the corresponding acid chlorides were available in the literature and these reported the use of a variety of reagents to effect the conversions. The most common reagents employed were phosphorous tri- and pentachloride, thionyl chloride,^{5,6} as well as oxalyl chloride.^{7,8} The latter two are the most favoured as the by-products formed are gaseous and thus work up of the acid chloride product is greatly simplified.⁹ However, the mechanistic principles of the reaction remain the same regardless of the reagent employed.

2.1.2 Review of literature methods

A brief description of each reported method used in the synthesis of 9-anthracoyl chloride, 1-pyrenebutanoyl chloride and 1-pyreneacetyl chloride is given below along with the percentage yield obtained in cases where this was given in the literature. The quantities of reactants and solvents used have been included as the ratio of these was thought to be of relevance to the outcome of the reactions, however this will be discussed in more detail in sections 2.1.3 and 2.1.4.

Method 1 (Morozumi *et al.*)¹⁰

A solution of 9-anthracenecarboxylic acid (2.22 g, 10.0 mmol), in SOCl₂ (30 ml) was refluxed for 1.5 hours. Excess SOCl₂ was distilled off *in vacuo*, and the product evaporated to dryness after four 10 ml additions of benzene. The percentage yield was not reported.

Method 2 (Weisler and Nakanishi)⁷

9-anthracenecarboxylic acid (1.00 g, 4.5 mmol) and SOCl₂ (4.5 ml) were refluxed in dry benzene for 1 hour. *In vacuo* removal of benzene and excess reagent afforded the aroyl chloride. The percentage yield was not reported.

Method 3 (Ciganek)¹¹

A mixture of 9-anthracenecarboxylic acid (18.85 g, 84.9 mmol) and SOCl₂ (60 ml), was heated under reflux for 1 hour. The excess reagent was removed *in vacuo*, and toluene (50 ml) was added, the mixture was concentrated again and repetition of this procedure afforded the product. The percentage yield was reported as being 95%.

Method 4 (Schuster)¹²

1-pyrenebutyric acid (4.90 g, 17.0 mmol) was added to dry diethyl ether (50 ml) and SOCl₂ (7.5 ml). Three drops of pyridine were added to the suspension followed by 1.5 hours of stirring at room temperature. Filtration of the solution removed the brown residue formed and *in vacuo* removal of the SOCl₂ and the

addition of four 20 ml volumes of diethyl ether followed by reconcentration of the solution afforded 1-pyrenebutanoyl chloride in 93% yield.

Method 5 (Lou, Hatton and Laibinis)¹³

A solution of SOCl_2 (0.22 ml) in CHCl_3 (3 ml) was added to a stirred suspension of 1-pyrenebutyric acid (0.10 g, 0.36 mmol) in CHCl_3 (5 ml) under a N_2 atmosphere. The mixture was stirred overnight at room temperature and excess solvent and thionyl chloride were removed *in vacuo* to yield 1-pyrenebutanoyl chloride. The percentage yield was not reported.

Method 6 (Tran and Fendler)¹⁴

1-pyrenebutyric acid (2.0 g, 6.9 mmol) and SOCl_2 (3 ml) were refluxed in dry benzene (800 ml) for 7 hours. The resulting 1-pyrenebutanoyl chloride was recrystallised from dry hexane in 71% yield.

As will become apparent during the course of the subsequent two sections (section 2.1.3 and 2.1.4) the products 9-anthracoyl chloride, 1-pyrenebutanoyl chloride and 1-pyreneacetyl chloride could not always be isolated in the pure form. The product precipitates obtained frequently being mixtures of the unconverted carboxylic acids and corresponding aroyl chlorides. For reasons that will become clear, chromatographic separations of these two species was not possible and consequently the yields of the aroyl chlorides could not be accurately calculated, however estimations of the degree of carboxylic acid to aroyl chloride conversion could be made.

2.1.3 Conversion of 9-anthracenecarboxylic acid to 9-anthracoyl chloride

In this work some of the reported methods described in the preceding section were varied in an attempt to improve the product yields of 9-anthracoyl chloride, in particular Methods 4 and 5 concerned with the conversion of 1-pyrenebutyric acid were adapted and applied to the conversion of 9-anthracenecarboxylic acid. Methods 1 to 5 were employed for the conversion of 9-anthracenecarboxylic acid and deviations from the reported text generally involved a scaling down of reagent quantities, an increase in reaction times, and on occasion the addition of a small amount of DMF to serve as a proton acceptor. The solvents used were also varied. Complete details of the synthetic procedures are given in Chapter 5.

Following a number of attempts with Method 1 a reasonable conversion ratio of 9-anthracenecarboxylic acid to 9-anthracoyl chloride was obtained, and between 50 to 70% of 9-anthracoyl chloride was estimated to have been formed. In an attempt to increase the yield of 9-anthracoyl chloride using this method the starting compound, 9-anthracenecarboxylic acid, was oven dried prior to the reaction as residual water in this compound could have contributed to the hydrolysis of the 9-anthracoyl chloride formed during the reaction. The drier 9-anthracenecarboxylic acid did not however significantly increase the yield of 9-anthracoyl chloride. A further experiment was performed using this method and the reaction time was

increased to a total of 40 hours, however instead of an improved yield of 9-anthracoyl chloride as expected, possible decomposition of the product was observed from the ^{13}C and ^1H NMR spectra. The large number of resonances in these spectra severely complicated the identification of any of the potential breakdown products, however the nature of these products will be discussed later in this section. Finally, it was found that an increase in the reaction time from the reported 1.5 hours to an optimal 6 hours affected an estimated 70% conversion ratio of 9-anthracenecarboxylic acid to 9-anthracoyl chloride.

Method 2 initially gave a fair conversion where the amount of 9-anthracoyl chloride formed was estimated to be 50%. Whilst this was not particularly high, the absence of decomposition products was encouraging. The use of a small amount of DMF as a base and the use of oxalyl chloride as reagent greatly improved the conversion ratio of 9-anthracenecarboxylic acid to 9-anthracoyl chloride and the final yield of 9-anthracoyl chloride was estimated to be 80%.

Method 3 yielded the best results as there was no sign of decomposition in any of the reactions carried out. The average yield of 9-anthracoyl chloride obtained using this method was greater than 95%.

Method 4 gave varying results and this was thought to be solvent dependant. When acetone was used as a solvent very poor results were obtained and severe decomposition was evident from the NMR spectra. The influence of acetone will be discussed later in this section. The use of diethyl ether as solvent however, gave very satisfactory results and no decomposition was apparent. The final yield of 9-anthracoyl chloride was 95%.

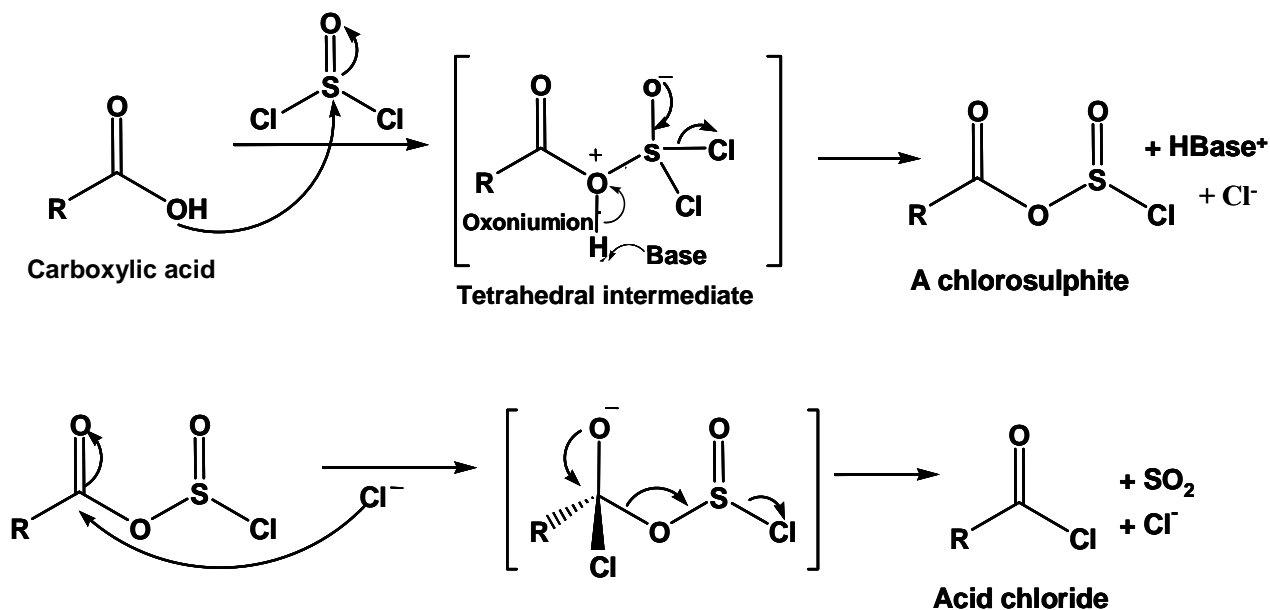
Method 5 was performed according to the reported procedure¹³ however dichloromethane was used as a solvent as opposed to chloroform. The reason for this substitution will be explained more fully in section 2.1.4. The conversion ratio of 9-anthracenecarboxylic acid to 9-anthracoyl chloride was generally very low and increased reaction times did little to improve this ratio, rather increasing the formation of possible decomposition products. The final yield of 9-anthracoyl chloride was estimated to be 40%.

Several factors resulting in the lack of success converting 9-anthracenecarboxylic acid to 9-anthracoyl chloride could be identified in the light of the above results.

Due to incomplete conversion in some of the syntheses, particularly using Method 1, the reaction times were increased, in some cases being as long as 40 hours. These attempts generally gave very poor results and mixtures of unidentifiable products. It was thought that light exposure may have played a role in the poor results obtained. Further investigation showed that reports have been made suggesting that this is likely. Lemmetyinen and co-workers¹⁵ studied the photodegradation of polycyclic aromatic compounds in aqueous solutions and found that anthracene and benzanthracene gave the fastest decomposition of the compounds studied. Abdel-Mottaleb *et al.*¹⁶ studied the photostability of 9-anthracenecarboxylic acid in different media and reported anthraquinone as being the main product of photodegradation. This supported

the idea that photodegradation of the starting compound had occurred during these reactions giving rise to the poor yields of 9-anthracoyl chloride obtained.

The addition of a base also influenced the outcome of the reaction, particularly in Methods 2 and 4, where DMF and pyridine were used respectively. This can be understood in terms of the reaction scheme below (Scheme 2). The reaction that takes place is a nucleophilic acyl substitution where the trigonal reactant forms a tetrahedral intermediate and deprotonation of the oxonium ion in this species results in the formation of the chlorosulphite intermediate. Further nucleophilic attack by the chloride ion and removal of the SO_2Cl moiety results in the formation of the acid chloride.¹⁷ It is apparent that the use of a base will aid the deprotonation of the oxonium ion and the formation of the chlorosulphite intermediate.



Scheme 2 Mechanism of carboxylic acid conversion to yield an acid chloride.¹⁸

In the light of the mechanistic principles of the reaction, it is interesting to note that the majority of reported methods did not allude to the use of a base. While this theory explains the results obtained using Methods 2 and 4 it is puzzling that the best yields of 9-anthracoyl chloride were obtained using Method 3, where no use was made of a base. This suggests that other factors are involved in the successful conversion of carboxylic acids to acid chlorides.

A third factor thought to influence the outcome of the reaction was the ratio of the solvent to reagent. This was demonstrated in the case of Method 4, where the ratio of the solvent to reagent scale was altered, with all other factors remaining constant. Better results were obtained where the solution was more concentrated, *i.e.* where 0.5 g of acid : 25 ml ether yielded relatively poor results, but 1 g of acid : 25 ml ether gave greatly improved conversion ratios of 9-anthracenecarboxylic acid to 9-anthracoyl chloride.

Using the same method but altering the choice of solvent also gave interesting results, which leads to the fourth factor thought to influence the outcome of the reaction. As previously mentioned, in Method 4 where acetone was used as a solvent very poor results were obtained. Figure 10 shows the “keto-enol” tautomerism exhibited by acetone which leads to the formation of another potentially reactive compound, namely the enol form of the acetone molecule. The NMR spectra obtained from the reaction showed the formation of a number of different species and some of these may have resulted from reaction with the solvent.

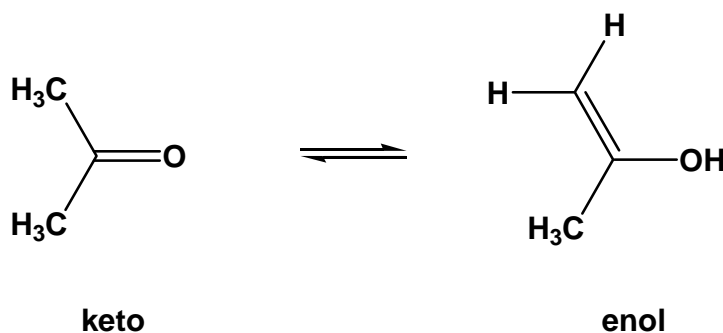


Figure 10 Keto-enol tautomerism exhibited by acetone.

As previously suggested, light exposure is known to influence reactions involving polycyclic aromatic hydrocarbons, anthracene in particular. This may be a further reason for the large amount of decomposition observed during this reaction in particular. Meyer and Eckert¹⁹ reported the formation of anthraquinone when dihydroanthracene was dissolved in acetone and exposed to light and they also found that anthranil acetate was a by-product of the reaction. Similar results were obtained when they subjected anthracene to these conditions. In our case, the presence of additional peaks in the carbonyl region of the NMR spectrum obtained from this reaction would appear to support the possibility of the formation of some of these compounds as by-products. While the chemical shifts of these resonances do not correspond exactly to the calculated shifts for anthraquinone, the presence of many other by-products in the solution could influence the chemical surroundings of the species leading to slight variations in their chemical shift positions.

2.1.4 Conversion of 1-pyrenebutyric acid and 1-pyreneacetic acid to their corresponding chlorides

Methods 1, 4, 5 and 6 were employed for the conversion of 1-pyrenebutyric acid and deviations from the literature methods were similar to those for 9-anthracenecarboxylic acid in that the scale of the reported reaction was usually decreased. Work up procedures sometimes involved the use of hexane in an attempt to yield a pure product (Method 6). The use of hexane as a solvent in recrystallisation was also reported elsewhere in a similar context.²⁰ Further details of the synthetic procedures are given in Chapter 5.

Only Method 4 was employed for the conversion of 1-pyreneacetic acid as the results obtained with this method were satisfactory.

In the case of the conversion of 1-pyrenebutyric acid, Method 1 gave very poor results. The best results were achieved using Method 4, which gave an estimated 91% yield of 1-pyrenebutanoyl chloride.

Method 5 was also attempted however poor yields of 1-pyrenebutanoyl chloride were obtained. The appearance of another potential carbonyl species was noted in the ^{13}C NMR spectrum and this was attributed to the formation of ethyl 1-pyrenebutanoate. In the published procedure the chloroform used had been stabilised with amylene, however the chloroform used in this reaction was stabilised with ethanol, thus resulting in the formation of the ethyl 1-pyrenebutanoate. Repeating the procedure and making use of dichloromethane as a solvent avoided the formation of the ester but did not improve the yield of the reaction.

Method 6 yielded better results than those previously obtained, giving an estimated 60% yield of 1-pyrenebutanoyl chloride.

As previously mentioned, for the conversion of 1-pyreneacetic acid to 1-pyreneacetyl chloride, only Method 4 was used and this was found to give satisfactory results with 90-95% yields of 1-pyreneacetyl chloride.

In the conversions of 1-pyrenebutyric acid and 1-pyreneacetic acid, similar factors to those identified for the 9-anthracenecarboxylic acid conversions were thought to play a role, in particular the choice of solvent. The use of halogenated solvents (*e.g.* chloroform in Method 5 for the conversion of 1-pyrenebutyric acid) giving the poorest results.

A further similarity for these two conversions was in the use of a base, particularly in Method 4 where the use of pyridine gave satisfactory results for both 1-pyrenebutyric acid and 1-pyreneacetic acid.

In general however, the pyrene derivatised compounds, 1-pyrenebutyric acid and 1-pyreneacetic acid were found to be more stable under harsh reaction conditions, including exposure to light and air, relative to the anthracene derivatised compound, 9-anthracenecarboxylic acid.

The above results are summarised in Table 1 where the estimated yield of 9-anthracoyl chloride, 1-pyrenebutanoyl chloride and 1-pyreneacetyl chloride obtained are given for each method used.

Table 1 Estimated yields of aromatic acyl chlorides for each method used.

Aroyl chloride (% yield)	Method					
	1	2	3	4	5	6
9-anthracoyl chloride	70	80	95	95	40	-
1-pyrenebutanoyl chloride	35	-	-	91	30	20
1-pyreneacetyl chloride	-	-	-	93	-	-

Understanding the reason for the varying success in conversion was complicated by the fact that the aroyl chlorides, in particular 9-anthracoyl chloride, was significantly more moisture sensitive and unstable than originally thought. Deuterated chloroform was used as a solvent in the NMR analyses of these compounds and it was found that the carboxylic acids, in particular 9-anthracenecarboxylic acid was relatively insoluble in this solvent, while the aroyl chloride was soluble. Initial NMR studies were performed where the 9-anthracoyl chloride obtained from the reaction was allowed to stand overnight prior to analysis, and its precipitation in chloroform led us to believe that the rate of hydrolysis to the corresponding carboxylic acid was a great deal faster than previously expected. Further analyses were then performed with a minimum amount of time spent between the preparation and subsequent testing of the NMR samples. Chromatographic separation of the carboxylic acids and the aroyl chlorides was not possible due to the acidity of the silica gel resulting in the hydrolysis of the aroyl chloride; this leading to plate and column “streaking”.

Available literature on the conversion of carboxylic acids to their aroyl chlorides is limited and the majority of literature available is in the form of patents.^{21,22,23} It would therefore appear that this apparently simple reaction is more complicated than initially thought. However, from the above results it would appear that no single factor can alone be held responsible for effecting good conversions, but rather that a combination of correct solvent choice, solvent to reagent ratio, limitation of exposure to light, and the use of a base all contribute to obtaining good product yields.

2.2 Synthesis of *N,N*-dialkyl-*N'*-aroylthiourea ligands

2.2.1 Introduction

2.2.1.1 *Douglass and Dains methods*

As mentioned in Section 2.1, the *N,N*-dialkyl-*N'*-acylthioureas are traditionally synthesised according to the procedure described by Douglass and Dains.¹ This was therefore the first procedure attempted in the synthesis of the series of *N,N*-dialkyl-*N'*-aroylthiourea ligands. In this procedure, the addition of potassium thiocyanate to the aroyl chloride was followed by 45 minutes of heating under reflux and cooling to room temperature yielded the aroyl isothiocyanate (Scheme 1). Slow dropwise addition of the amine in acetone solution was followed by a further 45 minutes of heating under reflux followed by cooling to room temperature. A small volume of water was added to increase the rate of product precipitation and the mixture was placed in the vent of the fumehood to allow slow volatilisation of the acetone and crystal formation. Single product precipitates were recrystallised from a combination of acetone and water or ethanol and water. Where the

product failed to crystallise and an oil was obtained extraction into chloroform was followed by separation and purification by column chromatography (silica gel). Further synthetic details are given in Chapter 5.

The anthracene derivatised ligands, *N,N*-diethyl-*N'*-9-anthracoylthiourea, *N*-morpholine-*N'*-9-anthracoylthiourea and *N,N*-di(2-hydroxyethyl)-*N'*-9-anthracoylthiourea, could be successfully synthesised using the Douglass and Dains method, however slight variations of the procedure were introduced for synthesis of the *N,N*-dialkyl-*N'*-[4-(pyrene-1-yl)butanoyl]thiourea and *N,N*-dialkyl-*N'*-[pyrene-1-ylacetyl]thiourea derivatives. These deviations included shortened periods of heating from 45 minutes (Douglass and Dains) to 10 minutes. Following the dropwise addition of the amine, the precipitated potassium chloride was removed by filtration and this was followed by the *in vacuo* removal of 80% of the solvent. The addition of 2 drops of 6M HCl to the remaining solution and the gradual volatilisation of the acetone enabled the formation of the *N,N*-dialkyl-*N'*-aroylthiourea product as a precipitate. The products were washed with cold ethanol and recrystallised from isopropyl alcohol. In cases where oils were obtained, these were extracted into chloroform followed by separation and purification by column chromatography (silica gel).

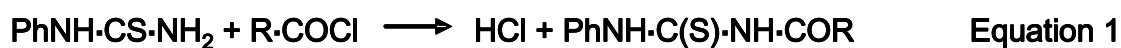
The latter method will be referred to as the “modified” Douglass and Dains method as despite the variations introduced in this procedure, the basic principles remain the same, namely the addition of an acyl halide to an isothiocyanate, followed by the addition of an amine to yield an *N,N*-dialkyl-*N'*-acylthiourea.

Of the large number of *N,N*-dialkyl-*N'*-acylthioureas that have been synthesised using the Douglass and Dains method in the literature most have been *N,N*-dialkyl-*N'*-benzoylthioureas.^{24,25,26} There have been very few reports of *N,N*-dialkyl-*N'*-acylthioureas *i.e.* with the use of an alkyl group attached to the carbonyl carbon.^{27,28} As has been previously noted this is not due to mere oversight²⁹ as the synthesis of acyl chloride derivatives using the Douglass and Dains procedure is generally less successful than for benzoyl chloride derivatives.

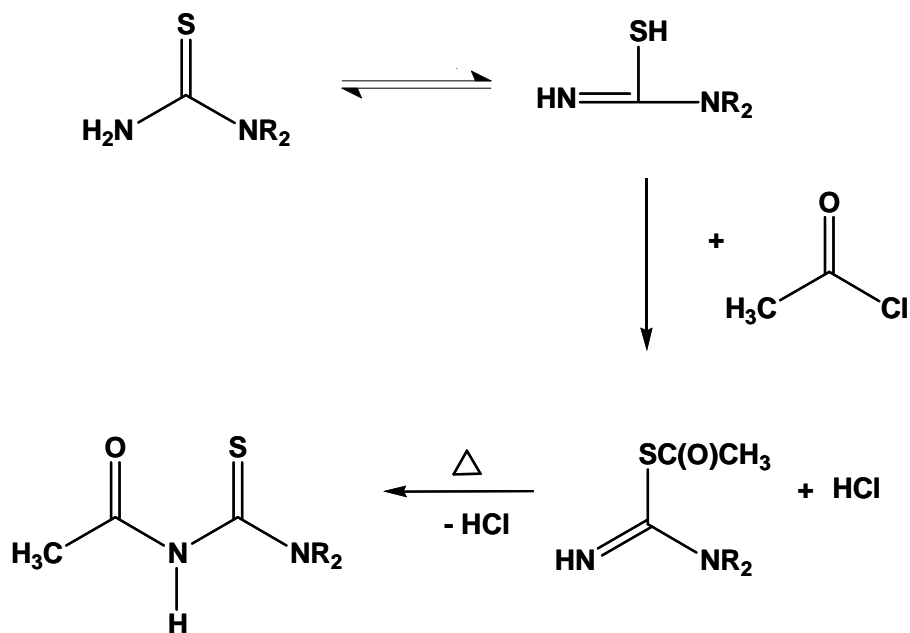
It was thus not unexpected that the *N,N*-dialkyl-*N'*-9-anthracoylthiourea derivatives could be obtained in satisfactory yields with the Douglass and Dains procedure, compared to those for the *N,N*-dialkyl-*N'*-[4-(pyrene-1-yl)butanoyl]thiourea derivatives in particular. The possible reasons for this will be discussed further in Section 2.2.2.

2.2.1.2 Dixon and Taylor method

An alternative synthetic method was therefore used in the synthesis of the *N,N*-dialkyl-*N'*-[4-(pyrene-1-yl)butanoyl]thiourea and *N,N*-dialkyl-*N'*-[pyrene-1-ylacetyl]thiourea derivatives. This method was first reported by Dixon and Taylor³¹ and involved the addition of acetyl chloride to 1-phenylthiourea in anhydrous acetone to yield an *N*-phenyl-*N'*-acylthiourea (Equation 1).



While this reaction initially appears to be similar to a condensation reaction, involving the elimination of HCl, the results of Dixon and Taylor indicate a somewhat different mechanistic route. In their study of allylthioureas and acetyl chloride, it was found that acylation initially occurred at the sulphur atom of the thiourea and not at the nitrogen as may be expected. This resulted in the formation of a hydrogen chloride salt of an *S*-substituted *pseudo*-thiourea.³⁰ It was found that the hydrogen chloride could be readily removed followed by heating which resulted in the transfer of the acyl group from the sulphur atom to the nitrogen atom, thus giving the desired product.³¹ This can be better understood by taking into account that the derivatised thiourea can exist in the form of a thiol (analogous to keto-enol tautomerism). This is illustrated in Scheme 3.

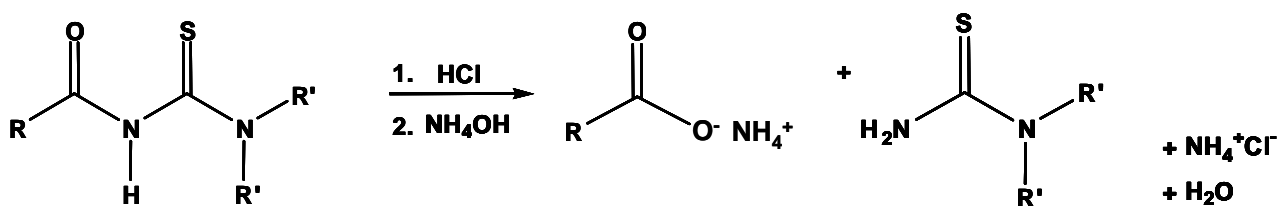


Scheme 3 Reaction mechanism of Dixon and Taylor method. Reaction occurs via acylation at the sulphur atom (*pseudo*-thiourea formation), leading to the formation of the desired *N,N*-dialkyl-*N'*-[4-(pyrene-1-yl)butanoyl]thiourea and *N,N*-dialkyl-*N'*-[pyrene-1-ylacetyl]thiourea derivatives.³¹

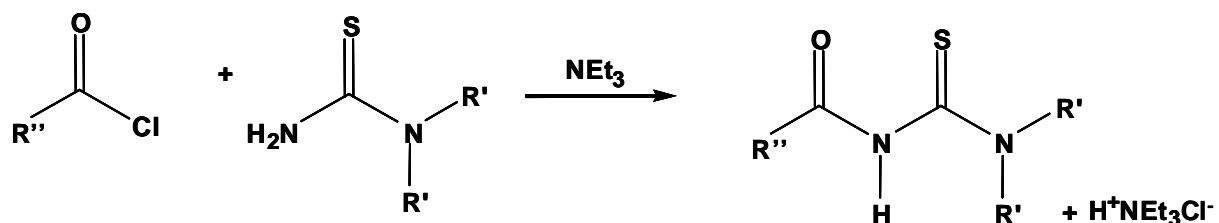
In the interests of simplicity, this method will be referred to as the Dixon and Taylor method in the subsequent sections. The *N,N*-disubstituted thioureas necessary for this procedure were not commercially available and therefore had to be synthesised. A brief examination of the literature yielded a variety of possible methods.^{32,33} Fairfull *et al.*³⁴ have described two methods for the synthesis of *N,N*-disubstituted thioureas. The first reported the use of thiocyanic acid and the appropriate amine to synthesise the *N,N*-disubstituted thiourea, however their alternative procedure involved the acid hydrolysis of an appropriate *N,N*-dialkyl-*N'*-substituted-thiourea and the latter method was followed. Despite the method of Fairfull *et al.* referring to the acid hydrolysis of benzoyl substituted *N,N*-dialkyl-*N'*-aroylthioureas, work subsequent to that of Fairfull *et al.* had shown that the hydrolysis of benzoylthiourea derivatives had given disappointingly low

yields.²⁹ It was for this reason that pivaloyl chloride* was used as a starting reagent as the acid hydrolysis of *N,N*-dialkyl-*N'*-pivaloylthioureas had been found to give satisfactory yields of *N*-substituted thioureas.²⁹ Three pivaloyl derivatives namely *N,N*-diethyl-*N'*-pivaloylthiourea HL⁴, *N*-morpholine-*N'*-pivaloylthiourea HL⁵ and *N,N*-di(2-hydroxyethyl)-*N'*-pivaloylthiourea HL⁶ were therefore synthesised for the purpose of subjecting these compounds to acid hydrolysis to yield the corresponding *N,N*-disubstituted thioureas. An outline of the two step procedure for the synthesis of the *N,N*-dialkyl-*N'*-[4-(pyrene-1-yl)butanoyl]thiourea and *N,N*-dialkyl-*N'*-[pyrene-1-ylacetyl]thiourea derivatives using the Dixon and Taylor method is given in Scheme 4.

Step 1: Acid hydrolysis of an *N,N*-dialkyl-*N'*-pivaloylthiourea to yield an *N,N*-disubstituted thiourea.



Step 2: Reaction of an aroyl halide with an *N,N*-disubstituted thiourea to yield an *N,N*-dialkyl-*N'*-acylthiourea.



R = pivalyl
 R' = alkyl
 R'' = 3-(pyrene-1-yl)propyl
 or pyrene-1-ylmethyl

Scheme 4 Dixon and Taylor method used for the synthesis of *N,N*-dialkyl-*N'*-[4-(pyrene-1-yl)butanoyl]thiourea and *N,N*-dialkyl-*N'*-[pyrene-1-ylacetyl]thiourea derivatives.³⁰

In this procedure all *N,N*-dialkyl-*N'*-pivaloylthioureas were synthesised in high yield according to the method of Douglass and Dains previously described. The subsequent hydrolysis of these ligands proceeded by heating the compounds with concentrated HCl for 3½ - 4 hours. The solution was cooled to room temperature and *carefully* neutralised by addition of 25% ammonium hydroxide solution. Numerous chloroform extractions and *in vacuo* removal of the solvent afforded the *N,N*-disubstituted thioureas in 80% yield. In the following stage of the synthesis the aroyl halide was dissolved in anhydrous acetone and an acetone solution

* Alternative nomenclature = 2,2-Dimethylpropanoyl chloride.

of the *N*-substituted thiourea and triethylamine was added dropwise. The solution was refluxed for 45 minutes and allowed to cool to room temperature, after which it was poured into a small volume of water. Gradual volatilisation of the acetone allowed the precipitation of single products and once again where the products were oils, these were extracted into chloroform and separated and purified by column chromatography (further synthetic details are given in Chapter 5).

2.2.2 Results and Discussion

2.2.2.1 Douglass and Dains method¹

The Douglass and Dains method proved successful in synthesising all the *N,N*-dialkyl-*N'*-pivaloylthiourea and *N,N*-dialkyl-*N'*-9-anthracoylthiourea derivatives. Table 2 shows the compounds synthesised using this method and includes their melting points and percentage yields. ¹³C and ¹H NMR chemical shifts as well as other details of their characterisation are included in Chapter 5 for all these compounds and a detailed discussion of the NMR spectra of the *N,N*-dialkyl-*N'*-9-anthracoylthiourea derivatives as well as X-ray analysis of *N,N*-diethyl-*N'*-9-anthracoylthiourea, *N*-morpholine-*N'*-9-anthracoylthiourea, *N,N*-di(2-hydroxyethyl)-*N'*-9-anthracoylthiourea and *N,N*-di(2-hydroxyethyl)-*N'*-pivaloylthiourea are given later in this chapter (Sections 2.2.3 and 2.2.4 respectively). Whilst the other details of characterisation are discussed further at the end of this chapter, the variation in melting points of these compounds deserves some attention at this point. While the melting points of *N,N*-diethyl-*N'*-9-anthracoylthiourea and *N,N*-di(2-hydroxyethyl)-*N'*-9-anthracoylthiourea are comparable, that of *N*-morpholine-*N'*-9-anthracoylthiourea is noticeably higher. This would imply that the intermolecular solid state interactions of the first two derivatives are of comparable strength, but that the morpholine derivative exhibits stronger intermolecular interactions in the crystalline state. The melting points of the pivaloyl derivatives show a different trend to those of the *N,N*-dialkyl-*N'*-9-anthracoylthiourea derivatives on variation of the amine substituent. In this series of ligands, the morpholine and di(2-hydroxyethyl)amine derivatives have comparable melting points, these being higher than that of the diethylamine analogue. As an oxygen donor atom is present in both *N*-morpholine-*N'*-pivaloylthiourea and *N,N*-di(2-hydroxyethyl)-*N'*-pivaloylthiourea, it is tempting to speculate on the possibility of hydrogen bonding in the crystalline state leading to the increased melting points. The solid state interactions of the *N,N*-dialkyl-*N'*-9-anthracoylthiourea derivatives as well as *N,N*-di(2-hydroxyethyl)-*N'*-pivaloylthiourea will be returned to at the end of this chapter (section 2.2.4).

Table 2* Compounds synthesised using Douglass and Dains method.

Compound	Structure	m.p. (°C)	Yield (%)
<i>N,N</i> -diethyl- <i>N'</i> -9-anthracoylthiourea (HL ¹)		157.5-160.3	86
<i>N</i> -morpholine- <i>N'</i> -9-anthracoylthiourea (HL ²)		181.2-183.6	79
<i>N,N</i> -di(2-hydroxyethyl)- <i>N'</i> -9-anthracoylthiourea (HL ³)		152.8-155.0	56
<i>N,N</i> -diethyl- <i>N'</i> -pivaloylthiourea (HL ⁴)		91.4-92.8	80
<i>N</i> -morpholine- <i>N'</i> -pivaloylthiourea (HL ⁵)		134.2-136.2	74

*

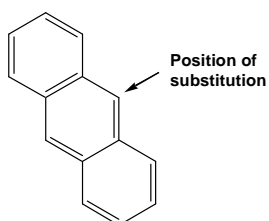
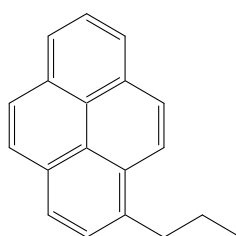
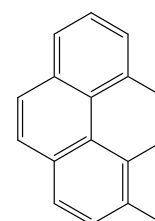
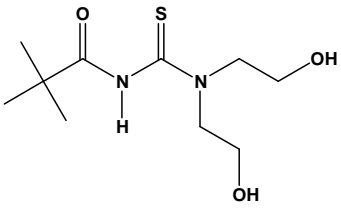
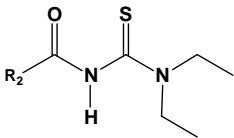
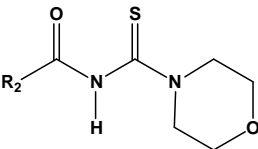
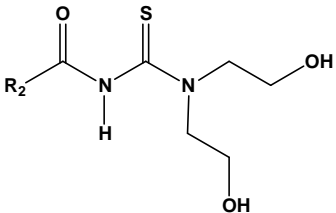
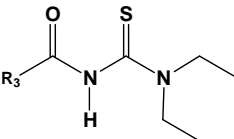
Where R₁ refersR₂ refers toand R₃ refers to

Table 2 contd. Compounds synthesised using Douglass and Dains method.

<i>N,N</i> -di(2-hydroxyethyl)- <i>N'</i> -pivaloylthiourea (HL ⁶)		137.9-141.5	65
<i>N,N</i> -diethyl- <i>N'</i> -[4-(pyrene-1-yl)butanoyl]thiourea (HL ⁷)		142.1-143.5	30
<i>N</i> -morpholine- <i>N'</i> -[4-(pyrene-1-yl)butanoyl]thiourea (HL ⁸)		161.6-163.0	3% yield of thiourea and 16% yield of amide
<i>N,N</i> -di(2-hydroxyethyl)- <i>N'</i> -[4-(pyrene-1-yl)butanoyl]thiourea (HL ⁹)		-	poor yield and mixture with no suitable elution system
<i>N,N</i> -diethyl- <i>N'</i> -[pyrene-1-ylacetyl]thiourea (HL ¹⁰)		141.7-142.5	poor yield and mixture with no suitable elution system

In the following sections the *N,N*-dialkyl-*N'*-[4-(pyrene-1-yl)butanoyl]thiourea and *N,N*-dialkyl-*N'*-[pyrene-1-ylacetyl]thiourea derivatives will be referred to as the pyrenebutanoylthiourea and pyreneacetylthiourea derivatives respectively; the *N,N*-dialkyl-*N'*-9-anthracoylthiourea derivatives will be referred to as the anthracoylthiourea derivatives.

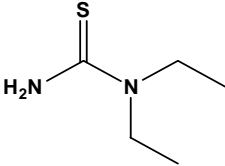
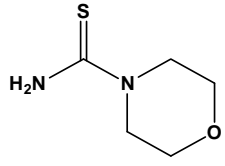
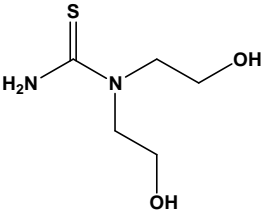
2.2.2.2 Synthesis of *N*-substituted thioureas

As is apparent from the percentage yields given in Table 2, the Douglass and Dains procedure was not particularly successful for the synthesis of the pyrenebutanoylthiourea or the pyreneacetylthiourea derivatives. In particular it was unfortunate that no suitable elution system for column chromatography (silica gel) could be found for the separation of *N,N*-di(2-hydroxyethyl)-*N'*-[4-(pyrene-1-yl)butanoyl]thiourea (HL⁹), and *N,N*-diethyl-*N'*-[pyrene-1-ylacetyl]thiourea (HL¹⁰) as this prohibited the isolation of pure compounds

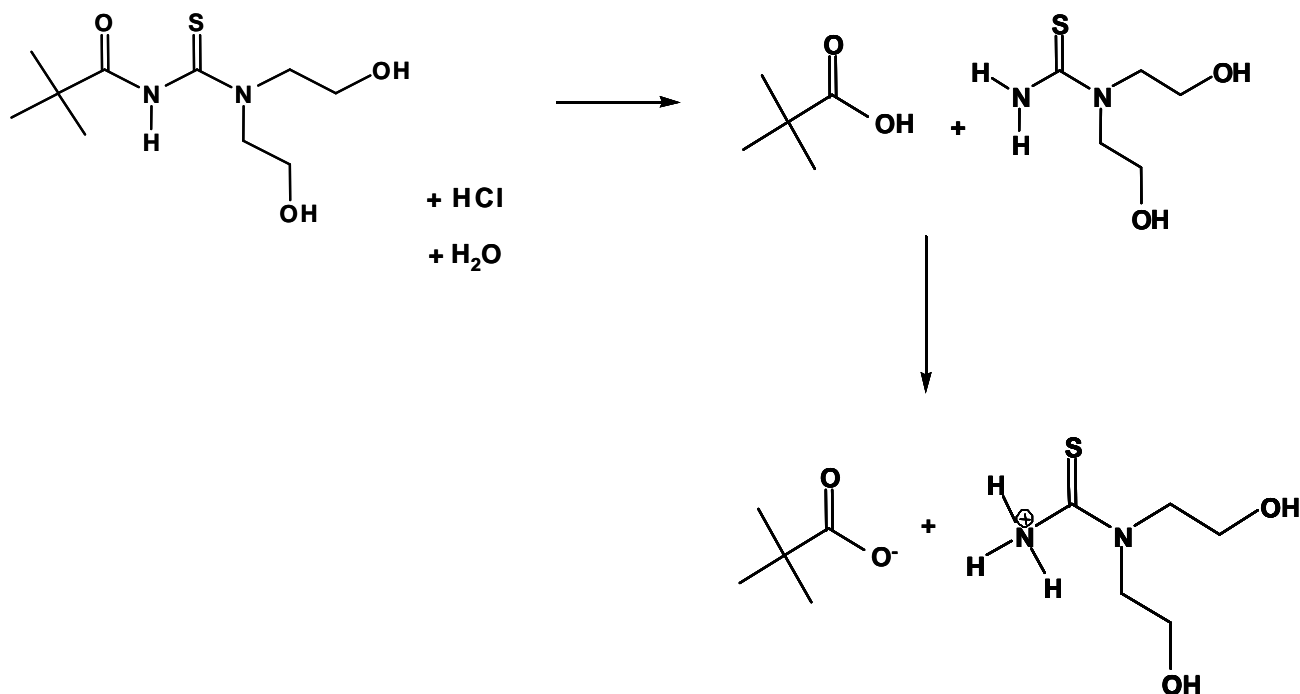
using this method. In these and other cases where no suitable elution system could be found, accurate percentage yields could obviously not be calculated for these compounds and therefore only a qualitative indication of the success of the method could be given. The inability to separate HL⁹ and HL¹⁰ chromatographically and the poor yields obtained for *N,N*-diethyl-*N'*-[4-(pyrene-1-yl)butanoyl]thiourea (HL⁷) and *N*-morpholine-*N'*-[4-(pyrene-1-yl)butanoyl]thiourea (HL⁸) led to the use of the “modified” Douglass and Dains method as well as the Dixon and Taylor method, which were then used to synthesise the pyrenebutanoylthiourea and pyreneacetylthiourea derivatives in an attempt to obtain higher yields of these compounds. However, before these compounds could be synthesised using the Dixon and Taylor method, the derivatised thioureas, *N,N*-diethylthiourea, *N*-morpholinethiourea and *N,N*-di(2-hydroxyethyl)thiourea had to be synthesised from the acid hydrolysis of their corresponding *N,N*-dialkyl-*N'*-pivaloylthiourea derivatives.

Acid hydrolysis of both *N,N*-diethyl-*N'*-pivaloylthiourea (HL⁴) and *N*-morpholine-*N'*-pivaloylthiourea (HL⁵) gave solid products identified to be *N,N*-diethylthiourea and *N*-morpholinethiourea respectively, however hydrolysis of *N,N*-di(2-hydroxyethyl)-*N'*-pivaloylthiourea (HL⁶) gave a slightly viscous liquid as a product, the nature of which will be discussed shortly. The results are summarised in Table 3 and the melting points and yields have been included. ¹³C and ¹H NMR chemical shifts as well as other details of characterisation for these compounds are included in Chapter 5. As is evident from Table 3, the synthesis of *N,N*-diethylthiourea and *N*-morpholinethiourea gave very satisfactory yields, however this was not true for *N,N*-di(2-hydroxyethyl)thiourea. NMR analysis of this liquid product suggested the formation of a type of ionic liquid. This seems feasible if the scheme below (Scheme 5) is considered.

Table 3 Yields of *N*-substituted thioureas.

Compound	Structure	m.p. (°C)	Yield (%)
<i>N,N</i> -diethylthiourea		101.8-102.9	91
<i>N</i> -morpholinethiourea		175.2-177.1	80
<i>N,N</i> -di(2-hydroxyethyl)thiourea		-	-

Acid hydrolysis of the ligand leads to the formation of pivalic acid and the desired *N,N*-di(2-hydroxyethyl)thiourea. Transfer of the acid proton to the primary NH_2 group seems feasible. This leads to the possible formation of an ionic liquid.



Scheme 5 Acid hydrolysis of *N,N*-di(2-hydroxyethyl)thiourea resulting in the possible formation of an ionic liquid.

The isolation of *N,N*-di(2-hydroxyethyl)thiourea was therefore not possible and thus the synthesis of *N,N*-di(2-hydroxyethyl)-*N'*-[4-(pyrene-1-yl)butanoyl]thiourea (HL^{10}) using the Dixon and Taylor method was not attempted.

2.2.2.3 “Modified” Douglass and Dains method¹² and Dixon and Taylor method³¹

Despite the synthesis of HL^{10} not being possible using the Dixon and Taylor method, the remaining pyrenebutanoylthiourea and pyreneacetylthiourea derivatives were synthesised using both the modified Douglass and Dains, and Dixon and Taylor methods. The results are summarised in Table 4 and the structures of the compounds as well as the melting points have been included. Only on rare occasions were solid products formed, the majority of cases resulting in oil formation and a mixture of products. Suitable elution solvents for column chromatography (silica gel) could be found for the *N,N*-diethyl-*N'*-[4-(pyrene-1-yl)butanoyl]thiourea and *N*-morpholine-*N'*-[4-(pyrene-1-yl)butanoyl]thiourea ligands enabling their separation and purification. However, successive chromatography was needed in some cases to achieve a pure product and this resulted in the final yields obtained being very low.

The “modified” Douglass and Dains synthesis of *N,N*-di(2-hydroxyethyl)-*N'*-[4-(pyrene-1-yl)butanoyl]thiourea proved particularly problematic as no suitable elution system could be found for this compound. A pure sample of this compound could therefore not be isolated as the synthesis using the Dixon and Taylor method was also not possible. The yield of *N,N*-diethyl-*N'*-[pyrene-1-ylacetyl]thiourea (HL¹⁰), while being only fair for the “modified” Douglass and Dains method, was greatly improved using the Dixon and Taylor method. As previously mentioned, ¹³C and ¹H NMR chemical shifts as well as other details of the characterisation for these compounds are included in Chapter 5 and a detailed discussion of the NMR spectra of these compounds follows at the end of this chapter as well as the X-ray analysis of *N,N*-diethyl-*N'*-[4-(pyrene-1-yl)butanoyl]thiourea (HL⁷) and *N*-morpholine-*N'*-[4-(pyrene-1-yl)butanoyl]thiourea (HL⁸).

As for the anthracoylthiourea and pivaloylthiourea derivatives, the melting points of the pyrenebutanoylthiourea and pyreneacetylthiourea derivatised compounds in Table 4 deserve some comment. The two diethylamine derivatives, HL⁷ and HL¹⁰, exhibit surprisingly similar melting points indicating analogous intermolecular interactions in the solid state, while that of *N*-morpholine-*N'*-[4-(pyrene-1-yl)butanoyl]thiourea (HL⁸) is slightly higher reflecting the trend observed in the case of the anthracoylthiourea and pivaloylthiourea derivatives. Once again it is tempting to speculate on the possibility of hydrogen bonding in the crystalline state leading to the increased melting point of HL⁸. The solid state interactions of this compound as well as those of HL⁷ will be returned to at the end of this chapter.

Table 4 Yields of pyrenebutanoylthiourea and pyreneacetylthiourea derivatives obtained using the “modified” Douglass and Dains, and Dixon and Taylor methods.

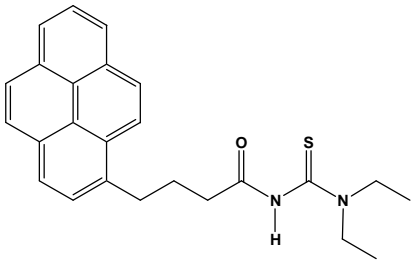
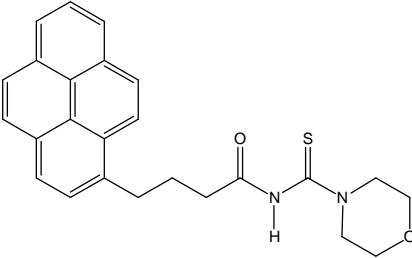
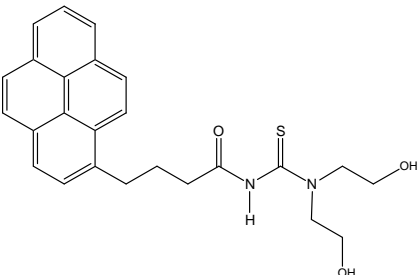
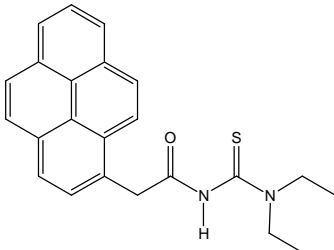
Compound	Structure	m.p. (°C)	Yield (%) from Modified Douglass and Dains Method	Yield (%) from Dixon and Taylor Method
<i>N,N</i> -diethyl- <i>N'</i> -[4-(pyrene-1-yl)butanoyl]thiourea (HL ⁷)		142.1- 143.5	90	40
<i>N</i> -morpholine- <i>N'</i> -[4-(pyrene-1-yl)butanoyl]thiourea (HL ⁸)		161.6- 163.0	9% yield of thiourea and 13% yield of amide	22

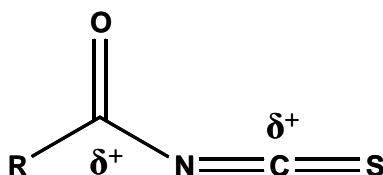
Table 4 contd. Yields of pyrenebutanoylthiourea and pyreneacetylthiourea derivatives obtained using the “modified” Douglass and Dains, and Dixon and Taylor methods.

<p><i>N,N</i>-di(2-hydroxyethyl)-<i>N'</i>-[4-(pyrene-1-yl)butanoyl]thiourea (HL⁹)</p>		-	-	Not possible
<p><i>N,N</i>-diethyl-<i>N'</i>-[pyrene-1-ylacetyl]thiourea (HL¹⁰)</p>		141.7-142.5	fair yield and mixture with no suitable elution system	60

During the course of the following discussion, in the interests of simplicity, the substituent on the carbonyl carbon will be referred to as the carbonyl substituent and that on the thiocarbonyl carbon as the thiocarbonyl substituent.

From the different yields obtained for the various compounds synthesised using the same Douglass and Dains procedure (Table 2), it is apparent that alteration of the carbonyl and thiocarbonyl substituents influences the amount of *N,N*-dialkyl-*N'*-aroylthiourea formed. This is evident as there is a marked difference in the yields of the anthracoylthiourea and pyrenebutanoylthiourea derivatives. This is largely because the one is essentially an aroyl substituent (anthracoyl) and the other an acyl substituent (1-pyrenebutanoyl). The many factors involved in the successful synthesis of these two classes of compounds have previously been discussed in detail²⁹ and several factors of relevance will be outlined here.

In the Douglass and Dains procedure the reaction of the acyl halide and potassium thiocyanate leads to the formation of the isothiocyanate intermediate. This moiety essentially has two electrophilic centers (Figure 11), the carbonyl and the isothiocyanate carbon atoms.

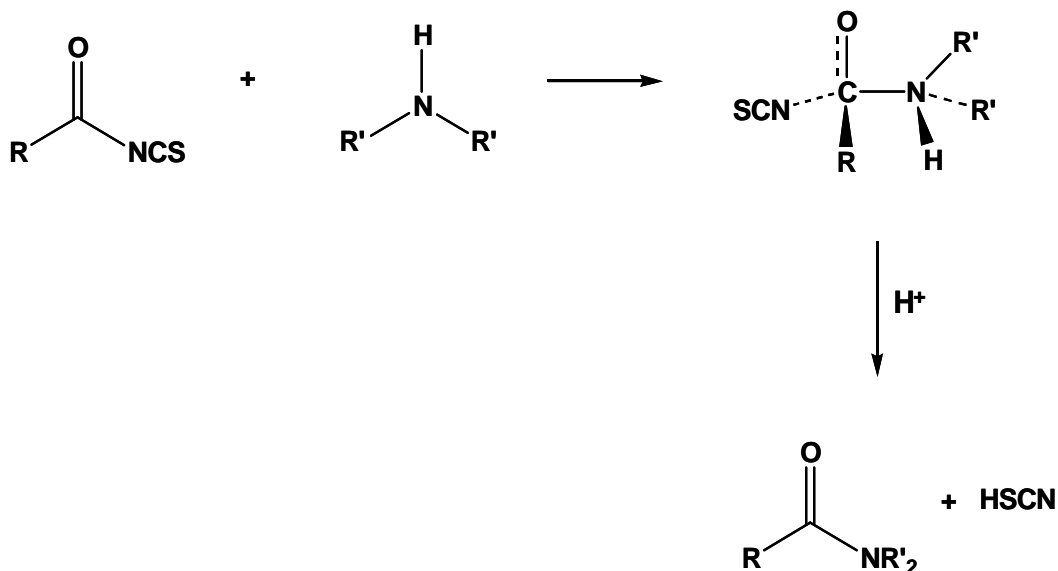
**Figure 11** Two electrophilic centers of isothiocyanate intermediate.

Nucleophilic attack by the amine can therefore lead to the formation of two different products: an *N*-substituted amide from attack at the carbonyl carbon and the addition product (attack at the thiocarbonyl carbon) leading to the desired acylthiourea. The latter reaction reportedly occurs preferentially in non-polar solvents.³⁵ The nature of attack at these two centres will be discussed first followed by the influence the nature of the attacking amine has on the outcome of the reaction.

2.2.2.4 Nature of the competing electrophilic centres

Where “hardness” is understood in terms of small atomic radius, high effective nuclear charge, low polarisability and low ease of oxidation,³⁶ amines can be thought of as being hard bases. Both carbonyl and thiocarbonyl carbons have been described as being hard acids, the thiocarbonyl being the softer of the two. The preferential site of nucleophilic attack would therefore appear to be the carbonyl carbon and it is interesting therefore that the acylthiourea product forms at all. However, the sp hybridisation of the thiocarbonyl carbon as well as the close proximity of the nitrogen atom are both factors which can be thought of as increasing the hardness of this centre.

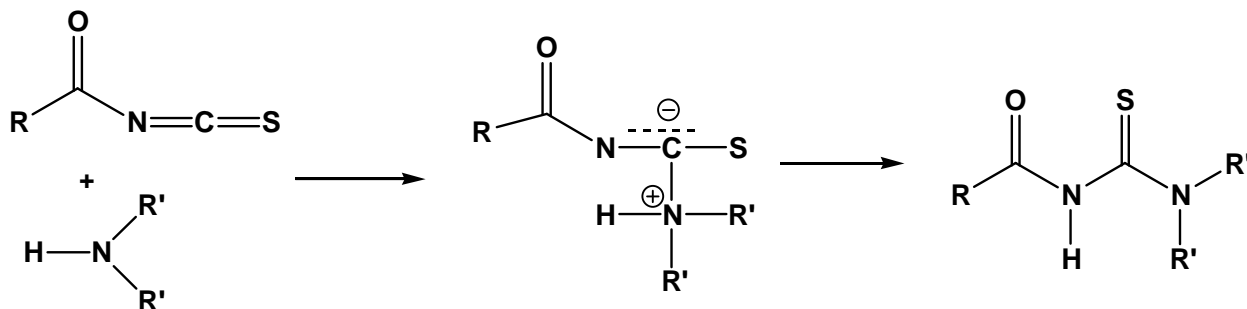
A closer look at the mechanism of amide formation shows that attack by the amine on the carbonyl carbon occurs via the formation of a tetrahedral intermediate (Scheme 6) in which both the carbonyl carbon and nitrogen atoms become sp^3 hybridised. This leads to the formation of a rather crowded transition state depending on the nature of the carbonyl and thiocarbonyl substituents.



Scheme 6 Nucleophilic attack at the carbonyl carbon leading to amide formation, *via* a tetrahedral intermediate.

In work done by Williams and Jencks³⁷ and others³⁸ the mechanism of amine addition to the isothiocyanate moiety is thought to occur via a trigonal zwitterionic intermediate (Scheme 7). In this species, the thiocarbonyl carbon becomes sp^2 hybridised and there is generally less congestion relative to the corresponding tetrahedral intermediate previously discussed (Scheme 6). Proton transfer from the amine

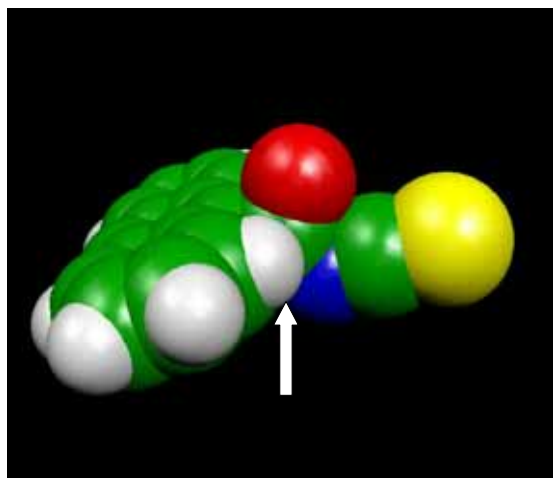
nitrogen to that of the isothiocyanate results in the formation of the *N,N*-dialkyl-*N'*-acylthiourea ligand as a product.



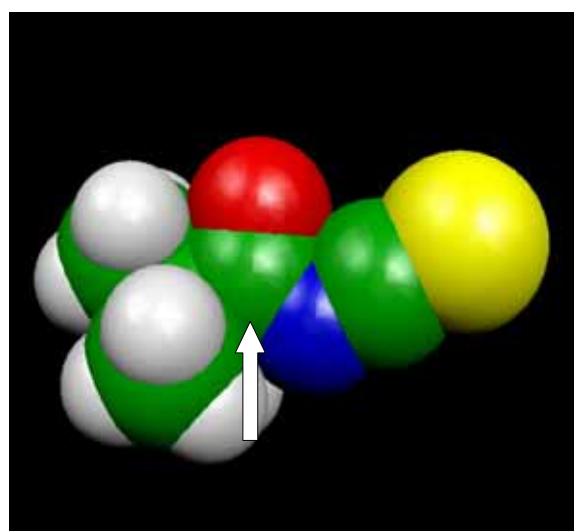
Scheme 7 Nucleophilic attack at the thiocarbonyl carbon leading to acylthiourea formation, *via* a trigonal zwitterionic intermediate.

Elmore and Ogle³⁵ stated that aroyl isothiocyanates with bulky substituents in the ortho positions, may react preferentially at the thiocarbonyl carbon atom due to steric retardation of nucleophilic substitution and this indeed appears to be the case. Where the substituent on this carbon was bulky, in the case of the pivaloyl or anthracene group, no significant amounts of amide were formed, and where the pyrene moiety was separated by a three carbon spacer from the carbonyl carbon atom, giving rise to a less sterically crowded electrophilic centre, there was significant amide formation. This may be illustrated in the derivatised isothiocyanate space filled models below, where it is clearly apparent that the anthracoyl and pivaloyl moieties lead to extensive congestion at the carbonyl carbon, as shown in Figure 12.* In these structures carbon atoms are indicated in green, oxygen atoms in red, nitrogen atoms in blue, sulphur atoms in yellow and hydrogen atoms in white.

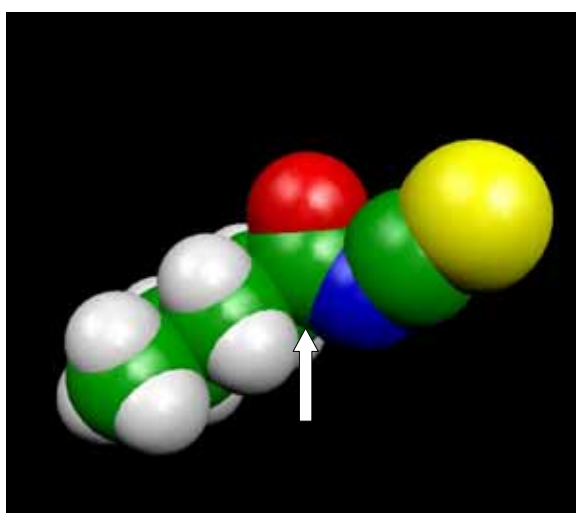
* These structures were plotted using MOLEKEL* and only serve as a graphical representation of the steric considerations described in the text.



Space filled model of anthracoylisothiocyanate



Space filled model of pivaloylisothiocyanate



Space filled model of butanoylisothiocyanate - the pyrenyl moiety has been excluded for clarity.

Figure 12 Space filled models of selected isothiocyanates illustrating steric congestion at the carbonyl carbon atom (white arrows).

This observation is limited however to attack by morpholine, and is not accurate when applied to comparisons in which the diethylamine was the attacking nucleophile, the nature of the amine therefore also plays a role.

2.2.2.5 Nature of the nucleophilic amine

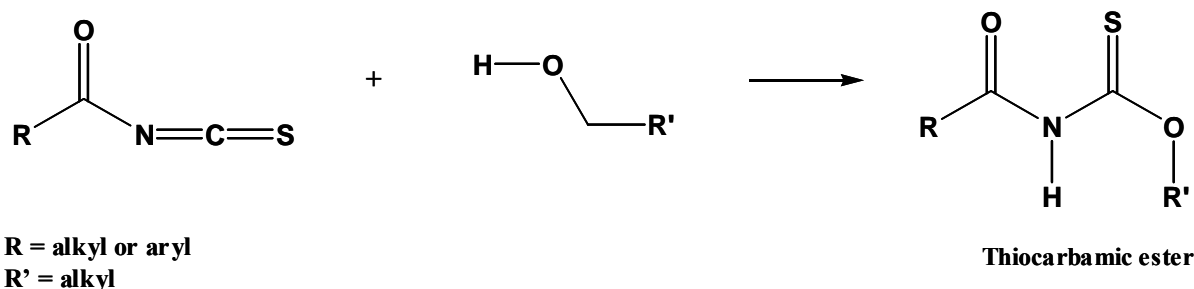
The reactions between isothiocyanates and amines have been investigated and the basic strength of the attacking nucleophile is found to have an influence on the rate of the reaction.³⁸ As previously alluded to, a stepwise mechanism of addition between these two species is thought to take place, *i.e.* initial amine attack followed by proton transfer from the amine nitrogen to that of the isothiocyanate species resulting in product formation (Scheme 7). Work done by Satchell *et al.*³⁸ confirmed that previously found by Williams and Jencks, where it was suggested that the reaction with strong amine nucleophiles was found to be first order with respect to amine concentration and weaker nucleophiles exhibited partially second order reactions.³⁷ The rate determining step changing from amine attack (for nucleophilic amines) to proton transfer (for weaker nucleophiles). A brief investigation of the effects of acid-base catalysis suggested that a catalytic effect was only observed for weak nucleophiles where proton transfer is rate determining. Nucleophilicity is comparable to basicity for 1° and 2° amines.

Secondary amines are generally regarded as being more basic than primary amines, however both diethylamine and morpholine have comparable basic strength (pK_a 10.98, 8.36 respectively).³⁹ The answer for the differing reactivity must therefore once again lie in steric considerations, and indeed this appears to be the case. Satchell³⁸ observed that bulky substituents at either the isocyanate or amine, will decrease the rate of the reaction and while this was said in reference to amine attack on isocyanates, the reactions of isocyanates and isothiocyanates are mechanistically very similar and it can therefore be thought to hold true for isothiocyanate systems such as ours.⁴⁰ Hanna *et al.* also reported that within a series of primary amines, it was the least branched amines that reacted most rapidly.⁴¹

A closer look at the geometry of diethylamine and morpholine reveals some interesting differences. Morpholine, a cyclic amine, has the methylene groups attached to the nitrogen held well away from this atom, enabling the nitrogen lone pairs to be at the molecular apex of the molecule and therefore more exposed. In the case of the diethylamine the nitrogen atom lies in the plane of the neighbouring methylene groups and the molecule is essentially linear, resulting in the available electrons being relatively more shielded with respect to nucleophilic attack.

Nucleophilic attack at the carbonyl carbon can therefore occur more readily in the case of the morpholine resulting in amide formation presumably because of reduced steric hindrance, whereas attack by the diethylamine is likely to be favoured at the thiocarbonyl carbon as there would otherwise be excessive congestion during the formation of the intermediate.

The above discussion has largely been in terms of diethylamine and morpholine, not di(2-hydroxyethyl)amine. Whilst all the considerations are applicable to this amine, the overriding reason for the consistently lower yields of desired acylthiourea obtained with this amine may be due to the fact that both nitrogen and oxygen atoms can be seen as potential nucleophiles. Nucleophilic attack by the OH group is therefore possible leading to the formation of thiocarbamic esters, as shown below (Scheme 8). Competing formation of the acylthiourea and thiocarbamic ester would thus explain the lower yields obtained with di(2-hydroxyethyl)amine.



Scheme 8 Nucleophilic attack by an alcohol resulting in thiocarbamate formation.

Before discussion of the Douglass and Dains method can be concluded, the difference in success between the two procedures used must first be examined.

The difference between the “modified” Douglass and Dains and Douglass and Dains procedures consisted of the order in which the aroyl acid and potassium thiocyanate were combined, length of reaction time, removal of KCl and the addition of a mineral acid prior to acetone volatilisation, without the addition of water. Essentially therefore these two procedures were the same and it would appear that the reason for the differing successes lie in practical considerations rather than mechanistic ones.

The synthetic procedure described by Dixon and Taylor avoided the competing reactions at the two electrophilic centers of the isothiocyanate intermediates and this was reflected in the improved yields of the pyrenebutanoylthiourea and pyreneacetylthiourea derivatives. This was also the first method where reasonable amounts of *N*-morpholine-*N'*-[4-(pyrene-1-yl)butanoyl]thiourea (HL⁸) were formed. It also gave the best results for the pyreneacetylthiourea derivative (HL¹⁰), however this is not necessarily due to a reflection on reactivity, but rather the formation of different by-products which enabled the efficient chromatographic separation of the product, *N,N*-diethyl-*N'*-[pyrene-1-ylacetyl]thiourea (HL¹⁰), this not previously having been possible.

The remainder of this chapter will focus on the detailed characterisation of the potentially fluorescent ligands synthesised *i.e.* the anthracoylthiourea, pyrenebutanoylthiourea and pyreneacetylthiourea derivatives. The NMR spectra of the compounds will be discussed followed by the X-ray analysis of selected compounds. The crystal structure of *N,N*-di(2-hydroxyethyl)-*N'*-pivaloylthiourea (HL⁶), though not strictly speaking a potentially fluorescent ligand, will be included in this section.

2.2.3 Characterisation of potentially fluorescent ligands by means of ^1H and ^{13}C NMR spectroscopy

Interest in the ^1H and ^{13}C NMR assignments of polycyclic aromatic hydrocarbons has largely been motivated by the carcinogenic nature of these compounds and attempts have been made to determine whether a correlation exists between the electronic structure and carcinogenic activity.^{42,43} The assignment of these complex aromatic systems was made using a variety of different methods prior to the availability of 1D and 2D FT NMR techniques. These included deuterium substitution⁴² which had the effect of reducing the intensity of the substituted carbons in the ^{13}C spectrum and thus aiding in assignment; the use of coupling constants;^{44,45,46} and ^{13}C labelling techniques.^{47,48,49} In particular Klaasen *et al.*⁵⁰ developed a method of ^{13}C labelling for benzo[α]pyrene and its derivatives which enabled the assignment of four carbon positions in this aromatic system. Changes in chemical shifts due to substituents has been used extensively for assignment purposes.^{51,52,53} This has included examining the nitration products of pyrene⁵⁴ and ^{13}C carboxy labelled acid derivatives.⁴⁵

As we had synthesised a range of anthracene and pyrene derivatives and with the availability of a high field spectrometer, we were presented with an ideal opportunity to attempt a full assignment of the carbon and proton NMR spectra of these systems and to look at the effect, if any, that altering the substituents has on the carbon and proton resonances of the aromatic systems.

2.2.3.1 ^1H and ^{13}C NMR spectra of N,N -dialkyl- N' -9-anthracoylthiourea derivatives

Table 5 shows the assigned proton shifts of the derivatised anthracene compounds investigated and Table 6 gives the corresponding ^{13}C shifts. The unsubstituted anthracene is included in both tables as a reference.⁴² The numbering scheme shown in Figure 13 was used for the assignments. The full proton assignments of N,N -di(2-hydroxyethyl)- N' -9-anthracoylthiourea (HL³) are not shown in Table 5, but are discussed further on in this section.

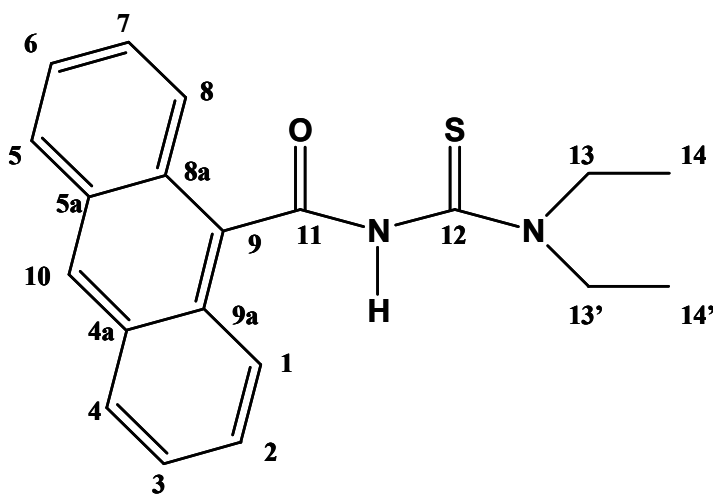


Figure 13 Numbering scheme used for N,N -dialkyl- N' -9-anthracoylthiourea derivatives.

Table 5 ¹H NMR chemical shifts (in ppm) of *N,N*-dialkyl-*N'*-9-anthracoylthiourea derivatives (25°C, CDCl₃).*

Compound	H1+H8	H2+H7	H3+H6	H4+H5	H10	N-H	H13+ H13'	H14+H14'
Anthracene ⁴²	8.02	7.48	7.48	8.02	8.44	-	-	-
9-anthracene carboxylic acid	8.22	7.50	7.42	7.95	8.49	-	-	-
9-anthracoyl chloride	8.13	7.62	7.52	8.02	8.49	-	-	-
HL¹	8.12	7.57	7.49	7.99	8.49	8.12	4.20/3.99	1.45
HL²	8.03	7.57	7.49	7.99	8.50	8.54	3.90	3.90
HL^{3†}	8.19	7.66	7.59	8.16	8.78	11.23	3.83/3.75	4.07/3.98

Despite ¹H and ¹³C chemical shifts for both anthracene and 9-anthracenecarboxylic acid being available in the literature, these two compounds were analysed with 2D NMR techniques in order to confirm the assignments. In most cases the chemical shift values obtained compared very well with those reported in the literature for similar solvents.

*

HL¹ (*N,N*-diethyl-*N'*-9-anthracoylthiourea)

HL² (*N*-morpholine-*N'*-9-anthracoylthiourea)

HL³ (*N,N*-dihydroxyethyl-*N'*-9-anthracoylthiourea)

† This compound was not sufficiently soluble in chloroform and the spectra were therefore obtained in DMSO-*d*₆.

Chapter 2: Synthesis and detailed characterisation of potentially fluorescent ligands.

Table 6 ^{13}C NMR chemical shifts (in ppm) of *N,N*-dialkyl-*N'*-9-anthracoylthiourea derivatives (25°C, CDCl_3).

Compound	C1+C8	C2+C7	C3+C6	C4+C5	C4a+C5a	C8a+C9a	C9	C10	C11	C12	C13	C14
Anthracene ⁴²	128.30	125.20	125.20	128.30	131.60	131.60	126.10	126.10	-	-	-	-
9-anthracene carboxylic acid	125.28	127.49	125.71	128.86	131.14	128.86	126.21	130.49	172.53	-	-	-
9-anthracoyl chloride	123.87	127.90	125.84	128.73	130.63/ 130.61	126.12	131.59	130.63/ 130.61	170.51	-	-	-
HL ¹	124.35	127.37	125.61	128.68	130.87	128.16	129.45	129.40	166.22	178.28	48.16/ 48.15	13.49/ 11.50
HL ²	124.31	127.68	125.80	128.94	130.98	128.27	129.07	129.87	165.75	178.62	52.89/ 51.73	66.21
HL ^{3*}	125.19	127.36	126.13	128.99	131.06	128.09	131.65	128.62	167.25	180.74	55.41/ 55.26	59.26/ 57.43

* This compound was not sufficiently soluble in chloroform and the spectra were therefore obtained in $\text{DMSO}-d_6$.

The assignment of anthracene was relatively simple as was that of 9-anthracenecarboxylic acid, however the latter will briefly be discussed here. The assignments of 9-anthracenecarboxylic acid were done using GHSQC and GHMQC spectra showing single and multiple bond carbon-hydrogen correlations respectively. The latter spectrum is shown in Figure 15. Identification of H10 is obvious as the only singlet proton resonance and the multiple bond correlation with a carbon resonance at 128.86 ppm enabled the assignment of this resonance as C4. The single bond correlation of H10 with a carbon resonance at 130.49 ppm in the GHSQC spectrum (not shown here), enabling the assignment of C10. The multiple bond correlation of C4 with one of the triplet proton resonances at 7.50 ppm enabled the assignment of H2, the other triplet resonance being H3. The multiple bond correlation shown by H3 with an upfield carbon resonance at 125.28 ppm being due to the coupling of H3 with C1, hence enabling the assignment of this carbon. The single bond correlation of C1 with the most downfield doublet proton resonance at 8.22 ppm making the assignment of H1 possible, the other doublet resonance necessarily being H4. The multiple bond correlation of H1 with a carbon resonance at 125.71 ppm enabled the assignment of C3. The multiple bond correlation between H4 and a carbon resonance at 127.49 ppm permitted the assignment of C2. Three carbon resonances now remain unassigned, namely C4a, C8a and C9. The multiple bond correlation of H3 with the most downfield carbon resonance at 131.14 ppm enabled the assignment of C4a. The low intensity carbon resonance at 126.21 ppm showing a correlation with H1 was preliminarily assigned as C9. From the multiple bond correlation of the assigned C4 resonance with H4, it became apparent that the remaining quaternary carbon (C8a) must be underneath this resonance at 128.86 ppm however the correlation with H1 exhibited by these two resonances was unexpected as neither C4 nor C8a are expected to couple to H1. This is because the experiment performed to obtain the GHMQC spectrum (Figure 15) was optimised for aromatic $^3J_{C-H}$ couplings as illustrated in Figure 14.

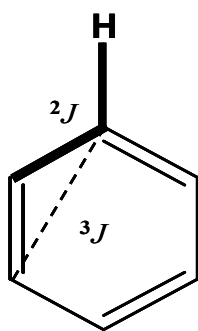


Figure 14 Illustration of $^2J_{C-H}$ and $^3J_{C-H}$ couplings in aromatic systems.

In aromatic molecules $^3J_{C-H}$ couplings are in the order of 7 to 11 Hz while the $^2J_{C-H}$ couplings are significantly smaller. This is in contrast to aliphatic systems where the $^2J_{C-H}$ couplings are in the order of 7 Hz. It was therefore thought that a third resonance lay underneath the C4 resonance, namely that of C9. It was however possible that the correlation with H1 shown by these carbon resonances may have been due to a $^2J_{C-H}$ coupling between C8a and H1, a similar 2J coupling being present between the assigned C4a and H4

leading to the second unexpected correlation indicated in Figure 15. The uncertainty surrounding the assignment of C9 at 126.21 ppm was further supported by this value not comparing well with the reported value¹⁵ for C9 of 9-anthracenecarboxylic acid. A brief examination of the literature however, revealed varying chemical shift values for this carbon atom. In particular, Marshall *et al.* reported a value of 127.1 ppm for C9 in a saturated acetone solution and Schuster reported a value of 129.57 ppm for a 0.2-0.5M chloroform solution while our initial assignment of 126.21 ppm was for a saturated chloroform solution. The difference between our and Marshall's value could be attributed to solvent effects, however Marshall's remaining assignments of the aromatic resonances were all in close agreement with those of Schuster (and ours) and the difference in solvent was therefore not thought to be significant. The chemical shift of the carbonyl resonance (C11) also differed, ours being 172.53 ppm and that of Schuster being 169.89 ppm. It is known that carboxylic acids form dimers by means of hydrogen bonding, these dimers and monomers co-existing in solution with the position of the equilibrium being dependant on concentration, temperature and solvent. Chemical shift changes of several ppm due to effects of the above nature are common.⁵⁵ It is therefore likely that a difference in conditions, concentration being one, may have led to the variation in the chemical shift positions of the carbonyl carbon atom. In an attempt to clarify the assignment of the C9 resonance in particular, a second analysis was performed under the conditions described by Schuster, however the acid was found to be insoluble at the concentrations reported. In conclusion, there is still some uncertainty surrounding the assignment of this resonance, however for the purpose of this discussion the value reported by Schuster will be used.

Chapter 2: Synthesis and detailed characterisation of potentially fluorescent ligands.

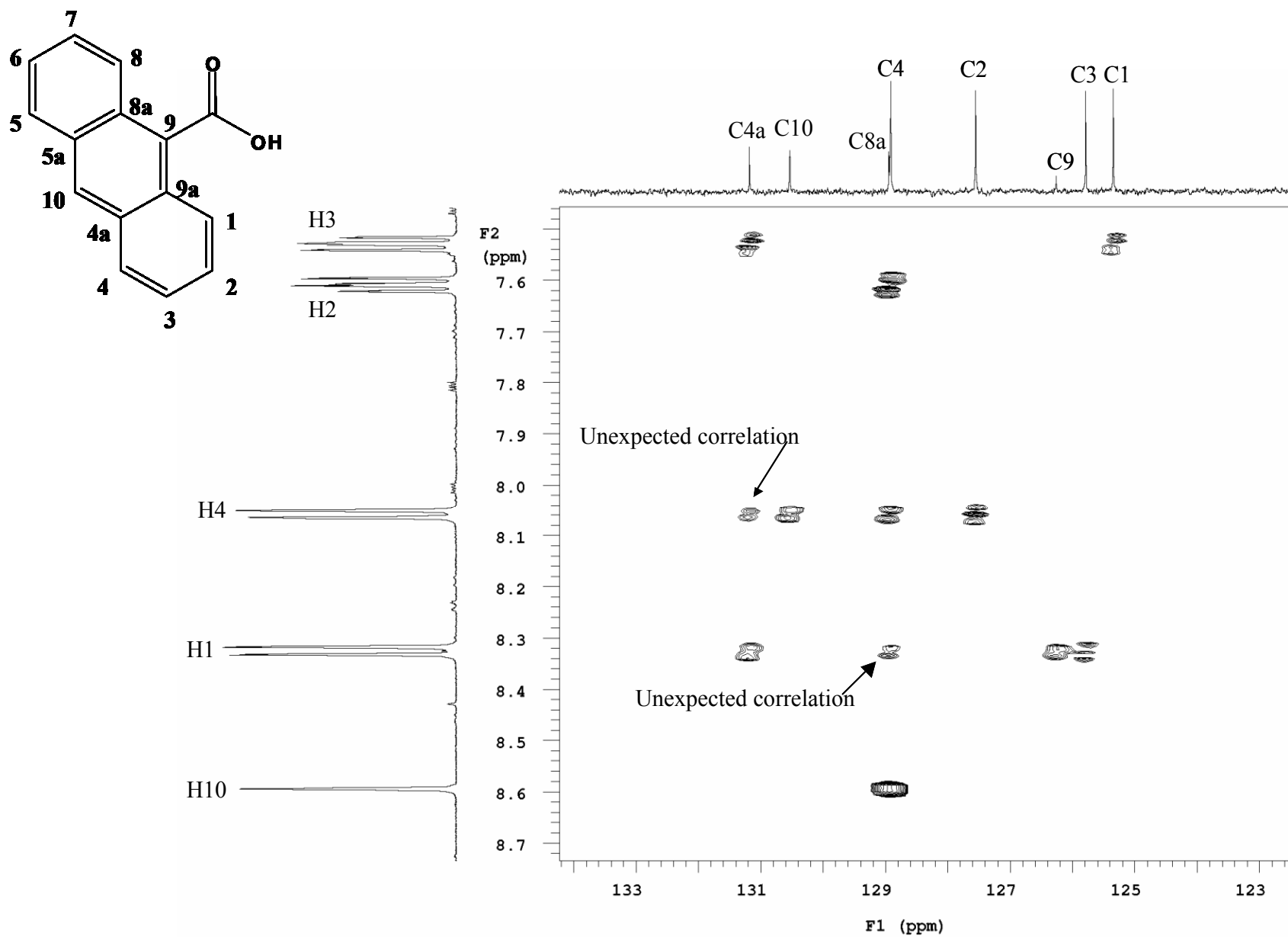
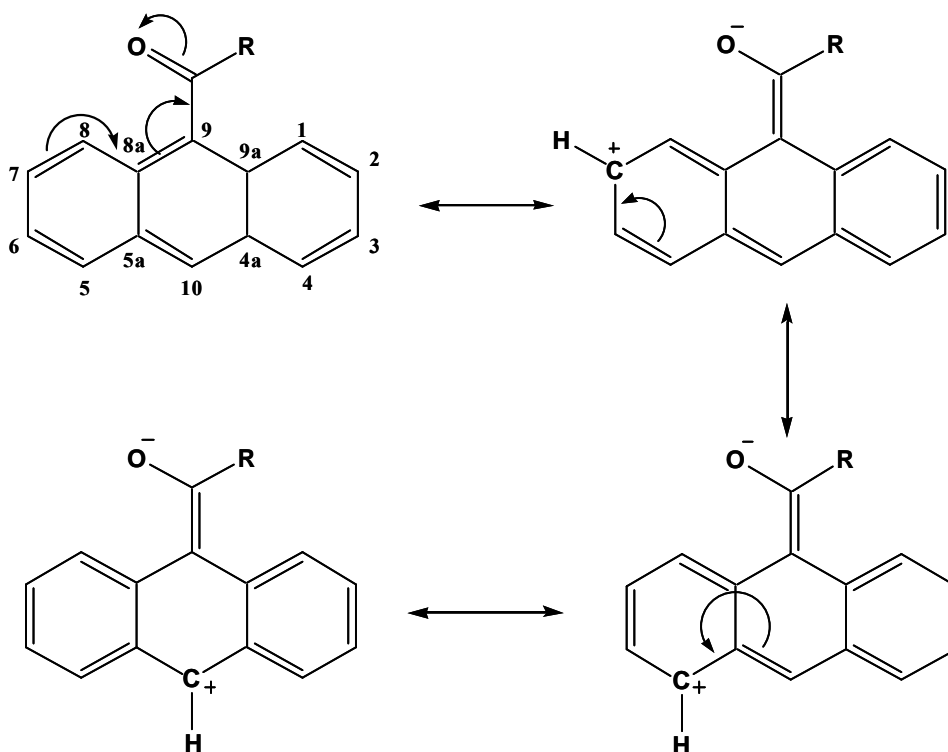


Figure 15 GHMOC 2D spectrum of 9-anthracenecarboxylic acid, showing multiple bond ^{13}C - ^1H correlations and unexpected correlations (25°C, CDCl_3).

A comparison of the ^{13}C chemical shifts of 9-anthracenecarboxylic acid, 9-anthracoyl chloride and HL¹ were made with those of unsubstituted anthracene and the shift differences are given in Table 7. A negative sign indicates an upfield shift, or shielding of the carbon atom and a positive sign indicates a downfield shift of the carbon resonance and deshielding of the carbon atom.

The carbonyl group is formally conjugated with the ring carbons and is therefore expected to exert a significant resonance effect on the fused ring system. The canonical structures are shown in Scheme 9 and result in a decrease in electron density at carbons C2 and C7, C4 and C5 and C10 (symmetry related structures not included).



Scheme 9 Canonical forms of carboxylated *N,N*-dialkyl-*N'*-9-anthracoylthiourea derivatives.

This deshielding effect is observed in the C2 and C7 and C10 resonances for all three the anthracoylthiourea compounds shown in Table 7, however there is little evidence of significant deshielding at C4 and C5 in these compounds.

Chapter 2: Synthesis and detailed characterisation of potentially fluorescent ligands.

Table 7 Difference in ^{13}C NMR chemical shifts (in ppm) of selected compounds relative to anthracene. *

	C1+C8	C2+C7	C3+C6	C4+C5	C4a+C5a	C8a+C9a	C9	C10
Δ[9-anthracene carboxylic acid]	-3.02	2.29	0.51	0.56	-0.46	-2.74	0.11	4.39
Δ[9-anthracoyl chloride]	-4.43	2.70	0.64	0.43	-0.99	-2.48	5.49	4.53
Δ[HL¹]	-3.96	2.17	0.41	0.38	-0.73	-3.44	3.35	3.44
Δ[HL²]	-3.99	2.48	0.60	0.64	-0.62	-3.33	2.97	3.77
Δ[HL³]	-3.11	2.16	0.93	0.69	-0.54	-3.52	5.55	2.52

* $\Delta = \delta^{13}\text{C}_{\text{compound}} - \delta^{13}\text{C}_{\text{anthracene}}$

HL¹ (*N,N*-diethyl-*N'*-9-anthracoylthiourea)

HL² (*N*-morpholine-*N'*-9-anthracoylthiourea)

HL³ (*N,N*-di(2-hydroxyethyl)-*N'*-9-anthracoylthiourea)

In work done by Schuster⁵⁶ it was found that the resonance effects in 9-substituted anthracenes are transmitted equally to all the conjugated positions of the adjacent aromatic rings, and it is therefore expected that C4 and C5 should be more deshielded than observed. Schuster studied a number of 9-monosubstituted anthracenes with a variety of different substituents including amino, cyano and methyl groups, all having different mesomeric and inductive properties. It was repeatedly found that the changes in chemical shift positions of C4 and C5 were very small. He concluded by suggesting that opposing influences were therefore involved. Schuster also noted that resonance effects due to the substituents in anthracenes were calculated to be transmitted more effectively to C10 (meso carbon) than to C2 and C7. This was supported by experimental evidence. It is therefore pleasing to note that a similar effect is observed for the compounds of the series shown here.

The shift differences of C2, C7 and C10 relative to anthracene are larger in 9-anthracoyl chloride than in 9-anthracenecarboxylic acid, indicating that the resonance effect of 9-anthracoyl chloride is greater than that of the corresponding carboxylic acid. This can be explained in terms of the hydroxyl group of 9-anthracenecarboxylic acid. This group enables delocalisation of electron density through the carbonyl carbon, leading to reduced electron withdrawal on the aromatic ring; this effect being less marked with the aroyl chloride. On addition of the thiourea moiety in the ligand, HL¹, the deshielding effects on the aromatic system are significantly reduced. This may be attributed to the electron donating ability of the central nitrogen atom of the thiourea moiety. This enables delocalisation of charge through both the carbonyl and thiocarbonyl carbons and a decrease in electron withdrawal from the ring system.

A closer look at the *ipso* carbon shifts show that in all cases this carbon is significantly deshielded relative to unsubstituted anthracene. The larger deshielding in the case of 9-anthracoyl chloride relative to the corresponding acid being understood in terms of the greater electronegativity of the chlorine atom relative to that of the hydroxyl group. The quaternary carbons C8a and C9a are shielded in all cases as are C1 and C8. This is expected in the case of 9-substituted anthracenes due to the steric effect of the substituent,^{57,56} however it is slightly greater in C1 and C8 than C8a and C9a and this is most likely due to the peri interactions of the substituents.⁵⁸ Whilst much of this discussion has focused on the differences between 9-anthracenecarboxylic acid, 9-anthracoyl chloride and *N,N*-diethyl-*N'*-9-anthracoylthiourea (HL¹), the arguments are also applicable to the ligands *N*-morpholine-*N'*-9-anthracoylthiourea (HL²) and *N,N*-di(2-hydroxyethyl)-*N'*-9-anthracoylthiourea (HL³).

In the three compounds (HL¹, HL² and HL³) the C13 and C13' resonances often give rise to two signals and a similar observation is possible for C14 and C14' (Table 6), this also extending to the corresponding hydrogen atoms (Table 5). This is somewhat unusual as rotation about the N2-C12 bond would be expected to give rise to equivalent chemical shift positions for the carbon and hydrogen atoms on the amine substituents. However, as will be explained in more detail in section 2.2.4, this bond has partial double bond character and therefore the rotation is limited, frequently giving rise to two separate resonances

in the carbon spectra *e.g.* HL¹ (Table 6), and in the proton spectra, either two separate resonances *e.g.* HL¹ (Table 5) or broad unresolved resonances, *e.g.* HL² (Table 5). On introduction of a metal ion the separation between these resonances is increased further however this will be explained in more detail in section 3.2.1.1. This phenomenon is common to the *N,N*-dialkyl-*N'*-acylthioureas⁵⁹ and is present in the pyrenebutanoylthiourea as well as the pyreneacetylthiourea derivatives synthesised.

N,N-di(2-hydroxyethyl)-*N'*-9-anthracoylthiourea (HL³) exhibited some interesting differences relative to unsubstituted anthracene, particularly the carbonyl (Table 6) and C9 resonances. This compound (HL³) was only sparingly soluble in CDCl₃ and the spectra were therefore acquired in DMSO-*d*₆. These differences may therefore be attributed to solvent effects rather than an electronic influence from the introduction of the terminal hydroxyl groups in the amine substituent.

The *N-H* resonance of the *N,N*-di(2-hydroxyethyl)-*N'*-9-anthracoylthiourea ligand was significantly deshielded relative to the corresponding resonances in the diethylamine and morpholine derivatised ligands. While the solvent used did differ, this downfield shift was thought to be large enough to be attributed to some form of molecular interaction rather than a solvent effect. A closer look at the methylene region of the spectrum revealed an interesting phenomenon. The two OH resonances were non-equivalent, the downfield resonance at 5.41 ppm appearing as a broad singlet and the more upfield resonance at 4.93 ppm appearing as a triplet. While a certain amount of non-equivalence of these two protons is expected due to restricted rotation about the N2-C12 bond, this effect was not as marked in the case of the diethylamine derivatised ligand (HL¹), where both methyl groups resonated at 1.45 ppm. Thus the non-equivalence could not be due to the restricted rotation about the N2-C12 bond alone. The differing rates of exchange (on the NMR timescale) of these two OH protons was therefore attributed to the presence of an intramolecular hydrogen bond between the N-H proton and the C14' oxygen, leaving the attached proton in fast exchange giving rise to the broad 5.41 ppm resonance. The presence of this intramolecular hydrogen bond was confirmed in the X-ray structure obtained and is discussed further in section 2.2.4.3. On the other pendant arm the slow exchange of the proton allows for coupling with the neighbouring methylene protons and gives rise to the triplet resonance at 4.93 ppm. A proton spectrum of the compound is given in Figure 16.

A similar phenomenon was observed in this work for the *N,N*-di(2-hydroxyethyl)-*N'*-pivaloylthiourea (HL⁶), and previously for *N,N*-di(2-hydroxyethyl)-*N'*-benzoylthiourea.²⁶ For the latter compound the coupling constant of the proton in slow exchange was reported as ${}^3J = 5.1$ Hz,²⁶ this value compares well with the observed coupling constant for HL³ being ${}^3J = 5.0$ Hz.

Chapter 2: Synthesis and detailed characterisation of potentially fluorescent ligands.

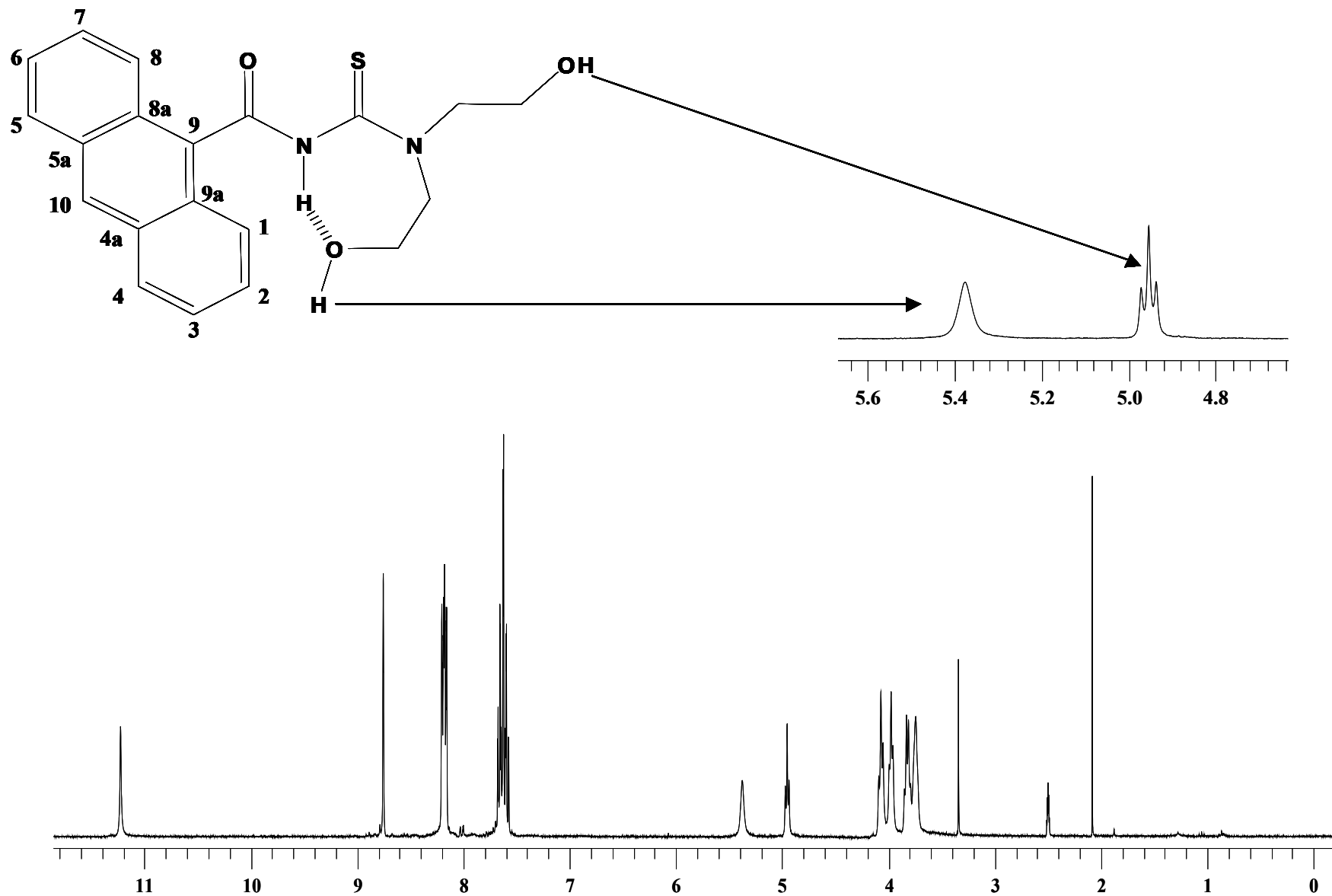


Figure 16 ¹H NMR spectrum of *N,N*-di(2-hydroxyethyl)-*N'*-9-anthracoylthiourea (25°C, DMSO-*d*₆).

2.2.3.2 ^1H and ^{13}C NMR spectra of N,N -dialkyl- N' -[4-(pyrene-1-yl)butanoyl]thiourea derivatives

Table 8 shows the proton assignments for the N,N -dialkyl- N' -[4-(pyrene-1-yl)butanoyl]thiourea derivatives investigated and the numbering scheme used is given in Figure 17.

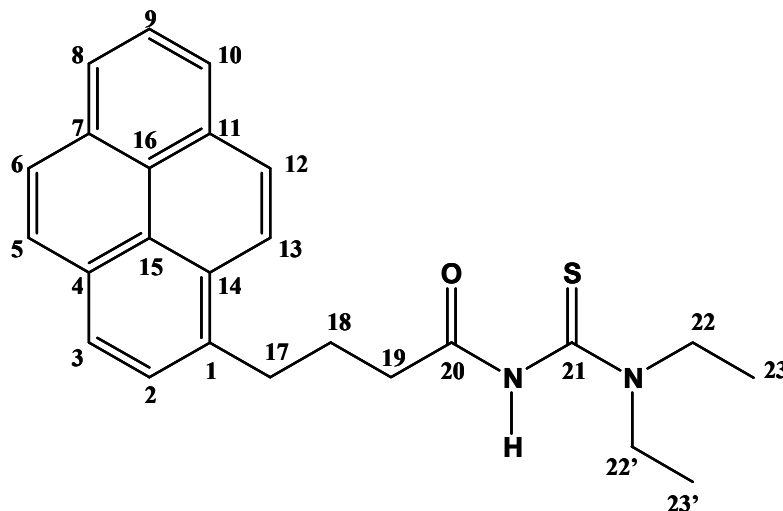


Figure 17 Numbering scheme for N,N -dialkyl- N' -[4-(pyrene-1-yl)butanoyl]thiourea derivatives.

The proton resonances of the pyrene moiety of the pyrenebutanoylthiourea derivatives occur very close together in some cases, in particular proton pairs H8 and H10, H12 and H3, H5 and H6. In the case of the 1-pyrenebutyric acid and 1-pyrenebutanoyl chloride, not all the ^1H resonances of the aromatic moiety could be unambiguously assigned due to resonance overlap at 300 MHz. Better dispersion was obtained at high magnetic field (600 MHz) and although this assisted in the identification of some of the individual protons, not all could be unambiguously assigned. In particular protons H8, H9, H10, H12 being far removed from the centre of asymmetry, were not clearly distinguishable.

Chapter 2: Synthesis and detailed characterisation of potentially fluorescent ligands.

Table 8 ^1H NMR chemical shifts (in ppm) of *N,N*-dialkyl-*N'*-[4-(pyrene-1-yl)butanoyl]thiourea derivatives (25°C, CDCl_3)*.

Compound	H2	H3	H5	H6	H8	H9	H10	H12	H13	H17	H18	H19	N-H	H22	H23
1-pyrene butyric acid	7.76	8.01	7.92	7.92	8.06	7.88	8.06	8.01	8.20	3.29	2.08	2.38	-	-	-
1-pyrene butanoyl chloride	7.72	8.01	7.94	7.94	8.08	7.91	8.08	8.01	8.13	3.27	2.12	2.86	-	-	-
HL⁷	7.84	8.08	8.01	8.01	8.15	7.98	8.15	8.09	8.27	3.38	2.20	2.48	8.20	3.90/ 3.48	1.23
HL⁸	7.84	8.12	8.03	8.03	8.16	7.99	8.17	8.11	8.26	3.40	2.23	2.41	7.98	4.10	4.11

* HL⁷ = *N,N*-diethyl-*N'*-[4-(pyrene-1-yl)butanoyl]thiourea

HL⁸ = *N*-morpholine-*N'*-[4-(pyrene-1-yl)butanoyl]thiourea

An example of a typical COSY spectrum of *N,N*-diethyl-*N'*-[4-(pyrene-1-yl)butanoyl]thiourea (HL⁷) is given in Figure 18, illustrating ¹H-¹H correlations. The correlations of interest are those lying off the diagonal as a result of ³*J*(¹H-¹H) coupling. Identification of H9 is the most obvious starting point as this is the only proton to exhibit coupling to two neighbouring protons (H8 and H10) resulting in a triplet at 7.98 ppm; all other protons being doublets. The correlation of H9 with a doublet at 8.15 ppm allows the assignment of H8 and H10. The assignment of the most downfield doublet as H13 was possible from a combination of single and multiple ¹³C-¹H correlations (Figure 20 and 21) these spectra will be discussed in more detail later in this section. H13 shows a correlation with two overlapping doublets at 8.09 ppm, the coupling constant of H13 being similar to that of the resonances at 8.09 ppm therefore allowing the assignment of this resonance as H12. The overlapping doublets at 8.09 ppm show a correlation to H13 as well as to the most shielded doublet at 7.84 ppm. This doublet (7.84 ppm) having been assigned as H2 from the spectra showing ¹³C-¹H correlations. In particular the coupling constant between the resonances at 8.10 ppm and 8.08 ppm is similar to that of H2 and one of these resonances can therefore be assigned as H3. The remaining singlet at 8.01 ppm represents 2 protons and exhibits no correlation to any other resonances. The remaining unassigned protons are H5 and H6 and due to these protons being in a similar environment and far removed from the centre of asymmetry it is likely that they will not be separated and hence the singlet at 8.01 ppm may be assigned to H5 and H6.

Figure 19 shows a ¹³C NMR spectrum of *N,N*-diethyl-*N'*-[4-(pyrene-1-yl)butanoyl]thiourea (HL⁷) and Table 9 gives the ¹³C shifts in relation to unsubstituted pyrene,⁴² the numbering in Figure 17 being used in the assignments. Relevant chemical shifts will be discussed together with those of the pyreneacetylthiourea derivatives in section 2.2.3.3. Figure 20 illustrates the single bond correlations between protons and carbons (*i.e.* GHSQC), both Figure 21 and 22 illustrate multiple bond correlations (*i.e.* GHMQC), where the former had a window optimised for the aromatic region and the latter has been expanded to include the methylene carbon chain, allowing the assignment of C17-C19, as well as confirming the carbonyl carbon chemical shift. A general outline of how the assignments were made is given following Table 9.

Chapter 2: Synthesis and detailed characterisation of potentially fluorescent ligands.

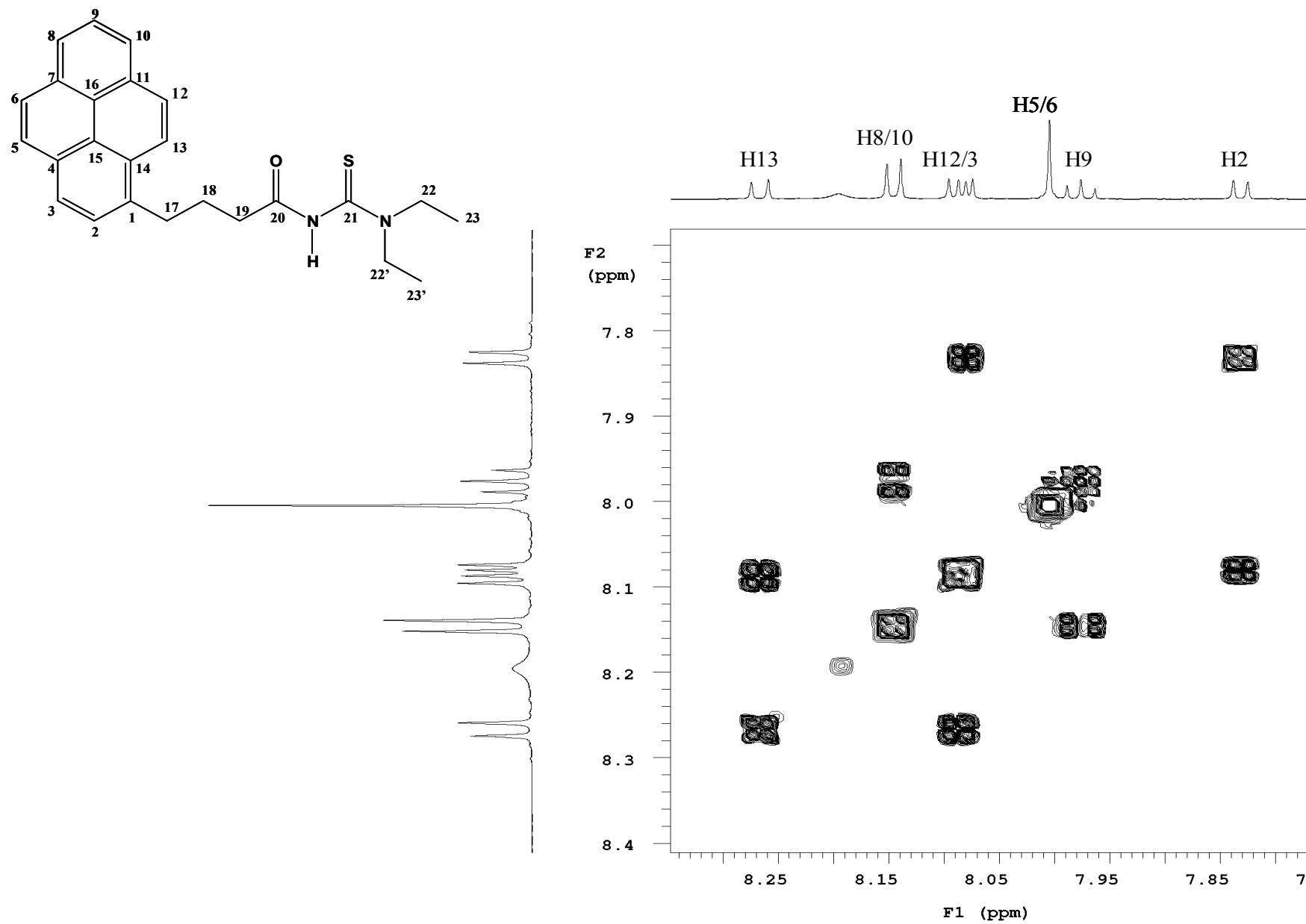


Figure 18 COSY spectrum of *N,N*-diethyl-*N'*-[4-(pyrene-1-yl)butanoyl]thiourea showing ¹H-¹H correlations (25°C, CDCl₃).

Chapter 2: Synthesis and detailed characterisation of potentially fluorescent ligands.

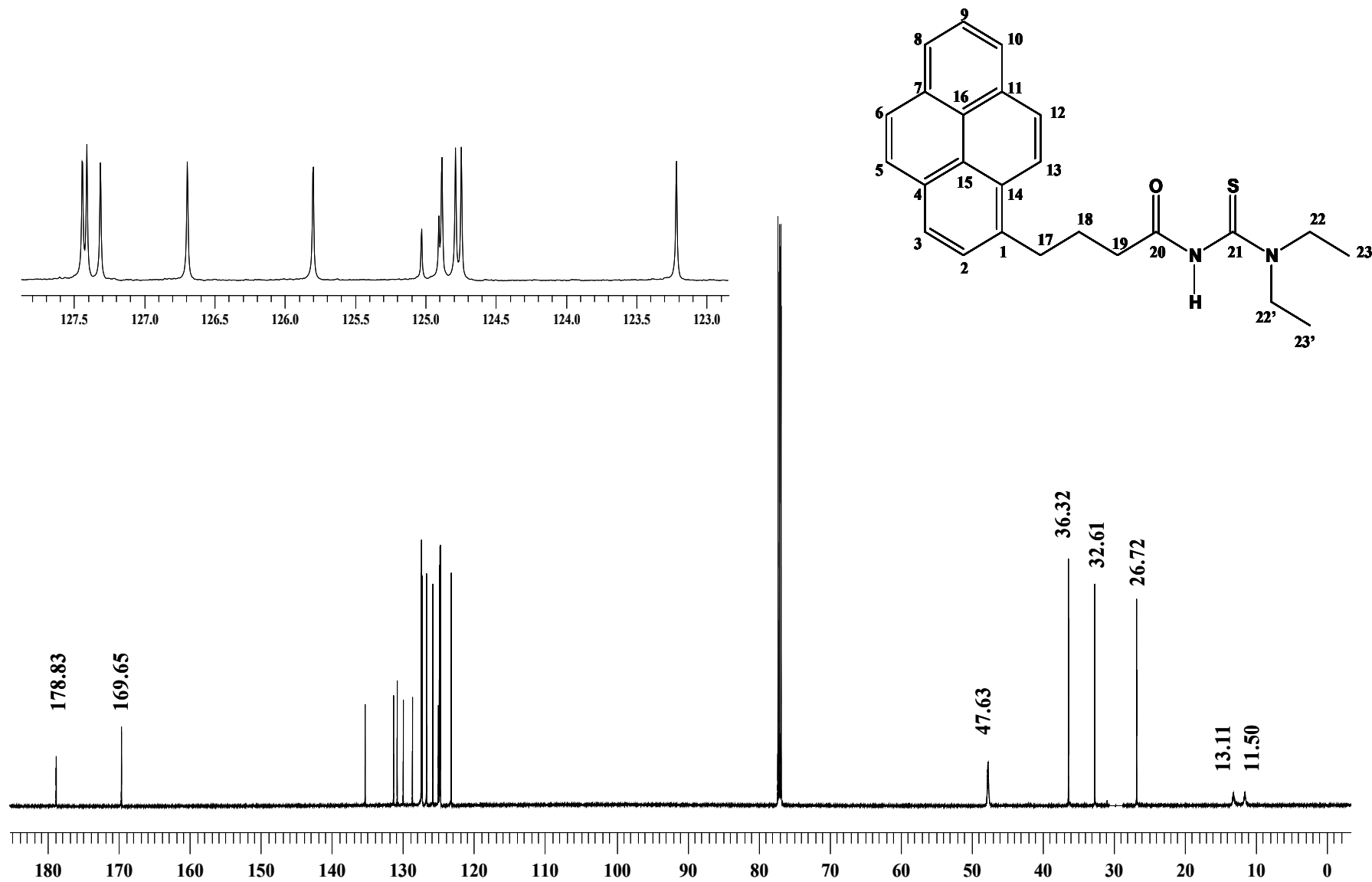


Figure 19 ^{13}C NMR spectrum of *N,N*-diethyl-*N'*-[4-(pyrene-1-yl)butanoyl]thiourea (25°C, CDCl_3).

Chapter 2: Synthesis and detailed characterisation of potentially fluorescent ligands.

Table 9 ^{13}C NMR chemical shifts (in ppm) of *N,N*-dialkyl-*N'*-[4-(pyrene-1-yl)butanoyl]thiourea derivatives (25°C, CDCl_3).

Compound	C1	C2	C3	C4	C5	C6	C7	C8	C9	C10
pyrene⁴²	124.6	125.5	124.6	130.9	127.0	127.0	130.9	124.6	125.5	124.6
1-pyrene butyric acid	135.64	127.51	-	130.21	-	126.90	131.58	-	126.01	-
1-pyrene butanoyl chloride	134.59	-	-	130.56	128.83	127.08	131.55	-	126.09	-
HL⁷	135.36	127.29	124.77	129.94	127.40	126.67	131.33	124.72	125.78	124.86
HL⁸	134.99	127.41	124.82	130.09	127.41	126.86	131.36	125.04	125.93	124.87

Chapter 2: Synthesis and detailed characterisation of potentially fluorescent ligands.

Table 9 contd. ^{13}C NMR chemical shifts (in ppm) of *N,N*-dialkyl-*N'*-[4-(pyrene-1-yl)butanoyl]thiourea derivatives (25°C, CDCl_3).

Compound	C11	C12	C13	C14	C15	C16	C17	C18	C19	C20	C21	C22	C23
pyrene ⁴²	130.9	127.0	127.0	130.9	124.6	124.6	-	-	-	-	-	-	-
1-pyrene butyric acid	131.07	-	123.37	128.91	-	-	32.50	26.31	33.14	178.22	-	-	-
1-pyrene butanoyl chloride	130.98	-	123.00	-	-	-	31.71	26.61	46.41	174.08	-	-	-
HL ⁷	130.81	127.41	123.21	128.65	125.01	124.89	32.61	26.72	36.32	169.65	178.83	47.63	12.85/ 11.50
HL ⁸	130.82	127.59	123.10	128.74	125.09	124.91	32.59	26.46	36.35	168.58	178.62	66.14	52.50

As the assignment of H9 is possible from the COSY spectrum (Figure 18), the single bond correlation this triplet shows with the carbon resonance at 125.78 ppm (Figure 20) enables the assignment of C9. The doublet in the proton spectrum assigned as H8 and H10 shows a single bond correlation to two peaks in the carbon spectrum which can be given the preliminary assignment of C8 or C10 (Figure 20), this will be referred to later. The carbon resonance at 135.36 ppm was preliminarily assigned as C1 (Figure 21). This was motivated by the fact that it is the most deshielded of the aromatic resonances and as the substituent is attached at this position, it should be the most electronically affected. This is further supported by the lower intensity of the peak, indicating a quaternary carbon, and the fact that it exhibits no single bond correlation with a proton. This carbon also shows a multiple bond correlation (Figure 21) to the doublet of doublets in the proton spectrum, previously assigned as H3 and H12 (Figure 18). Using these proton resonances and returning to the single bond correlations enables the preliminary assignment of C12 and C3.

A closer look at the GHMQC (Figure 21) shows 4 resonances in a similar region (132 ppm-128 ppm) with a lower intensity, indicating quaternary carbons. H9 exhibits a multiple bond correlation to the first two carbons at 131.33 ppm and 130.81 ppm and these are therefore either C7 or C11, leaving the remaining two resonances at 129.94 ppm and 128.65 ppm to be either C4 or C14. H12/H3 shows a correlation with the resonance at 130.81 ppm therefore enabling this resonance to be assigned as C11, the first resonance is therefore assigned as C7 (131.33 ppm). H5/H6 shows a correlation with C7 and with the resonance at 129.94 ppm and therefore this resonance must be C4, leaving the remaining resonance to be assigned as C14 (128.65 ppm, Figure 21). The newly assigned C4 and C14 both show a multiple bond correlation with the most shielded doublet in the proton spectrum, thus confirming its assignment as H2, and the most downfield doublet as H13. Returning to the single bond correlations, the assignments of C2 and C13 are now possible. While these correlations may not be clear on the spectra given, expansions of these regions enabled their assignments.

From the single bond correlation between H5/6 and the carbon resonances at 126.7 ppm and 127.4 ppm these can be assigned as C5 and C6 respectively, the unambiguous assignment enabled by the multiple bond correlation between H12/3 and the peak at 127.4 ppm (C5) and the multiple bond correlation between H10/8 and the peak at 126.7 ppm (C6).

Four carbon resonances remain unassigned: C15 and C16 being the remaining quaternary carbons at 125.01 ppm and 124.89 ppm, and C8 and C10 at 124.86 ppm and 124.72 ppm. Large expansions of these regions showed a correlation between H13 and the low intensity peak at 125.01 ppm enabling the assignment of C15, the remaining low intensity resonance therefore being C16 (124.89 ppm). A further expansion revealed a multiple bond correlation between the H12/H3 two doublets and the carbon resonance at 124.86 ppm allowing the assignment of C10, the remaining carbon resonance therefore being C8 (124.72 ppm).

Figure 22 shows the multiple bond ^{13}C - ^1H correlations and includes the methylene chain of the pyrenebutanoyl moiety. The correlation that H18 and H19 exhibit with C20 confirm the assignment of this resonance at 169.65 ppm as the carbonyl carbon as opposed to the thiocarbonyl carbon.

As is apparent from Table 9, the assignment of certain ^{13}C resonances was uncertain particularly for 1-pyrenebutyric acid and 1-pyrenebutanoyl chloride. This was due to poor separation of the carbon resonances. For the assignment of the ^{13}C NMR spectra, a HETCOR, (^{13}C detected 1J H-C correlation experiment) should give better resolution in the ^{13}C dimension than a ^1H detected GHSQC, however this would most likely still not have been sufficient to assign the peaks due to the overlap in the ^1H dimension. An INADEQUATE experiment (indicating ^{13}C - ^{13}C correlations) could also have been run, however the 1-pyrenebutyric acid was not sufficiently soluble in CDCl_3 for this experiment, as an extremely high concentration is required for this experiment to be successful in a reasonable time period (e.g. 48 hours). In cases where the assignment was uncertain, these peaks have been omitted.

Chapter 2: Synthesis and detailed characterisation of potentially fluorescent ligands.

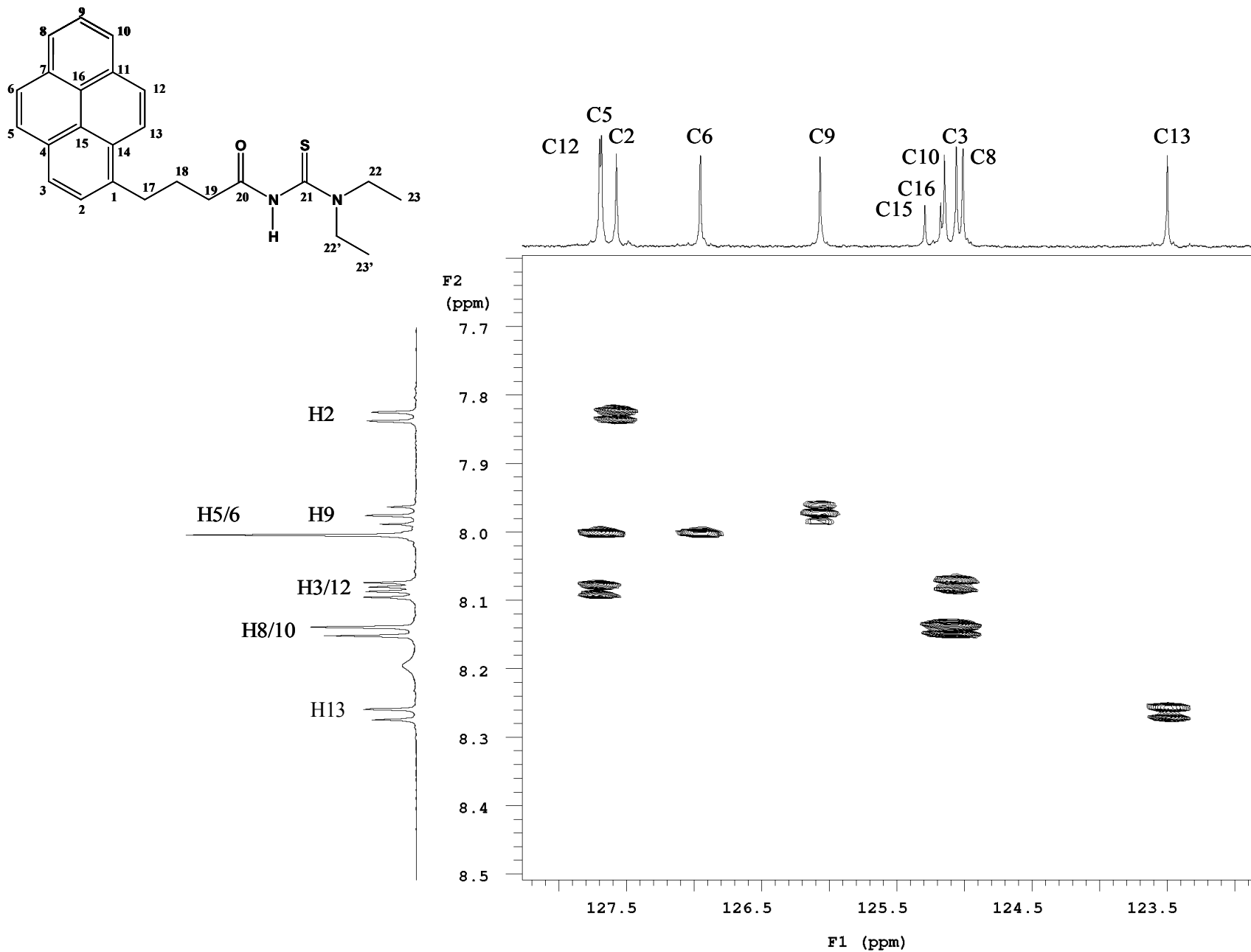


Figure 20 GHSQC spectrum of *N,N*-dialkyl-*N'*-[4-(pyrene-1-yl)butanoyl]thiourea showing single bond ^{13}C - ^1H correlations (25°C, CDCl_3).

Chapter 2: Synthesis and detailed characterisation of potentially fluorescent ligands.

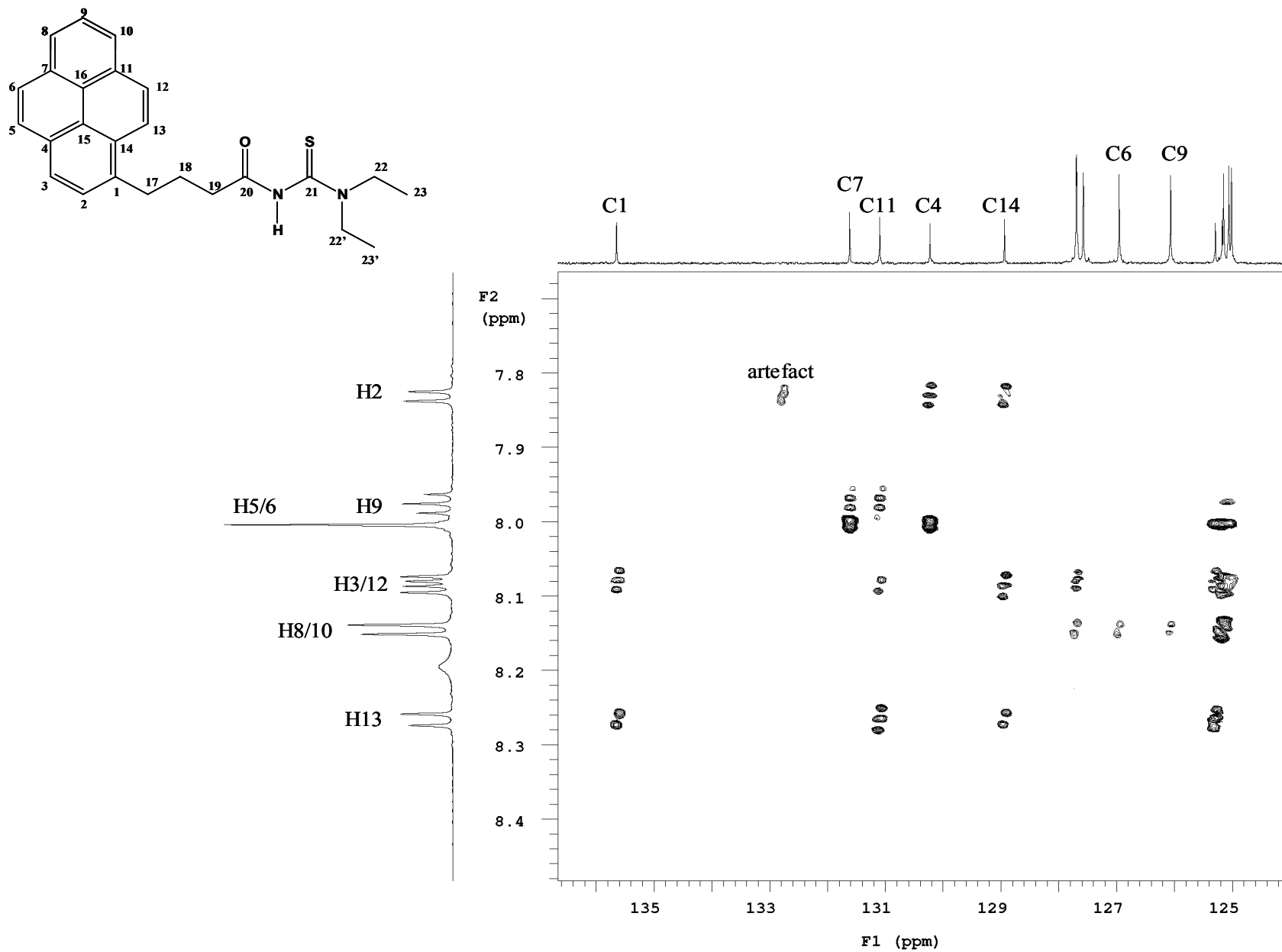


Figure 21 GHMQC spectrum of *N,N*-dialkyl-*N'*-[4-(pyrene-1-yl)butanoyl]thiourea showing multiple bond ¹³C-¹H correlations (25°C, CDCl₃).

Chapter 2: Synthesis and detailed characterisation of potentially fluorescent ligands.

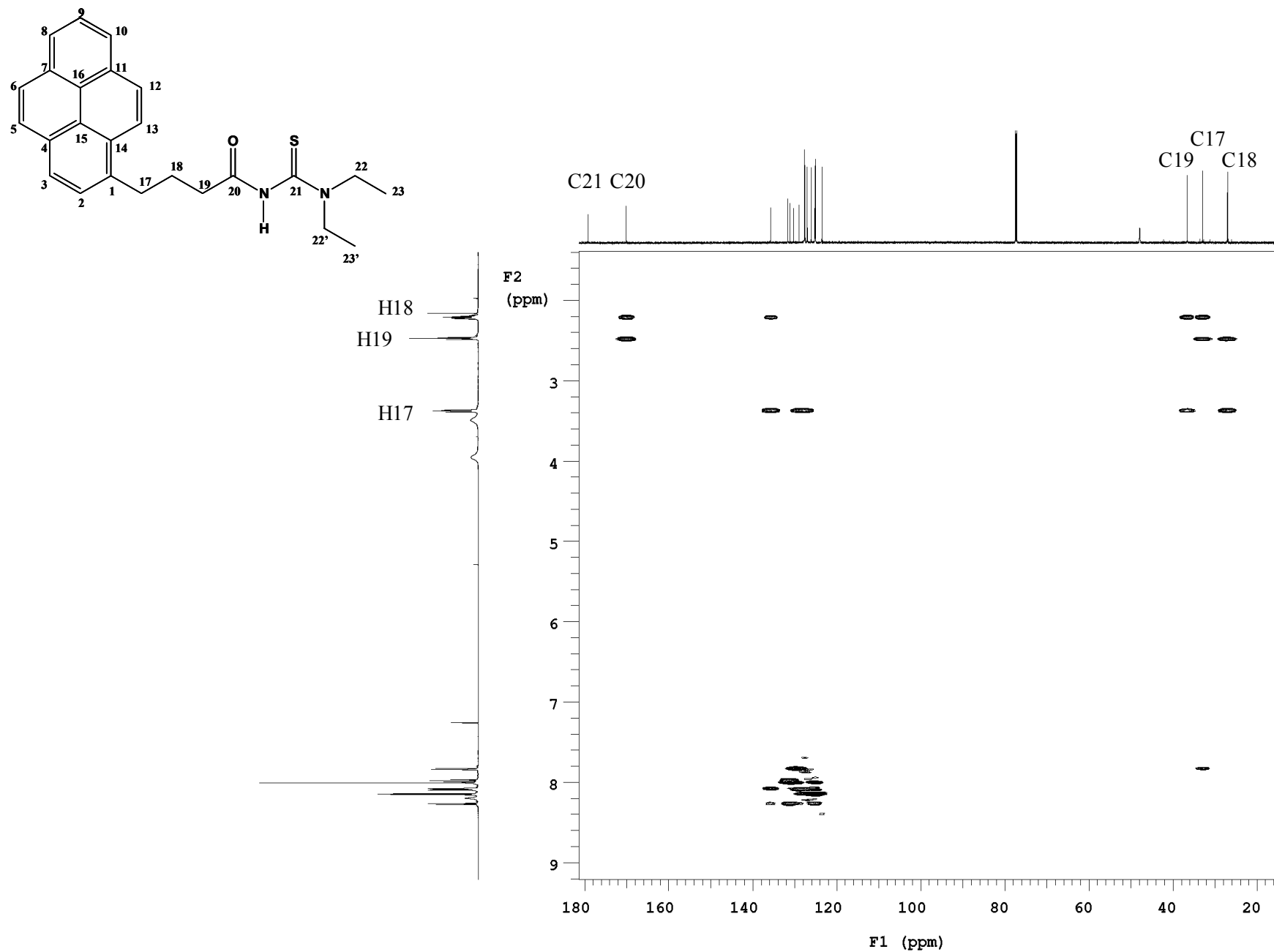


Figure 22 GHMQC spectrum of *N,N*-dialkyl-*N'*-[4-(pyrene-1-yl)butanoyl]thiourea showing multiple bond ¹³C-¹H correlations (25°C, CDCl₃).

2.2.3.3 ^1H and ^{13}C NMR spectra of N,N -dialkyl- N' -[pyrene-1-ylacetyl]thiourea derivatives

Table 10 shows the proton assignments for the investigated compounds and the corresponding ^{13}C shifts are given in Table 11. Figure 23 illustrates the numbering scheme used in these assignments.

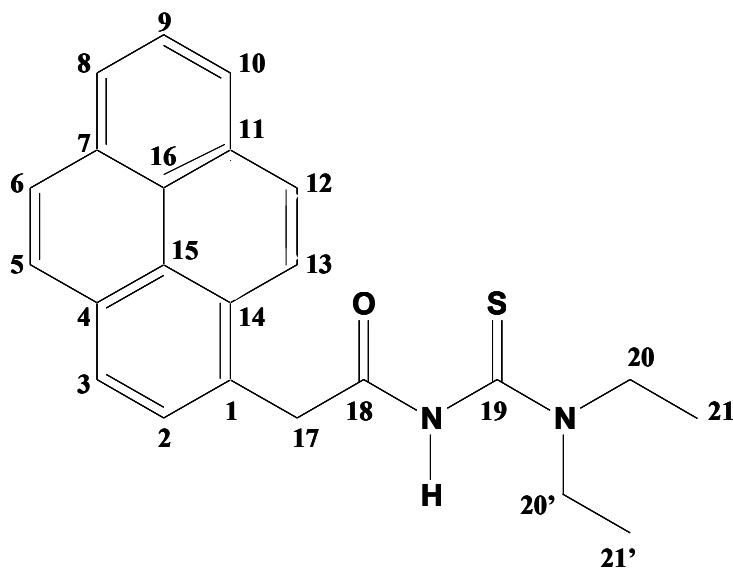


Figure 23 Numbering scheme for N,N -dialkyl- N' -[pyrene-1-ylacetyl]thiourea derivatives.

Table 10 ^1H NMR chemical shifts (in ppm) of N,N -dialkyl- N' -[pyrene-1-ylacetyl]thiourea derivatives (25°C, CDCl_3)*

Compound	H2	H3	H5	H6	H8	H9	H10	H12	H13	N-H	H17	H20	H21
1-pyreneacetic acid	7.93	8.15	8.05	8.05	8.20	8.00	8.20	8.13	8.24	-	4.35	-	-
1-pyreneacetyl chloride	7.88	8.14	8.01	8.06	8.19	8.02	8.19	8.14	8.07	-	4.80	-	-
HL ¹⁰	7.91	8.19	8.02	8.05	8.18	8.01	8.18	8.11	8.18	7.94	4.38	3.85/ 3.30	1.22/ 0.92

In the series of pyrenebutanoylthiourea derivatives there was very little change in any of the ring carbon resonances with varying substituents and some difficulty was experienced in assigning the shifts as many of

* HL¹⁰ = N,N -diethyl- N' -[pyrene-1-ylacetyl]thiourea

the resonances fell very close together. The pyreneacetylthiourea derivatives were, however, easier to assign, especially in the case of C12 and 3, C8 and 10, and C15 and 16, as these resonances were generally better separated.

In the case of pyreneacetylthiourea derivatives, alteration of the carbonyl substituent resulted in a significant change of only the C1 aromatic resonance position. The shift of the spacer carbon C17 however, did show a sensitivity to the carbonyl substituent being the most shielded in the case of the 1-pyreneacetylcarboxylic acid, moving downfield in the ligand, *N,N*-diethyl-*N'*-[pyrene-1-ylacetyl]thiourea (HL¹⁰), and 1-pyreneacetyl chloride giving rise to the most downfield shift. This trend was similar for C19 in the pyrenebutanoylthiourea derivatives and in these compounds the chemical shift of C17, the *ipso* carbon and the remaining aromatic resonances altered very little.

These observations indicate that with a longer spacer group the electronic system of the pyrene and thiourea moieties are distinct and there is very little interaction between the two. In the pyreneacetylthiourea derivatives the single methylene group is too short to afford distinction between these two systems and as a result, there appears to be delocalisation of electrons from one to the other. This would account for the change in shift position of the C1 carbon when changing the carbonyl substituent, in the pyreneacetylthiourea derivatives as well as the greater separation of the aromatic carbon resonances.

The shift of the *ipso* carbon (C1) of the pyreneacetylthiourea derivatives deserves closer examination. In the case of 1-pyreneacetyl chloride this carbon (C1) is significantly shielded relative to the carboxylic acid, most probably due to the increased electron density caused by the introduction of the chlorine atom, this being similar in the case of the anthracoylthiourea derivatives. On changing the carbonyl substituent of 1-pyreneacetyl chloride to introduce the thiourea moiety in the ligand (*N,N*-diethyl-*N'*-[pyrene-1-ylacetyl]thiourea) a deshielding effect on C1 is observed and a shielding of the carbonyl carbon. This is possibly due to a combination of electron withdrawal by the carbonyl group from the aromatic system and a potential delocalisation through the nitrogen atoms and the carbonyl and thiocarbonyl groups.

Chapter 2: Synthesis and detailed characterisation of potentially fluorescent ligands.

Table 11 ^{13}C NMR chemical shifts (in ppm) of *N,N*-dialkyl-*N'*-[pyrene-1-ylacetyl]thiourea derivatives (25°C, CDCl_3).

Compound	C1	C2	C3	C4	C5	C6	C7	C8	C9	C10
Pyrene ⁴²	124.6	125.5	124.6	130.9	127.0	127.0	130.9	124.6	125.5	124.6
1-pyreneacetic acid	127.25	128.57	124.86	131.15	127.42/ 127.36	129.42/ 127.56	131.46	125.36	126.17	125.20
1-pyreneacetyl chloride	124.93/ 124.87	128.49	124.86	131.51	127.21	127.65	131.15	125.68	126.17	125.50
HL ¹⁰	127.27	128.57	125.33	131.39	127.44	127.81	131.39	125.73	126.33	125.55

Chapter 2: Synthesis and detailed characterisation of potentially fluorescent ligands.

Table 11 contd. ^{13}C NMR chemical shifts (in ppm) of *N,N*-dialkyl-*N'*-[pyrene-1-ylacetyl]thiourea derivatives (25°C, CDCl_3).

Compound	C11	C12	C13	C14	C15	C16	C17	C18	C19	C20	C21
Pyrene ⁴²	130.9	127.0	127.0	130.9	124.6	124.6	-	-	-	-	-
1-pyreneacetic acid	130.92	128.12	123.22	129.63	125.02	124.70	38.81	176.21			
1-pyreneacetyl chloride	130.54	128.60	122.30	129.38	124.93/ 124.87	124.48	51.04	171.81			
HL ¹⁰	130.83	128.64	122.72	129.65	125.24	124.68	42.40	167.92	178.49	47.83/ 47.23	12.99/ 10.99

2.2.4 Single Crystal X-Ray Diffraction Analysis

A brief survey of the literature revealed that relatively little structural information on the anthracoylthioureas, pyrenebutanoylthioureas as well as their metal complexes was available.^{2,60} The fluorescent tags, anthracene and pyrene have however been studied in detail particularly by Desiraju *et al.*⁶¹ This group systematically studied 32 different polynuclear aromatic hydrocarbons and identified four basic structure types, which could be clearly differentiated by energetic and geometrical criteria.⁶¹ The major motifs of these four prototypes were classified as stack, layer, glide or herringbone, the importance of C...C and C...H interactions in the various molecules studied influencing the adoption of a particular structure type.⁶² It was therefore considered of interest to carry out crystal and molecular structure determinations of the molecules *N,N*-diethyl-*N'*-9-anthracoylthiourea (HL¹), *N*-morpholine-*N'*-9-anthracoylthiourea (HL²), *N,N*-di(2-hydroxyethyl)-*N'*-9-anthracoylthiourea (HL³), *N,N*-di(2-hydroxyethyl)-*N'*-pivaloylthiourea (HL⁴), *N,N*-diethyl-*N'*-[4-(pyrene-1-yl)butanoyl]thiourea (HL⁷) and *N*-morpholine-*N'*-[4-(pyrene-1-yl)butanoyl]thiourea (HL⁸) by means of single crystal x-ray diffraction to investigate the interactions (if any) of the aromatic moieties and the influence of the acylthiourea moiety on the crystal packing.

2.2.4.1 Crystal and molecular structure of *N,N*-diethyl-*N'*-9-anthracoylthiourea (HL¹)

Yellow crystals of HL¹ were isolated from a solvent mixture of chloroform and pentane. This compound crystallised out in the $P2_1/n$ space group with four molecular units in the unit cell. Further details are given in Table 17 at the end of this chapter, and relevant bond lengths and torsion angles will be discussed together with the other anthracoylthiourea derivatives at the end of this section. A numbered molecular structure is given in Figure 24.

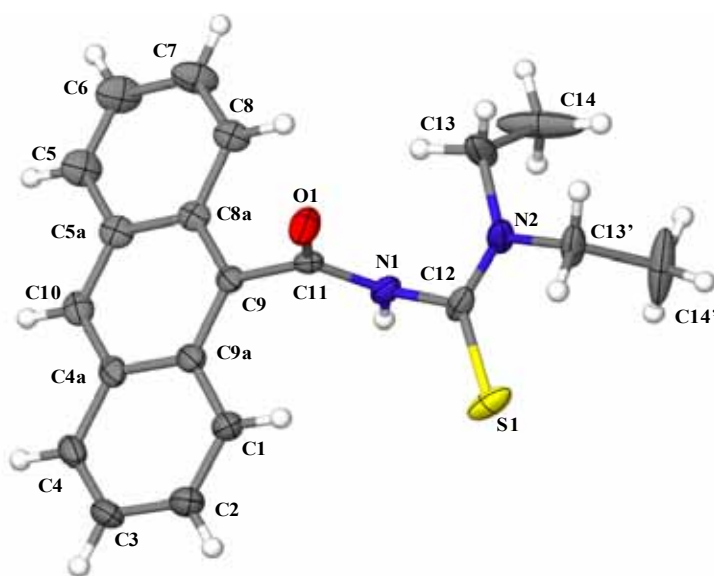


Figure 24 Molecular structure of *N,N*-diethyl-*N'*-9-anthracoylthiourea (HL¹).

There was a certain degree of disorder surrounding the terminal methyl groups presumably as a result of thermal motion. Attempts to model this disorder did not however significantly improve the overall quality of the structure and for the sake of clarity is not shown in the diagram.

There was evidence of an intermolecular hydrogen bond between the thioamidic N-H proton (located from the difference fourier map) of one molecule and the S atom of an adjacent molecule (symmetry operator 1-X, 1-Y, 1-Z) ($N(H)\dots S = 2.62(3) \text{ \AA}$, and $N1-S1 = 3.388(2) \text{ \AA}$), leading to a form of dimerisation where the aromatic systems were in opposite arrangements (Figure 25). A similar phenomenon was reported for the closely related pyrrolidine analogue with average $H\dots S$ distances of 3.445 \AA .⁶³ The aromatic rings in HL^1 exhibited face to edge interactions ($H4\dots C8 = 2.767 \text{ \AA}$) in the crystal (Figure 25). Interestingly this molecule did not exhibit any π interactions in the unit cell packing, which might have been expected between the anthracene rings.⁶³ The opposing orientation of the oxygen and sulphur atoms is noteworthy. In the complexed form, both the thiocarbonyl and carbonyl groups are necessarily in a similar orientation and the opposing arrangement observed between these two atoms in this compound is presumably as a result of the $N(H)\dots S$ hydrogen bonding present. The thiocarbonyl and carbonyl orientations of HL^1 as well as the other anthracoylthiourea derivatives will be discussed further in section 2.2.4.5.

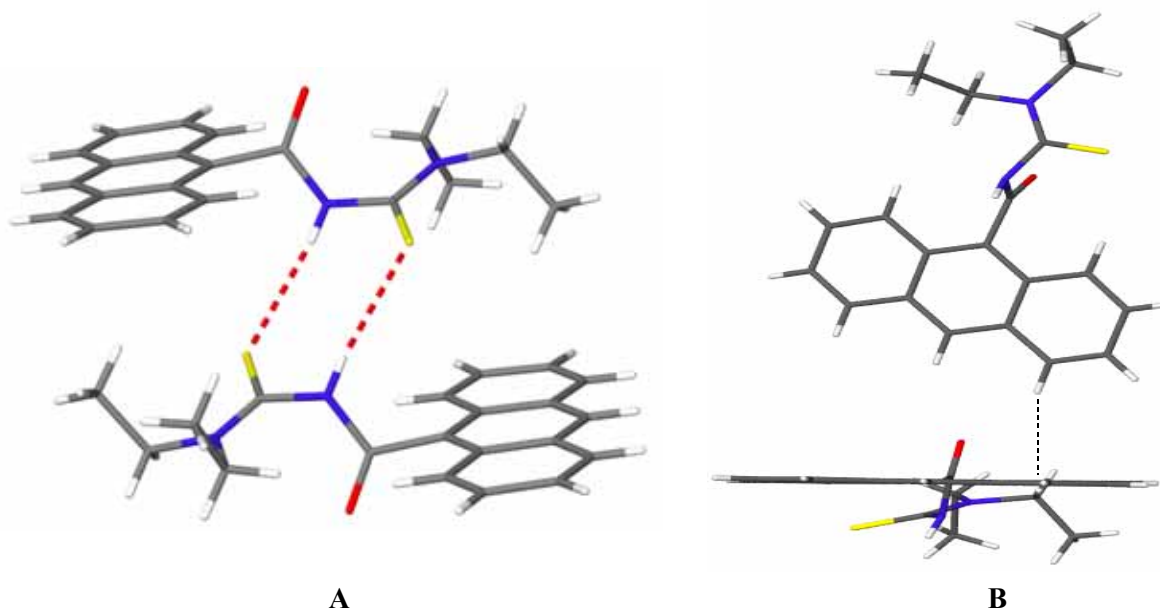


Figure 25 Intermolecular hydrogen bonding ($N(H)\dots S = 2.62(3) \text{ \AA}$) leading to dimerisation of HL^1 (A) and face to edge interactions ($H4\dots C8 = 2.767 \text{ \AA}$) in N,N -diethyl- N' -9-anthracoylthiourea (B).

2.2.4.2 Crystal and molecular structure of N -morpholine- N' -9-anthracoylthiourea (HL^2)

Pale yellow crystals of HL^2 were obtained from a solvent mixture of chloroform and pentane and crystallised out in the $P-1$ (No. 2) space group with 2 molecular units per unit cell (Table 18). Figure 26 illustrates the numbered molecular structure.

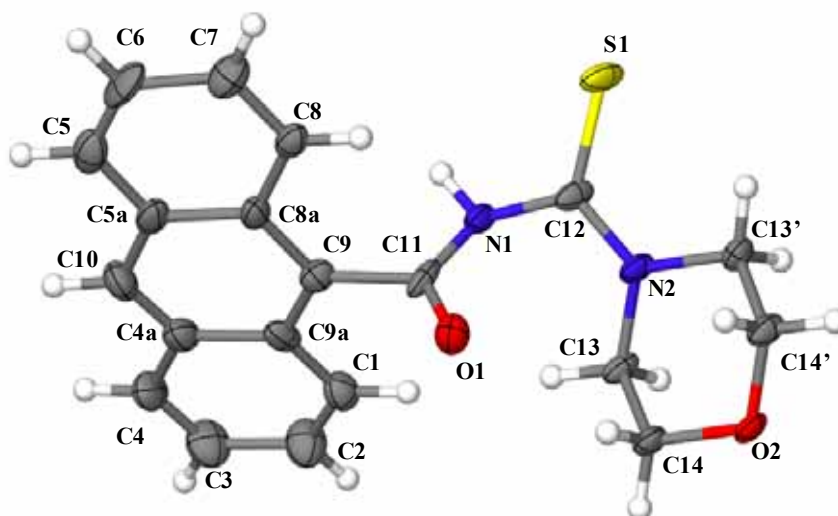


Figure 26 Molecular structure of *N*-morpholine-*N'*-9-anthracoylthiourea (HL^2).

This was the only anthracoylthiourea ligand to exhibit a π interaction between the aromatic rings (Figure 27). Two molecules are orientated in opposite directions and related by the symmetry operator $(-X, 1-Y, 2-Z)$ with an offset π overlap; the closest carbon – carbon distance between C10 and C9a being 3.309(62) Å. These values compare well with those previously reported for π - π stacking distances, 3.43(1) and 3.47(1) Å, between phenanthroline residues.⁶⁴ The thioamidic N-H was located from the difference fourier map and an intermolecular hydrogen bond linking this proton and O2 of the adjacent molecule (symmetry operator $1+X, Y, Z$) had a distance of 2.19(4) Å, where $N1-O2 = 2.971(4)$ Å. These interactions resulted in alternating planes of aromatic and heteroatomic nature through the crystal. Interestingly there were no face to edge contacts, since all the aromatic moieties are parallel.

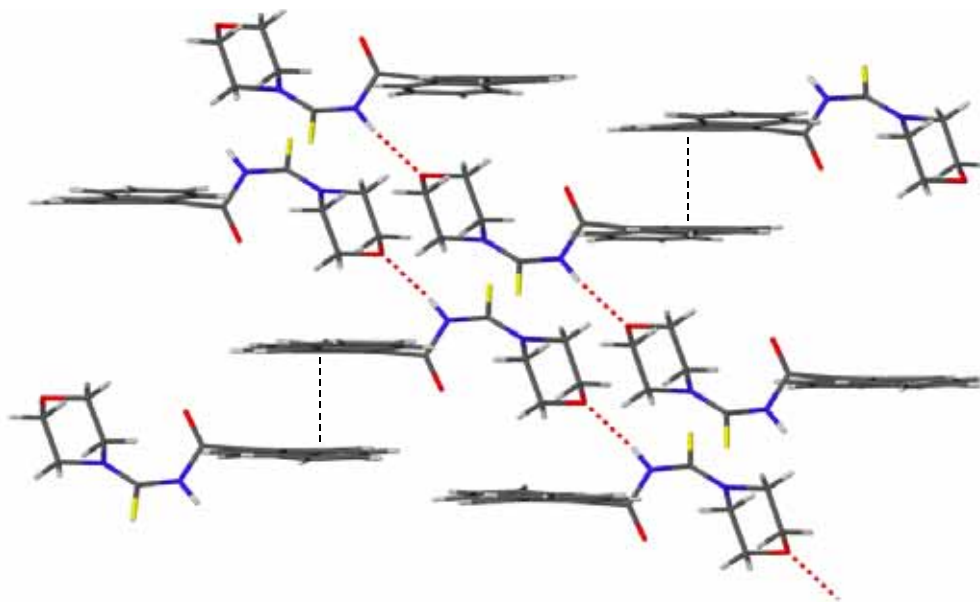


Figure 27 π - π Interactions between anthracene moieties and hydrogen bonding between N(H)...O2 of an adjacent molecule (symmetry operator $1+X, Y, Z$) in *N*-morpholine-*N'*-9-anthracoylthiourea.

2.2.4.3 Crystal and molecular structure of *N,N*-di(2-hydroxyethyl)-*N'*-9-anthracoylthiourea (HL^3)

Orange crystals of HL^3 were isolated from a chloroform/pentane solvent system and crystallised in the $P2_12_12_1$ (No 19) space group with 4 molecular units per unit cell (Table 19). Figure 28 illustrates the molecular structure.

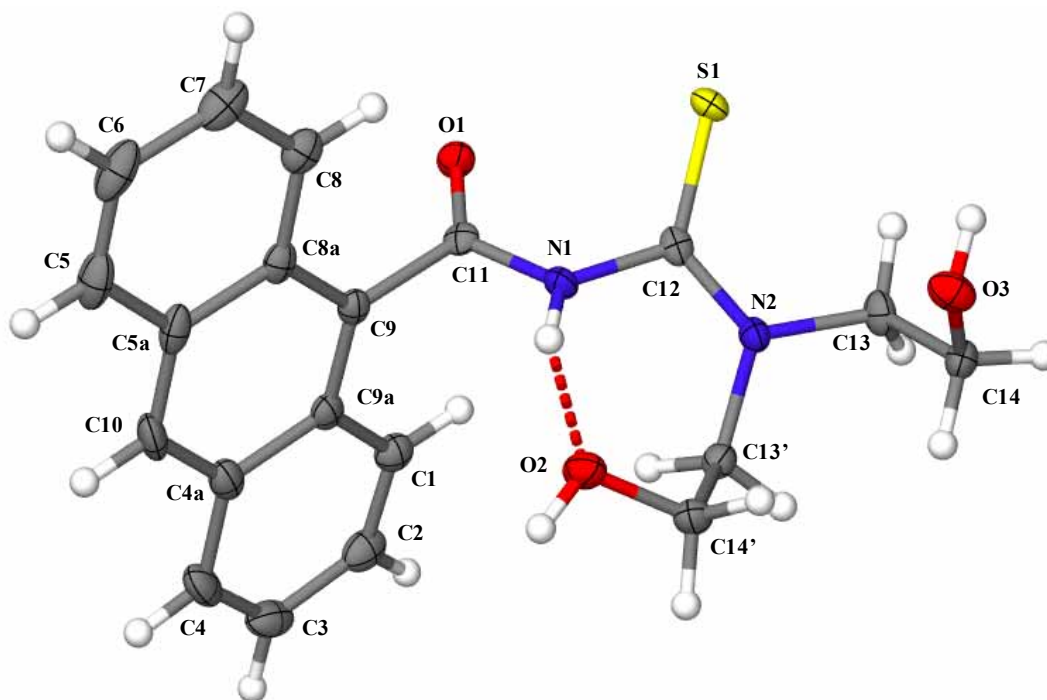


Figure 28 Molecular structure of *N,N*-di(2-hydroxyethyl)-*N'*-9-anthracoylthiourea (HL^3).

The intramolecular hydrogen bond between N(H) and O2 has a length of 1.906(28) Å, and the corresponding hydrogen of the hydroxyl group involved in this bond also formed an intermolecular hydrogen bond with the oxygen atom on the pendant arm of an adjacent molecule (symmetry operator $\frac{1}{2}+X, \frac{3}{2}-Y, 1-Z$) where O2(H)...O3 = 1.873 Å and O2...O3 = 2.680(2) Å (Figure 29). Similar observations were reported for *N,N*-di(2-hydroxyethyl)-*N'*-benzoylthiourea²⁶ with O...O distances of 2.739 Å (H...O = 1.96 Å). A further interaction was observed in HL^3 between the carbonyl oxygen O1 and the hydroxyl group of an adjacent molecule (symmetry operator $\frac{1}{2}+X, \frac{1}{2}-Y, 1-Z$) on the pendant arm not involved in the intramolecular hydrogen bond, (O3(H)...O1 = 2.299 Å and O1...O3 = 2.945(2) Å). The corresponding (O...O) distances in *N,N*-di(2-hydroxyethyl)-*N'*-benzoylthiourea are slightly longer at 3.213 Å.²⁶ The aromatic rings in HL^3 were characterised by face to edge interactions between adjacent molecules (symmetry operator $1-X, \frac{1}{2}+Y, \frac{3}{2}-Z$) where closest C1...H5 distance = 2.681 Å and C1...C5 = 3.613(3) Å, the molecular orientation precluding any pi interaction. These interactions led to alternating planes of edge to face aromatic contacts and hydrogen bonding in the crystal packing (Figure 30).

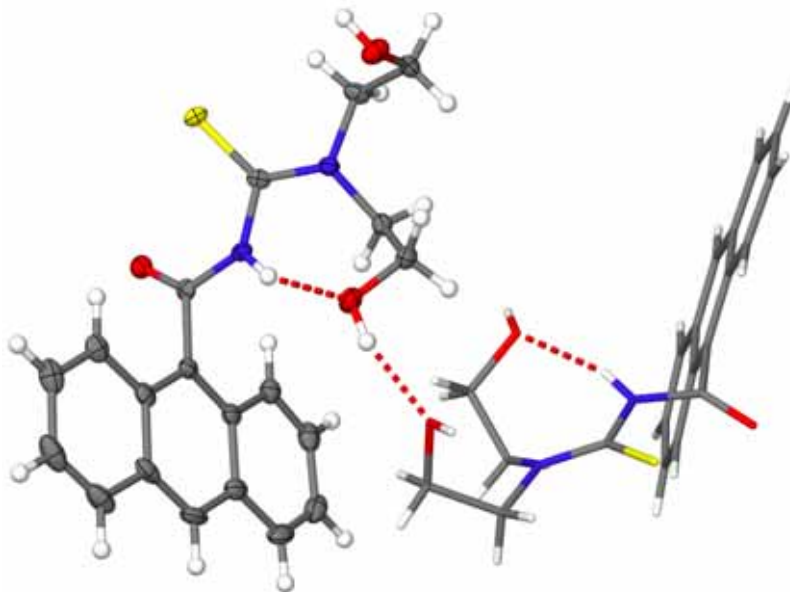


Figure 29 Intramolecular and intermolecular hydrogen bonding exhibited by *N,N*-di(2-hydroxyethyl)-*N'*-9-anthracoylthiourea (HL³).

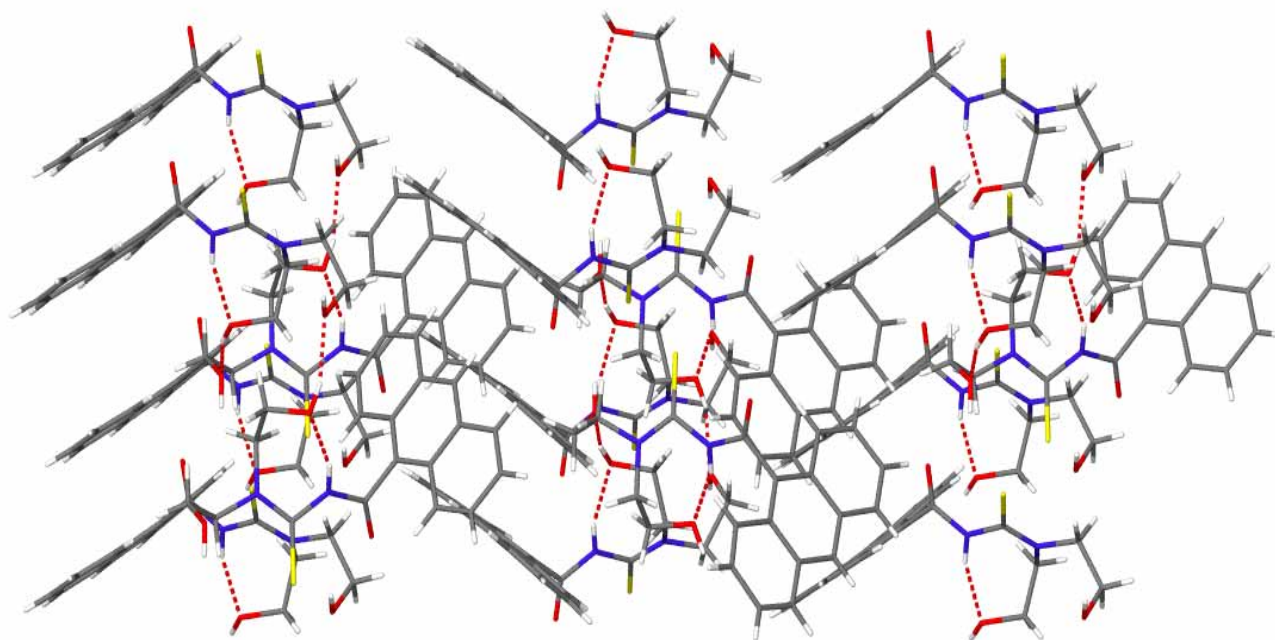


Figure 30 Molecular packing of *N,N*-di(2-hydroxyethyl)-*N'*-9-anthracoylthiourea (HL³).

2.2.4.4 Crystal and molecular structure of *N,N*-di(2-hydroxyethyl)-*N'*-pivaloylthiourea (*HL*⁶)

Colourless crystals of *HL*⁶ were isolated from a solvent mixture of methanol and pentane and crystallised out in the $P2_1/n$ space group with 4 molecular units per unit cell (Table 20). The molecular structure is given in Figure 31.

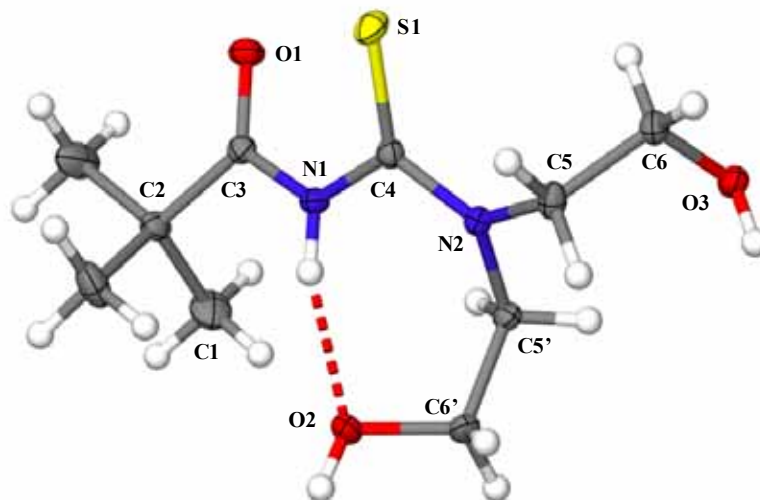


Figure 31 Molecular structure of *N,N*-di(2-hydroxyethyl)-*N'*-pivaloylthiourea (*HL*⁶).

This compound formed inter- and intramolecular hydrogen bonds, in a similar fashion to that of the anthracene analogue (*HL*³). The intramolecular hydrogen bond N(H)...O2 being 1.946(17) Å and the intermolecular hydrogen bond with the adjacent molecule ($X-\frac{1}{2}, \frac{1}{2}-Y, \frac{1}{2}+Z$) O2(H)...O3 being 1.915 Å, and O2...O3 = 2.745(1) Å. The intermolecular hydrogen bond between the carbonyl oxygen and hydrogen atom of the hydroxyl group on the pendant arm of the adjacent molecule (symmetry operator $\frac{1}{2}+X, \frac{1}{2}-Y, \frac{1}{2}+Z$) O1...(H)O3 had a distance of 2.033 Å, and O1...O3 = 2.835(1) Å, these being shorter than the corresponding distances in both of *N,N*-di(2-hydroxyethyl)-*N'*-9-anthracoylthiourea and the benzoyl analogue.

Of the various hydrogen bonds in the preceding two ligands, (*HL*³ and *HL*⁶), it is apparent from the NMR spectra that only the intramolecular hydrogen bond between N-H and O2 persist in DMSO-*d*₆ solution. (section 2.2.3.1).²⁶

2.2.4.5 Discussion of the *N,N*-dialkyl-*N'*-9-anthracoylthiourea and *N,N*-dialkyl-*N'*-pivaloylthiourea derivatives

It is interesting to note that *N*-morpholine-*N'*-9-anthracoylthiourea (*HL*²) was the only ligand to exhibit π - π interactions and this compound has the highest melting point (182-185°C). *N,N*-di(2-hydroxyethyl)-*N'*-9-anthracoylthiourea (*HL*³) despite the extensive hydrogen bonding, having a comparable melting point to that of *N,N*-diethyl-*N'*-9-anthracoylthiourea (*HL*¹) which exhibited fewer intermolecular interactions (152.8-155°C and 158-160°C respectively).

In work done previously by Grimmbacher⁶⁵ a comparison was drawn between the dibutylamine acylthiourea derivatives of anthracene, naphthalene and benzene, and it was noted that the melting points

of these ligands were 115-117°C, 97-99°C and 70-71°C²⁴ respectively. Interest was expressed as to the nature of the intermolecular interactions in these compounds, the higher melting point of *N,N*-dibutyl-*N'*-9-anthracoylthiourea possibly being indicative of a π - π interaction. The analogous series of diethylamine derivatised compounds namely *N,N*-diethyl-*N'*-9-anthracoylthiourea HL¹, *N,N*-diethyl-*N'*-naphthoylthiourea and *N,N*-diethyl-*N'*-benzoylthiourea, however show a different trend, where the naphthoyl and benzoyl ligands have melting points of 174-176°C and 97-98°C⁶⁶ respectively. The anthracene analogue's (HL¹) lying between these at 158-160°C. This slightly unexpected behaviour can now be better understood in the light of the available crystallographic data as *N,N*-diethyl-*N'*-9-anthracoylthiourea (HL¹) did not show any π - π interactions in the solid state as expected.

Table 12 Bond lengths of selected *N,N*-dialkyl-*N'*-acylthiourea ligands (Å).

Bond	HL ¹	HL ²	HL ³	HL ⁶	HL ¹¹
C9-C(O)	1.503(3)	1.513(6)	1.510(2)	1.537(1)	1.498(4)
C=O	1.218(3)	1.235(5)	1.213(2)	1.220(1)	1.230(3)
(O)C-N	1.373(3)	1.343(6)	1.373(2)	1.377(1)	1.362(4)
N-C(S)	1.417(3)	1.391(5)	1.401(2)	1.398(1)	1.448(4)
C=S	1.676(2)	1.667(4)	1.673(8)	1.667(1)	1.672(3)
S(C)-N	1.321(3)	1.323(5)	1.3442(2)	1.349(1)	1.320(4)

The relevant bond lengths of four of the ligands have been shown in Table 12 and data from *N,N*-diethyl-*N'*-benzoylthiourea⁶⁷ (HL¹¹) has been included for comparison. It is apparent that the (O)C-N, N-C(S) and S(C)-N bonds are all shorter than the average C-N single bond distance of 1.472(5) Å. In general the N-C(S) bonds are slightly longer than both the (O)C-N and S(C)-N bonds, with the latter being the shortest of the three bond types hence giving rise to the trend N-C(S) > (O)C-N > S(C)-N. This would appear to confirm the NMR observations of electronic delocalisation in this region; particularly the partial double bond character of the S(C)-N bond giving rise to the inequivalent carbon and proton NMR resonances of the amine substituents section 2.2.3.1. The C9-C(O) bond in the acyl substituted ligand (HL⁶) is marginally longer than the corresponding bond in the aroyl substituted ligands, possibly indicating a degree of resonance between the carbonyl group and aromatic groups. This would be consistent with the NMR results obtained where an alteration in the carbonyl substituent affected the position of the aromatic carbon resonances (section 2.2.3.1).

Table 13 shows relevant torsion angles which give an indication of the differing orientations of the carbonyl and thiocarbonyl groups relative to each other. In general, the oxygen and sulphur atoms are orientated away from each other, however this is not observed for the di(2-hydroxyethyl)amine derivatives (HL³ and HL⁶), where these two atoms are almost in the same plane, most likely due to the intramolecular hydrogen bonding in these structures. A similar observation has been made of the closely related *N,N*-di(2-hydroxyethyl)-*N'*-benzoylthiourea.²⁶ The opposite orientation of the oxygen and sulphur

atoms observed in HL¹ presumably being due to the intermolecular hydrogen bond (N(H)...S) as previously mentioned. The torsion angle C9a-C9-C11-O1 has been included to illustrate the orientation of the carbonyl group relative to the plane of the aromatic ring, and in all three cases (HL¹-HL³) the oxygen atom is roughly perpendicularly orientated above the aromatic plane. This is in contrast to the structure of 9-anthraldehyde determined by Trotter where the carbonyl group lies approximately in the plane of the aromatic moiety.⁶⁸ The angles are also on average larger than in the benzoyl derivative, where the torsion angle is significantly smaller than 90°.

Table 13 Torsion angles of selected *N,N*-dialkyl-*N'*-acylthiourea derivatives.

Torsion Angle	HL ¹	HL ²	HL ³	HL ⁶	HL ¹¹
C9a-C9-C11-O1	-78.4°	-92.1°	-84.0°	-	-34.3°
O1-C11-N1-C12	-20.7°	-14.0°	0.6°	15.8°	12.5°
S1-C12-N1-C11	-106.2°	-122.5°	33.5°	27.9°	100.4°

2.2.4.6 Crystal and molecular structure of *N,N*-diethyl-*N'*-[4-(pyrene-1-yl)butanoyl]thiourea (HL⁷)

Crystals of HL⁷ were isolated by the slow evaporation of a chloroform solution of the compound and crystallised out in the *P2₁/a* space group with four molecular units per unit cell (Table 21). Figure 32 illustrates the molecular structure. Relevant torsion angles are given in Table 14 and 15 and relevant bond lengths are given in Table 16.

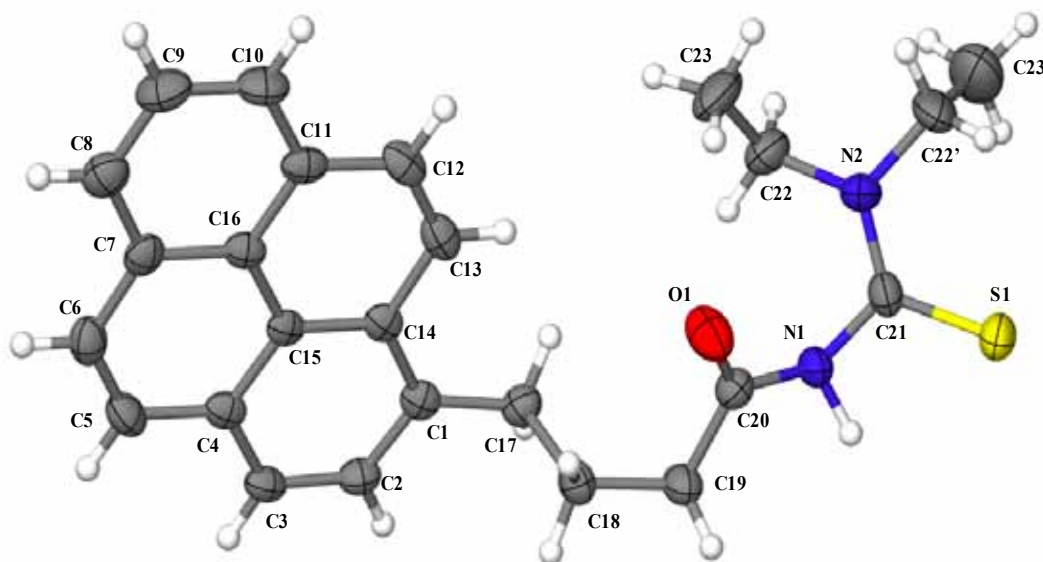


Figure 32 Molecular structure of *N,N*-diethyl-*N'*-[4-(pyrene-1-yl)butanoyl]thiourea (HL⁷).

This compound (HL⁷), like its anthracene analogue (HL¹), also exhibits a form of dimerisation, with hydrogen bonds between the N-H and S1 of an adjacent molecule (1-X, 1-Y, -Z-1) having a distance of 2.59(8) Å, and N1-S1 = 3.448(6) Å (Figure 33), these comparing well with the corresponding distances in the anthracene analogue (H-S = 2.62(3) Å).

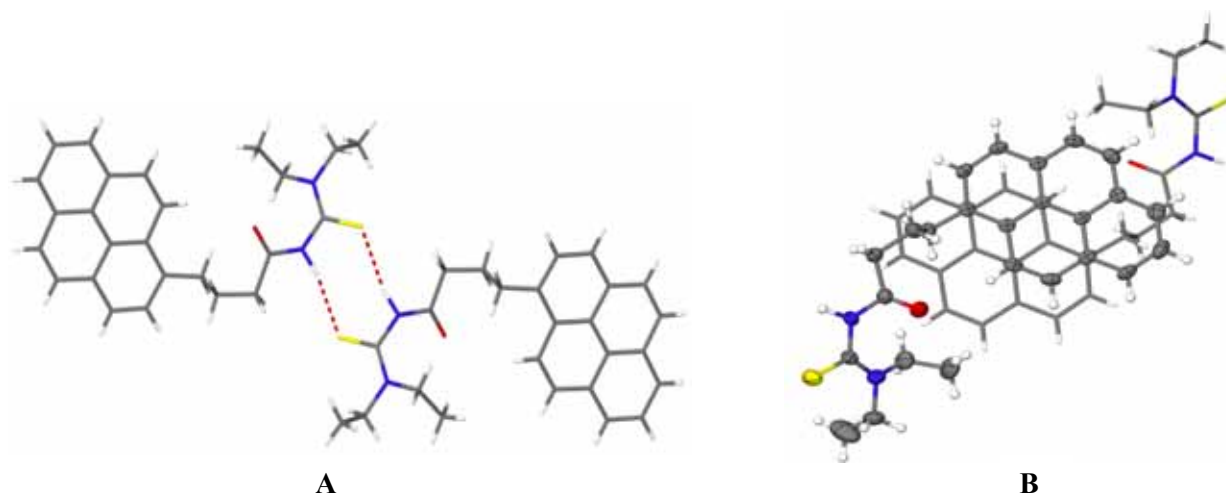


Figure 33 Intermolecular hydrogen bonding ($N(H)\dots S = 2.59(8) \text{ \AA}$) leading to dimerisation of HL^7 (**A**) and offset π - π overlap (**B**).

The pyrene moiety is planar with the maximum deviation from the least squares plane of the aromatic carbons being 0.0068 \AA , significantly less than in the case of the anthracene derivatives. Two adjacent molecules in opposite orientations (symmetry operator $1-X, 2-Y, -Z$) exhibited an offset (Figure 33) π - π overlap with the closest carbon-carbon distance between C13 and C15 being $3.429(8) \text{ \AA}$, (Figure 33), this comparing well with the face-to-face dimers found in unsubstituted pyrene⁶⁹ (3.47 \AA). The closest C-H distance in a T shaped contact was between H2 and C14 on an adjacent molecule (symmetry operator $\frac{1}{2}-X, Y-\frac{1}{2}, -Z$) and had a distance of 2.773 \AA , where $C2-C14 = 3.590(8) \text{ \AA}$. This compound showed a dimeric herringbone packing structure (Figure 34).

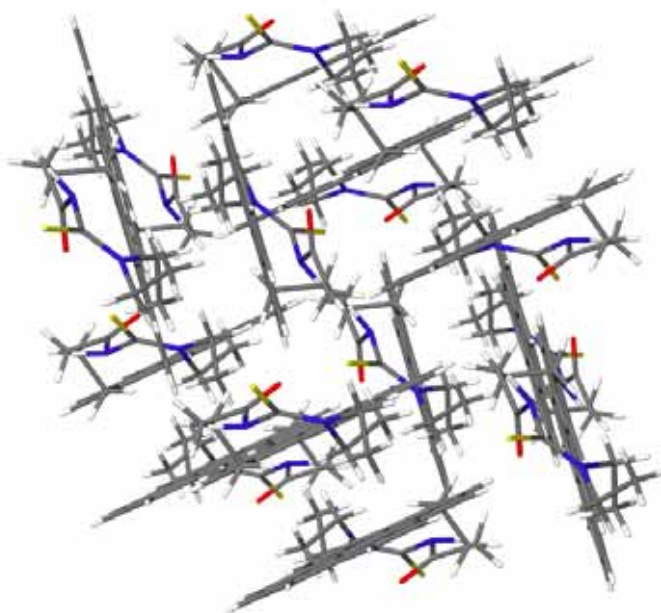


Figure 34 Molecular packing of N,N -diethyl- N' -[4-(pyrene-1-yl)butanoyl]thiourea (HL^7).

2.2.4.7 Crystal and molecular structure of *N*-morpholine-*N'*-[4-(pyrene-1-yl)butanoyl]thiourea (HL^8)

Crystals of HL^8 were isolated from a solvent mixture of chloroform and pentane, and these, similarly to the diethylamine derivative, crystallised out in the $P2_1/c$ space group with four molecular units per unit cell (Table 22). Figure 35 gives the atomic numbering.

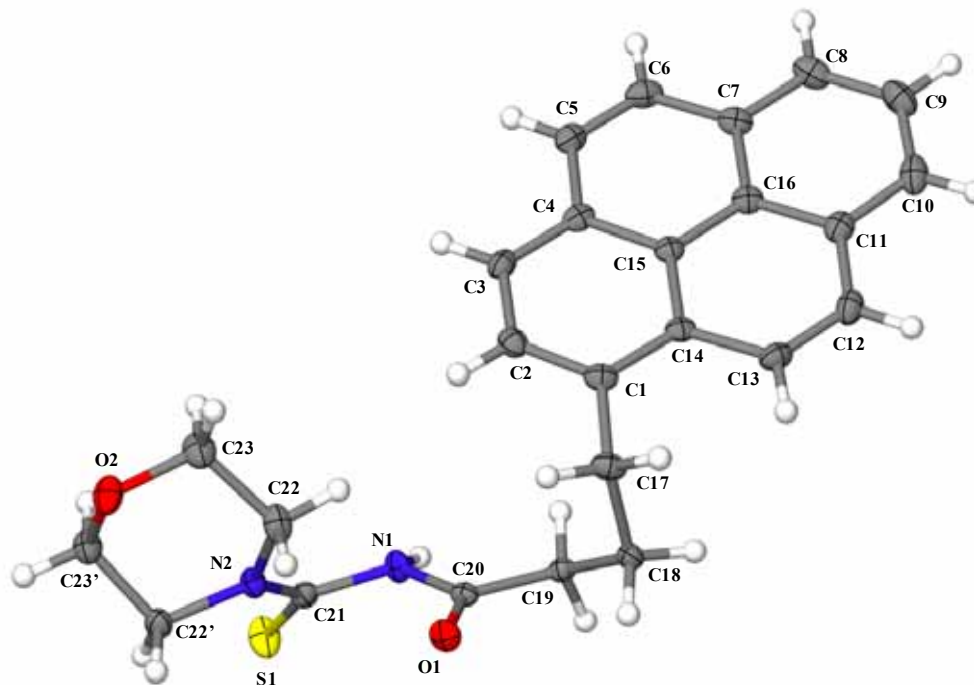


Figure 35 Molecular structure of *N*-morpholine-*N'*-[4-(pyrene-1-yl)butanoyl]thiourea (HL^8).

This compound exhibited hydrogen bonding between the thioamidic proton (located from the difference fourier map) and carbonyl oxygen of an adjacent molecule (symmetry operator $X, \frac{1}{2}-Y, Z-\frac{1}{2}$) $N(H) - O1 = 2.18(3) \text{ \AA}$ and $N1-O1 = 3.019(2) \text{ \AA}$). Interestingly no hydrogen bonding is observed between the thioamidic proton and $O2$ of the morpholine moiety as was the case with the anthracene analogue (HL^2). The morpholine moiety was however in a similar orientation to that in *N*-morpholine-*N'*-9-anthracoyl thiourea, (torsion angles $N2-C22'-C23'-O2 = 57.7$ and 56.9° respectively). The pyrene moiety was slightly concave with the maximum deviation from the least squares plane of the aromatic carbons being 0.0361 \AA . The $\pi-\pi$ overlap was also offset in this compound, however in a different fashion to that of the diethylamine derivatised analogue (HL^7) (Figure 36) – the closest carbon - carbon distances being $3.354(3) \text{ \AA}$ ($C11 - C3$). The two moieties involved in this interaction were related by the $1-X, -Y, 1-Z$ symmetry operator. The pyrene moieties of the two adjacent molecules connected by the intermolecular hydrogen bond, were in a perpendicular orientation with the closest carbon - hydrogen ($C9 - H12$) distance being 2.911 \AA , $C9-C12 = 3.763(3) \text{ \AA}$.

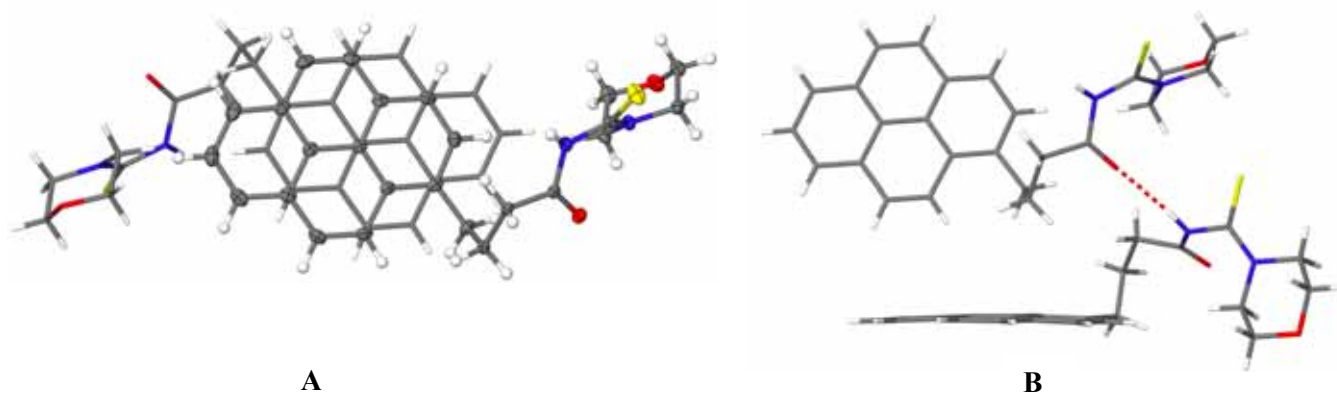


Figure 36 Offset π overlap between pyrene moieties (A) and intramolecular hydrogen bond N(H)-O1 = 2.59(8) Å with T shaped contact between aromatic moieties of HL⁸ (B).

The compound exhibited a similar dimeric herringbone packing structure to that of the diethylamine derivative, and formed planes of alternating aromatic and hydrogen bonding sections (Figure 37).

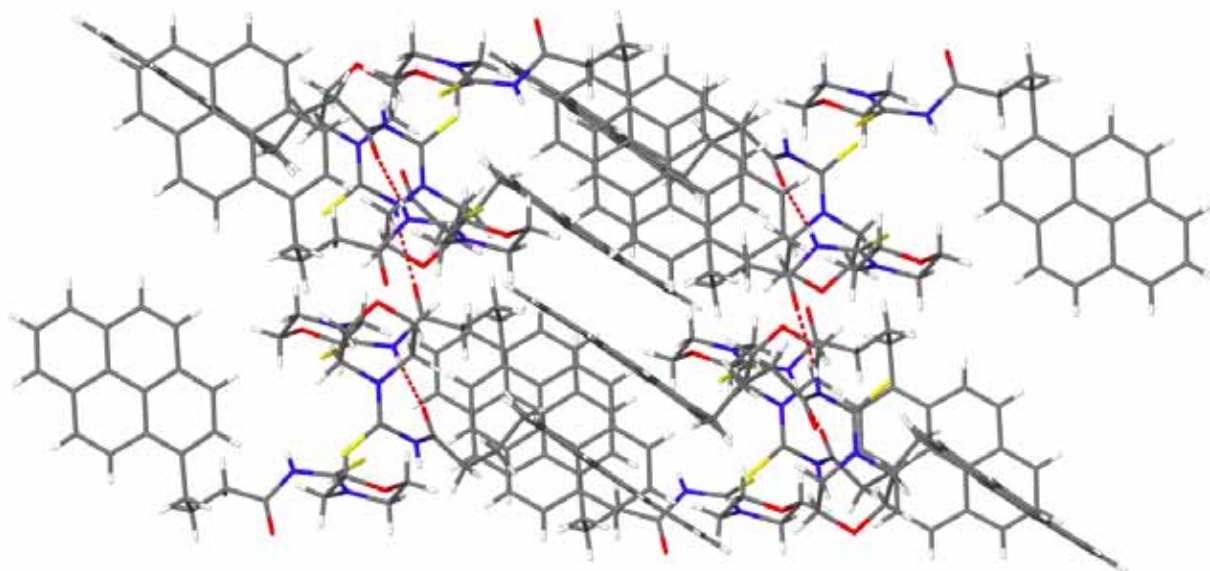


Figure 37 Molecular packing of *N*-morpholine-*N'*-[4-(pyrene-1-yl)butanoyl]thiourea (HL⁸).

In the case of the diethylamine derivative (HL⁷), only 2 of the pyrene rings show an appreciable overlap, whereas in HL⁸ all four rings overlap with the adjacent molecule. It is therefore interesting to note that the latter compound has the higher melting point of the two (161.6-163°C and 142.1-143.5°C respectively) and it is tempting to speculate on the degree of overlap between the rings and the strength of the intermolecular interaction, however other factors can not be excluded such as the presence of hydrogen bonding etc. The melting point of *N,N*-diethyl-*N'*-[pyrene-1-ylacetyl]thiourea is 141.7-142.5°C, and very close to that of the pyrenebutanoyl analogue (HL⁷). While crystals of this compound could be isolated, they did not refract sufficiently to enable the collection of a data set. This was unfortunate as an examination of the intermolecular interactions exhibited by this compound would be most interesting in light of the crystal packing exhibited by *N,N*-diethyl-*N'*-[4-(pyrene-1-yl)butanoyl]thiourea (HL⁷).

The alkyl chains of the two pyrenebutanoylthiourea derivatives were in slightly different orientations as can be seen from the torsion angles in Table 14.

Table 14 Torsion angles of pyrenebutanoylthiourea derivatives illustrating the differing alkyl chain orientations.

Torsion angles	HL ⁷	HL ⁸
C2-C1-C17-C18	-82.0°	-100.5°
C1-C17-C18-C19	-175.5°	53.6°
C17-C18-C19-C20	73.9°	67.6°
C18-C19-C20-O1	24.7°	27.2°

The torsion angles below (Table 15) give an indication of the positions of the carbonyl and thiocarbonyl groups relative to each other. *N,N*-diethyl-*N'*-benzoylthiourea⁶⁷ (HL¹¹) has been included for comparison and it is apparent that the two groups are in opposite orientations as in the corresponding anthracene analogues, indicating again that the deviation in the case of *N,N*-di(2-hydroxyethyl)-*N'*-9-anthracoylthiourea and *N,N*-di(2-hydroxyethyl)-*N'*-pivaloylthiourea is most likely due to the presence of the intramolecular hydrogen bond.

Table 15 Torsion angles of pyrenebutanoylthiourea derivatives.

Torsion angles	HL ⁷	HL ⁸	HL ¹¹
O1-C20-N1-C21	10.8°	-6.3°	12.5°
S1-C21-N1-C20	120.6°	127.7°	100.4°

Table 16 Selected bond lengths of pyrenebutanoylthiourea derivatives (Å).

Bond	HL ⁷	HL ⁸	HL ¹¹
C(20)-C(O)	1.512(11)	1.509(3)	1.498(4)
C=O	1.218(10)	1.216(2)	1.230(3)
(O)C-N	1.387(10)	1.388(3)	1.362(4)
N-C(S)	1.401(10)	1.406(3)	1.448(4)
C=S	1.677(8)	1.674(2)	1.672(3)
S(C)-N	1.341(10)	1.332(3)	1.320(4)

The relevant bond lengths of the two pyrenebutanoylthiourea ligands are shown in Table 16, these again being compared to *N,N*-diethyl-*N'*-benzoylthiourea (HL¹¹).⁶⁷ The bond lengths are very similar to those of the *N,N*-dialkyl-*N'*-9-anthracoylthioureas and similar conclusions can be drawn, in that the partial double bond character of the C-N bonds is more apparent in the alkyl substituted S(C)-N bonds than in the amide (O)C-N bonds. The C19-C(O) bonds are of a comparative length to the anthracoylthiourea derivatives,

however the pivaloylthiourea derivative (HL⁶) shows on average a slightly longer bond. This is interesting because these compounds (pyrenebutanoylthiourea and pivaloylthiourea derivatives) can be classified as acylthioureas as opposed to aroylthioureas. In the latter a certain amount of resonance would be expected between the aromatic moieties and carbonyl carbon (possibly leading to a shortening of this bond), especially in light of the NMR results obtained. This is however not observed, as the bond lengths of these two compounds compare well with those of the anthracene analogues.

2.2.5 Conclusion

It is fitting to conclude this work on ligand synthesis by briefly summarising the results outlined in the sections above.

The conversion of 9-anthracenecarboxylic acid, 4-(1-pyrene)butyric acid and 1-pyreneacetic acid to their corresponding aroyl chlorides was achieved, ultimately in high yields. From the series of experiments completed in this area of work it was apparent that 9-anthracenecarboxylic acid exhibited a greater sensitivity to harsh reaction conditions including extended periods of heating and exposure to light, than 4-(1-pyrene)butyric acid and 1-pyreneacetic acid.

Various anthracoylthiourea and pivaloylthiourea derivatives were successfully synthesised using the Douglass and Dains method of ligand synthesis. In this procedure the isothiocyanate intermediate exhibits two electrophilic centres. Preferential nucleophilic attack is governed by the steric constraints of both the acyl group and the nucleophile. This was illustrated by the differing yields obtained for the anthracoylthiourea and pyrenebutanoylthiourea derivatives using the Douglass and Dains method. Increased steric congestion at the carbonyl carbon, by use of a carbonyl substituent such as anthracene, and the use of an amine in which the lone pair of electrons on the nitrogen atom is less exposed, such as diethylamine, leads to preferential attack at the thiocarbonyl carbon, and the formation of the desired *N,N*-dialkyl-*N'*-aroylthiourea ligand. In cases where the carbonyl substituent is not bulky, such as the pyrenebutanoylthiourea derivatives and the lone pair of electrons on the nitrogen atom of the amine is exposed, such as morpholine, preferential nucleophilic attack at the carbonyl carbon leads to the formation of the undesired *N*-substituted amide.

The Dixon and Taylor method provides an elegant synthetic alternative as the presence of competing electrophilic centres is avoided and this method could be used to synthesise *N,N*-dialkyl-*N'*-aroylthiourea ligands where the acyl substituent was not bulky, or where the amine had an apical nitrogen atom leading to greater exposure of the lone pair of electrons on this atom.

NMR spectra of all the potentially fluorescent compounds could be obtained and the use of two-dimensional spectroscopy enabled the full assignments of all the aromatic resonances in these compounds. From the results it was evident that the “electronic” communication between the

coordinating thiourea moiety and the pyrene system was limited where a spacer group was present as in the case of the pyrenebutanoylthiourea derivatives. The shorter methylene spacer in the pyreneacetylthiourea derivatives afforded a certain degree of “electronic communication” between the thiourea moiety and the pyrene fluorophore. A certain amount of resonance between the anthracene fluorophore and the thiourea moiety was apparent. These observations could have important implications in the fluorescent properties of these compounds.

Crystal structures of all the anthracoylthiourea derivatives could be obtained and these exhibited interesting inter- and intramolecular interactions. *N,N*-diethyl-*N'*-9-anthracoylthiourea exhibits an intramolecular hydrogen bond between the sulphur atom and thioamidic N-H proton. *N*-morpholine-*N'*-9-anthracoylthiourea was the only ligand in this series to exhibit π interactions. A crystal structure of *N,N*-di(2-hydroxyethyl)-*N'*-pivaloylthiourea was acquired and this exhibited similar inter- and intramolecular hydrogen bonding to that of its anthracoyl analogue, namely *N,N*-di(2-hydroxyethyl)-*N'*-9-anthracoylthiourea. X-ray analysis of *N,N*-diethyl-*N'*-[4-(pyrene-1-yl)butanoyl]thiourea and *N*-morpholine-*N'*-[4-(pyrene-1-yl)butanoyl]thiourea was also possible. Similarly to its anthracoyl analogue, *N,N*-diethyl-*N'*-[4-(pyrene-1-yl)butanoyl]thiourea also exhibited an intramolecular hydrogen bond between the sulphur atom and the thioamidic N-H proton. *N*-morpholine-*N'*-[4-(pyrene-1-yl)butanoyl]thiourea exhibited intermolecular hydrogen bonding between the carbonyl oxygen atom and the thioamidic N-H proton, this was in contrast to its anthracoyl analogue where the intermolecular hydrogen bond occurred between the oxygen atom situated in the morpholine ring and that of the thioamidic N-H proton. Both these pyrenebutanoylthiourea derivatives exhibited π - π interactions, however the degree of overlap between the aromatic rings differed.

Table 17 Crystallographic data for *N,N*-diethyl-*N'*-9-anthracoylthiourea (HL¹).

Empirical Formula	C ₂₀ H ₂₀ N ₂ OS	
Formula Weight /gmol ⁻¹	336.44	
Crystal system	Monoclinic	
Space Group	<i>P</i> 2 ₁ / <i>n</i>	
Unit cell dimensions	<i>a</i> /Å	7.4431 (16)
	<i>b</i> /Å	10.373 (2)
	<i>c</i> /Å	22.083 (5)
	β /°	92.190 (4)
	<i>V</i> /Å ³	1703.7 (6)
	<i>Z</i>	4
<i>D_c</i> /gcm ⁻³	1.312	
<i>F</i> (000)	712	
Temperature /K	100 (2)	
Absorption coefficient /mm ⁻¹	0.199	
Crystal size /mm ³	0.310 x 0.241 x 0.194	
Theta range for data collection /°	1.85 - 26.00	
Limiting Indices	-9 ≤ <i>h</i> ≤ 9 ; -12 ≤ <i>k</i> ≤ 12 ; -27 ≤ <i>l</i> ≤ 27	
Reflections collected / unique	16985 / 3333	
Completeness to theta /%	99.7	
Radiation	MoK α , graphite monochromated	
Refinement method	Full-matrix-least-squares on <i>F</i> ²	
Data / restraints / parameters	3333 / 0 / 235	
Goodness-of-fit on <i>F</i> ²	1.028	
Final <i>R</i> indices [<i>I</i> > 2 σ (<i>I</i>)]	5.35, 14%	
<i>R</i> indices (all data)	<i>R</i> = 0.0584; <i>wR</i> ₂ = 0.1441	
Largest diff. peak and hole	1.093, -0.402	

Table 18 Crystallographic data for *N*-morpholine-*N'*-9-anthracoylthiourea (HL²).

Empirical Formula	C ₂₀ H ₁₈ N ₂ O ₂ S	
Formula Weight /gmol ⁻¹	350.42	
Crystal system	Triclinic	
Space Group	<i>P</i> -1	
Unit cell dimensions	<i>a</i> /Å	7.781 (4)
	<i>b</i> /Å	9.249 (5)
	<i>c</i> /Å	13.283 (8)
	α /°	81.848 (10)
	β /°	73.897 (10)
	γ /°	71.250 (9)
	<i>V</i> /Å ³	868.3 (9)
<i>Z</i>	2	
<i>D_c</i> /gcm ⁻³	1.340	
<i>F</i> (000)	368	
Temperature /K	100 (2)	
Absorption coefficient /mm ⁻¹	0.202	
Crystal size /mm ³	0.25 x 0.125 x 0.1	
Theta range for data collection /°	1.6 - 27	
Limiting indices	-9 ≤ <i>h</i> ≤ 9; -11 ≤ <i>k</i> ≤ 11; -16 ≤ <i>l</i> ≤ 16	
Reflections collected / unique	9634 / 3738	
Completeness to theta /%	98.8	
Radiation	MoK α , graphite monochromated	
Refinement method	Full-matrix-least-squares on <i>F</i> ²	
Data / restraints / parameters	3738 / 0 / 226	
Goodness-of-fit on <i>F</i> ²	1.030	
Final R indices [<i>I</i> > σ (<i>I</i>)]	10.0; 24.1%	
R indices (all data)	R = 0.1234 <i>w</i> R ₂ = 0.258	
Largest diff. peak and hole	1.387 ; -0.565	

Table 19 Crystallographic data for *N,N*-di(2-hydroxyethyl)-*N'*-9-anthracoylthiourea (HL³).

Empirical Formula		C ₂₀ H ₂₀ N ₂ O ₃ S
Formula Weight /gmol ⁻¹		368.44
Crystal system		Orthorhombic
Space Group		<i>P</i> 2 ₁ 2 ₁ 2 ₁
Unit cell dimensions	<i>a</i> /Å	7.8352 (5)
	<i>b</i> /Å	9.4013 (6)
	<i>c</i> /Å	24.141 (2)
	<i>V</i> /Å ³	1778.28 (19)
<i>Z</i>		4
<i>D_c</i> /gcm ⁻³		1.376
<i>F</i> (000)		776
Temperature /K		100 (2)
Absorption coefficient /mm ⁻¹		0.205
Crystal size /mm ³		0.237 x 0.193 x 0.114
Theta range for data collection /°		1.69 – 26.99
Limiting indices		-10 ≤ <i>h</i> ≤ 10; -11 ≤ <i>k</i> ≤ 12; -30 ≤ <i>l</i> ≤ 30
Reflections collected / unique		19985 / 3870
Completeness to theta /%		100
Radiation		MoKα, graphite monochromated
Refinement method		Full-matrix-least-squares on <i>F</i> ²
Data / restraints / parameters		3870 / 0 / 237
Goodness-of-fit on <i>F</i> ²		1.091
Final <i>R</i> indices [<i>I</i> > σ(<i>I</i>)]		3.81; 8.88%
<i>R</i> indices (all data)		<i>R</i> = 0.04 <i>wR</i> ₂ = 0.090
Largest diff. peak and hole		0.311, -0.178

Table 20 Crystallographic data for *N,N*-di(2-hydroxyethyl)-*N'*-pivaloylthiourea (HL⁶).

Empirical Formula	C ₁₀ H ₂₀ N ₂ O ₃ S	
Formula Weight /gmol ⁻¹	248.34	
Crystal system	Monoclinic	
Space Group	<i>P</i> 2 ₁ / <i>n</i>	
Unit cell dimensions	<i>a</i> /Å	9.7242 (6)
	<i>b</i> /Å	11.7682 (7)
	<i>c</i> /Å	11.0942 (6)
	<i>β</i> /°	93.657 (1)
	<i>V</i> /Å ³	1266.99 (13)
<i>Z</i>	4	
D _c /gcm ⁻³	1.302	
<i>F</i> (000)	368	
Temperature /K	100 (2)	
Absorption coefficient /mm ⁻¹	0.251	
Crystal size /mm ³	0.359 x 0.312 x 0.186	
Theta range for data collection /°	2.53 – 28.24	
Limiting indices	-12 ≤ <i>h</i> ≤ 12; -15 ≤ <i>k</i> ≤ 15; -14 ≤ <i>l</i> ≤ 14	
Reflections collected / unique	14230 / 3025	
Completeness to theta /%	96.5	
Radiation	MoKα, graphite monochromated	
Refinement method	Full-matrix-least-squares on <i>F</i> ²	
Data / restraints / parameters	3026 / 0 / 154	
Goodness-of-fit on <i>F</i> ²	1.056	
Final R indices [<i>I</i> > σ(<i>I</i>)]	3.20; 8.6%	
R indices (all data)	R = 0.0336 <i>w</i> R ₂ = 0.0873	
Largest diff. peak and hole	0.418 ; -0.211	

Table 21 Crystallographic data for *N,N*-diethyl-*N'*-[4-(pyrene-1-yl)butanoyl]thiourea (HL⁷).

Empirical Formula	C ₂₅ H ₂₆ N ₂ OS	
Formula Weight /gmol ⁻¹	402.54	
Crystal system	Monoclinic	
Space Group	<i>P</i> 2 ₁ / <i>a</i>	
Unit cell dimensions	<i>a</i> /Å	13.7970 (2)
	<i>b</i> /Å	9.6919 (2)
	<i>c</i> /Å	16.2624 (3)
	β	103.8100 (10)°
	<i>V</i> /Å ³	2111.73 (7)
<i>Z</i>	4	
D _c /gcm ⁻³	1.266	
<i>F</i> (000)	856	
Temperature /K	173 (2)	
Absorption coefficient /mm ⁻¹	0.172	
Theta range for data collection /°	2.59 – 25.00	
Limiting Indices	-16 ≤ <i>h</i> ≤ 16 ; -11 ≤ <i>k</i> ≤ 11 ; -19 ≤ <i>l</i> ≤ 19	
Reflections collected / unique	7188 / 3714	
Completeness to theta /%	99.7	
Radiation	MoK α , graphite monochromated	
Refinement method	Full-matrix-least-squares on <i>F</i> ²	
Data / restraints / parameters	3714/ 0 / 269	
Goodness-of-fit on <i>F</i> ²	1.136	
Final <i>R</i> indices [<i>I</i> > 2 σ (<i>I</i>)]	12.24; 36.28%	
<i>R</i> indices (all data)	<i>R</i> = 0.1365 <i>wR</i> ₂ = 0.3696	
Largest diff. peak and hole	1.169, -0.394	

Table 22 Crystallographic data for *N*-morpholine-*N'*-[4-(pyrene-1-yl)butanoyl]thiourea (HL⁸).

Empirical Formula	C ₂₅ H ₂₄ N ₂ O ₂ S	
Formula Weight /gmol ⁻¹	416.52	
Crystal system	Monoclinic	
Space Group	<i>P</i> 2 ₁ / <i>c</i>	
Unit cell dimensions	<i>a</i> /Å	14.1775 (15)
	<i>b</i> /Å	14.3336 (16)
	<i>c</i> /Å	9.8092 (11)
	β	93.344 (2)°
	<i>V</i> /Å ³	1990.0 (4)
<i>Z</i>	4	
Dc /gcm ⁻³	1.390	
<i>F</i> (000)	880	
Temperature /K	100 (2)	
Absorption coefficient /mm ⁻¹	0.189	
Theta range for data collection /°	2.02 – 28.22	
Limiting Indices	-18 ≤ <i>h</i> ≤ 18 ; -14 ≤ <i>k</i> ≤ 18 ; -12 ≤ <i>l</i> ≤ 11	
Reflections collected / unique	12331 / 4633	
Completeness to theta /%	94.4	
Radiation	MoK α , graphite monochromated	
Refinement method	Full-matrix-least-squares on <i>F</i> ²	
Data / restraints / parameters	4633/ 0 / 271	
Goodness-of-fit on <i>F</i> ²	1.063	
Final <i>R</i> indices [<i>I</i> > 2 σ (<i>I</i>)]	6.26; 14.14%	
<i>R</i> indices (all data)	<i>R</i> = 0.0756 <i>wR</i> ₂ = 0.1414	
Largest diff. peak and hole	0.474, -0.441	

References

1. I. Douglass, F. Dains, *J. Am. Chem. Soc.*, **1934**, 56, 719-721.
2. J. Bricks, K. Rurack, R. Radeglia, G. Reck, B. Schulz, H. Sonnenschein, U. Resch-Genger, *J. Chem. Soc., Perkin Trans. 2*, **2000**, 2, 1209-1214.
3. A. Dixon, J. Hawthorne, *Pr. Chem. Soc.*, **1907**, 22, 322-323.
4. J. Brindley, J. Caldwell, G. Meakins, S. Plackett, S. Price, *J. Chem. Soc., Perkin Trans. 1.*, **1987**, 1153-1158.
5. H. Salari, M. Yeung, S. Douglas, W. Morozowich, *Anal. Biochem.*, **1987**, 165, 220-229.
6. N. Goeckner, H. Snyder, *J. Org. Chem.*, **1972**, 38, 3, 481-483.
7. W. Wiesler, K. Nakanishi, *J. Am. Chem. Soc.*, **1989**, 111, 26, 9205-9213.
8. Aldrich Chemical Advertisement, *J. Org. Chem.*, **1995**, 60, 6.
9. A. Jackson, G. Angoh, *Chemistry in Britain*, **1993**, 1046-1048.
10. T. Morozumi, T. Anada, H. Nakamura, *J. Phys. Chem. B*, **2001**, 105, 2923-2931.
11. E. Ciganek, *J. Org. Chem.*, **1980**, 45, 1407-1505.
12. M. Schuster, *Technical University München, Germany*, personal correspondence, **2003**.
13. J. Lou, A. Hatton, P. Laibinis, *Anal. Chem.*, **1997**, 69, 1262-1264.
14. C. Tran, J. Fendler, *J. Am. Chem. Soc.*, **1979**, 102, 2923-2928
15. K. Lehto, E. Vourimaa, H. Lemmetyninen, *J. Photochem. Photobiol. A*, **2000**, 136, 53-60.
16. M. Abdel-Mottaleb, H. Galal, A. Dessouky, M. El-Naggar, D. Mekkawi, S. Ali, G. Attya, *Int. J. Photoenergy*, **2000**, 2, 47-53.
17. R. Morrison, R. Boyd, *Organic Chemistry*, Allyn and Bacon Inc, London, 3rd Edn, **1981**.
18. J. McMurry, *Organic Chemistry*, Brooks Cole London, 5th Edition, **2000**.
19. H. Meyer, A. Eckert, *J. Chem. Soc. Abstracts*, **1918**, 114, 385-386.
20. M. Winnik, A. Sinclair, *Can. J. Chem.*, **1985**, 63, 1300-1307.
21. R. Busch, H. Kneuper, T. Weber, *German Patent* 19943844, **2001**.
22. P. Swiatkowski, M. Nilsson, *Swedish Patent* 19871221, **1987**.
23. A. Stamm, J. Henkelmann, *International patent* 2000026171, **2000**.
24. L. Beyer, E. Hoyer, H. Hennig, R. Kirmse, R. Hartmann, H. Liebscher, *J. fur Prakt. Chem.*, **1975**, 317, 829-839.
25. M. Schuster, *Fresenius' J. Anal. Chem.*, **1986**, 324, 127-129.
26. K. Koch, C. Sacht, S. Bourne, *Inorg. Chim. Acta*, **1995**, 232, 109-115.
27. A. Mautjana, J. Miller, A. Gie, S. Bourne, K. Koch, *Dalton Trans*, **2003**, 1952-1960.
28. M. Schuster, B. Kugler, K. Konig, *Fresenius' J. Anal. Chem.*, **1990**, 338, 717-720.
29. J. Miller, *PHD Thesis*, University of Cape Town, **2000**.
30. A. Dixon, J. Taylor, *J. Chem. Soc.*, **1912**, 101, 558-571.
31. A. Dixon, J. Taylor, *J. Chem. Soc., Abstracts*, **1908**, 93-94, 18-31.
32. T. Birkinshaw, D. Gillon, S. Harkin, G. Meakins, M. Tirel, *J. Chem. Soc., Perkin Trans. 1*, **1984**, 2, 147-153.
33. R. Bartsch, Y. Chae, S. Ham, D. Birney, *J. Am. Chem. Soc.*, **2001**, 123, 7479-7486.
34. A. Fairfull, D. Peak, *J. Chem. Soc. Abstracts*, **1955**, 796-802.
35. D. Elmore, J. Ogle, *J. Am. Chem. Soc.*, **1958**, 1141-1145.
36. B. Saville, *Angew. Chem.*, **1967**, 6, 11.
37. A. Williams, W. Jencks, *J. Chem. Soc.*, **1974**, 1753-1760.

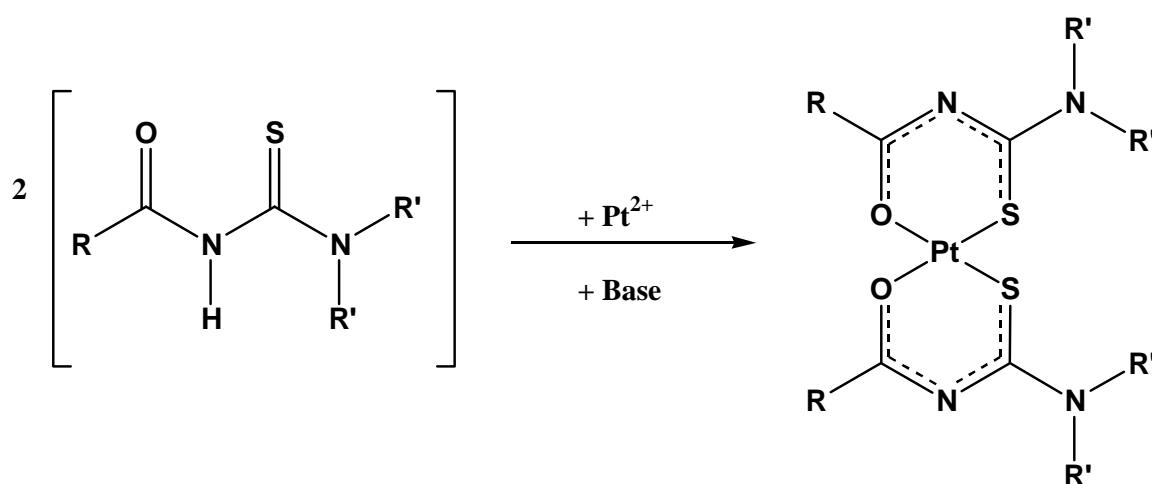
-
38. D. Satchell, R. Satchell, *J. Chem. Soc., Perkin Trans. 2*, **1990**, 1415-1420.
 39. H. Hall, *J. Am. Chem. Soc.*, **1957**, 79, 5441.
 40. D. Satchell, R. Satchell, *Chem. Soc. Reviews*, **1975**, 4, 231-251.
 41. J. Hanna, S. Siggia, *Anal. Chem.*, **1962**, 34, 547.
 42. G. Buchanan, R. Ozubko, *Can. J. Chem.*, **1975**, 53, 1829-1832.
 43. K. Laali, P. Hansen, *J. Org. Chem.*, **1997**, 62, 5804-5810.
 44. P. Hansen, A. Berg, *Org. Mag. Res.*, **1979**, 12, 50-54.
 45. J. Marshall, L. Faehl, A. Ihrig, M. Barfield, *J. Am. Chem. Soc.*, **1976**, 98, 3406-3410.
 46. J. Marshall, A. Ihrig, *J. Am. Chem. Soc.*, **1972**, 94, 1756-1757.
 47. C. Unkefer, R. London, T. Whaley, G. Daub, *J. Am. Chem. Soc.*, **1983**, 105, 733-735.
 48. P.E. Hansen, O. Poulsen, A. Berg, *Org. Mag. Res.*, **1975**, 7, 23-25.
 49. P. Hansen, O. Poulsen, A. Berg, *Org. Mag. Res.*, **1975**, 7, 475-477.
 50. S. Klaasen, G. Daub, D. Vanderjagt, *J. Am. Chem. Soc.*, **1983**, 105, 4361-4366.
 51. M. Bullpit, W. Kitching, *J. Org. Chem.*, **1976**, 41, 760-766.
 52. J. Bromilow, R. Brownlee, R. Topsom, *J. Am. Chem. Soc.*, **1976**, 98, 2020-2022.
 53. W. Adcock, M. Aurangzeb, W. Kitching, N. Smith, D. Doddrell, *Aust. J. Chem.*, **1974**, 27, 1817-1821.
 54. S. Kaplan, *Org. Mag. Res.*, **1981**, 15, 197-199.
 55. H. Friebolin, *Basic 1 and 2 Dimensional NMR spectroscopy*, **1998**, 3rd Edition, Wiley, Toronto, 68-69.
 56. I. Schuster, *J. Am. Chem. Soc.*, **1981**, 103, 5110-5118.
 57. B. Cheney, D. Grant, *J. Am. Chem. Soc.*, **1967**, 89, 21.
 58. G. Anderson, R. Parish, L. Stock, *J. Am. Chem. Soc.*, **1971**, 93, 25.
 59. K. Koch, C. Sacht, T. Grimmbacher, S. Bourne, *S. African J. Chem*, **1995**, 48, 71-77.
 60. M. Schuster, E. Unterreitmaier, *Fresenius' J. Anal. Chem.*, **1993**, 346, 630-633.
 61. G. Desiraju, A. Gavezzotti, *Acta Crystallogr. Sect. C*, **1989**, B45, 473-482.
 62. G. Desiraju, A. Gavezzotti, *Chem. Commun.*, **1989**, 621-623.
 63. F. Yang, P. Fanwick, C. Kubiak, *Inorg. Chem.*, **2002**, 41, 4805-4809.
 64. M. Kato, J. Takahashi, Y. Sugimoto, C. Kosuge, S. Kishi, S. Yano, *Dalton Trans*, **2001**, 747-752.
 65. T. Grimmbacher, *PhD Thesis*, **1995**, University of Cape Town, RSA.
 66. C. Sacht, M. Datt, S. Otto, A. Roodt, *Dalton Trans*, **2003**, 1952-1960.
 67. M. Bolte, L. Fink, *Private communication to CCD*, **2003**, Crystal nm - CCDC214315.
 68. J. Trotter, *Acta Crystallogr. Sect. C*, **1959**, 12, 922.
 69. T. Olszak, F. Willig, W. Durfee, W. Dreissig, H. Bradaczek, *Acta Crystallogr. Sect. C*, **1989**, 45, 803-805 and references therein.

3.1 Synthesis of Pt(II) and Pd(II) complexes

3.1.1 Introduction

It is well known that the *N,N*-dialkyl-*N'*-acylthioureas form stable metal complexes with a variety of different transition metal ions.¹⁻³ Coordination takes place through the sulphur and oxygen atoms and this distinguishes these compounds as ligands, in that coordination to the softer metals can be promoted by the sulphur atom and coordination to harder metals by the oxygen atom, resulting in complexation to a variety of metal ions, traditionally considered to be both “hard” *e.g.* Cu(II), Ni(II)^{1,2} and “soft” *e.g.* Pd(II), Pt(II) and Hg(II).³ The *N,N*-dialkyl-*N'*-acylthiourea ligands have been shown to have an affinity for the platinum group metals and their selective complexation to the PGM's has been demonstrated in chloride rich solutions where complexation to Pt(II), Pd(II) and Rh(III) takes place at pH < 2 while at pH conditions where pH > 3, complexation to Ni(II), Zn(II) and Co(II) also takes place.⁴ Further work has been carried out on these metal chelates in order to study the influence that different substituents on the ligand have on the metal-ligand bond in particular, however these studies have thus far been limited to the Ni(II) and Cu(II) complexes.⁵ This study focuses on complex formation with Pt(II) and Pd(II), this being motivated by the impact these two metals have on the South African economy (section 1.1). These metals have a well established chemistry in their (II) and (IV) oxidation states, as well as chemistry in the (0) state with some tertiary phosphine and carbonyl ligands.⁶ In general Pt(II) and Pd(II) show a preference for nitrogen and softer heavy donor atoms such as P, As and S, with a relatively lower affinity for harder donors such as O and F.⁷ It is therefore interesting that these ligands exhibit bidentate coordination in which both the oxygen and sulphur atoms are bound to the metal ion. The thioamidic proton (N-H) is marginally acidic and deprotonation of this nitrogen most likely results in the carbonyl oxygen exhibiting a negative charge thus enabling its coordination. The bidentate coordination consequently results in a six membered chelate ring with relatively extensive electronic delocalisation (Scheme 10).

In the case of Pt(II) and Pd(II), coordination takes place with a 2:1 stoichiometry with the metal centre adjoining two chelate rings (Scheme 10). The concomitant loss of the two thioamidic protons results in the formation of *cis*-[M(L-S,O)₂] complexes, where M represents the metal and L the deprotonated ligand; S and O, indicating coordination through the sulphur and oxygen atoms respectively.



Scheme 10 Bidentate coordination of *N,N*-dialkyl-*N'*-acylthioureas to d^8 metal ions, resulting in square planar metal complexes.

The literature is dominated by examples of *N,N*-dialkyl-*N'*-benzoylthioureas involved in Pt(II) and Pd(II) coordination, however very little synthetic detail was available, reporting the coordination of acylthioureas, as opposed to aroylthioureas, to Pd(II) in particular,⁸ and it was with interest that this metal was reacted with the pyrenebutanoylthiourea derivatives. Whilst the Ni(II) and Cu(II) complexes of *N,N*-dioctyl-*N'*-9-anthracoylthiourea have been reported,⁹ the Pt(II) and Pd(II) complexes of *N,N*-diethyl-*N'*-9-anthracoylthiourea, to the best of our knowledge, had yet to be synthesised.

A particularly interesting study of the related *N,N*-tetramethylene-*N'*-9-anthracoylthiourea ligand done by Bricks *et al.*¹⁰ deserves further mention here. In an attempt to synthesise the Cu(II) complex of this ligand, the aroylthiourea was reacted with $\text{Cu}(\text{ClO}_4)_2$ in acetonitrile. Instead of isolating the cationic Cu(II) complex however, (previously thought to have given rise to an enhanced fluorescence spectrum¹⁰), a rearrangement of the ligand occurred giving rise to a new molecule, *S*-(9-anthryl)-*N,N*-tetramethyleisothiuronium perchlorate, in which the sulphur atom was bound to the aromatic moiety (Figure 38).

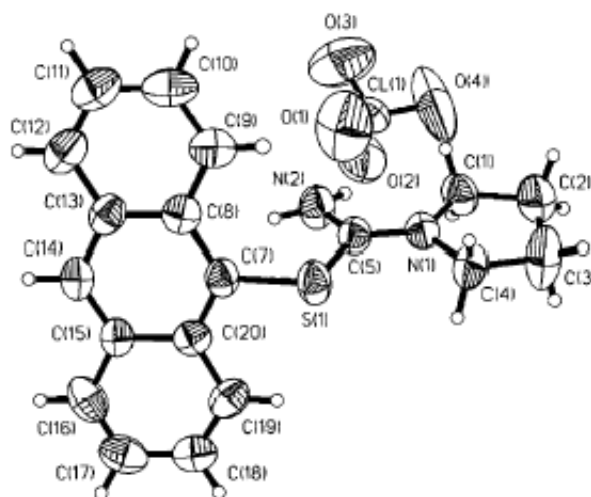
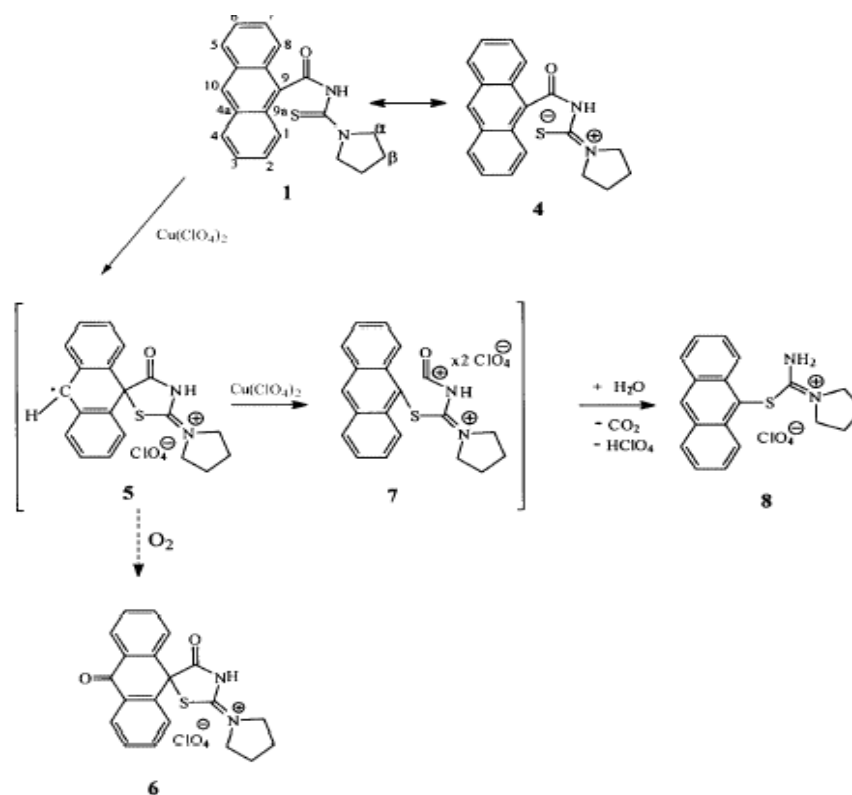


Figure 38 Molecular structure of *S*-(9-anthryl)-*N,N*-tetramethyleisothiuronium perchlorate (**8**).¹⁰

The formation of this molecule, **8** (Scheme 11) reportedly occurred *via* a two step oxidation mechanism, resulting in the formation of a Cu(I) species. The mechanism suggested by Bricks *et al.* is given in Scheme 11.



Scheme 11 Suggested two step oxidative mechanism for the rearrangement observed for *N,N*-tetramethylene-*N'*-9-anthracoylthiourea.¹⁰

Oxidation of the anthracene species by the copper complex, occurs at the most reactive sites of the aromatic moiety (C9 and C10) and this initial oxidation results in the formation of the spiro intermediate **5** (Scheme 11). In terms of the resonance form of the ligand, **4**, the formation of the C9-S bond can be better understood. A further oxidation step restores the aromaticity of the anthracene system, **7**, following which, hydrolysis and stabilisation yielded the observed compound **8**. Interestingly, as a possible confirmation of this proposed mechanistic route, the crystal structure of a derivative of the spiro intermediate could also be obtained, **6**. Further study indicated the instability of the ligand in acetonitrile solution as well as THF under acidic conditions. The addition of HClO_4 also yielded the rearrangement product, even in the absence of an oxidising agent. A proposed protonation mechanism was also postulated, but is not shown here.

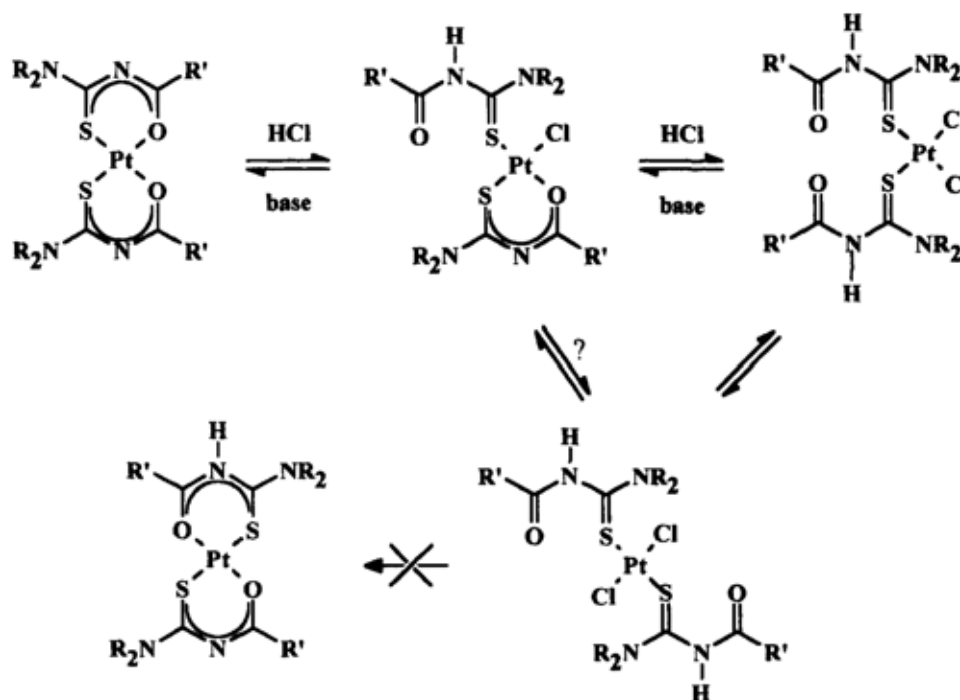
It is interesting that in the synthesis of the Cu(II) complex of the *N,N*-dioctyl-*N'*-9-anthracoylthiourea ligand, no mention was made of the formation of the rearrangement species observed by Bricks *et al.*⁹ The high yield in which this complex was obtained also make it unlikely that a significant quantity of this compound could have been formed as a by-product. It is possible that the use of metal acetate solutions as starting reagents as well as the DMF/water solvent combination, may have prevented the formation of this rearrangement species. It is however noteworthy that the presence of the

anthracene ring gives rise to a potential for rearrangement reactions not observed for naphthyl or benzyl groups being used as carbonyl substituents in such ligands.

From the various crystal structures of metal complexes in the literature, it has been shown that the four donor atoms adopt a square planar geometry around the central metal ions as is expected for d^8 metal centres.⁷ In all except one instance, the crystal structures obtained from the *N,N*-dialkyl-*N'*-acylthiourea ligands exhibiting bidentate coordination to the d^8 metal centres have adopted a *cis* conformation around the central metal ion. This has been attributed to the *trans influence* of the polarisable sulphur atoms where “two soft ligands in mutual *trans* positions will have a destabilising effect on each other when attached to class b metal atoms”.¹¹ There are very few reported cases of where sulphur, for example has exhibited *trans* coordination to a soft metal ion.¹² The unique case in which an *N,N*-dialkyl-*N'*-acylthiourea ligand did give rise to a *trans* metal complex was observed for *trans*-bis(*N,N*-dibutyl-*N'*-naphthoylthioureato)platinum(II).¹³ The large size of the carbonyl substituent on the ligand was initially thought to have affected the conformation of the complex through steric factors, and it was with interest that the anthracoylthiourea ligands in particular were coordinated with Pt(II) and Pd(II); as the larger bulk of the anthracoyl group might be expected to increase the possibility of the formation of a *trans* complex. However, as will become apparent later in this section, only the *cis* complex is formed with anthracoylthiourea ligands, suggesting that other factors in the *cis-trans* isomerisation of these compounds are operative.

Further work has been reported on the complexes of the *N,N*-dialkyl-*N'*-acylthiourea ligands, in particular the chromatographic separation of mixtures of metal complexes has been reported and work has been done on normal phase systems¹⁴ as well as the use of reversed phase separations.⁸ Whilst not all the metal complexes proved to be stable on silica gel, the PGM's reportedly gave good separations with minimal decomposition.¹⁴ The potential for the analytical applications of these systems in metal complex separation is thus apparent.

Coordination of the *N,N*-dialkyl-*N'*-acylthiourea ligands to platinum (II) in particular, is protonation dependant, as has been demonstrated by Koch *et al.*^{15,34} The addition of HCl results in the protonation of the bidentately coordinated ligand, and affords a variety of species in solution. As protonation of one of the ligands takes place, ring opening of the bidentate coordination occurs followed by the coordination of the halide ion, in place of the oxygen atom on the metal centre. Further protonation affords similar results in the second chelating ligand. The $[Pt(HL-S)_2Cl_2]$ species formed can take on either a *cis* or *trans* conformation, the former however predominating in solution at steady-state. The reversible nature of these reactions was demonstrated by treating the acidic solutions with aqueous ammonia which led to the rapid conversion of the species to yield the initial *cis*- $[Pt(L-S,O)_2]$ complex. These observations are summarised in Scheme 12.



Scheme 12 Representation of the effects of HCl addition to *cis*-[Pt(L-S,O)₂] complexes.¹⁵

The monitoring of these species was done using ¹⁹⁵Pt NMR due to the sensitivity of the chemical shifts of this nucleus to changes in the coordination sphere of the Pt(II).¹⁶

The monoalkyl analogues of these ligands, namely the *N*-alkyl-*N'*-acylthioureas, also coordinate to metal ions, however coordination in these cases is generally monodentate taking place through the sulphur atom, resulting in the formation of *cis* and *trans* metal complex isomers.¹⁷ Coordination is limited to the sulphur atom as the oxygen is locked into a planar 6 membered ring through a hydrogen bond with the N-H proton, this presumably preventing coordination of the acyl-carbonyl group.^{18,19}

3.1.2 Synthesis of Platinum (II) complexes

In general these compounds could be synthesised by making use of a mixed solvent system of water and acetonitrile. This was necessary to ensure that both the ligand (generally only soluble in organic solvents) and metal salt (soluble in more polar solvents) remained in solution, until product formation occurred. Two mole equivalents of ligand and a four mole excess of base (sodium acetate) were added to one mole equivalent of Pt(II) salt (usually K₂PtCl₄) at elevated temperatures. In general, yellow product precipitates were collected by centrifugation on cooling of the reaction mixtures to 4°C. Recrystallisation from a combination of chloroform and ethanol⁹ usually yielded solid products. In cases where an “oil” was obtained, sequential extractions with chloroform and removal of the solvent usually yielded a solid product that could be recrystallised from chloroform and ethanol. A slight variation was necessary in the case of the pyrenebutanoylthiourea and pyreneacetylthiourea derivatised ligands as these compounds

were not sufficiently soluble in acetonitrile and acetone was therefore used as a second solvent. More detailed experimental conditions are given in Chapter 5.

Despite the formation of the Cu(II) and Ni(II) complexes of *N,N*-dioctyl-*N'*-9-anthracoylthiourea having been reported,⁹ the Pt(II) complex of *N,N*-diethyl-*N'*-9-anthracoylthiourea could not be formed using K_2PtCl_4 as a starting compound. Whilst a colour change was observed, indicating the occurrence of a reaction and at times a yellow precipitate was formed, the resulting NMR spectra were a very complex collection of peaks, indicating the formation of a mixture of products. Assignment of these varying species was not practically possible, however the appearance of additional resonances in the carbonyl region appeared to indicate that some coordination had occurred, although this was not quantitative as expected. The reported Cu(II) and Ni(II) complexes were synthesised from the metal acetate solutions in a DMF/water solvent combination, and it was thought that the choice of solvent may have influenced the outcome of the reaction. It is well known that acetonitrile is a coordinating solvent, and indeed, K_2PtCl_4 , water and MeCN have been used to synthesise the bis(nitrile) complexes *cis* and *trans* $Pt(NCCH_3)_2Cl_2$.²⁰ The use of dioxane as a solvent did not however do anything to reduce the complexity of the resulting NMR spectra of the products obtained using this as an alternative solvent. In the light of the results obtained during the conversions of 9-anthracenecarboxylic acid to 9-anthracoyl chloride (Section 2.1.3.), where prolonged heating appeared to cause decomposition, the use of heat in this synthetic procedure was a second possible source of concern and may have contributed to the low yield and possible decomposition of the *N,N*-diethyl-*N'*-9-anthracoylthiourea.

Hence an extractive synthetic method similar to that used in the formation of the palladium complexes was attempted (see section 3.1.3). As platinum is known to be less labile than palladium,⁷ this reaction was allowed to proceed for 4 days with intermittent monitoring by TLC. Whilst this too was unsuccessful in affording a satisfactory yield of the complex, the NMR spectra obtained were noticeably cleaner, and it was possible to assign certain ligand peaks, as well as peaks thought to belong to the *cis*- $[Pt(L^1-S,O)_2]$ complex. In an attempt to obtain a Pt(II) complex of an anthracoylthiourea derivative, the morpholine analogue, *N*-morpholine-*N'*-9-anthracoylthiourea, was reacted with K_2PtCl_4 in dioxane and left to recrystallise in the dark, however once again, the NMR spectra indicated a complex mixture of species. Attempted separation of this mixture on a preparative TLC plate and analysis of the resulting fractions did not help to identify the various components.

The unsatisfactory coordination of the *N,N*-dialkyl-*N'*-9-anthracoylthiourea ligands using K_2PtCl_4 as a starting compound, indicated a possible coordination competition between Cl^- ions and the ligand to Pt(II). Thus a different Pt(II) containing starting material was considered. Nitrile complexes of Pt(II) *i.e.* $Pt(NCPr_i)_2Cl_2$, are frequently used as precursors for other coordination compounds due to their general lability and ease of replacement, for example by an organic moiety.²¹ Both the *cis* and *trans* isomers exist,²² however in our case, only the *trans* was available. Reactions with *N,N*-diethyl-*N'*-9-anthracoylthiourea and *N*-morpholine-*N'*-9-anthracoylthiourea using *trans*- $Pt(NCPr_i)_2Cl_2$ were performed

in solvent combinations of acetonitrile and water. The formation of yellow precipitates that did not disappear on addition of excess water showed more promising results. The yellow solids could be isolated by centrifugation and separated on a preparative TLC plate and in both cases NMR evidence of coordination having taken place was clear. However only in the case of the *N,N*-diethyl-*N'*-9-anthracoylthiourea (HL¹) could the platinum complex, *cis*-[Pt(L¹-S,O)₂], be isolated in sufficient yield. *N,N*-diethyl-*N'*-[4-(pyrene-1-yl)butanoyl]thiourea (HL⁷) formed a light brown oil which was extracted with chloroform and recrystallised from an ethanol and chloroform solvent combination to yield a yellow complex *cis*-[Pt(L⁷-S,O)₂].

In the complexation of *N,N*-diethyl-*N'*-[pyrene-1-ylacetyl]thiourea (HL¹⁰) with Pt(II), an oil was obtained and this was extracted with a solvent combination of ethanol and chloroform and a solid product could be isolated and recrystallised from an ethanol and chloroform mixture.

Details of the characterisation of the platinum complexes are given in Chapter 5 and the NMR spectra as well as the X-ray analysis performed will be discussed further in section 3.2.

3.1.3 Synthesis of Palladium (II) complexes

The palladium complexes of *N,N*-diethyl-*N'*-9-anthracoylthiourea, *N,N*-diethyl-*N'*-[4-(pyrene-1-yl)butanoyl]thiourea and *N,N*-diethyl-*N'*-[pyrene-1-ylacetyl]thiourea were synthesised using a method of liquid-liquid extraction. Two mole equivalents of ligand were dissolved in chloroform and mixed with a mole equivalent of K₂PdCl₄ in water. The complete solubility of both compounds was essential to avoid emulsion formation. The aqueous layer usually lost its colour and a colour change in the organic layer was observed after phase contact. The addition of a small amount of base and further shaking of the mixture followed by extraction was usually sufficient to afford high yields of the complexes. More complete experimental details are given in Chapter 5.

The palladium complex of *N,N*-diethyl-*N'*-9-anthracoylthiourea, *cis*-[Pd(L¹-S,O)₂], was easily formed using the liquid-liquid extraction method and found to have poor solubility in almost all solvents except chloroform. The synthesis of the palladium complex of *N*-morpholine-*N'*-9-anthracoylthiourea, *cis*-[Pd(L²-S,O)₂], was also attempted and the formation of a yellow precipitate appeared encouraging, however, the solubility of this compound was limited in all solvents and was insufficient to enable NMR analysis. ESMS results however, indicated the presence of the M⁺ ion (M⁺H⁺ = 805.42).

N,N-diethyl-*N'*-[4-(pyrene-1-yl)butanoyl]thiourea also reacted rapidly with palladium to form the complex *cis*-[Pd(L⁷-S,O)₂] in almost quantitative yields.

The reaction of *N,N*-diethyl-*N'*-[pyrene-1-ylacetyl]thiourea (HL¹⁰) with palladium was less rapid and facile than for the preceding cases, and resulted in the formation of an emulsion despite the ensured solubility of both phases prior to mixing. Careful addition of chloroform however, enabled the separation

of the organic layer and the palladium complex cis -[Pd(L¹⁰-S,O)₂] could be isolated as a solid product following *in vacuo* removal of the solvent.

There was no apparent visible difference in the reaction between the essentially acyl and aroyl thiourea ligands with palladium.

3.1.4 Discussion of complex formation

The differing reactivities of the two starting compounds of platinum, namely K₂PtCl₄ and *trans*-Pt(NCPr_i)₂Cl₂ deserves further discussion. The increased lability of the nitrile complexes is a result, presumably of the weaker donation by the triply bonded nitrogen to the metal ion, than in the case of the bonded chloride ion. The chloride ion, being a charged species most likely has an increased bond strength with the metal ion and it may be for this reason that ligand coordination of the *N,N*-dialkyl-*N'*-9-anthracoylthiourea ligands took place with the former and not the latter. It is also interesting to note that the formation of the palladium complex of a similar starting material (K₂MCl₄) was much more facile than in the case of the platinum. Whilst this may be expected in terms of the increased lability of palladium complexes relative to their platinum counterparts, the increased softness of the platinum ion could be expected to aid complexation. In the *N,N*-dialkyl-*N'*-acylthiourea ligands, the close proximity of the carbonyl group to any aromatic system, such as anthracene in the case of the anthracoylthiourea derivatives, would be expected to result in a certain amount of resonance (section 2.2.3.1) and increased electronic movement through the carbonyl bond, possibly resulting in an increased electron density at the carbonyl oxygen atom. This resonance effect would be expected to increase with the addition of aromatic rings, therefore being more pronounced in the anthracoylthiourea derivatives relative to that of the naphthoyl or benzoylthiourea derivatives. This could possibly further soften the oxygen atom, presumably favouring coordination to the softer metal ions, it is therefore intriguing that this is not observed, as coordination to the palladium was far more facile than in the case of the platinum ion. The reticence of the *N,N*-dialkyl-*N'*-9-anthracoylthiourea ligands to react with the chloro species of Pt(II) could be a limitation in their potential application as many PGM ions exist as chloro species in effluent streams (section 1.1).

As in Chapter 2, the remainder of this chapter will focus on the detailed characterisation of the Pt(II) and Pd(II) complexes of the anthracoylthiourea, pyrenebutanoylthiourea and pyreneacetylthiourea derivatives. The NMR spectra will be discussed followed by the X-ray analysis of *cis*-bis(*N,N*-diethyl-*N'*-9-anthracoylthioureato)palladium(II) and *cis*-bis(*N,N*-diethyl-*N'*-9-anthracoylthioureato)platinum(II). IR spectra will also be referred to.

3.2 Characterisation of Pt(II) and Pd(II) complexes

3.2.1 Characterisation of potentially fluorescent complexes by means of ^1H , ^{13}C and ^{195}Pt NMR spectroscopy

3.2.1.1 ^1H and ^{13}C NMR spectra of *N,N*-diethyl-*N'*-9-anthracoylthiourea derivatives

The proton chemical shifts of *cis*-bis(*N,N*-diethyl-*N'*-9-anthracoylthioureato)palladium(II), *cis*-[Pd(L¹-S,O)₂] and *cis*-bis(*N,N*-diethyl-*N'*-9-anthracoylthioureato)platinum(II), *cis*-[Pt(L¹-S,O)₂] are given in Table 23 and the ^{13}C chemical shifts are given in Table 24. Chemical shift values of both anthracene²³ and the free ligand, *N,N*-diethyl-*N'*-9-anthracoylthiourea (HL¹) have been included. The numbering scheme used in these tables is given in Figure 39 for *cis*-[Pd(L¹-S,O)₂].

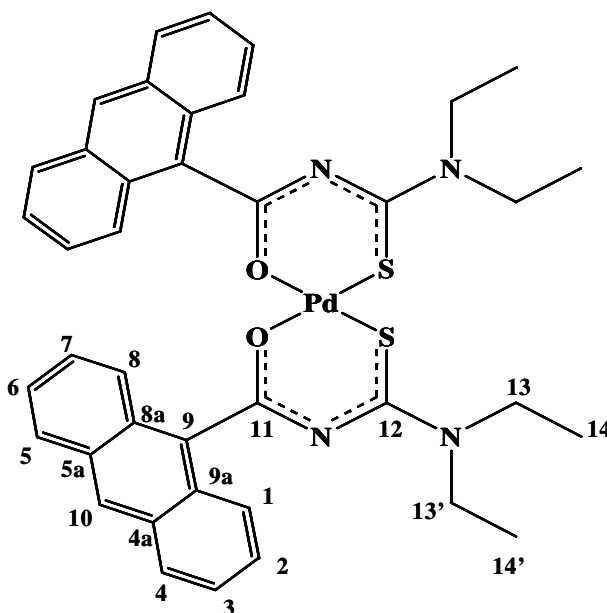


Figure 39 Numbering scheme shown for *cis*-[Pd(L¹-S,O)₂] and is applicable to all *N,N*-diethyl-*N'*-9-anthracoylthiourea derivatives.

Table 23 ^1H NMR chemical shifts (in ppm) of anthracene and *N,N*-diethyl-*N'*-9-anthracoylthiourea derivatives (25°C, CDCl₃).

Compound	H1+H8	H2+H7	H3+H6	H4+H5	H10	N-H	H13+ H13'	H14+ H14'
Anthracene ²³	8.02	7.48	7.48	8.02	8.44	-	-	-
HL ¹	8.12	7.57	7.49	7.99	8.49	8.12	4.04	1.45
<i>cis</i> -[Pd(L ¹ -S,O) ₂]	8.17	7.34	7.34	7.86	8.29	-	3.92/ 3.60	1.40/ 1.09
<i>cis</i> -[Pt(L ¹ -S,O) ₂]	8.19	7.34	7.34	7.85	8.29	-	3.83/ 3.55	1.39/ 1.05

Table 24 ^{13}C NMR chemical shifts (in ppm) of anthracene and *N,N*-diethyl-*N'*-9-anthracoylthiourea derivatives (25°C, CDCl_3).

Compound	C1+C8	C2+C7	C3+C6	C4+C5	C4a+C5a	C8a+C9a	C9	C10	C11	C12	C13	C14
Anthracene ²³	128.30	125.20	125.20	128.30	131.60	131.60	126.10	126.10	-	-	-	-
HL ¹	124.35	127.37	125.61	128.68	130.87	128.16	129.45	129.40	166.22	178.28	48.16/ 48.15	13.49/ 11.50
<i>cis</i> -[Pt(L ¹ -S,O) ₂]	126.30	125.56	124.90	128.01	132.17	127.98	134.34	127.16	172.56	166.70	46.77/ 45.58	13.32/ 12.32
<i>cis</i> -[Pd(L ¹ -S,O) ₂]	126.41	125.51	124.91	128.05	131.21	128.13	134.06	126.96	174.66	170.80	47.04/ 45.78	13.35/ 12.59

It is apparent from Table 23 that the proton chemical shifts of cis -[Pd(L¹-S,O)₂] and cis -[Pt(L¹-S,O)₂] are practically identical, indicating that the electronic environments of the hydrogens are independent of the metal centre in these complexes. There are however some differences between the chemical shifts of the complexes and those of the uncoordinated ligand, in particular those of H13, H13' and H14, H14'. These resonances were previously mentioned in section 2.2.3.1 with reference to the uncomplexed *N,N*-diethyl-*N'*-9-anthracoylthiourea ligand. It was noted that while separate resonances are observed for H13, H13' in the free ligand, the peaks remain broad and the coupling unresolved. In cis -[Pd(L¹-S,O)₂] and cis -[Pt(L¹-S,O)₂] however, the corresponding H13, H13' resonances are distinct and well separated with clear coupling present. A similar observation can be made for the resonances of H14, H14'. The increased separation of these resonances upon complexation would appear to confirm the accentuated partial double bond character between the thiocarbonyl carbon atom and the neighbouring nitrogen atom of the amine substituent which would serve to limit the rotation about this bond (Figure 40).

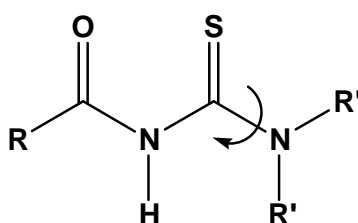


Figure 40 Restricted rotation about partial double bond in the *N,N*-dialkyl-*N'*-aroylthiourea ligands.

Further differences between the uncoordinated ligand and complexes are seen in the proton NMR spectra, particularly in the aromatic region (Figure 41). Three distinctive sets of peaks are still clearly visible in the aromatic region of the spectra of the complexes, but the coupling between the aromatic protons is significantly less well-defined than in the *N,N*-diethyl-*N'*-9-anthracoylthiourea. The expected disappearance of the thioamidic proton (N-H) in the complexes is also observed.

Similarly to the proton NMR spectra, the carbon chemical shifts, particularly in the aromatic regions of cis -[Pd(L¹-S,O)₂] and cis -[Pt(L¹-S,O)₂] (Table 24), are comparable, indicating that the electronic environment of the carbons in this region are also independent of the choice of metal centre in these complexes. Differences between the carbon chemical shifts of the complexes and ligand are however apparent. In particular C13, C13' being very broad in the uncoordinated ligand, becomes more clearly defined and separated in cis -[Pd(L¹-S,O)₂] and cis -[Pt(L¹-S,O)₂]. This appears to confirm the possibility of increased double bond character between the thiocarbonyl carbon atom and the neighbouring nitrogen atom in the complexes. Other differences between HL¹, cis -[Pd(L¹-S,O)₂] and cis -[Pt(L¹-S,O)₂] are apparent in the chemical shift positions of C11 and C12, the carbonyl and thiocarbonyl carbon atoms respectively. Discussion of these resonances will however be deferred to section 3.2.1.2 where they will be examined in detail with the other complexes synthesised.

As for the anthracoylthiourea derivatives in Chapter 2, the ¹³C chemical shift differences between the Pt(II) and Pd(II) complexes and underivatized anthracene have been calculated

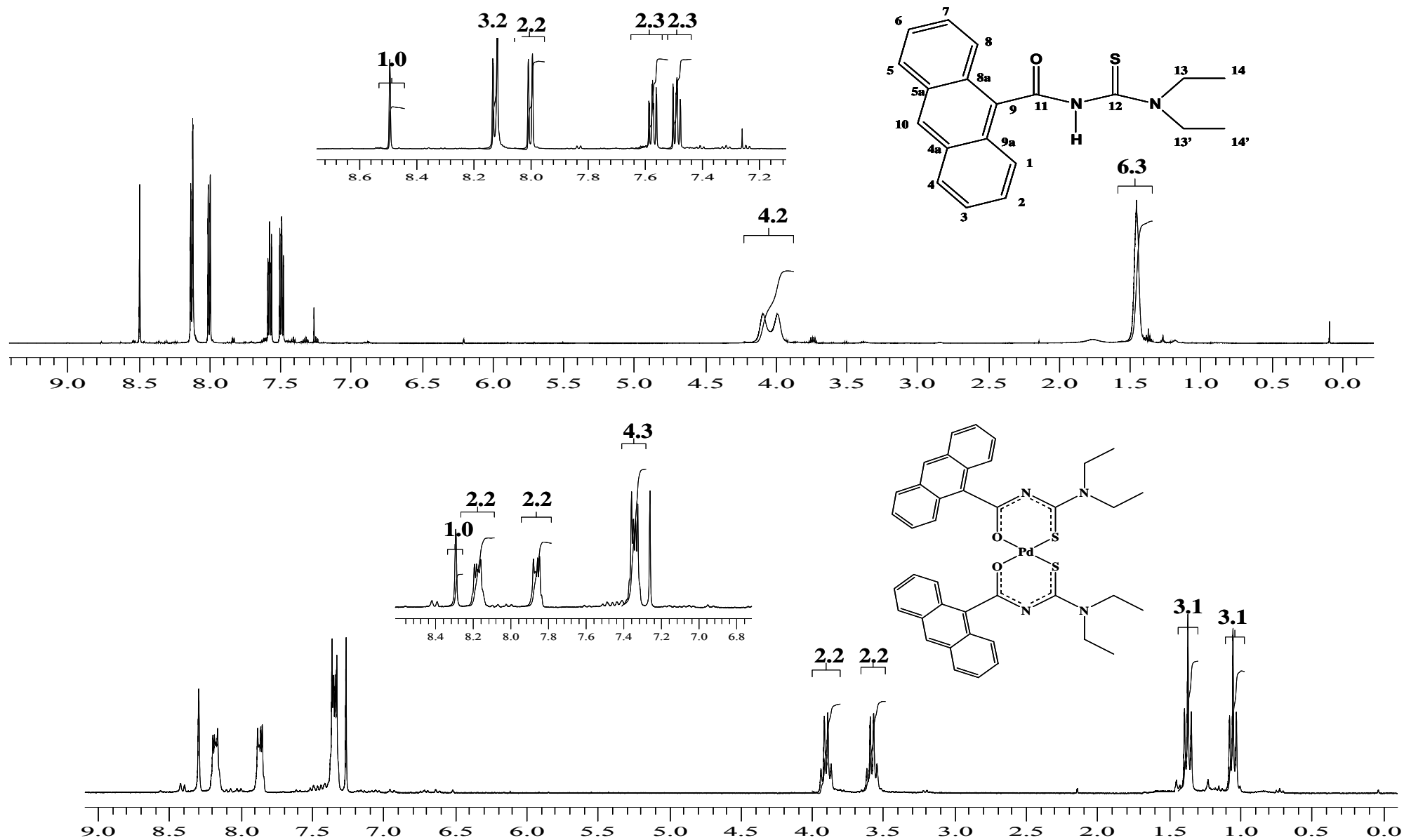


Figure 41 ¹H NMR spectra of *N,N*-diethyl-*N'*-9-anthracoylthiourea and *cis*-Bis(*N,N*-diethyl-*N'*-9-anthracoylthioureato)palladium(II) (25°C, CDCl₃), with expanded aromatic regions inserted.

and are given in Table 25, where $\Delta = \delta^{13}\text{C}_{\text{compound}} - \delta^{13}\text{C}_{\text{anthracene}}$. The values obtained for HL¹ have also been included for comparison. As explained previously, a negative sign indicates an upfield shift, or shielding of the carbon atom and a positive sign indicates a decrease in electron density and hence a downfield shift of the carbon resonance.

Table 25 Difference in ¹³C NMR chemical shifts (in ppm) of selected compounds relative to anthracene ($\Delta = \delta^{13}\text{C}_{\text{compound}} - \delta^{13}\text{C}_{\text{anthracene}}$).

	C1+C8	C2+C7	C3+C6	C4+C5	C4a+ C5a	C8a+ C9a	C9	C10
$\Delta[\text{HL}^1]$	-3.96	2.17	0.41	0.38	-0.73	-3.44	3.35	3.44
$\Delta\text{cis-}[\text{Pt}(\text{L}^1\text{-S},\text{O})_2]$	-1.89	0.31	-0.30	-0.25	-0.40	-3.47	7.96	0.86
$\Delta\text{cis-}[\text{Pd}(\text{L}^1\text{-S},\text{O})_2]$	-2.00	0.36	-0.30	-0.29	0.57	-3.62	8.24	1.06

The differences between the carbon chemical shifts of the complexes and those of underivatised anthracene (Table 25) can be partially understood in terms of the possible resonance effect resulting from the direct attachment of a carbonyl or electron withdrawing substituent to the anthracene system (see Chapter 2, Scheme 9). As is apparent from Table 25 however, the effect of the resonance withdrawal of electrons from the ring system is not nearly as pronounced in *cis*-[Pd(L¹-S,O)₂] and *cis*-[Pt(L¹-S,O)₂] as it is in the ligand (HL¹). This can be seen by the smaller positive numbers in the chemical shift differences of C2 (C7) and C10, and the slightly negative numbers of C4 and C5. Were the resonance interaction to be as strong in the complexes as it is in the ligand, the chemical shift differences would all be of comparative value. A further point of variation between the uncoordinated ligand and complexes is seen in the chemical shift difference of C9. In the case of the ligand, HL¹, the positive value of 3.35 indicates a degree of deshielding and this is more than doubled in the case of the Pt(II) and Pd(II) complexes, where the shift differences are 7.96 and 8.24 respectively. Upon complexation, the oxygen and sulphur atoms behave as electron donors and it is therefore understandable that this should result in a deshielding effect on the *ipso* carbon of the ring system, as seen here for C9. It is also possible that the electron donation by the oxygen atom in particular should lead to increased resonance electron withdrawal from the ring system, but as previously noted this is not observed and it may therefore be speculated that the inductive effect could be a contributory factor in this case. The chemical shift differences of C1 (C8) and C8a (C9a) are negative values indicating shielding of these carbon atoms. In the case of the quaternary carbons (C8a and C9a), these values differ little between the complexes and the ligand, indicating similar substituent steric effects.²⁴ The values of C1 (C8) however, differ between the ligand and complexes. It is therefore likely that the *peri* interactions of these carbons differ (as expected) in the complexes and free ligand.

3.2.1.2 ^1H and ^{13}C NMR spectra of N,N -diethyl- N' -[4-(pyrene-1-yl)butanoyl]thiourea and N,N -diethyl- N' -[pyrene-1-ylacetyl]thiourea derivatives

The proton and carbon chemical shifts of *cis*-bis(N,N -diethyl- N' -[4-(pyrene-1-yl)butanoyl]thioureato)palladium(II) (*cis*-[Pd(L⁷-S,O)₂]) and *cis*-bis(N,N -diethyl- N' -[4-(pyrene-1-yl)butanoyl]thioureato)platinum(II) (*cis*-[Pt(L⁷-S,O)₂]) are given in Tables 26 and 27 respectively. The numbering scheme used in these tables is given in Figure 42 for *cis*-[Pt(L⁷-S,O)₂]. The chemical shifts of pyrene and N,N -diethyl- N' -[4-(pyrene-1-yl)butanoyl]thiourea (HL⁷) have also been included in the tables, where applicable.

Following on from Tables 26 and 27, the proton and carbon chemical shifts of *cis*-bis(N,N -diethyl- N' -[pyrene-1-ylacetyl]thioureato)palladium(II), (*cis*-[Pd(L¹⁰-S,O)₂]) and *cis*-bis(N,N -diethyl- N' -[pyrene-1-ylacetyl]thioureato)platinum(II), (*cis*-[Pt(L¹⁰-S,O)₂]) as well as N,N -diethyl- N' -[pyrene-1-ylacetyl]thiourea, (HL¹⁰) are given in Tables 28 and 29 respectively. The numbering scheme used in these tables is given in Figure 43 for *cis*-[Pt(L¹⁰-S,O)₂]. The pyrenebutanoylthiourea and pyreneacetylthiourea derivatised compounds are discussed together following Table 29.

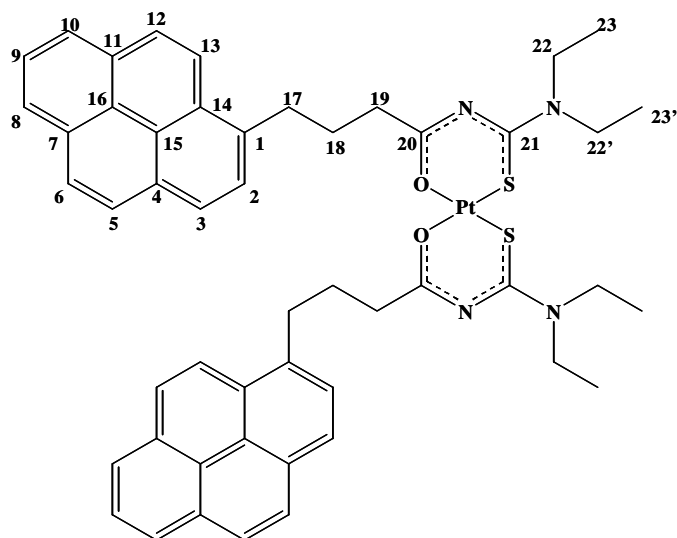


Figure 42 Numbering scheme shown for *cis*-[Pt(L⁷-S,O)₂] is applicable to all pyrenebutanoylthiourea derivatives

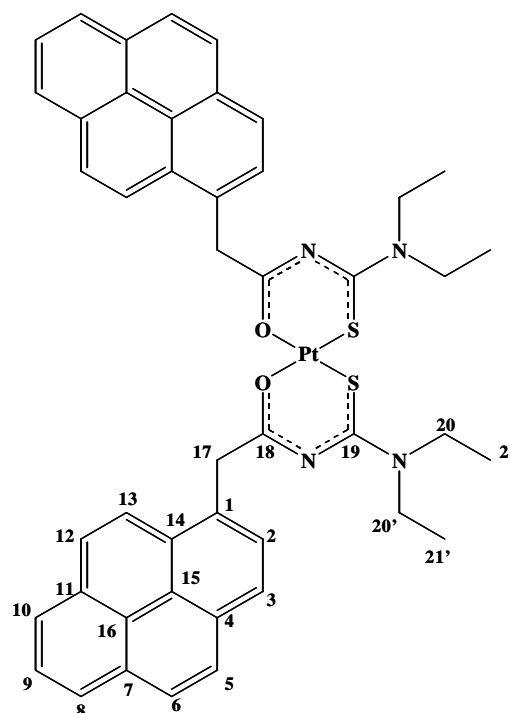


Figure 43 Numbering scheme shown for *cis*-[Pt(L¹⁰-S,O)₂] is applicable to all pyreneacetylthiourea derivatives

Table 26 ^1H NMR chemical shifts (in ppm) of *N,N*-diethyl-*N'*-[4-(pyrene-1-yl)butanoyl]thiourea derivatives (25°C, CDCl_3).

Compound	H2	H3	H5	H6	H8	H9	H10	H12	H13	H17	H18	H19	N-H	H22	H23
HL⁷	7.84	8.08	8.01	8.01	8.15	7.98	8.15	8.09	8.27	3.38	2.20	2.48	8.20	3.90/ 3.48	1.23
<i>cis</i> -[Pt(L ⁷ -S,O) ₂]	7.80	8.00	7.95	7.95	8.10	7.94	8.12	8.00	8.25	3.33	2.17	2.51	-	3.66	1.21/ 1.09
<i>cis</i> -[Pd(L ⁷ -S,O) ₂]	7.82	8.00	7.95	7.95	8.10	7.94	8.09	8.00	8.25	3.50	2.20	2.61	-	3.75/ 3.65	1.27/ 1.11

Table 27 ^{13}C NMR chemical shifts (in ppm) of pyrene and *N,N*-diethyl-*N'*-[4-(pyrene-1-yl)butanoyl]thiourea derivatives (25°C, CDCl_3).

Compound	C1	C2	C3	C4	C5	C6	C7	C8	C9	C10
pyrene ²³	124.6	125.5	124.6	130.9	127.0	127.0	130.9	124.6	125.5	124.6
HL ⁷	135.36	127.29	124.77	129.94	127.40	126.67	131.33	124.72	125.78	124.86
<i>cis</i> -[Pt(L ⁷ -S,O) ₂]	136.83	127.40	124.81	129.79	127.50	126.50	131.51	124.74	125.73	124.62
<i>cis</i> -[Pd(L ⁷ -S,O) ₂]	136.72	127.27	124.68	129.64	127.46	126.35	131.36	124.60	125.59	124.47

Table 27 contd. ^{13}C NMR chemical shifts (in ppm) of pyrene and *N,N*-diethyl-*N'*-[4-(pyrene-1-yl)butanoyl]thiourea derivatives (25°C, CDCl_3).

Compound	C11	C12	C13	C14	C15	C16	C17	C18	C19	C20	C21	C22	C23
pyrene ²³	130.9	127.0	127.0	130.9	124.6	124.6	-	-	-	-	-	-	-
HL ⁷	130.81	127.41	123.21	128.65	125.01	124.89	32.61	26.72	36.32	169.65	178.83	47.63	12.85/ 11.50
<i>cis</i> -[Pt(L ⁷ -S,O) ₂]	131.03	127.13	123.72	128.76	125.07	125.07	32.72	25.22	40.14	177.79	166.54	46.46/ 45.31	12.66/ 12.12
<i>cis</i> -[Pd(L ⁷ -S,O) ₂]	130.89	126.99	123.64	128.62	124.95	124.95	32.99	28.74	39.80	179.57	170.29	46.86/ 45.58	12.92/ 12.60

Table 28 ^1H NMR chemical shifts (in ppm) of *N,N*-diethyl-*N'*-[pyrene-1-ylacetyl]thiourea derivatives (25°C, CDCl_3).

Compound	H2	H3	H5	H6	H8	H9	H10	H12	H13	N-H	H17	H20	H21
HL¹⁰	7.91	8.19	8.02	8.05	8.18	8.01	8.18	8.11	8.18	7.94	4.38	3.85/ 3.30	1.22/ 0.92
<i>cis</i> -[Pt(L ¹⁰ -S,O) ₂]	7.94	8.10	8.03	8.03	8.15	7.98	8.15	8.05	8.37	-	4.52	3.46/ 2.80	1.04/ 0.19
<i>cis</i> -[Pd(L ¹⁰ -S,O) ₂]	7.93	8.10	8.02	8.02	8.14	7.97	8.14	8.04	8.36	-	4.46	3.37/ 2.73	1.03/ 0.14

Table 29 ^{13}C NMR chemical shifts (in ppm) of pyrene and *N,N*-diethyl-*N'*-[pyrene-1-ylacetyl]thiourea derivatives (25°C, CDCl_3).

Compound	C1	C2	C3	C4	C5	C6	C7	C8	C9	C10
Pyrene ²³	124.6	125.5	124.6	130.9	127.0	127.0	130.9	124.6	125.5	124.6
HL ¹⁰	127.27	128.57	125.33	131.39	127.44	127.81	131.39	125.73	126.33	125.55
<i>cis</i> -[Pt(L ¹⁰ -S,O) ₂]	131.82	128.62	124.45/ 124.41	130.03	127.39	127.17/ 126.61	131.21	124.78/ 124.71	125.63	124.78/ 124.71
<i>cis</i> -[Pd(L ¹⁰ -S,O) ₂]	132.31	128.64	124.55/ 124.51	130.06	127.47	126.63	131.30	124.73/ 124.70	125.67	124.73/ 124.70

Table 29 contd. ^{13}C NMR chemical shifts (in ppm) of pyrene and *N,N*-diethyl-*N'*-[pyrene-1-ylacetyl]thiourea derivatives (25°C, CDCl_3).

Compound	C11	C12	C13	C14	C15	C16	C17	C18	C19	C20	C21
Pyrene ²³	130.9	127.0	127.0	130.9	124.6	124.6	-	-	-	-	-
HL ¹⁰	130.83	128.64	122.72	129.65	125.24	124.68	42.40	167.92	178.49	47.83/ 47.23	12.99/ 10.99
<i>cis</i> -[Pt(L ¹⁰ -S,O) ₂]	130.79	127.17/ 126.61	124.45/ 124.41	129.59	124.87/ 124.80	124.87/ 124.80	46.34	175.59	168.00	45.17/ 44.61	11.97/ 11.95
<i>cis</i> -[Pd(L ¹⁰ -S,O) ₂]	130.89	127.17	124.55/ 124.51	129.63	124.87	124.80	44.30	177.70	170.14	46.68/ 45.41	12.25/ 12.09

Similarly to the anthracoylthiourea derivatives, the proton chemical shifts of the metal complexes *cis*-[Pt(L⁷-S,O)₂] and *cis*-[Pd(L⁷-S,O)₂] (Table 26) differ very little relative to each other. This is also reflected in the proton chemical shifts of *cis*-[Pt(L¹⁰-S,O)₂] and *cis*-[Pd(L¹⁰-S,O)₂] (Table 28). This indicates that the electronic environment of the protons are independent of the choice of metal centre in both the pyrenebutanoylthiourea and pyreneacetylthiourea derivatives, as was observed for *cis*-[Pt(L¹-S,O)₂] and *cis*-[Pd(L¹-S,O)₂]. From Tables 26 and 28, it is also apparent that the proton chemical shift positions in the aromatic region vary very little between the free ligands HL⁷, HL¹⁰ and the complexes *cis*-[M(L⁷-S,O)₂] and *cis*-[M(L¹⁰-S,O)₂]. This indicates little change in the electronic environment of the protons in the aromatic region upon complexation.

From Table 27 it is evident that there are negligible differences in the chemical shifts of the carbon atoms in the aromatic region between HL⁷, *cis*-[Pt(L⁷-S,O)₂] and *cis*-[Pd(L⁷-S,O)₂]. This suggests that (similarly to the case of the protons) the electronic environment of the carbons in the aromatic region is not significantly altered by the introduction of a metal ion. There are however some differences between the free ligand and the complexes, in particular C19 which appears slightly upfield in HL⁷ relative to *cis*-[Pt(L⁷-S,O)₂] and *cis*-[Pd(L⁷-S,O)₂]. Moving along the alkyl chain, slight variations in C18 between HL⁷ and the complexes are evident, however this phenomenon does not extend to C17 for which the electronic environment appears to be similar in HL⁷, *cis*-[Pt(L⁷-S,O)₂] and *cis*-[Pd(L⁷-S,O)₂]. This would appear to indicate that the electronic systems of the acylthiourea moiety and the pyrene moiety are distinct in the case of the pyrenebutanoylthiourea derivatives, where the three carbon spacer is long enough to reduce “electronic communication” between the two electronic centres, thereby confirming the results obtained in section 2.2.3.2.

From Table 29 it is clear that the chemical shifts of the carbon atoms in the pyrene moieties of *cis*-[Pt(L¹⁰-S,O)₂] and *cis*-[Pd(L¹⁰-S,O)₂] do not display a sensitivity to the metal centre; similar observations have been made for the pyrenebutanoylthiourea derivatives. There are however differences in the chemical shift positions of the carbons in the aromatic region between the free ligand HL¹⁰, *cis*-[Pt(L¹⁰-S,O)₂] and *cis*-[Pd(L¹⁰-S,O)₂]. In particular C13 appears further upfield in HL¹⁰ relative to *cis*-[Pt(L¹⁰-S,O)₂] and *cis*-[Pd(L¹⁰-S,O)₂] and a similar observation can be made for C1. The chemical shift position of C17 differs between HL¹⁰, *cis*-[Pt(L¹⁰-S,O)₂] and *cis*-[Pd(L¹⁰-S,O)₂] indicating that it too displays a sensitivity to the introduction of a metal ion. It would therefore appear that the single methylene spacer (C17) in the pyreneacetylthiourea derivatives is too short to afford a distinction between the electronic systems of the pyrene moiety and acylthiourea moiety. Consequently there may be a non-negligible electronic interaction between the two regions. These observations would appear to further support the results found in section 2.2.3.2. As will be discussed later, the extent of “electronic communication” between the acylthiourea moiety and the pyrene moiety, can have a significant influence on the fluorescent properties of these compounds.

In the anthracoylthiourea, pyrenebutanoylthiourea and pyreneacetylthiourea derivatives the thiocarbonyl and carbonyl carbon chemical shifts exchange relative positions in the spectrum and appear

with a smaller difference in the shift values. The thiocarbonyl resonance shifts upfield in the complexes, and the carbonyl resonance downfield, the latter becoming the most downfield resonance upon introduction of the metal ion. The assignment of these two peaks were confirmed with 2D spectra, where the coupling between the thiocarbonyl carbon and the CH₂ of the alkyl fragment gave a correlation enabling the identification of this carbon. The exchange in the position of these two resonances is illustrated in Figure 44, for the ligand, *N,N*-diethyl-*N'*-9-anthracoylthiourea and the complex *cis*-bis(*N,N*-diethyl-*N'*-9-anthracoylthioureaato)palladium(II).

Whilst the thiocarbonyl and carbonyl carbon resonances shift upon complexation with both platinum and palladium, the extent of these shift changes differs depending on the metal centre. This is seen in more detail in Table 30, where the shift differences (Δ defined as $\delta^{13}\text{C}_{\text{complex}} - \delta^{13}\text{C}_{\text{ligand}}$) are given.

Table 30 Chemical shift displacements in selected complexes.

Complex	$\Delta [\delta^{13}\text{C}(\text{S})]/\text{ppm}$	$\Delta[\delta^{13}\text{C}(\text{O})]/\text{ppm}$
<i>cis</i> -[Pt(L ¹ -S,O) ₂]	-11.58	6.34
<i>cis</i> -[Pd(L ¹ -S,O) ₂]	-7.48	8.44
<i>cis</i> -[Pt(L ⁷ -S,O) ₂]	-12.29	8.14
<i>cis</i> -[Pd(L ⁷ -S,O) ₂]	-8.54	9.92
<i>cis</i> -[Pt(L ¹⁰ -S,O) ₂]	-12.49	7.67
<i>cis</i> -[Pd(L ¹⁰ -S,O) ₂]	-8.35	9.78

In all cases the thiocarbonyl carbon becomes more shielded, however this effect is more marked in the case of the platinum complexes; and the carbonyl resonances move downfield, this generally being more significant in the case of the palladium complexes. Similar effects have been observed for related thiourea complexes⁷ and these observations are in accordance with the delocalisation of charge within the coordination sphere of the complexes.

Taking into account the inversion of the average trend, *i.e.* Δ (Pt(II) complexes) > Δ (Pd(II) complexes) for C(S) and Δ (Pd(II) complexes) > Δ (Pt(II) complexes) for C(O), and the fact that coordination takes place through the oxygen and sulphur atoms, it has previously been speculated that the shift displacement values could reflect the relative order of HSAB ‘softness’ of the metal center in the order Pt(II) > Pd(II).⁸

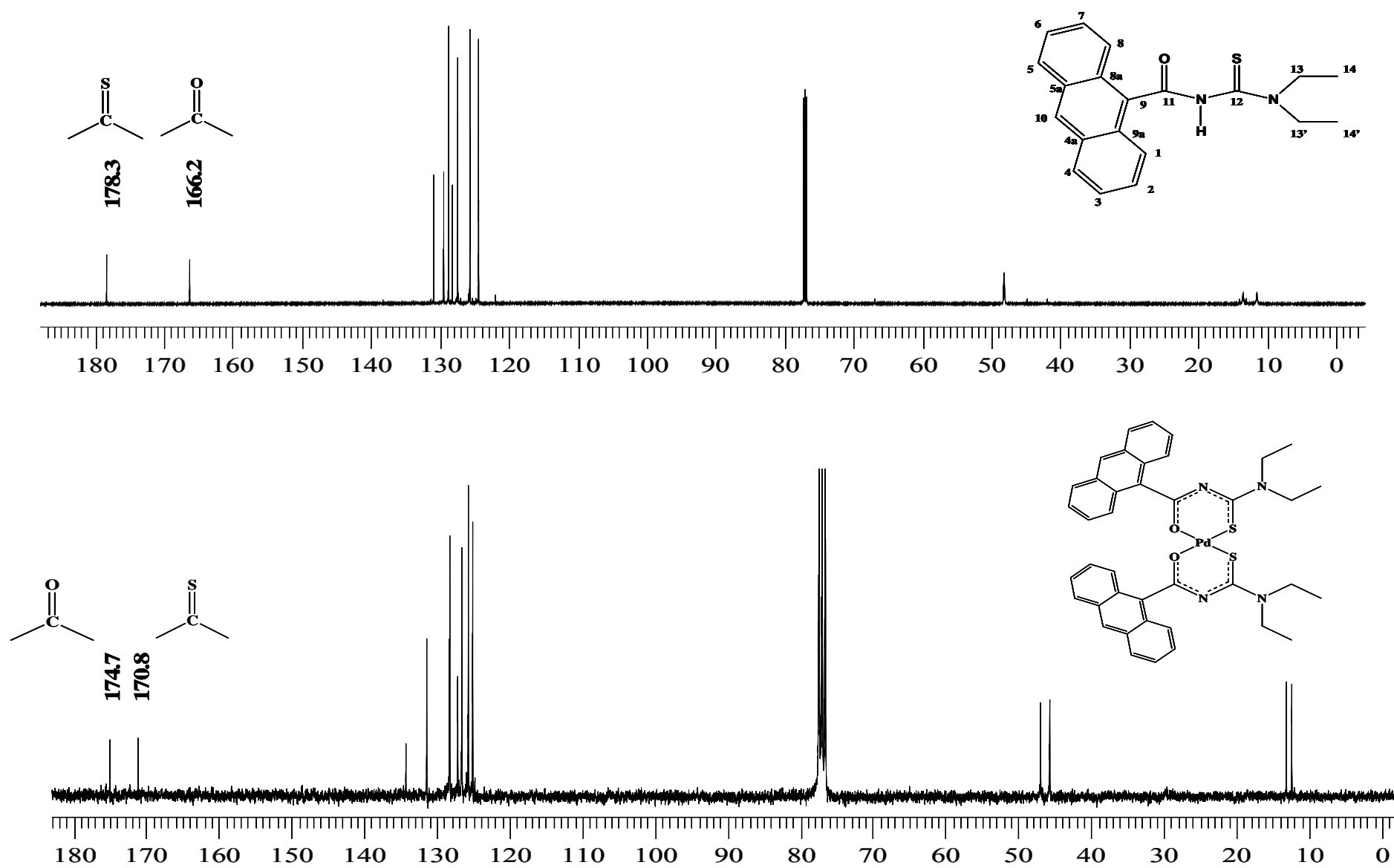


Figure 44 ^{13}C NMR spectra of *N,N*-diethyl-*N'*-9-anthracoylthiourea and *cis*-bis(*N,N*-diethyl-*N'*-9-anthracoylthioureaato)palladium(II), illustrating the exchange in chemical shift position of the thiocarbonyl and carbonyl resonances (25°C, CDCl_3).

3.2.1.3 ¹⁹⁵Pt NMR of potentially fluorescent complexes

The ¹⁹⁵Pt chemical shifts of the three complexes, $\delta_{\text{Pt}} = -2707$ ppm for [Pt(L¹-S,O)₂], $\delta_{\text{Pt}} = -2734$ ppm (major peak with relative intensity 96.5%) for [Pt(L⁷-S,O)₂] and -2723 ppm (major peak with relative intensity 96.9%) for [Pt(L¹⁰-S,O)₂] (Table 31), all fall within the range of previously reported $\delta^{195}\text{Pt}$ values for *cis*-[Pt(L-S,O)₂] complexes.^{8,25} The appearance of minor resonances in the NMR spectra run for *cis*-[Pt(L⁷-S,O)₂] and *cis*-[Pt(L¹⁰-S,O)₂] occurred at -2682 ppm (relative intensity 3.5%) and -2691 ppm (relative intensity 3.1%) respectively.

Table 31 ¹⁹⁵δPt chemical shifts (in ppm) of complexes.

Complex	<i>cis</i> -[Pt(L ¹ -S,O) ₂]	<i>cis</i> -[Pt(L ⁷ -S,O) ₂]	<i>cis</i> -[Pt(L ¹⁰ -S,O) ₂]
¹⁹⁵ δPt shift	-2707	-2734 (96.5%)	-2723 (96.9%)

Whilst the formation of a *trans* isomer is possible, it is unlikely that the minor resonances can be assigned to *trans* complexes of [Pt(L⁷-S,O)₂] and [Pt(L¹⁰-S,O)₂] since preliminary experimental results have indicated that the ¹⁹⁵Pt resonances for bidentately coordinated *trans* complexes of this type, appear 700 ppm downfield relative to that of the *cis* complex (studies with *cis*-bis(*N,N*-diethyl-*N'*-3,4,5-trimethoxybenzoylthioureato)Pt(II) have been performed).²⁶ The downfield shift of the minor resonances relative to the major are 52 ppm and 32 ppm for [Pt(L⁷-S,O)₂] and [Pt(L¹⁰-S,O)₂] respectively. Furthermore, no evidence of a *trans* isomer could be found in either the proton or carbon NMR spectra of these complexes.

The presence of excess starting material, K₂PtCl₄, is possible despite stoichiometric quantities of the ligand having been used. Pesek and Mason report the ¹⁹⁵Pt chemical shift position of H₂PtCl₄ and Na₂PtCl₄ in aqueous solution as being -1614 ppm.²⁷ For [(*n*-C₄H₉)₄N]₂[PtCl₄] in CH₂Cl₂ the chemical shift of the platinum nucleus was reported as -1416 ppm. It is therefore unlikely that the presence of the minor resonances at -2682 ppm and -2691 ppm can be assigned to uncomplexed starting compound, considering also the sparse solubility of K₂PtCl₄ in the organic solvent used to obtain the NMR spectra.

As previously mentioned, the protonation of *cis*-[Pt(L-S,O)₂] complexes leads to the formation of a variety of different species (Scheme 12). The ¹⁹⁵Pt chemical shifts of these species however, all appear upfield relative to that of the bidentately coordinated *cis* complex.²⁸ This phenomenon and the basic environment in the reaction mixture, due to the addition of excess base, make it unlikely that the presence of the minor resonances can be attributed to protonated species. It has not been possible to unambiguously assign the resonances which appear at -2682 ppm and -2691 ppm in the ¹⁹⁵Pt spectra for [Pt(L⁷-S,O)₂] and [Pt(L¹⁰-S,O)₂] respectively.

The absence of a *trans* species was somewhat unexpected as the larger carbonyl substituents, particularly the anthracene moiety, might be expected to lead to increased steric hinderance in the *cis* form of the complex, thereby possibly increasing the potential for the *trans* complex to form. With the isolation and characterisation of the first *trans* complex, *trans*-bis(*N,N*-dibutyl-*N'*-

naphthoylthioureato)platinum(II),¹³ it was speculated that the increased steric bulk of the naphthoyl group led to the formation of this complex. The absence of a *trans* species in the case of *cis*-bis(*N,N*-diethyl-*N'*-[4-(pyrene-1-yl)butanoyl]thioureato)platinum(II), is less surprising as the longer alkyl chain would enable the rotation of the large aromatic group, out of the plane of complexation, thereby reducing the steric congestion in the *cis* conformation of the complex. Due to the absence of a *trans* species in the anthracoylthiourea, pyrenebutanoylthiourea and pyreneacetylthiourea derivatives, it is likely that factors other than the bulkiness of the carbonyl substituents play a role in the *cis-trans* isomerisation of these compounds.

3.2.2 Characterisation of potentially fluorescent complexes by means of Infra-Red Spectroscopy

The complexation of the potentially fluorescent ligands was further supported by IR evidence. The IR spectra of the *N,N*-dialkyl-*N'*-acylthiourea ligands and their complexes are surprisingly intricate and not frequently reported. In the few cases where the peak shifts have been mentioned, no assignment attempts have been made,³³ however the convenient exceptions are the N-H and C=O stretches which reportedly appear in the 3200 cm⁻¹ and 1660-1700 cm⁻¹ regions respectively.³⁴ Their disappearance necessarily indicates the removal of the thioamidic (N-H) proton and the increased single bond character in the C=O bond, expected on complexation. The disappearance of this carbonyl peak was observed in the case of all the palladium complexes, as well as the disappearance of the N-H out of plane bend. This is illustrated in Figure 45 where the IR spectrum of *N,N*-diethyl-*N'*-[4-(pyrene-1-yl)butanoyl]thiourea HL⁷, is shown, Figure 46 being the palladium complex, *cis*-[Pd(L⁷-S,O)₂]. Whilst the insolubility of the *cis*-bis(*N*-morpholine-*N'*-9-anthracoylthioureato)palladium (II) complex, prevented its NMR analysis, the disappearance of the carbonyl and N-H stretches in the IR spectra support the ESMS evidence indicating complex formation. The IR spectrum of each compound is reported in Chapter 5.

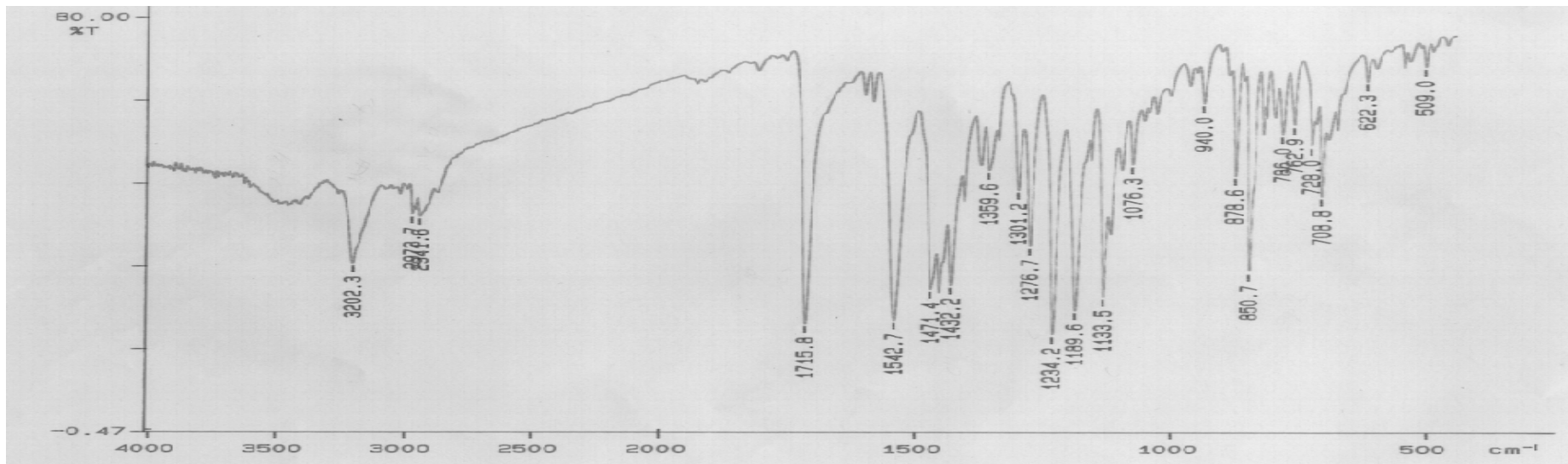


Figure 45 IR spectrum of *N,N*-diethyl-*N'*-[4-(pyrene-1-yl)butanoyl]thiourea.

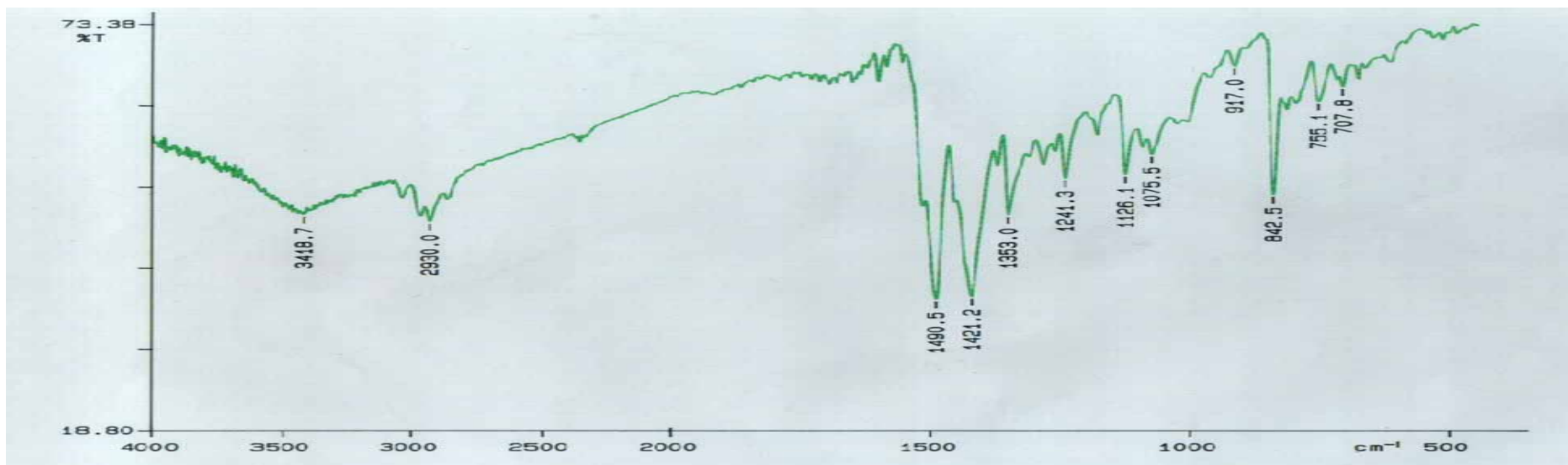


Figure 46 IR spectrum of *cis*-bis(*N,N*-diethyl-*N'*-[4-(pyrene-1-yl)butanoyl]thioureato)palladium(II).

3.2.3 Single Crystal X-Ray Diffraction Analysis

As previously mentioned in Chapter 2, structural information on these potentially fluorescent compounds is severely limited in the literature, particularly in the case of the metal complexes.¹⁰ It was therefore fortunate that crystals of both the Pt(II) and Pd(II) complexes of *N,N*-diethyl-*N'*-9-anthracoylthiourea could be isolated.

3.2.3.1 Crystal and molecular structure of *cis*-bis(*N,N*-diethyl-*N'*-9-anthracoylthioureato)palladium(II)

Orange yellow crystals of $[\text{Pd}(\text{L}^1\text{-S},\text{O})_2]$, with a prismatic platelike morphology were isolated from a combination of acetonitrile and pentane, and in a second attempted crystallisation, yellow needles were obtained from a mixture of chloroform and pentane. It was thought that the differing morphologies and solvent combinations would result in the *cis* and *trans* isomers of the palladium complex however on analysis they both proved to be the *cis* isomer. The orange yellow crystals crystallised out in the $P2_1/c$ space group with four molecular units in the unit cell. Further crystallographic details are given in Table 34 at the end of this chapter.

The anthracene rings are orientated perpendicularly to the plane of co-ordination with torsion angles $\text{C8a-C9-C11-O1} = 93.2^\circ$ and $\text{C8aA-C9A-C11A-O1A} = 94.5^\circ$ (Figure 47).

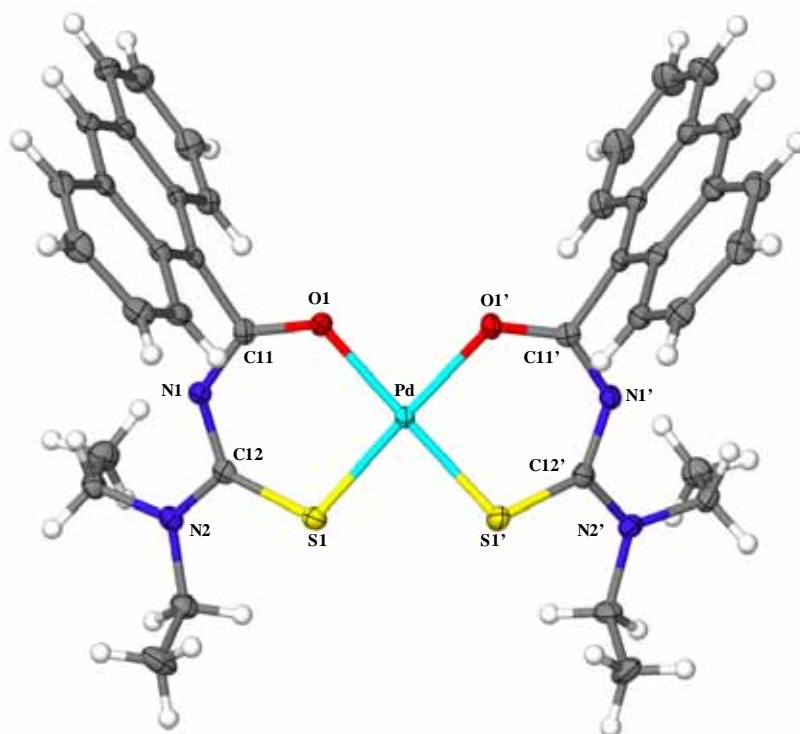


Figure 47 Molecular structure of *cis*-bis(*N,N*-diethyl-*N'*-9-anthracoylthioureato)palladium(II), *cis*- $[\text{Pd}(\text{L}^1\text{-S},\text{O})_2]$. Numbering of the aromatic rings and amine substituent follows that of the uncoordinated ligand (Figure 13).

No significant intramolecular π interactions were apparent however intermolecular π - π interactions were observed in the crystal packing with the anthracene rings of two adjacent molecules (symmetry operator

1-X, 1-Y, 2-Z) having a slightly offset facial overlap (Figure 48). The distance between the two centroids (generated using all the aromatic carbon atoms) being 3.813 Å and the closest carbon - carbon distance being 3.572(4) Å; (C9...C5a), these values comparing well with those previously reported for interplanar separation between parallel anthracene rings (3.54 Å).²⁹

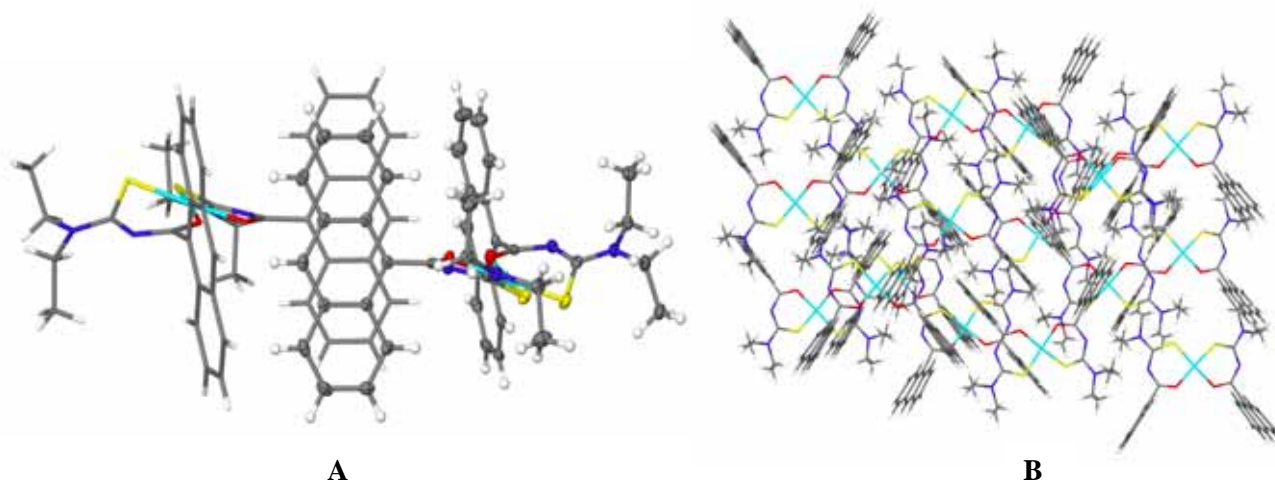


Figure 48 Offset π overlap between adjacent molecules (A) and crystal packing of *cis*-[Pd(L¹-S,O)₂] (B).

The anthracene moieties are slightly distorted, the one to a greater degree than the other. Maximum deviation from the least squares plane (defined using the aromatic carbon atoms) being 0.0396 Å (-0.0697(27) Å for C5) for the first anthracene moiety and 0.8247 Å (-1.3819(31) Å for C8') for the second anthracene moiety. The angle between the two aromatic planes being 54.35° (5), however these were oriented slightly more towards each other on one end where C8'...C1 = 6.549(5) Å than the other where C1'...C8 = 7.321(5) Å. Coordination takes place through the oxygen and sulphur atoms and a side view (Figure 49) shows the atoms in the co-ordination plane to be slightly buckled. The two chelating rings do not lie in the same plane. The two planes are defined by the following atoms (S1/C12/N1/C11/O1/Pd1) and (O1A/C11A/N1A/C12A/S1A/Pd1) and are orientated at a 22.07° (7) angle relative to each other. The coordination plane defined by (O1/O1A/S1/S1A and Pd) is almost planar, the root mean squared deviation of the atoms being 0.0508 Å and the maximum deviation being exhibited by O1 (0.061(1) Å). It is however interesting to note that the maximum deviation from a least squares plane through (C11/O1/N1/C12/S1/Pd1/S1A/C12A/N1A/C11A/O1A) is 0.2833 Å with S1 = 0.536(1) Å. The relevant bond lengths and angles are discussed further following Table 32 and further discussion of the buckled coordination plane will be included.

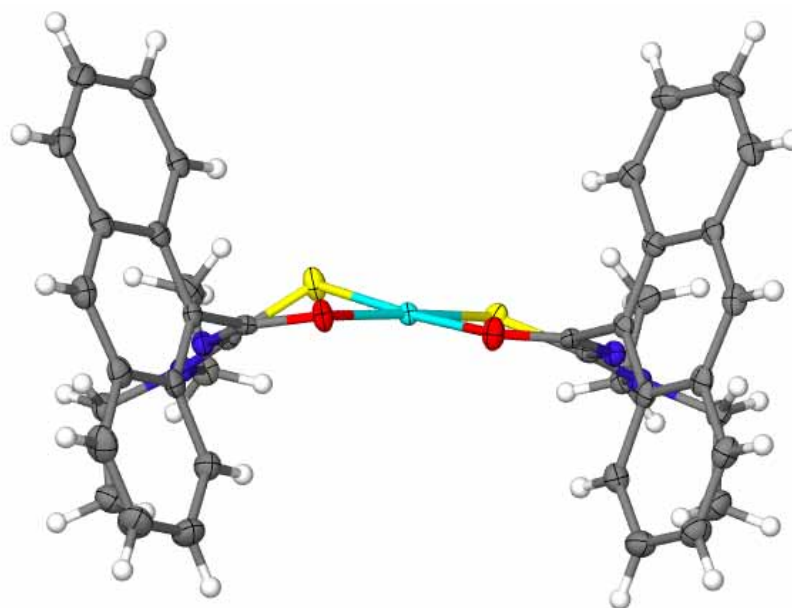


Figure 49 Buckled coordination sphere of *cis*-[Pd(L¹-S,O)₂] illustrating the deviation of the sulphur atom from the coordination plane.

3.2.3.2 Crystal and molecular structure of *cis*-bis(*N,N*-diethyl-*N'*-9-anthracoylthioureato)platinum(II)

Yellow crystals of [Pt(L¹-S,O)₂] were isolated from a chloroform/pentane solvent combination and crystallised in the *Cmc*2₁ orthorhombic system with 4 molecular units per unit cell. Further crystallographic details are given in Table 35 at the end of this chapter. One half of the molecule was generated using the symmetry operator (1-*X*,*Y*,*Z*) and from the difference fourier map there was a certain amount of disorder that could not be accurately modelled, giving rise to the large R factor for the crystal (Figure 50). The ellipsoid plot of the complex is shown and some interesting observations can be made.

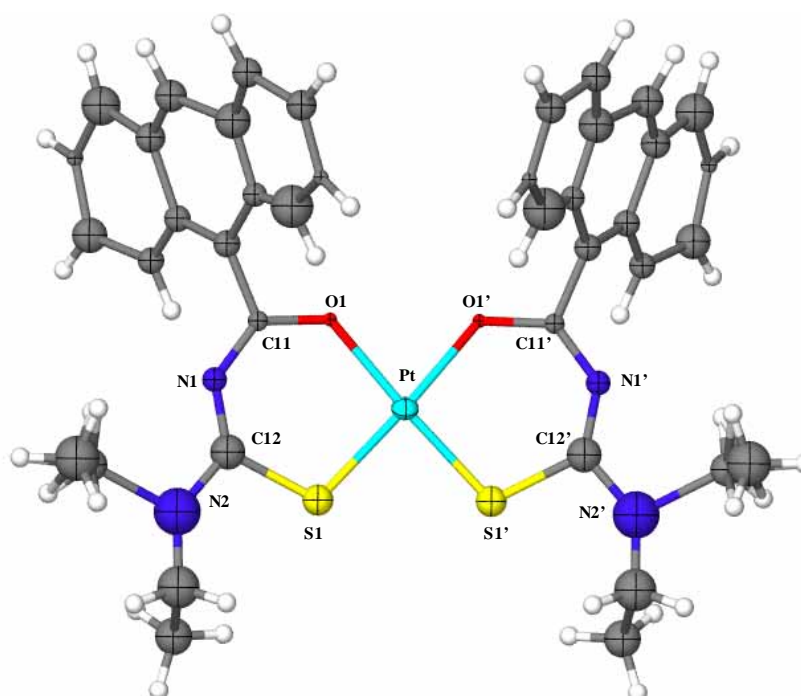


Figure 50 Molecular structure of *cis*-bis(*N,N*-diethyl-*N'*-9-anthracoylthioureato)platinum(II), *cis*-[Pt(L¹-S,O)₂].

The aromatic rings appeared to be less distorted (max deviation from the least squares plane of the aromatic carbons = 0.0662 and 0.1224(48) Å for C4a) than in the palladium analogue. The coordination plane is also significantly less buckled where the maximum deviation from the root mean squared plane defined using the following atoms (Pt1/O1/C11/N1/C12/N2/S1) is 0.0822 (-0.129(19) Å for O1). The anthracene moiety is orientated perpendicularly to the coordination plane however once again the rings are tilted towards each other more on one side than the other (Figure 51). The distances corresponding to those given for the palladium complex between C1-C8 being 4.3867(1321) Å and 8.7462(687) Å, however the closest carbon – carbon distances being between C2-C7' = 3.58(7) Å and the furthest distance between C3'-C6 = 11.39(7) Å (Figure 51).

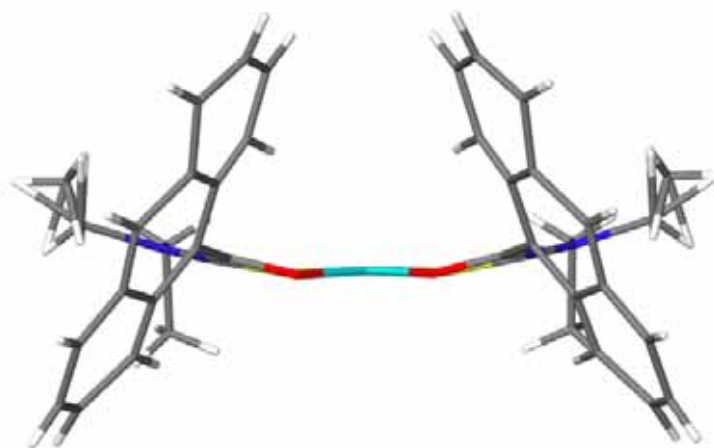


Figure 51 Coordination sphere of *cis*-[Pt(L¹-S,O)₂].

Relevant bond lengths and angles of the two complexes are given in Table 32. Data from *cis*-bis(*N,N*-diethyl-*N'*-benzoylthioureato)palladium(II), (*cis*-[Pd(L¹¹-S,O)₂]³² and the corresponding platinum complex, (*cis*-[Pt(L¹¹-S,O)₂]³³ have been included for reference. The melting points of the platinum and palladium complexes, (*cis*-[Pt(L¹-S,O)₂] and *cis*-[Pd(L¹-S,O)₂]), (252.0-253.4 °C and 252.5-253.8 °C respectively) are surprisingly high relative to the benzoylthiourea analogues (170-172 °C³³ and 128-130 °C³⁰ respectively). It is also interesting to note that in the latter the melting points of the two complexes differ, whilst in the case of the anthracoylthiourea analogues, the difference in melting point between the two metal centres is negligible. In the light of the crystallographic data however, this is readily understandable as both complexes exhibit very similar intermolecular interactions in the solid state.

It is evident from Table 35 that the M-O bonds of both the platinum (II) and palladium (II) complexes are all shorter than the M-S bonds as expected. This is consistent with bond lengths in *cis*-bis(*N,N*-dibutyl-*N'*-benzoylthioureato)platinum(II) where the average M-O bond of 2.022(4) Å is shorter than the average M-S bond of 2.232(2) Å.³⁴ However, the Pd-O bond 2.043(2) Å in *cis*-[Pd(L¹-S,O)₂] is not equivalent to its Pd-O' counterpart 2.024(2) Å, the longer bond being greater than the corresponding bond in the benzoylthiourea analogue as well. A similar observation can be made for the Pd-S bonds, where Pd-S >

Pd-S' in *cis*-[Pd(L¹-S,O)₂]. Arslan *et al.*³¹ elucidated the structure of *cis*-bis(*N,N*-dimethyl-*N'*-4-chlorobenzoylthioureaato)palladium(II) and also mentioned a slightly distorted square planar coordination of the central palladium atom. In their structure however, the Pd-O bonds were reportedly equal within experimental error as were the Pd-S bonds.

Table 32 Bond distances and angles of selected complexes (Å),(°).

Distance/ angle	<i>cis</i> -[Pd(L ¹ -S,O) ₂]	<i>cis</i> -[Pd(L ¹¹ -S,O) ₂] ³²	<i>cis</i> -[Pt(L ¹ -S,O) ₂]	<i>cis</i> -[Pt(L ¹¹ -S,O) ₂] ³³
M-O	2.043(2)	2.015(3)	2.020(19)	2.018(5)
M-O'	2.024(2)	2.016(3)	-	-
M-S	2.241(1)	2.224(2)	2.202(11)	2.231(2)
M-S'	2.232(9)	2.231(1)	-	-
O-M-S	92.54(7)	93.41(8)	95.3(6)	94.8(2)
O-M-S'	176.96(6)	176.7(1)	176.5(6)	177.5(2)
O'-M-S	176.23(7)	178.9(1)	-	177.1(2)
O-M-O'	86.29(9)	86.3(1)	82.0(11)	82.7(2)
S-M-S'	85.93(4)	86.79(4)	87.3(6)	88.10(7)

The distance of the Pd from the best plane through the coordination sphere was reported to be 0.008(1) Å, our value essentially being similar at 0.0076(7) Å. In Arslan's complex the chelate ring systems Pd-O-C-N-C-S were nearly planar, the maximum deviation being 0.139(2) Å for S1. A similar situation was seen in our complex, *cis*-[Pd(L¹-S,O)₂], for the one side of the chelate ring system, the maximum deviation of the sulphur atom being 0.131(1) Å, however the other chelate ring system was less planar, the deviation of the sulphur atom being significantly larger at 0.340(1) Å.

Further deviations exhibited by our *cis*-[Pd(L¹-S,O)₂], relative to the benzoylthiourea analogue, *cis*-[Pd(L¹¹-S,O)₂], can be seen in the O'-M-S angle being slightly smaller in our case, than in the *cis*-[Pd(L¹¹-S,O)₂]. These longer bonds and differing angle are seen in the buckling observed in the coordination sphere, however the reason for this anomalous behaviour is as yet, not fully understood. No mention was made of a lack of planarity in the *cis*-[Pd(L¹¹-S,O)₂],³² and the platinum complexes of the *N,N*-dialkyl-*N'*-acylthiourea ligands generally exhibit a planar geometry in the coordination sphere. The bond lengths in *cis*-[Pt(L¹-S,O)₂] compare well with those of the benzoyl analogue as do the listed bond angles.

Table 33 shows the remaining bond lengths in the coordination sphere. The corresponding bond lengths of the uncoordinated ligands, HL¹ and HL¹¹ have been included for reference. It is evident that the bond lengths of both the C-O and C-S bonds in our *cis*-[Pd(L¹-S,O)₂] and *cis*-[Pt(L¹-S,O)₂] have increased relative to those of the uncoordinated ligand, HL¹ indicating a decrease in the bond order of these bonds upon complexation. A similar observation can be made for *cis*-[Pd(L¹¹-S,O)₂] and *cis*-[Pt(L¹¹-S,O)₂] relative to HL¹¹. Further differences in the chelate rings of *cis*-[Pd(L¹-S,O)₂] and *cis*-[Pt(L¹-S,O)₂] are

apparent in the shortening of the C-N bonds, (O)C-N and N-C(S), relative to those of the ligand, HL¹. The shortening of these bonds combined with the increased C-O and C-S bond lengths indicates the delocalisation of charge in this region upon complexation.^{34,7} It is noteworthy that the C(S)-N' bond is slightly longer in *cis*-[Pd(L¹-S,O)₂] and *cis*-[Pt(L¹-S,O)₂] than in the uncoordinated ligand HL¹, indicating a lowering of the bond order of this bond upon complexation. This is also reflected in *cis*-[Pd(L¹¹-S,O)₂] and *cis*-[Pt(L¹¹-S,O)₂]. However it is evident from the ¹H NMR data obtained for *cis*-[Pd(L¹-S,O)₂] and *cis*-[Pt(L¹-S,O)₂] that a non-equivalence of the ethyl fragments is present indicating that despite the increased bond length of this bond, a degree of double bond character is still maintained. Similar observations have been made for *cis*-bis(*N,N*-dibutyl-*N'*-benzoylthiourea)platinum(II).³⁴

Table 33 Relevant bond lengths of the chelate ring. (Å).

Bond	HL ¹	<i>cis</i> -[Pd(L ¹ -S,O) ₂]	<i>cis</i> -[Pt(L ¹ -S,O) ₂]	HL ¹¹	<i>cis</i> -[Pd(L ¹¹ -S,O) ₂] ³²	<i>cis</i> -[Pt(L ¹¹ -S,O) ₂] ²⁷
C9-C(O)	1.503(3)	1.513(4)	-	1.498(4)	1.480(9)	-
C=O	1.218(3)	1.272(3)	1.33(4)	1.230(3)	1.285(9)	1.271(8)
(O)C-N	1.373(3)	1.317(4)	1.30(4)	1.362(4)	1.324(9)	1.313(9)
N-C(S)	1.417(3)	1.349(4)	1.27(5)	1.448(4)	1.337(8)	1.341(9)
C=S	1.676(2)	1.740(3)	1.81(5)	1.672(3)	1.728(7)	1.731(7)
C(S)-N'	1.321(3)	1.332(4)	1.34(7)	1.320(4)	1.344(8)	1.350(9)

3.3 Conclusions

Platinum complexes of *N,N*-diethyl-*N'*-9-anthracoylthiourea, *N,N*-diethyl-*N'*-[4-(pyrene-1-yl)butanoyl]thiourea and *N,N*-diethyl-*N'*-[pyrene-1-ylacetyl]thiourea were successfully synthesised. The anthracoylthiourea derivatised ligands did however exhibit a reticence to react with platinum (II) where K₂PtCl₄ was used as a starting material. Complexation was however found to be possible where the more labile nitrile complex, *trans*-Pt(NCPr_i)₂Cl₂ was used as a starting material. This reticence to react with platinum was not reflected in the pyrenebutanoylthiourea or pyreneacetylthiourea derivatised ligands, where coordination to the metal ion was relatively facile.

Palladium complexes of *N,N*-diethyl-*N'*-9-anthracoylthiourea, *N,N*-diethyl-*N'*-[4-(pyrene-1-yl)butanoyl]thiourea and *N,N*-diethyl-*N'*-[pyrene-1-ylacetyl]thiourea were also successfully synthesised, and there was no visibly apparent difference between the complexation of the essentially aroyl and acyl thioureas to Pd(II).

NMR spectra of all the complexes were obtained and the use of two-dimensional spectroscopy enabled full assignments of the aromatic regions of these complexes. Similarly to the free ligands, the electronic systems of the pyrene and thiourea moieties appear distinct in compounds with a longer spacer group between the two electronic systems such as the pyrenebutanoylthiourea derivatives, and in the compounds with a shorter single carbon spacer *i.e.* the pyreneacetylthiourea derivatives, an “electronic communication” between the two electronic systems was observed. An exchange of the chemical shifts of thiocarbonyl and carbonyl ^{13}C resonances was observed in both the platinum and palladium complexes, this observation being in accordance with other *N,N*-dialkyl-*N'*-acylthiourea complexes. Increased separation of the methyl and methylene carbon and proton resonances of the amine substituent in the complexes indicated that conditions for coalescence for the groups about the C(S)-N' bond change in favour of slow exchange on the NMR time-scale in the metal complexes as opposed to the free ligand. The NMR results also indicated the formation of *cis* complexes in all cases and this was confirmed for *cis*-bis(*N,N*-diethyl-*N'*-9-anthracoylthioureato)palladium(II) and *cis*-bis(*N,N*-diethyl-*N'*-9-anthracoylthioureato)platinum(II) with X-ray analysis. The palladium complex exhibited intermolecular π interactions between the anthracene moieties of neighbouring molecules and no further inter- or intramolecular interactions were apparent.

Table 34 Crystallographic data for *cis*-bis(*N,N*-diethyl-*N'*-9-anthracoylthioureato)Pd(II)

Empirical Formula	$\text{C}_{40}\text{H}_{38}\text{N}_4\text{O}_2\text{PdS}_2$	
Formula Weight / g mol^{-1}	777.26	
Crystal system	Monoclinic	
Space Group	$P2_1/c$	
Unit cell dimensions	$a/\text{\AA}$	11.827 (2)
	$b/\text{\AA}$	22.109 (4)
	$c/\text{\AA}$	14.644 (3)
	$\beta/^\circ$	111.62 (3)
	$V/\text{\AA}^3$	3559.6 (12)
<i>Z</i>	4	
<i>D_c</i> / g cm^{-3}	1.450	
<i>F</i> (000)	1600	
Temperature /K	173 (2)	
Absorption coefficient / mm^{-1}	0.680	
Crystal size / mm^3	0.12 x 0.08 x 0.06	
Theta range for data collection / $^\circ$	1.76 - 26.99	
Limiting Indices	$-15 \leq h \leq 15$; $-28 \leq k \leq 28$; $-18 \leq l \leq 18$	

Reflections collected / unique	39414 / 7749
Completeness to theta /%	99.8
Radiation	MoK α , graphite monochromated
Refinement method	Full-matrix-least-squares on F^2
Data / restraints / parameters	7749 / 0 / 446
Goodness-of-fit on F^2	1.060
Final R indices [$I > 2\sigma(I)$]	4.25, 9.7%
R indices (all data)	$R = 0.0517$; $wR_2 = 0.1007$
Largest diff. peak and hole	1.093, -0.402

Table 35 Crystallographic data for *cis*-bis(*N,N*-diethyl-*N'*-9-anthracoylthioureato)Pt(II)

Empirical Formula	$C_{40}H_{38}N_4O_2PtS_2$
Formula Weight / $gmol^{-1}$	865.95
Crystal system	Orthohombic
Space Group	$Cmc2_1$
Unit cell dimensions	$a/\text{\AA}$ 23.073 (19)
	$b/\text{\AA}$ 40.46 (3)
	$c/\text{\AA}$ 8.823 (7)
	$V/\text{\AA}^3$ 8237 (12)
Z	4
D_c / gcm^{-3}	1.397
$F(000)$	3456
Temperature /K	100 (2)
Absorption coefficient / mm^{-1}	3.544
Theta range for data collection / $^\circ$	1.01 – 27.00
Limiting Indices	$-29 \leq h \leq 28$; $-38 \leq k \leq 51$; $-11 \leq l \leq 9$
Reflections collected / unique	24019 / 8467
Completeness to theta /%	100
Radiation	MoK α , graphite monochromated
Refinement method	Full-matrix-least-squares on F^2
Data / restraints / parameters	8467 / 1 / 106
Goodness-of-fit on F^2	2.796
Final R indices [$I > 2\sigma(I)$]	28.64; 57.11%
R indices (all data)	$R = 0.324$ $wR_2 = 0.622$
Largest diff. peak and hole	1.093, -0.402

References

1. L. Beyer, E. Hoyer, H. Hennig, R. Kirmse, R. Hartmann, H. Liebscher, *J. fur Prakt. Chem.*, **1975**, 317, 829-839.
2. S. Behrendt, L. Beyer, F. Dietze, E. Hoyer, L. Eberhard, E. Uhlemann, *Inorg. Chim. Acta*, **1980**, 43, 141-144.
3. R. Richter, J. Sieler, L. Beyer, O. Lindqvist, L. Andersen, *Z. Anorg. Allg. Chem.*, **1985**, 522, 171-183.
4. M. Schuster, E. Unterreitmaier, *Fresenius' J. Anal. Chem.*, **1993**, 346, 630-633.
5. M. Ribiero da Silva, M. Ribiero da Silva, L. da Silva, J. Gomes, A. Damas, F. Dietze, E. Hoyer, *Inorg. Chim. Acta*, **2003**, 356, 95-102.
6. F. Hartley, *Chemistry of the Platinum Group Metals*, Elsevier, Amsterdam, **1991**.
7. Cotton, Wilkinson, *Advanced Inorganic Chemistry*, **1972**, 3rd Edition, John Wiley & Sons, London.
8. A. Mautjana, J. Miller, A. Gie, S. Bourne, K. Koch, *Dalton Trans*, **2003**, 1952-1960.
9. T. Grimmbacher, *phD Thesis*, University of Cape Town, 1995.
10. J. Bricks, K. Rurack, R. Radechia, G. Reck, B. Schulz, H. Sonnenschein, U. Resch-Genger, *J. Chem. Soc., Perkin Trans. 2*, **2000**, 1209-1214.
11. R. G. Pearson, *Inorg. Chem.*, **1973**, 12, 712-713.
12. A. Antsishkina, M. Porai-Koshits, A. Nivorozhkin, I. Vasilchenko, L. Nivorozhkin, A. Garnovsky, *Inorg. Chim. Acta*, **1991**, 180, 151-2.
13. K. Koch, J. du Toit, M. Caira, C. Sacht, *Dalton Trans*, **1994**, 785-786.
14. M. Schuster, *Fresenius' J. Anal. Chem.*, **1986**, 324, 127-129.
15. K. Koch, T. Grimmbacher, C. Sacht, *Polyhedron*, **1998**, 17, 267-274.
16. P. Pregosin, *Coord. Chem Reviews*, **1981**, 44, 247-291.
17. S. Bourne, K. Koch, *Dalton Commun.*, **1993**, 1, 2071-2072.
18. K. Koch, C. Sacht, T. Grimmbacher, S. Bourne, *S. African J. Chem*, **1995**, 48, 71-77.
19. A. Dago, Y. Shepelev, F. Fajardo, F. Alvarez, R. Pomes, *Acta Crystallogr., Sect. C.*, **1989**, 34, 1192-1194.
20. D. Fraccarollo, R. Bertani, M. Mozzon, U. Belluco, R. Michelin, *Inorg. Chim. Acta*, **1992**, 201, 15-22.
21. D. Fogg, B. James, *J. Am. Chem. Soc.*, **1997**, 36, 1961-1966.
22. F. Rochon, R. Melanson, E. Thouin, A. Beauchamp, C. Bensimon, *Can. J. Chem.*, **1995**, 74, 144-152.
23. G. Buchanan, R. Ozubko, *Can. J. Chem.*, **1975**, 53, 1829-1832.
24. B. Cheney, D. Grant, *J. Am. Chem. Soc.*, **1971**, 93, 25.
25. J. Miller, *phD Thesis*, University of Cape Town, **2000**.
26. D. Hanekom, *Msc Thesis*, University of Stellenbosch, **2005**.
27. J. Pesek, W. Mason, *J. Magn. Reson.*, **1977**, 25, 519-529.
28. A. Westra, J. Miller, K. Koch, *Proceedings of the International Solvent Extraction Conference, ISEC*, **2002**, K. Sole, P. Cole, J. Preston, D. Robinson, ed., SAIMM, p327.
29. H. Rzepa, M. Webb, A. Slawin, D. Williams, *Chem Commun.*, **1991**, 765-768.
30. M. Dominguez, E. Antico, L. Beyer, A. Aguirre, S. Garcia-Granda, V. Salvado, *Polyhedron*, **2002**, 1429-1437.
31. H. Arslan, D. Vanderveer, F. Emen, N. Kuelcue, *New Crystal Structures*, **2003**, 218, 479-480.
32. M. Bolte, L. Fink, *Private communication to CCDC*, **2003**, Crystal nm - CCDC214313.
33. C. Sacht, M. Datt, S. Otto, A. Roodt, *Dalton Trans*, **2000**, 727-733.
34. A. Irving, K. Koch, M. Matoetoe, *Inorg. Chim. Acta*, **1993**, 206, 193-199.

4.1 Principles of Luminescence

Luminescence refers to the emission of light from any substance in an electronically excited state. It can be broadly classified into two categories namely fluorescence and phosphorescence depending on the nature of the excited state.¹ The discovery of luminescence dates back as far as the sixteenth century² and more “recent” reports by Sir John Herschel in 1845¹ describe a mysterious blue tinge observed in a glass of tonic water, this being more apparent when the angle of observation was at 90° to the direction of sunlight and was attributed to the emission of the quinine present in the beverage. It is therefore interesting that luminescence spectroscopy can be considered as one of the oldest analytical techniques in use today, despite the fact that it is not as widely used today as might be expected.³

The basic theory underlying luminescence processes will briefly be described and Jablonski diagrams are frequently used in this context (Figure 52) as these concisely summarise the varying excitation and deactivation processes taking place. In these diagrams the molecules are depicted as having three major contributions to their energy namely electronic, vibrational and rotational,² however the latter are not resolved on conventional instrumentation and have therefore been excluded.

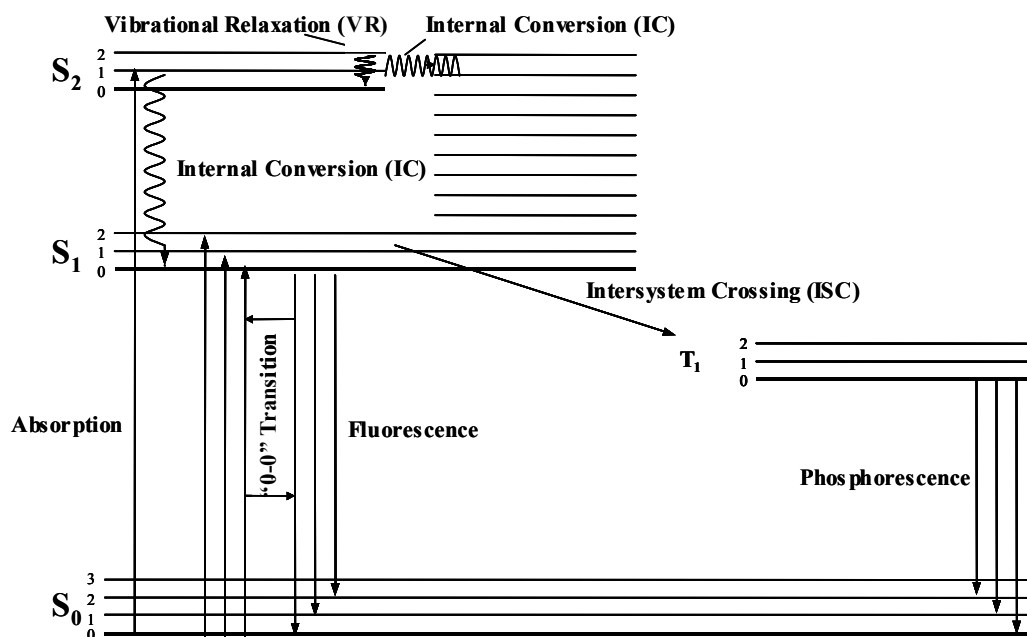


Figure 52 Jablonski diagram. (Adapted from Reference 1).
Where S_0 is the ground state (always singlet), S_1 and S_2 the first and second excited singlet states respectively, and T_1 is the first triplet excited state. Further explanations are given in the text.

4.1.1 Electronic Excitation Process

A molecule will absorb a photon of visible or UV light, when the energy of the incident photon is comparable to the energy difference between two allowed electronic states. The absorption of a photon will then result in the transition of an electron from a lower occupied molecular orbital to a higher unoccupied molecular orbital, leaving the molecule in a higher energy state. Many compounds are

absorbent, in particular, conjugated aromatic systems. In general for organic molecules, the ground state is a **singlet state** where $M=2S+1$ (M being the multiplicity and S being the total spin angular momentum quantum number).⁴ Organic molecules generally have an even number of electrons and all the spins are paired. This is depicted as the S_0 line in Figure 52. Absorption of a photon can result in one of two excited electronic states. In one, the spins are paired and the state is a singlet (S_1) and in the other, the spins are parallel (unpaired) giving rise to the **triplet state** (T_1). S_0 is therefore the ground singlet state, S_1 the lowest energy excited singlet state and T_1 is the lowest excited triplet state.^{2,3}

In the Jablonski diagram, the transitions between states are depicted as vertical lines to illustrate the instantaneous nature of light absorption. These electronic transitions occur in the order of 10^{-15} seconds in a time scale much higher than the molecular translation time scale (10^{-13} - 10^{-15} s) and this gives rise to the **Franck-Condon principle** which states that:

“Since electronic motions are much faster than nuclear motions, electronic transitions occur most favourably when the nuclear structure of the initial and final states are most similar.”⁵

More detailed photophysical and quantum mechanical explanations are beyond the scope of this work, but can be found in Turro *et al.*⁵ and Birks *et al.*⁶ In most organic molecules at room temperature, absorption of a photon corresponds to an electronic transition from the vibrational levels of the ground state to one of the vibrational levels of the first or second electronic excited states of the same multiplicity. The spacing of the vibrational and rotational levels in these higher electronic states is what gives rise to the generally broad absorption spectrum of the molecule.⁷ The energy difference between the S_0 and S_1 ground state is too large to allow for thermal population of S_1 and it is for this reason that UV/Visible light (with shorter wavelengths) and not heat, is used as a source of excitation in fluorescence spectroscopy.¹

4.1.2 Electronic De-excitation processes

De-excitation processes can be classified into two categories. The first of these are **radiative transitions** where the excited molecule attains a lower electronic state and this results in the observable emission of a photon (luminescence). In the second category of **radiationless transitions**, the excited molecule relaxes back to its ground state *via* non-radiative pathways that do not give rise to an observable photon emission. If the absorption of a photon by an organic molecule results in the molecule being in the S_2 excited state, it can rapidly dissipate the excess vibrational energy through collision with solvent molecules. This process is called **vibrational relaxation** (VR Figure 52) and results in the excited electron in the molecule attaining the lowest vibrational level of the S_2 state without photon emission and the excess energy is thus thermally dissipated.

Internal conversion (IC Figure 52) is a second deactivation process that can take place whereby the molecule can pass from a lower vibrational level of S_2 to an isoenergetic vibrational level of S_1 . These two processes occur very rapidly (10^{-12} sec) until the electron reaches the vibrational levels of S_1 . The

Boltzmann distribution is then rapidly established and as a result, the lowest vibrational level ($V=0$) has the greatest probability of electron occupation. As this energy loss is so rapid, emission from excited states higher than the first excited state are rare, although few molecules are found to be exceptions to this rule (azulene being one).²

Once the electron in the molecule has reached the lowest vibrational level of the first excited state, internal conversion to the ground state is a relatively slow process with a low probability and emission of a photon can now effectively compete with these and other decay processes. Emission of a photon from the first excited singlet state to the ground state is classified as **fluorescence** and occurs in a time frame of 10^{-9} - 10^{-7} seconds following excitation. Consequently it is not possible for the human eye to perceive fluorescence after removal of the excitation source. Because fluorescence occurs from the lowest excited state, the wavelengths of emitted radiation (*i.e.* the fluorescence spectrum) are generally independent of the wavelength of excitation.⁷ This must however not be confused with the intensity of the emitted radiation which is proportional to the number of photons absorbed *i.e.* the intensity of the incident light, and often measured as the quantum yield.

As previously mentioned, the absorption of a photon can also result in the reversal of an electron spin giving rise to an excited triplet state. This process of spin reversal results in the molecule going from a higher singlet state to a lower triplet state and is also classified as being a non-radiative pathway, namely **intersystem crossing** (ISC Figure 52). After attaining the triplet state, the molecule can dissipate its excess vibrational energy and relax to the lowest vibrational level of the T_1 state (VR). Return of the molecule to the S_0 state *via* emission of a photon is now called **phosphorescence**. Because these transitions between states of different multiplicities are quantum mechanically strictly spin forbidden, these have relatively longer lifetimes (order of 10^{-4} sec) compared to fluorescence in which singlet to singlet transitions are spin allowed. Consequently a faint “afterglow” is often observable upon removal of the excitation source, which suggests phosphorescence. As these transitions have longer lifetimes, radiationless processes can often compete more effectively with phosphorescence than with fluorescence and it is as a result of this that phosphorescence is only rarely observed at room temperature; collisions with the solvent or oxygen can effectively dissipate the energy of the electron in such molecules. These collisions are minimised by performing phosphorescence measurements under cryogenic conditions.⁷ It should be noted here that distinction between fluorescence and phosphorescence is not always clear, in particular for transition-metal-ligand complexes which frequently exhibit mixed singlet-triplet states.¹

It should now be apparent that whilst almost all molecules absorb photons of appropriate energy, relatively few are able to fluoresce or phosphoresce significantly at room temperatures. Compounds able to do this most effectively are referred to as **fluorophores** and in most cases they are generally rigid conjugated systems with specific structures, where energy loss from the excited state is slow and able to compete with the non-radiative decay pathways.

All fluorescent molecules can be characterised by two types of spectra, the **excitation spectrum** and the **emission spectrum**. The excitation spectrum is reported as a plot of fluorescence intensity observed as a function of the exciting wavelength at some fixed or variable emission wavelength. As will become apparent in section 4.1.4, this is essentially the same as an absorption spectrum in that the absorption of a photon of light is described as a function of wavelength, however excitation spectra are obtained by different means to absorption spectra and can therefore be determined at much lower concentrations than true absorption spectra. More frequently reported however, is the emission spectrum of a compound, where the relative fluorescence intensity is observed as a function of emitted wavelengths at some fixed or variable excitation wavelength. From the Jablonski diagram it is apparent that the energy of emission is generally lower than that of absorption and hence emission occurs at longer wavelengths. This phenomenon was initially observed by Stokes and is therefore referred to as a Stokes shift.¹ Stokes shifting observed in emission spectra is primarily caused by the radiationless relaxation of the excited molecule to the lowest vibrational level of S_1 (*via* VR and IC presumably due to strong overlap of numerous states of nearly equal energy). This is a rapid process and generally complete prior to emission, causing a Stokes shift. Excited fluorophores generally tend to relax to higher vibrational levels of S_0 and the loss of excess vibrational energy (*via* thermal dissipation) is a further cause of emission occurring at longer wavelengths. Other factors also playing a role in the Stokes shift may be solvent effects, excited state reactions and complex formation. In general only the longer wavelength band of absorption and the shorter wavelength band of emission will overlap. These are commonly called the 0-0 transitions of absorption and emission (Figure 53).

A second feature of the emission spectrum is stated in Kasha's rule,¹ namely that qualitatively, the same emission spectrum is generally observed irrespective of the excitation wavelength, as has previously been explained.

A third feature of the emission spectrum is that it appears to be an approximate mirror image of the absorption spectrum. This is as a consequence of an excited molecule initially relaxing back to a higher vibrational ground state level before attaining thermal equilibrium. Because the electronic excitation does not greatly alter the nuclear geometry (Franck – Condon principle), the spacing of the vibrational levels of the excited state S_1 are similar to those of the ground state S_0 , hence, the vibrational structures seen in the absorption and emission spectra are similar; substructure present in the spectrum necessarily resulting from different rotational levels at each vibrational level.⁵ It should be noted that the mirror image rule only applies to the S_0 - S_1 absorption and that the emission spectrum is not the mirror image of the total absorption spectrum. Figure 53 illustrates the relationship between the Franck-Condon principle and the mirror image rule.

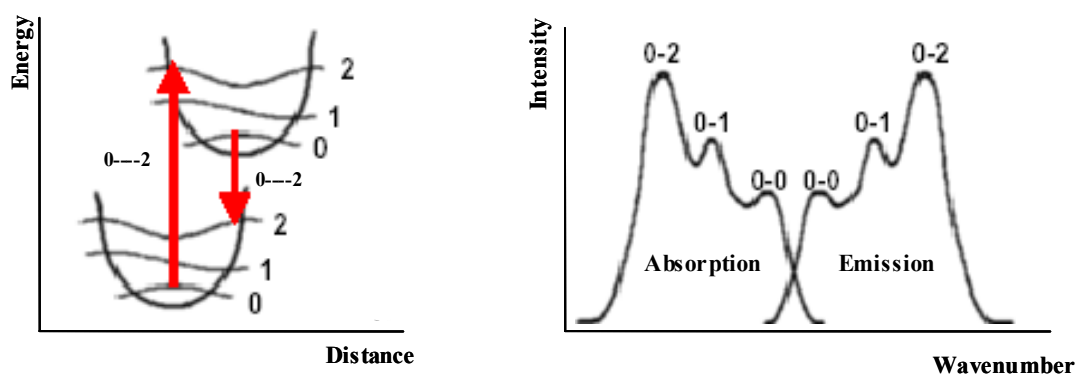


Figure 53 Mirror image rule and Franck-Condon principle.⁸

As a result of the nuclei not altering their position in the time of electronic absorption, if a particular transition is most probable in the absorption spectrum (*i.e.* 0-2 vibrational level) the reciprocal transition is most probable in the emission spectrum. Exceptions to this rule do exist, in particular for anthracene in which its excited state is known to form a charge transfer complex with diethylaniline, resulting in an unstructured emission at longer wavelengths. At certain concentrations pyrene also exhibits a longer wavelength emission and this is due to the formation of excited state dimers, generally referred to as **excimers**.¹

From Figure 53 it can be seen that the 0-0 transitions of absorption and emission should theoretically occur at the same wavelength, however this is not often observed in practice due to the energy of the emitted photon being altered by solvation differences between the excited and ground state species.⁷

The most important characteristics of a fluorophore are its **fluorescence lifetime** and **quantum yield** (also referred to as quantum efficiency). In steady-state fluorescence measurements, the compound is illuminated with a constant source of excitation and its emission is observed simultaneously. Time resolved measurements make use of a short pulse of light which excites the compound and this enables the decay time (lifetime) of the fluorophore to be recorded. The pulse width of the exciting light necessarily needs to be shorter than the lifetime of the fluorophore. Steady state measurements are therefore essentially the average of time resolved measurements, however much information about the fluorophore is lost in this process. From the decay curve of the fluorophore, obtained in time resolved measurements, information with regards to the shape and conformation can frequently be obtained. It is apparent though, that the instrumentation necessary for these types of experiments is expensive, complex and not generally available. As the fluorescence work in this project was intended to be a preliminary investigation into the luminescent properties of the compounds, steady-state measurements only were carried out. Further discussion of time resolved spectroscopy is therefore not directly applicable, but can be found in the text-book by Lacowicz.¹

The quantum yield of a fluorophore is the ratio of the number of photons emitted relative to the number absorbed. This process is determined by the two rate constants Γ and k_{nr} , these being the rate constants for the radiative and non-radiative decay processes respectively, both necessarily leading to a depopulation of the excited state.

The quantum yield is then given by

$$Q = \frac{\Gamma}{\Gamma + k_{nr}} \quad \text{Equation 2}$$

where Q - quantum yield
 Γ - rate constant for the radiative decay processes
 k_{nr} - rate constant for the non-radiative decay processes

It is apparent that the quantum yield will approach unity if the radiationless decay rate is much smaller than the rate of radiative decay *i.e.* $k_{nr} \ll \Gamma$. It should be noted that the energy yield of fluorescence is always less than unity due to Stokes losses, and for convenience all possible non-radiative decay processes have been combined to give the single rate constant k_{nr} .

This is a rather fundamental explanation of the quantum yield and the practical methods of determination will be explained in more detail in Section 4.2

4.1.3 Rayleigh and Raman scatter

The processes of Rayleigh and Raman scatter are illustrated in Figure 54. When a monochromatic beam of light is used as an excitation source and passes through a sample, there are three things that can happen to the light. Some is transmitted in the original direction, some, as in the case of the “inner filter” effect can be absorbed (see section 4.1.4) and a small percentage is scattered in all directions. The wavelength of the transmitted light remains the same and the scattered light can either remain at the same wavelength, in which case it is referred to as Rayleigh scatter, or at wavelengths in positive or negative increments of the vibrational levels of the molecule, in which case it is referred to as Raman scatter. Figure 54 illustrates this in the case of non-absorbing matter. The energy of the incident beam ($h\nu$) is not sufficient to allow the molecule to reach the S_1 state and hence, no absorption of light can occur. It is however sufficient to promote the molecule to a virtual state (S_{virt}), from which it must fall back to the ground state (S_0). This virtual state is extremely short lived. The transmitted light is re-emitted without a change of direction, but a small percentage of the light is re-emitted at a different angle, but with the same wavelength, and the remaining light is re-emitted to other vibrational levels of the ground state. The Raman spectrum of scattered light shows lines at the long wavelength side of the Rayleigh scattered beam ($h\nu$), the differences then corresponding to the vibrational levels $\nu_1, \nu_2, \text{etc.}$

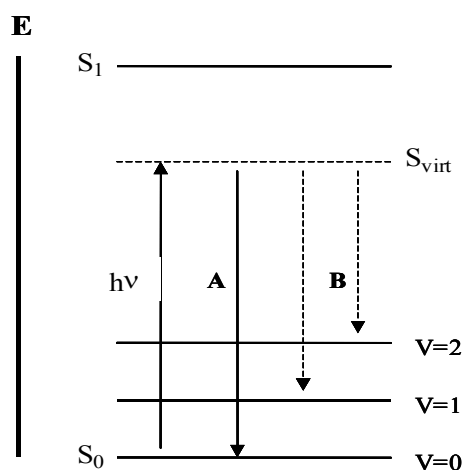


Figure 54 Outline of the processes of Rayleigh and Raman Scattering.⁹ Where A represents Rayleigh scatter, B represents Raman scatter, S_{virt} represents a virtual excited singlet state, $V=0,1,2$ are the vibrational levels of the ground state and all other terms and symbols are as defined in Figure 49.

4.1.4 Fluorescence Quenching

The phenomenon of quenching results in a decrease of the fluorescence quantum yield by in effect, providing competing pathways for the electronic excitation energy to be dissipated. A variety of mechanisms and compounds lead to quenching, however all result in the deactivation of the S_1 or T_1 state through radiationless processes involving some form of interaction with a “quencher” molecule. These processes are generally first order or pseudo first order reactions.² A brief summary of the various mechanisms is given below.

Collisional quenching. This occurs when a molecule in the excited state is deactivated by contact with some other molecule in solution (the quencher). The molecules are not chemically altered in the process. The Stern - Volmer equation describes the decrease in intensity.

$$F_0/F = 1 + K[Q] = 1 + k_q\tau_0[Q] \quad \text{Equation 3}$$

F is the emission intensity, τ_0 is the unquenched lifetime and k_q is the bimolecular rate constant for the dynamic reaction of the quencher with the fluorophore, the product of these two constants gives the Stern-Volmer quenching constant (K). $[Q]$ is the concentration of the quencher.

A wide variety of molecules can act as “quencher” molecules, in particular, oxygen, halogens and amines. The precise mechanism of quenching differs for each group of compounds and of particular relevance here is that due to halogen containing solvents, as some of the spectra were run in chloroform.

Halogens and heavy atoms cause quenching by spin-orbit coupling and intersystem crossing to the triplet state. Strictly speaking, triplet - singlet transitions are spin forbidden and only occur due to spin-orbit coupling between the wavefunctions of the two states. In these interactions, triplet states acquire a small component of singlet state character and singlet states acquire a small amount of triplet state character due to spin-orbit coupling. The magnitude of this coupling in an atom, increases with the

atomic number Z , and hence the effectiveness of fluorescence quenching has been found to be $I \gg Br > Cl > F$.¹⁰ As aromatic hydrocarbons only contain light atoms (low Z) this effect is small for T_1-S_1 transitions. However substitution of atoms with a greater atomic number, such as halogens, can increase the probability of the T_1-S_0 transition and this is known as the **internal heavy atom effect**. The energy of the electronic radiationless transition is little affected by the halogen substitution, rather it is only the transitional probability which is increased.¹⁰

An alternative method of increasing the transitional probability, without modification of the aromatic hydrocarbon is the substitution of atoms of higher atomic number into the solvent environment.¹¹ This is then referred to as the **external heavy atom effect**.⁶ Whilst this effect is an unwanted phenomenon in the measurement of fluorescence, it enhances the rate of the singlet – triplet transition and has been used to enhance phosphorescence.¹²

Generally the magnitude of the external heavy atom effect is less than that of the internal effect due to the spin-orbit coupling being less direct.⁶ The full photophysical details and explanations of how this process works are beyond the scope of this study, but further details can be found in Chapters 4 and 6 of Birks *et al.* and Chapter 3.6 Turro *et al.*

Static quenching can also occur in the ground state of a fluorophore without dependence on diffusion or molecular collisions, and an example of this phenomenon, is the formation of non-fluorescent complexes with “quencher” molecules. Other causes of quenching include the attenuation of the incident light by the fluorophore itself (self absorption) or other absorbing species, these non-molecular mechanisms will be discussed in more detail in Section 4.1.2.

4.1.5 Instrumentation and practical considerations in fluorimetry

The six major components of fluorescence spectrometers are schematically represented in Figure 55. Two basic types are available. Filter fluorometers (or fluorophotometers), in which both the excitation and emission wavelengths are fixed, and grating instruments (usually referred to as spectrofluorophotometers or fluorescence spectrometers)¹³ where wavelength selection is possible. The latter was used in the experiments in this work as these generally produce better resolution than their less expensive counterparts.¹⁴ A comprehensive review of the various instruments available can be found in references 11 and 12. A brief description of the major components will be given here.

The radiation source is generally a Xenon arc lamp, these being preferred as light sources due to their relatively continuous output from 250-700 nm; furthermore they are ozone free,¹ which is an important health consideration, although their output is still wavelength dependant.

Lenses enable the efficient transfer of excited and emitted radiation in the region of 200-380 nm for quartz and glass lenses are used for longer wavelengths of 380-700 nm.

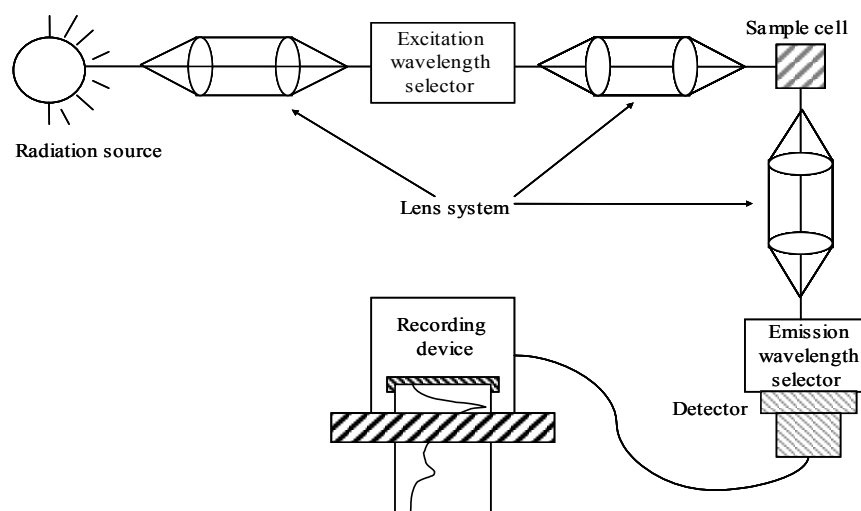


Figure 55 Major components of a fluorometer or spectrofluorometer.¹

Isolation of the excitation wavelength from the radiation source can be effected by either making use of filters or a grating monochromator. In this work, the instrument used had a grating monochromator, this having the advantage of being more versatile than a filter as it reduces the possibility of interferences from other wavelengths. The sample cell used was a 1 cm quartz cuvette in which all four sides were polished, as fluorometers make use of a 90° geometry unlike absorption spectrometers where 180° geometry is used. The selection of the emission wavelengths is achieved by a grating monochromator (similarly to excitation).

In modern instrumentation the detectors used are almost always photomultiplier tubes (PMT's), and are placed at the exit slit of the emission wavelength system. PMT's are widely used for low level light detection as they have a low noise amplification, and very little additional noise is generated when electrons pass through the photomultiplier tube in amplifying the final electrical signal. PMT's are however sensitive to excessive photocurrents which result in the detector displaying high dark currents (dark current is the current generated in the absence of incident light).¹

In ideal spectrofluorometers, the individual components should have the following general characteristics.

1. At all wavelengths, the light source should yield a constant photon output.
2. The monochromator should pass photons of all wavelengths with equal efficiency.
3. The monochromator efficiency should be independent of polarisation.
4. The detector should detect photons of all frequencies with equal efficiency.

From the above description of the varying components in the instrument it should however be apparent that components with these ideal characteristics are not always available and hence there is a need for spectral correction, this will be elaborated on in section 4.1.8.

4.1.6 Difference between Absorption and Fluorescence spectroscopy

Absorption spectrophotometers contain the same components as fluorescence spectrometers, however spectral correction is not necessary in the acquisition of absorption spectra. In this technique, the difference between two finite signals is measured, *i.e.* between the blank and the sample giving rise to a relative signal. The sensitivity is then governed by the ability to distinguish between these two, this is dependant on the stability of the instrument amongst other factors, however the non-ideal behaviour of the spectral components is largely cancelled out in these comparative measurements.

Fluorescence, on the other hand, measures the difference between zero and a finite number of photons giving rise to an absolute signal and so in principle at least, the detection limit is governed by the intensity of the source and the stability and sensitivity of the detector.⁷ Comparison of the sample with a blank is not useful as the blank displays no signal (theoretically) and the weak background signal which is present, is of an unknown spectral distribution and can therefore not be used to correct for the wavelength dependence of the individual components.¹

Whilst the high sensitivity of fluorescence is an advantage, this technique is limited to low fluorophore concentrations which gives rise to practical problems not normally encountered with more concentrated solutions as in the case of absorption spectroscopy. Dilute solutions are difficult to work with in that significant losses of analyte occur due to various factors which will be discussed shortly. Whilst similar deterioration does occur in more concentrated solutions, it forms a negligible percentage of the sample still in solution; at lower concentrations such losses become significantly more important.

One of the factors requiring careful work is the adsorption of the fluorophore onto the surfaces of glass containers. This results in a limited time being available for testing of the sample once it has been prepared. Fluorophoric organic substances at less than 1 ppm are especially prone to being adsorbed onto glass surfaces from organic solvents.⁷

The oxidation of trace substances is a further problem, as well as the concentration of dissolved oxygen. Whilst photodecomposition occurs in more concentrated solutions, its effect is much more evident in dilute solutions and this becomes a serious problem in fluorescence measurements, because the energy of the exciting radiation may cause the substance to decompose, necessitating rapid measurements. A further reason for rapid measurements being necessary, is to avoid the possible thermal decomposition of the solution as it becomes heated by the source, xenon lamps in particular emitting large amounts of infrared radiation.¹

4.1.7 The “inner filter” effect

The relative fluorescence intensity should be proportional to fluorophore concentration, however at higher fluorophore concentrations this is not observed as a result of the “inner filter” effect. This arises because the incident light is strongly absorbed by the solution containing a higher concentration of the fluorophore, or (more rarely), the emitted light is strongly re-absorbed by a high concentration of the fluorophore; both these effects result in a decrease in emitted light intensity and in the extreme case, loss of apparent emission.

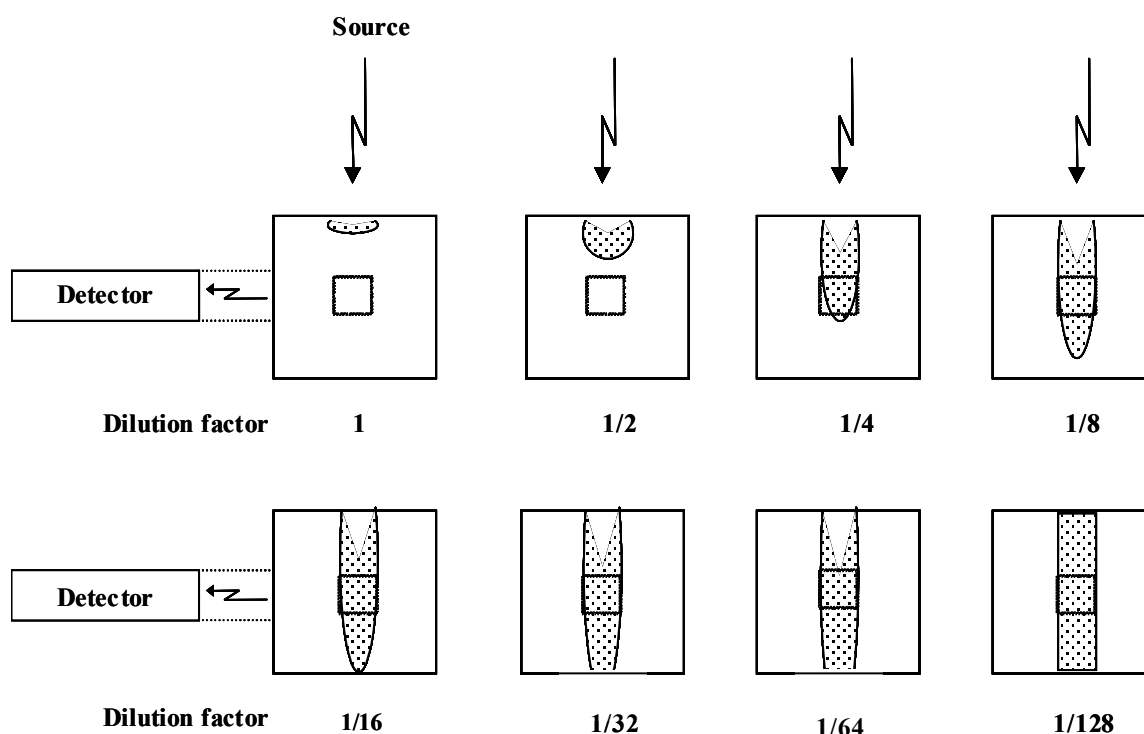


Figure 56 Graphical depiction of the inner filter effect – effect of dilution on the detected signal. (Adapted from Bashford *et al.*)¹⁵

The effect of dilution on the “inner filter” effect is illustrated in Figure 56. In a concentrated solution, (high optical density), most of the incident light is absorbed by the sample within the first few millimetres of the cuvette. None of the light reaches the molecules in the centre of the sample cell and as a result they are not excited and do not emit any light, giving rise to little or no signal. As the sample is consecutively diluted, an increasing amount of light reaches the molecules in the centre of the sample cell enabling them to emit irradiation and therefore produce an accurate signal. The “inner filter” effect can not always be sufficiently reduced in all cases and sample vessel geometry can then be altered to still enable a fairly accurate measurement. Conventionally, a 90° geometry is used (Figure 56), as this reduces Raman and Rayleigh scatter from the solvent as well as any stray incident light, although the “inner filter” effect is accentuated. Off-centre illumination decreases the path length (using cuvettes with path lengths of less than 1 cm) and can be used for samples with a higher optical density or samples in which turbidity is unavoidable. Front-face illumination is also used in samples with high optical densities.

Samples with high optical densities, not only affect the apparent intensity of the emission spectra, they can also distort them. An example of this is anthracene fluorescence with a 90° geometry, the shorter wavelength emissions are selectively attenuated relative to the emissions at longer wavelengths. This is due to the absorption of these shorter wavelengths by anthracene, and this can be understood by examination of the excitation and emission spectra which show significant overlap. This effect is less pronounced in compounds which exhibit a greater Stokes shift. In general however these problems can be greatly reduced by working with dilute solutions.

4.1.8 Spectral correction and quantum efficiency

The intensity of fluorescence is by definition equal to the intensity of light absorbed, measured in quanta, multiplied by the quantum efficiency of fluorescence, as given below.

$$F = [I_o(1-10^{-\epsilon cd})][\Phi] \quad \text{Equation 4}^{16}$$

Where F = the total fluorescence intensity in quanta per second

I_o = intensity of exciting light in quanta per second

c = concentration of solution

d = optical depth of solution

ϵ = molecular extinction coefficient

Φ = quantum efficiency of fluorescence.

For dilute solutions, for which only a small fraction of light is absorbed, F is approximately given by

$$F \approx [I_o(2.3 \epsilon cd)][\Phi] \quad \text{Equation 5}^{16}$$

Hence, under these conditions, the detector response is directly proportional to concentration of a given fluorophore, at a particular cell geometry and provided the exciting light wavelength and intensity are kept constant. Equation 5 also illustrates that the intensity of the relative fluorescence varies when the wavelength of the exciting light is varied. For a given solution the fluorescence intensity is proportional to $I_o\epsilon\Phi$ and it happens that for many substances the fluorescence efficiency (Φ) is approximately independent of the excitation wavelength. Thus, if the intensity of exciting light, in quanta per second, is kept constant as the wavelength is varied, the fluorescence intensity is proportional to ϵ , the molar extinction coefficient of the compound, which is wavelength dependant. Hence, the true excitation spectrum usually corresponds to the absorption spectrum of the compound (however the excitation spectrum being obtainable at much lower concentrations).¹⁶ From the above, it is apparent that the relative fluorescence intensity is thus proportional to the fluorophore concentration and the quantum efficiency of the molecular system.

The above conditions are not always observed in practice however as the detector response is not always linear and the lamp intensity is not always constant over a range of wavelengths and therefore the need for spectral correction arises. Spectral correction compensates for the wavelength dependant response of the detector as well as other instrumental components. Corrected emission spectra are

required in the determination of the absolute quantum yields of compounds. Correction of excitation spectra is also necessary, as the apparent excitation spectrum recorded is a plot of the product $I_o\varepsilon\Phi$ against frequency or wavelength. To obtain the true excitation spectrum, the intensity of the incident (or exciting) light I_o must be determined as a function of frequency, and there are various methods to do this, however none are completely satisfactory. Excitation spectra are mainly distorted by the wavelength dependency of the intensity of the incident (or exciting) light and frequently a quantum counter is used to provide automatically corrected spectra. A quantum counter is a compound whose fluorescence efficiency is independent of the excitation wavelength and the most frequently used compound is Rhodamine B (RhB) in ethylene glycol (3g/l),¹ however other substances used include coumarins in PVA films, and fluorescein (2 g/l) in 0.1N NaOH.¹ Split beam instruments can provide automatically corrected excitation spectra as the beam of incident (or exciting) light is split so that most of the incident light falls on the sample, while a small fraction is diverted to a reference photodetector and the quantum counter is placed in front of the reference photodetector to enable correction of the spectrum, as the detector must have a linear response to the quantum intensity of the incident beam exciting the sample. Of more relevance here, however is the need for spectral correction of emission spectra.

Parker and Rees¹⁶ attribute the difference between the apparent emission spectra (recorded on the instrument) and true corrected emission spectra to three factors:

1. The variation in quantum sensitivity of the photomultiplier with frequency,
2. The varying band width of the spectrometer and
3. The internal light losses of the spectrometer.

4.1.9 Practical methods of spectral correction

There are various methods available for spectral correction. The correction factors can be obtained by observing the wavelength-dependant output from a calibrated light source, usually obtainable from a National Bureau of Standards or similar institution, however this is a long and tedious process and the spectral output of the lamp varies with the age and usage of the lamp.¹ A second method to obtain correction factors is by using a quantum counter and scatterer, *i.e.* to calibrate the xenon lamp for its spectral output, however once again this is a long and tedious process.¹ A more detailed description of these methods can be found elsewhere.¹

The most frequently used correction method and thus a method in which the quantum yield of the analyte can be determined, is one which relies on comparison to known emission spectra.

Weber and Teale¹⁷ made use of the dipolar scattering of monochromatic light from glycogen solutions as a standard of unit quantum efficiency against which the fluorescence from a solution with the same apparent optical density (for comparative exciting wavelengths) was compared. This method was modified and used further by Dawson and Windsor in 1968.¹⁸ Quinine bisulphate in aqueous H₂SO₄ solutions has frequently been used as a reference emission standard¹⁹ however more recent reports prefer

the use of fluorescein in 0.1M NaOH and anthracene in ethanol¹⁸ as the use of quinine is complicated by variation in its fluorescence yield with H₂SO₄ concentration and excitation wavelength.¹⁸ It is apparent from the above discussion however, that the acquisition of corrected spectra is generally a long and tedious process and not always accurate as is apparent from the varying literature values available for the quantum efficiencies of the same compounds.²⁰ As the measurements undertaken in this study were preliminary and only an approximate value of quantum yield was necessary, none of the emission spectra recorded were corrected. The method used in the determination of the quantum yield will be explained in section 4.2.

4.2 Fluorescence as a means of detection

The main purpose of work in this thesis was to observe the effect that the addition of the thiourea moiety had on the emission spectrum of the fluorescent tag (anthracene or pyrene), as well as to observe the effect that coordination to platinum and palladium had on the emission of the fluorophores. The compounds synthesised can be thought of as chemical sensors, based on the binding site-signaling subunit approach,²¹ where the signaling subunit (anthracene or pyrene) is covalently attached to the binding sites (acylthiourea moiety) (Figure 57). This approach has been used in the detection of both anions²¹ and cations,²³ where the coordination of the substrate alters the properties of the signaling subunit in some way, such as colour variation (chromogenic sensor), or its fluorescence behaviour (fluorogenic chemosensor), the latter naturally being more applicable in this case. The signaling subunit acts as a transducer *i.e.* it translates the chemical information taking place at a molecular level (such as the binding of the substrate) into a detectable signal. The word chemosensor implies the reversibility of the reaction (chemodosimeter being used in the case where coordination of the substrate is irreversible). Despite the reversibility of metal coordination not having been specifically tested in this case, previous work on the acylthioureas has shown coordination to be reversible in the presence of acid²² (see Chapter 3), hence justifying the use of this term with these systems.

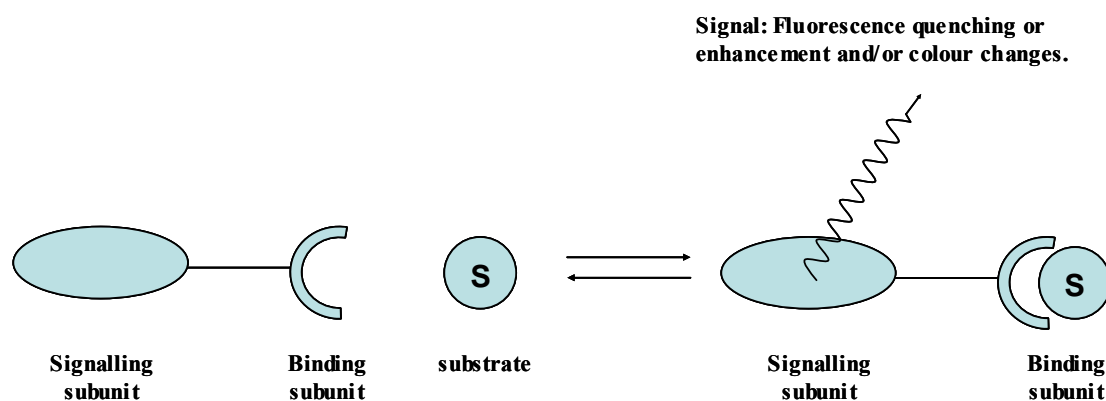


Figure 57 Chemosensor based on the binding site-signaling subunit approach.²¹

In the field of fluorogenic chemosensors, photoinduced electron transfer (PET) is a process that has been widely used for the processes of sensing both anions²¹ and cations.²³ As previously outlined, fluorescence in a molecule occurs when an excited electron in for example, the lowest unoccupied molecular orbital (LUMO) relaxes back to the highest occupied molecular orbital (HOMO). The excess energy being released as light. In the context of this scheme, it may be that a molecular orbital either from another part of the molecule or from a separate molecular entity altogether, has an energy which lies between that of the LUMO and HOMO of the fluorescing entity. In the case of this “foreign” orbital being fully occupied (*i.e.* if there is a donor group), a PET can take place resulting in the occupation of the HOMO by the electron previously occupying the “foreign” orbital. A second electron transfer from the LUMO of the fluorescing entity to the now empty “foreign” orbital will achieve the stable ground state (Figure 58). This sequence results in substantial fluorescence quenching because the transition from the excited to the ground state follows a non-radiative path. Hence, what is observed²³ is a macroscopic reduction in the intensity of the emission, or simply no fluorescence at all.

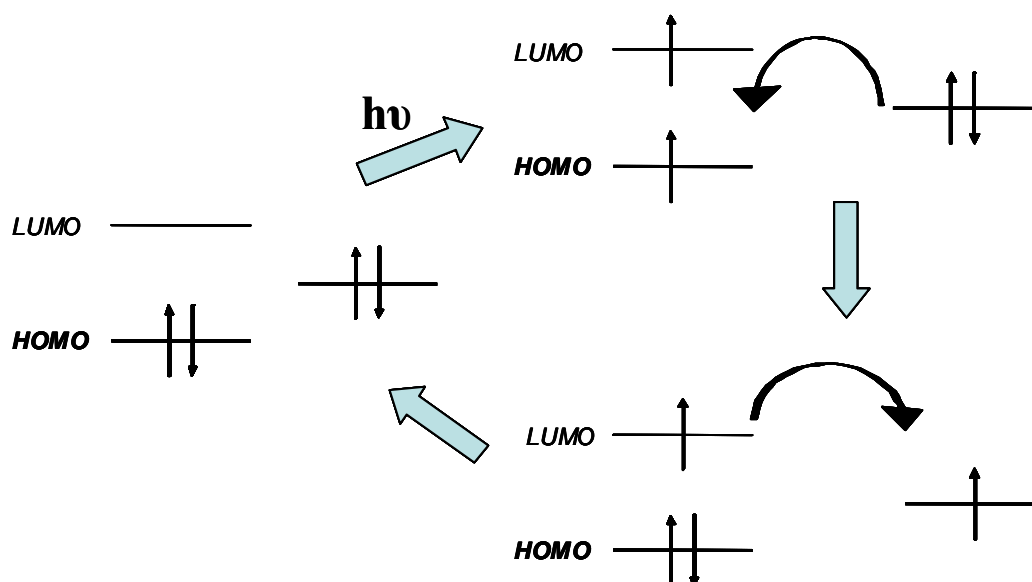


Figure 58 PET process with participation from the HOMO, LUMO and an external molecular orbital.²¹

A related scheme is also possible. In this case an empty orbital from a separate molecular unit or from another part of the molecule lies between the HOMO and LUMO of the fluorescing entity. In this scheme a PET from the LUMO to the unoccupied “foreign” orbital can take place followed by a second PET from this orbital to that of the HOMO of the fluorophore (Figure 59). As in the above case, the de-excitation takes place without radiation and a decrease in the emission intensity is observed.

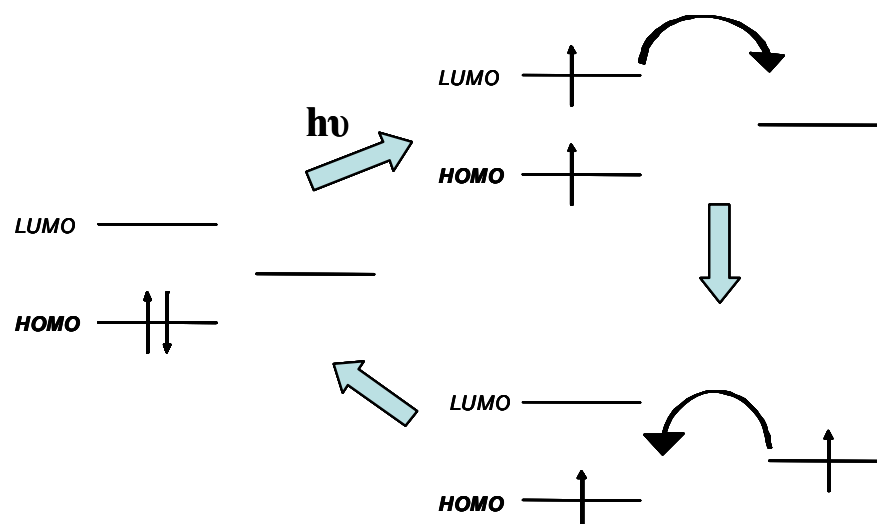


Figure 59 PET process with participation from the HOMO, LUMO and an empty external molecular orbital.²¹

A second mechanism which also leads to fluorescence quenching is electronic energy transfer (EET). In this scheme the external molecular group has some empty or half-filled orbitals that lie between the HOMO and LUMO of the fluorophore. A simultaneous electron exchange can occur (from the LUMO to the foreign orbital and from the foreign orbital to the HOMO) (Figure 60). This double electron exchange once again achieves the ground state of the fluorophore *via* a non-radiative pathway, leading to a reduction in fluorescence intensity. Close contact between the fluorophore and the molecular group is required for this double and simultaneous electron transfer to occur. Flexible linkers between signaling and binding subunits are therefore thought to favour the occurrence of an intramolecular electron transfer of this type.

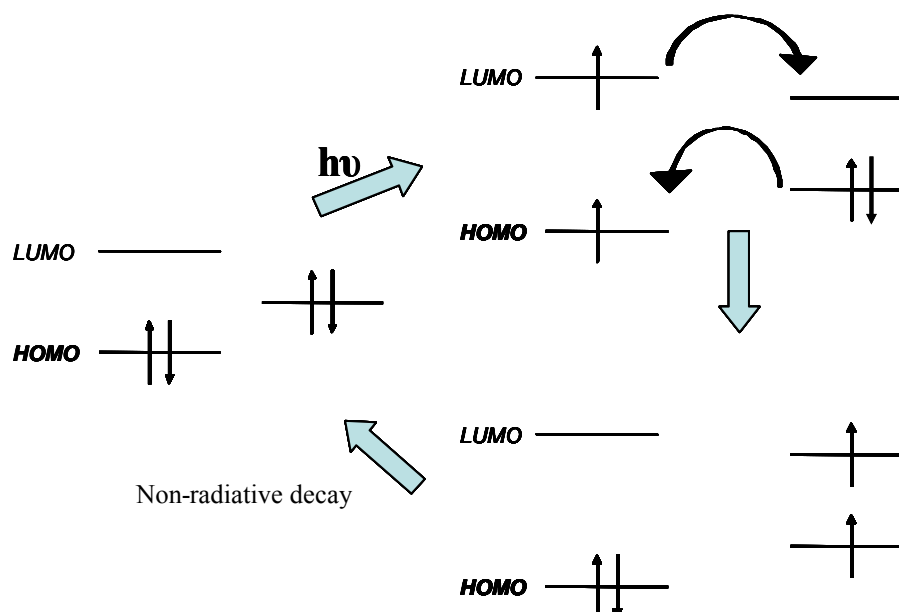


Figure 60 EET process with participation of the HOMO and LUMO of the fluorophore and an external molecular orbital.²¹

A vast amount of work has been done in the study of PET mechanisms and the role of the spacer group gives rise to various fluorophore-receptor configurations that are possible.²⁵ Amongst these, the potentially most applicable for our systems are the Integral model, Orthogonal model and Proximal, non-adjacent models, where a decreasing interaction is observed between the fluorescent unit (fluor) and receptor as shown in Figure 61.

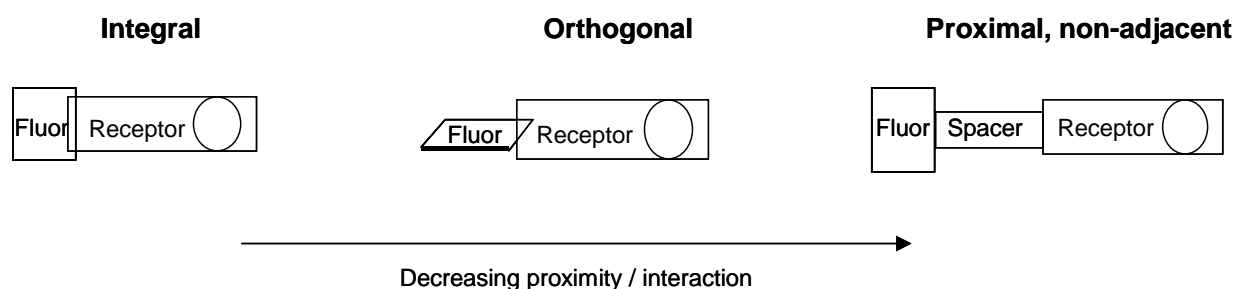


Figure 61 Fluor-receptor configurations potentially applicable to the studied systems.²⁵

The majority of known fluorescent indicators for protons and other cationic species fall into the category of integral systems, where optical excitation leads to internal charge transfer (ICT).²⁴ In orthogonal systems the π molecular orbitals of the fluorophore and receptors are separated due to a steric clash of their molecular frameworks and the signalling behaviour in these systems can be thought of as a PET process with a virtual C_0 spacer (this will be elaborated on further in Section 4.4.3). Finally, proximal, non-adjacent systems have the fluor-spacer-receptor module with molecular spacer lengths varying between 1 and 3 carbon atoms generally and signalling behaviour which can be interpreted as a PET process. In general, the majority of compounds designed as chemosensors exhibit off-on logic, *i.e.* binding of the substrate results in fluorescence enhancement, however reversed PET logic (on-off) is also possible, resulting in fluorescence attenuation.^{24,25}

Anthracene has been widely used as a fluorophore in PET designed systems for the detection of protons,²⁶ as well as alkali and alkali earth metal ions.^{27,28} and more recently for Cu(II)²⁹ and Zn(II) ions.³⁰ Pyrene has also been incorporated as a fluorophore³¹ in particular work done by Aoki.³² In this case a metal induced conformational change in a calixarene based host-guest sensory system led to the enhanced fluorescence of the pyrene moiety on addition of Na^+ . The receptors in PET systems naturally vary in design, although numerous cases have been reported using aza-crown ethers for alkali metals^{27,33} and derivatised cryptands for both non-transition³⁴ and transition metal ions.³⁵ In these cases the lone pairs on the nitrogen atoms which lead to PET in the free state are bound in the presence of the guest molecule and hence enable chelation-enhanced fluorescence (CHEF). In this work, the acylthioureas can therefore be seen as receptors for selective binding to Pt(II) and Pd(II), and some work in this context has been reported previously.^{36,37}

Whilst the majority of PET signalling processes have been focussed on the sensing of protons and s-block metal ions, few systems have been reported for transition metal ions. This is not particularly surprising due to the potential quenching influence of these metal ions.³⁸ Despite this however, Ghosh

reported the first fluorescence enhancement due to transition metal binding.³⁹ In the PET mechanism active, the receptor (R) –fluorophore (F) interaction switches off the fluorescence and binding by the guest metal ion (M) results in the switching on of the fluorescence. This mechanism requires the M-F communication to be less than the M-R interaction. With transition metal ions however, the M-F communication is frequently too strong and thus enhanced fluorescence is not observed. The success of Ghosh's systems has been ascribed to the topology of the cryptand systems that bind the metal so strongly within the cavity so as to make it unavailable for fluorescence quenching. In other words, the M-R interaction has been increased to reduce, indirectly the communication between M and F.⁴⁰ Following this work several transition metal ion sensors have subsequently been reported.^{41,42,43}

4.2.1 Measurement of quantum yield of the anthracoylthiourea and pyrenebutanoylthiourea derivatives

In the light of the potential application of these compounds it was of interest to determine the quantum yield of the ligands as well as the complexes to gain an idea of their fluorescing ability. The determination of the absolute quantum efficiency directly, without any reference to a standard solution of known quantum yield is a difficult task, as has previously been elaborated on and this is reflected in the different values quoted in the literature for the same substances.⁴⁴ Various methods are however available for the determination of quantum yields relative to that of a known substance. By obtaining the emission spectrum of the substance with a known quantum yield as well as that of a substance whose quantum yield is to be determined on the same instrument, errors due to variations in lamp intensity *etc* can largely be eliminated. The method outlined by Russo⁴⁵ was found to be very similar to that discussed by Hrdlovic^{46,47} and Parker and Rees⁴⁴ and the following general approach was used in this work, as expressed by Equation 6.

$$\Phi_u = \Phi_s \cdot \frac{\text{Area}_u \cdot (1-10^{-A_s})}{\text{Area}_s \cdot (1-10^{-A_u})} \quad \text{Equation 6}$$

Where Φ_u and Φ_s = quantum yield of the unknown and standard solution respectively
 Area_u and Area_s = area under the emission spectrum of the unknown and standard solution
 A_u and A_s = Absorbance of the unknown and standard solutions.

The concentration of the analyte exhibiting an absorbance not greater than 0.4 was determined. A 1:9 dilution was prepared and the emission spectrum of the diluted sample was obtained. The wavelength of excitation for both the standard and unknown solutions was kept constant and the absorbance at this wavelength was used in the calculation. This method theoretically appeared suitable, however some practical difficulties will be discussed later in this chapter.

As the ultimate goal of this work was to detect metal ions at very low concentrations, the maximum intensity of the fluorescent signal was very important. As previously mentioned, one way of increasing the signal would be to increase the intensity of the light source, this does however have the limitation of

potential photodegradation of the sample. In the case of anthracene, this was particularly relevant as previous experience had shown that the anthracoylthiourea derivatives exhibited light sensitivity.

The intensity of fluorescence of all frequencies, emitted by dilute solutions (such as the ones we were studying) of substances irradiated by light of a certain frequency is proportional to $I\Phi\epsilon cd$ (Equation 5). The product $\Phi\epsilon$ therefore is characteristic of the substance at a chosen frequency for excitation and is a measure of its fluorescence sensitivity at this frequency. For most substances the quantum yield is substantially independent of the excitation frequency and therefore maximum sensitivity is obtained at the peak of the most intense absorption band, in other words by irradiating at wavelengths where the maximum absorption occurs, the greatest intensity of emission will be obtained.⁴⁴ It was therefore necessary to obtain the UV/Visible spectra of all the compounds studied in order to determine the wavelengths of maximum absorption.

4.2 Experimental

All glassware (volumetric flasks and pipettes) used were of Grade A quality to ensure the accurate concentrations of solutions, and rinsed with the solvent in which the spectra were to be determined to minimise the effect of any contaminants as well as dust particles that would lead to increased scatter (Rayleigh and Raman) in the spectra obtained. Once the solutions had been prepared the volumetric flasks were covered in aluminium foil and kept in the dark to minimise any photodegradation. Solutions were also kept at 4°C however not for extended periods of time as the organic compounds in particular adhered to the glass sides of the containers, lowering the effective concentrations of the solutions and thus fresh solutions were made before each test session to achieve repeatable results. The cuvettes used in both the UV spectrometer and the fluorescence spectrophotometer were heated in acid to remove any impurities before being thoroughly washed with water and acetone. They were then stored in the solutions in which the spectra were to be run. Gloves were worn at all times as fingerprints are known to be fluorescent and would have given rise to anomalous values. Care was also taken when cleaning the apparatus used to ensure that no traces of soap remained on the glassware as some detergents contain fluorescent compounds. The concentrations of interest were naturally very low ($<10^{-5}$), and stock solutions of the samples at higher concentrations were therefore made to ensure that the mass of compound needed could be accurately weighed.

All compounds, including the anthracene and pyrene were purified chromatographically to remove any fluorescent impurities. In the case of these two compounds, elution with chloroform gave suitable separation and in the case of the synthesised compounds, 5-10% acetone in dichloromethane was used as eluent. All solvents were purified according to conventional methods⁴⁸ in order to remove excess water the presence of which would lead to a reduction in the fluorescence intensity of the tested compounds. The instrument specifications are given in Chapter 5.

4.4 Results

4.4.1 UV/Visible Spectra of *N,N*-diethyl-*N'*-9-anthracoylthiourea and its metal complexes

As the determination of the quantum yield called for the UV/Visible absorbance, absorption spectra of anthracene, *N,N*-diethyl-*N'*-9-anthracoylthiourea (HL^1), *cis*-bis(*N,N*-diethyl-*N'*-9-anthracoylthioureato) palladium(II) *cis*-[Pd(L¹-S,O)₂] and *cis*-bis(*N,N*-diethyl-*N'*-9-anthracoylthioureato)platinum(II) *cis*-[Pt(L¹-S,O)₂] were determined, some of which are shown in Figure 62. Whilst sufficient sample of *cis*-[Pd(L¹-S,O)₂] was available to obtain repeatable results, the amount of pure *cis*-[Pt(L¹-S,O)₂] available was limited. The UV/Visible spectrum of *cis*-[Pt(L¹-S,O)₂] exhibited an approximately similar absorption spectrum to that of *cis*-[Pd(L¹-S,O)₂] in dichloromethane. The absorbance of *cis*-[Pt(L¹-S,O)₂] was however slightly lower than that of *cis*-[Pd(L¹-S,O)₂] and as no more sample was available to ensure the repeatability of these results, the spectrum is not shown here.

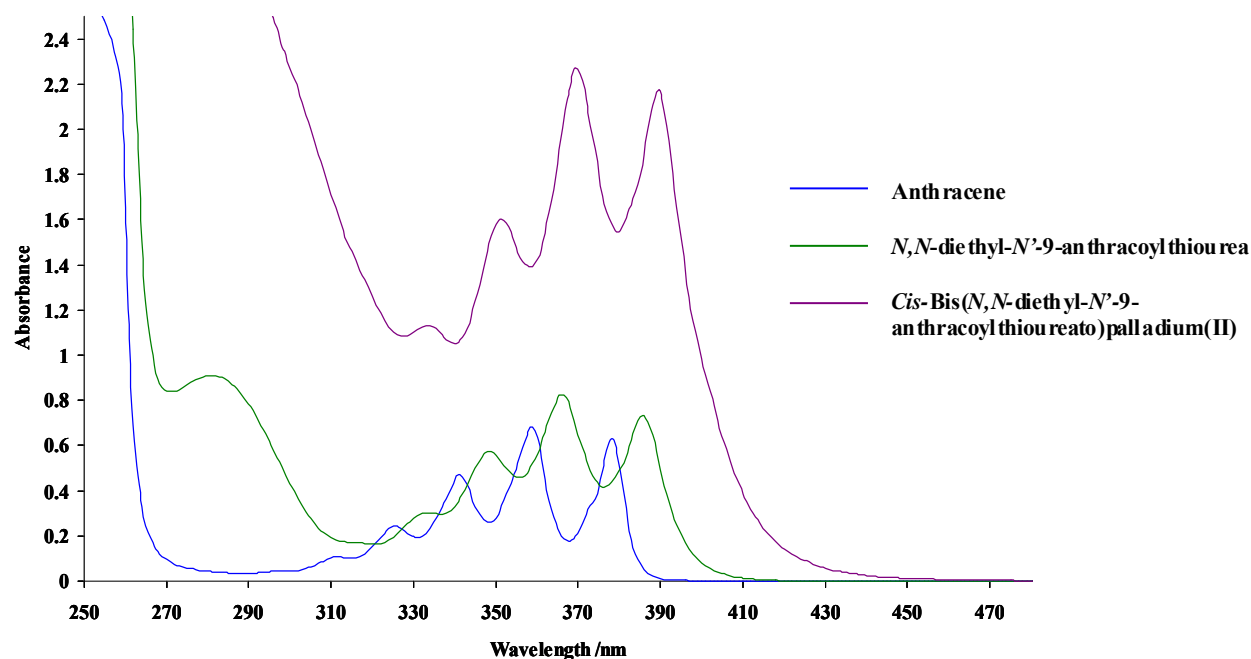


Figure 62 UV/Visible spectra of anthracene, *N,N*-diethyl-*N'*-9-anthracoylthiourea and *cis*-bis(*N,N*-diethyl-*N'*-9-anthracoylthioureato)palladium(II) in dichloromethane at 1×10^{-4} M.

The absorption spectra of *N,N*-diethyl-*N'*-9-anthracoylthiourea and *cis*-[Pd(L¹-S,O)₂] closely resembles that of the unsubstituted anthracene particularly in the region of 330 – 430 nm as shown in Figure 62. It can therefore be assumed that the absorbance in this area exhibited by these compounds is largely due to the anthracene moiety.

Table 36 Molar absorptivities ($\text{cm}\cdot\text{mol}^{-1}\cdot\text{dm}^3$) of *N,N*-dialkyl-*N'*-9-anthracoylthiourea derivatives at selected wavelengths in dichloromethane.

Anthracene		<i>N,N</i> -diethyl- <i>N'</i> -9-anthracoylthiourea		<i>cis</i> -bis(<i>N,N</i> -diethyl- <i>N'</i> -9-anthracoylthioureato)Pd(II)	
Wavelength (nm)	log ϵ	Wavelength (nm)	log ϵ	Wavelength (nm)	log ϵ
312	3.03	281	3.96	278	4.54
326	3.39	333	3.48	334	4.05
341	3.67	348	3.76	351	4.21
359	3.83	366	3.92	369	4.36
378	3.80	386	3.87	390	4.34

The molar absorptivity (Table 36) of *N,N*-diethyl-*N'*-9-anthracoylthiourea is slightly higher than that of the unsubstituted anthracene, and that of *cis*-[Pd(L¹-S,O)₂] is significantly higher than that of anthracene and the uncomplexed ligand (HL¹). From the UV/Visible spectra it is apparent that the introduction of the acylthiourea substituent at position 9 on the aromatic ring results in a bathochromic shift of approximately 7 nm as well as the appearance of a peak centred around 280 nm, this peak presumably being due to the thiourea chromophore. The shorter wavelength absorption of the anthracene moiety (312 nm) is not visible in *N,N*-diethyl-*N'*-9-anthracoylthiourea since the stronger 280 nm absorbance overlaps with this band. Discussion of the bathochromic shift in the spectra will be deferred to section 4.4.3. The absorbance of *cis*-[Pd(L¹-S,O)₂] is almost twice that of HL¹ in the region of 330 - 430 nm, however as the absorbance is due to the anthracene moiety, this is expected as *cis*-[Pd(L¹-S,O)₂] contains two anthracene rings relative to HL¹'s one.

The absorption spectra of *cis*-[Pd(L¹-S,O)₂] was only very slightly shifted to longer wavelengths relative to that of HL¹. The stronger unstructured absorbance of *cis*-[Pd(L¹-S,O)₂] in the shorter wavelength region of 270 - 330 nm suffers from partial overlap from the absorbance of anthracene.

From the UV/Visible spectrum of *cis*-bis(*N,N*-diethyl-*N'*-benzoylthioureato)platinum(II) (Figure 63), it is apparent that there is a strong absorbance in the region of 230 – 310 nm and whilst it decreases, this absorption extends through to approximately 420 nm. Whilst the benzoyl moiety in *cis*-bis(*N,N*-diethyl-*N'*-benzoylthioureato)platinum(II) is UV active, it only absorbs in the region of 170 – 270 nm⁴⁹ so that the 270-430 nm absorption may therefore be attributed to a charge-transfer transition of the *cis*-bis(*N,N*-diethyl-*N'*-benzoylthioureato)platinum(II) complex. The precise nature of this transition (*i.e.* ligand to metal or metal to ligand) is however not known and requires detailed study. It is not unreasonable therefore that a similar situation occurs in the case of *cis*-bis(*N,N*-diethyl-*N'*-9-anthracoylthioureato)palladium(II), this being less clear however, due to the superposition of the anthracoyl moiety absorptions, especially in the region of 330 – 410 nm. The overall increased absorption of the complex, *cis*-[Pd(L¹-S,O)₂], can therefore be attributed to a contribution from a M-L or L-M charge transfer interaction. The tailing above 410 nm present in the absorption spectrum of *cis*-bis(*N,N*-diethyl-

N'-benzoylthioureato)platinum(II) is reflected to a greater degree in the absorption spectrum of *cis*-[Pd(L¹-S,O)₂]. Previous work by Cicogna *et al.* on anthracene derivatised metal complexes also reported the presence of tailing in the absorption spectrum and suggested that this may be attributed to interactions between the anthracene chromophore and metal-containing moiety, and this may be occurring in the complexes studied here.⁵⁰

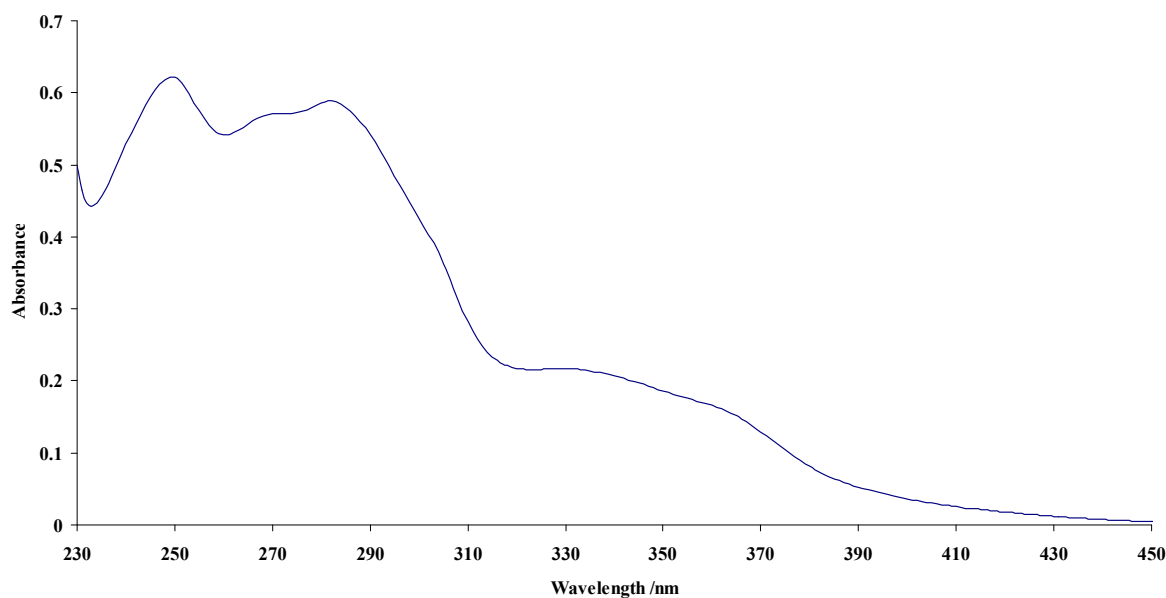


Figure 63 UV/Visible spectrum of *cis*-bis(*N,N*-diethyl-*N'*-benzoylthioureato)platinum(II) in chloroform. Conc. = 1×10^{-4} M and $\lambda_{\max} = 249$ nm with $\log \epsilon = 3.79$.⁵¹

4.4.2 Emission spectra of *N,N*-diethyl-*N'*-9-anthracoylthiourea and its metal complexes

An indication of the quantum yield of the *N,N*-dialkyl-*N'*-9-anthracoylthiourea derivatives was of interest in this work and the choice of a reference solution to this end, was of importance. Birks⁶ suggests the use of a 5×10^{-6} M ethanolic anthracene solution as reference solution for the determination of the quantum yield of an unknown substance and this was thought to be ideally suited to the *N,N*-dialkyl-*N'*-9-anthracoylthiourea derivatives. Literature values for the quantum yield of anthracene in ethanol varied in the range 0.22 – 0.30,^{6,11,16,17} depending on the concentration of the solution, this in some cases not being reported,¹⁷ as well as the excitation wavelength used (which also varied).^{11,17} As the aim of this work was only to provide an indication of the quantum efficiency of the *N,N*-dialkyl-*N'*-9-anthracoylthiourea derivatives, it was therefore decided to assume a value of 0.30 for the quantum yield of anthracene in 99% ethanolic solution, at a concentration of 5×10^{-6} M and with an excitation wavelength of 320 nm. The reason for the choice of this excitation wavelength will become apparent later in this section. As the method of Russo⁴⁵ was being followed in the determination of the quantum yield, it was fortunate that *N,N*-diethyl-*N'*-9-anthracoylthiourea was soluble in ethanol as unnecessary complications could be avoided in its quantum yield determination. The solubilities of *cis*-[Pd(L¹-S,O)₂] and *cis*-[Pt(L¹-S,O)₂]

were however limited to dichloromethane. The emission spectrum of *N,N*-diethyl-*N'*-9-anthracoylthiourea was therefore determined in both solvents to enable accurate comparison with those of *cis*-[Pd(L¹-S,O)₂] and *cis*-[Pt(L¹-S,O)₂]. The emission spectra obtained in ethanol will be discussed first, followed by those determined in dichloromethane.

In order to establish an accurate working procedure, varying concentrations of anthracene were tested and an example of the emission spectrum obtained is given in Figure 64, with emission maxima at 378.5 nm, 400.5 nm, 423.5 nm and 445.5 nm.

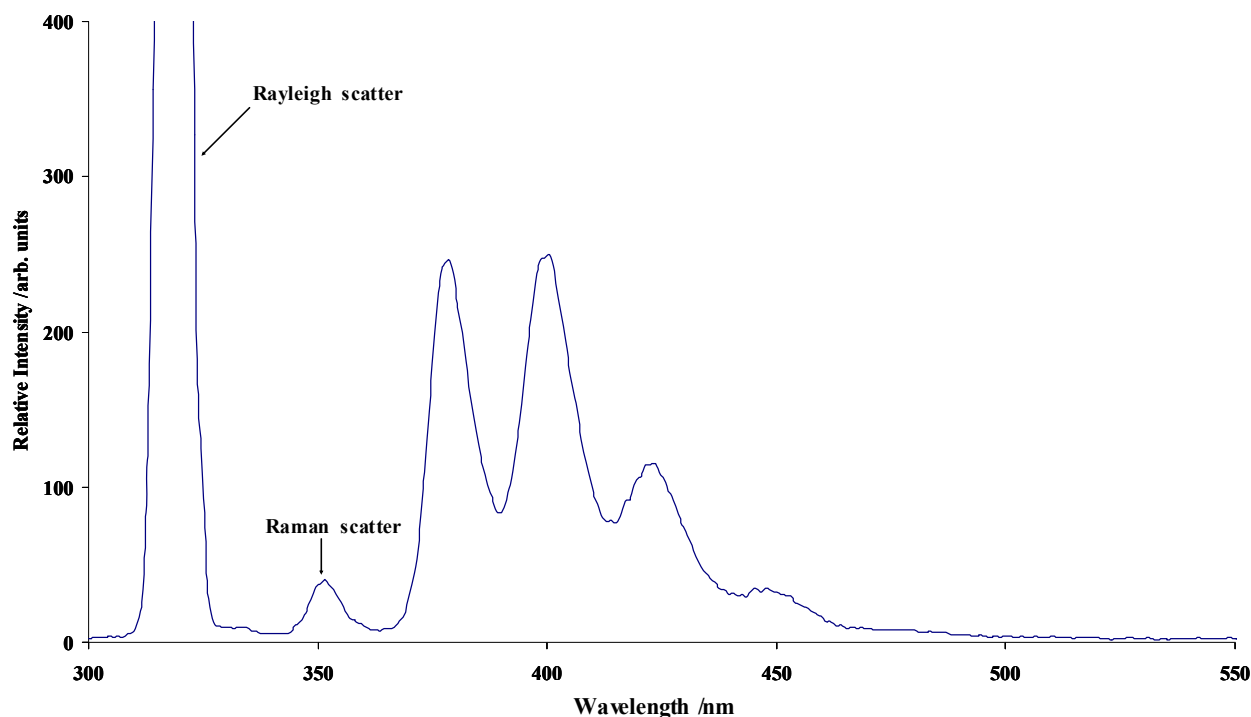


Figure 64 Emission spectrum of anthracene. $\lambda_{\text{Ex}} = 320 \text{ nm}$ at $1 \times 10^{-6} \text{ M}$ in ethanol.

As this sample was excited at 320 nm the Rayleigh scatter peak is clearly visible in the spectrum, the smaller peak at 350 nm is most likely due to Raman scatter.

Figure 65 shows a plot of the intensities of the peak at 398 nm against the concentration of anthracene. It is apparent that the fluorescence intensity varies linearly with concentration up to a limit of approximately $5 \times 10^{-6} \text{ M}$. Above an anthracene concentration of approximately $5 \times 10^{-6} \text{ M}$, the intensity of the fluorescence decreases and deviations from linearity are observed, presumably due to the “inner filter” effect as well as self absorption. Concentrations below $2 \times 10^{-7} \text{ M}$ were observable, however the signal to noise ratio of the emission spectra obtained was very poor and an accurate working range on the available instrumentation was therefore determined to be between $2 \times 10^{-7} \text{ M}$ and $5 \times 10^{-6} \text{ M}$ for anthracene in ethanol.

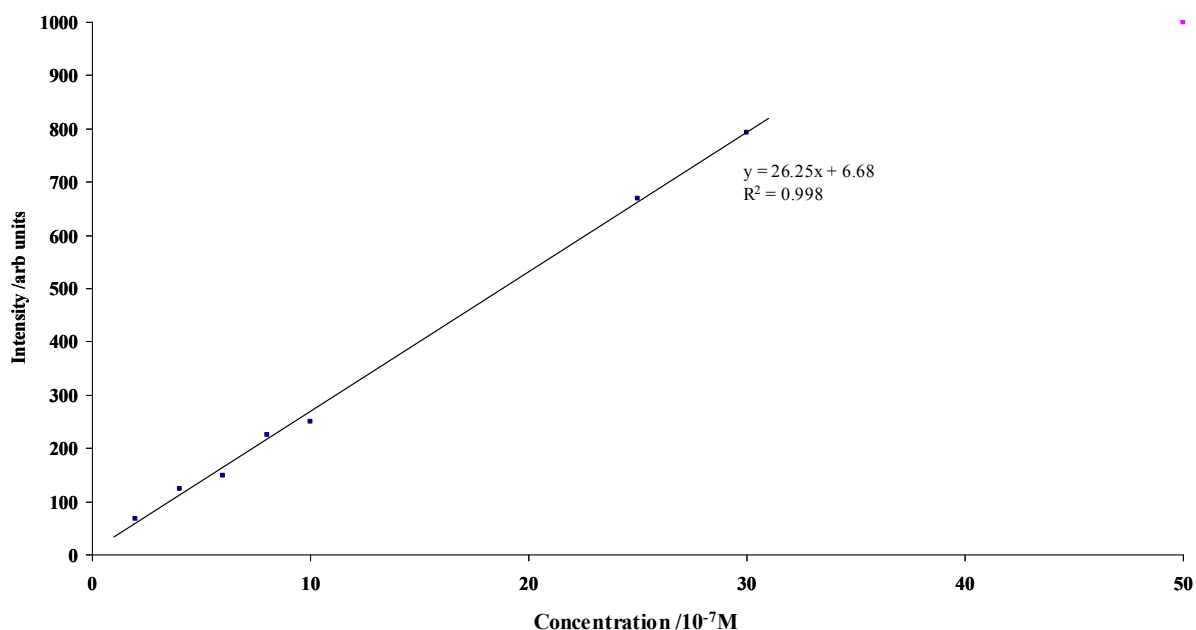


Figure 65 Graph depicting linear correlation between fluorescence intensity and anthracene concentration (mol dm^{-3}). $\lambda_{\text{Ex}} = 320 \text{ nm}$. Best fit equation and R^2 value as indicated. Fluorescence intensity at $5 \times 10^{-6} \text{ M}$ deviates from linearity and has therefore not been included in the trend line.

Various excitation wavelengths were also examined. The UV/Visible spectrum of anthracene shows strong absorbance peaks at wavelengths of 359 nm and 378 nm. Irradiation at these wavelengths would therefore increase the intensity of the signal observed, however this would have given rise to undesirable Rayleigh scatter. Despite various precautions being taken, the presence of the Rayleigh scatter peak in the emission spectrum is never practically avoidable and irradiation of the sample at wavelengths of 359 nm and 378 nm would have caused an overlap of this peak, with that of the emission spectra and hence given rise to an unquantifiable source of error. It was for this reason that an excitation wavelength of 320 nm was used as this wavelength gave a linear response between fluorescence intensity and concentration in the range $2 \times 10^{-7} \text{ M}$ to $5 \times 10^{-6} \text{ M}$ and avoided overlap of the Rayleigh scatter peak with the emission spectrum.

In order to determine the quantum yield of *N,N*-diethyl-*N'*-9-anthracoylthiourea in ethanol, it would be necessary to irradiate a sample of the ligand at 320 nm (wavelength established for anthracene) and at the same concentration as that of anthracene, *i.e.* in the range $2 \times 10^{-7} \text{ M}$ to $5 \times 10^{-6} \text{ M}$. This was however not possible as under these conditions (*i.e.* concentration and excitation wavelength), no emission for *N,N*-diethyl-*N'*-9-anthracoylthiourea could be observed. The concentration of HL¹ was therefore increased in order to establish if an observable emission signal could be found; and the lowest detectable concentration was observed at $2 \times 10^{-5} \text{ M}$. The concentration was increased in increments to a limit of $1 \times 10^{-4} \text{ M}$ and as is apparent (Figure 66) only a very limited linear range ($1 \times 10^{-5} \text{ M}$ – $5 \times 10^{-5} \text{ M}$) was obtained before self absorption occurred. It was therefore not possible to accurately determine the quantum yield for any of the *N,N*-dialkyl-*N'*-9-anthracoylthiourea derivatives, however if certain assumptions were made, an estimate of the quantum yield of *N,N*-diethyl-*N'*-9-anthracoylthiourea could be obtained.

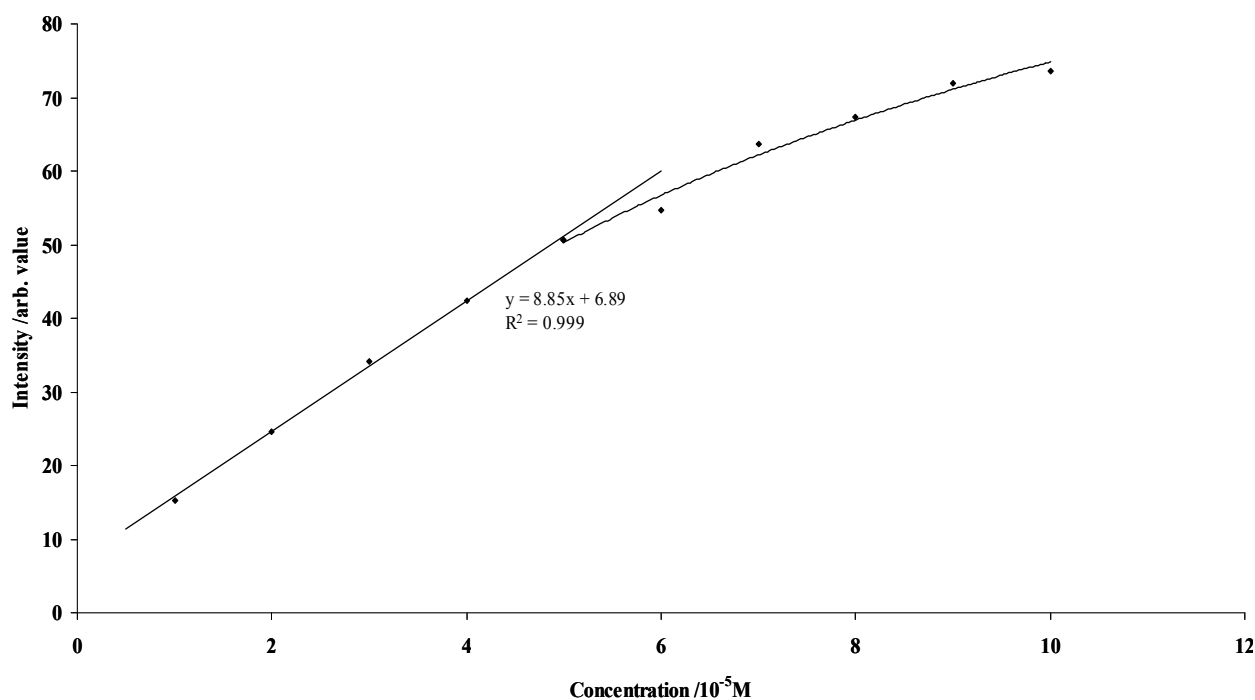


Figure 66 Graph depicting limited linear correlation between fluorescence intensity and concentration of *N,N*-diethyl-*N'*-9-anthracoylthiourea in ethanol. $\lambda_{\text{Ex}} = 320$ nm. Intensity of emission plotted for peak at 410 nm. Best fit equation and R^2 value as indicated.

As stated previously, the quantum yield of anthracene in ethanolic solution was assumed to be 0.3 at an excitation wavelength of 320 nm. If this is assumed to be accurate for a 1×10^{-6} M solution of anthracene as well, an estimate of the quantum efficiency of *N,N*-diethyl-*N'*-9-anthracoylthiourea could be determined to be 0.003, a 100 fold decrease in the quantum efficiency relative to anthracene, upon introduction of the acylthiourea moiety (the method by which the estimated quantum yield calculation was performed will be described further in section 4.4.6 for the pyrenebutanoylthiourea derivatives). The decrease in emission intensity of *N,N*-diethyl-*N'*-9-anthracoylthiourea may be attributable to the close proximity of the carbonyl group to the fluorescent moiety, as this has been found to cause quenching in other systems.^{52,53} The mechanism by which this occurs will be discussed in more detail in Section 4.4.3 although the decrease in quantum yield was rather more dramatic than anticipated.

A sample of 9-anthracenecarboxylic acid was available which was reasonably soluble in ethanol, so for comparison, solutions with a range of concentrations were prepared to determine whether the quenching was due to the carbonyl group only and what influence the acylthiourea moiety had on the intensity of the emission spectrum. The results are shown in Figure 67 where the emission spectrum of anthracene was obtained at a concentration of 5×10^{-6} M, half that of 9-anthracenecarboxylic acid and HL¹ to enable a comparison. It is apparent that the introduction of the carbonyl group in such close proximity to the aromatic fluorophore leads to a reduction of emission intensity, the effect being very pronounced for 9-anthracenecarboxylic acid.

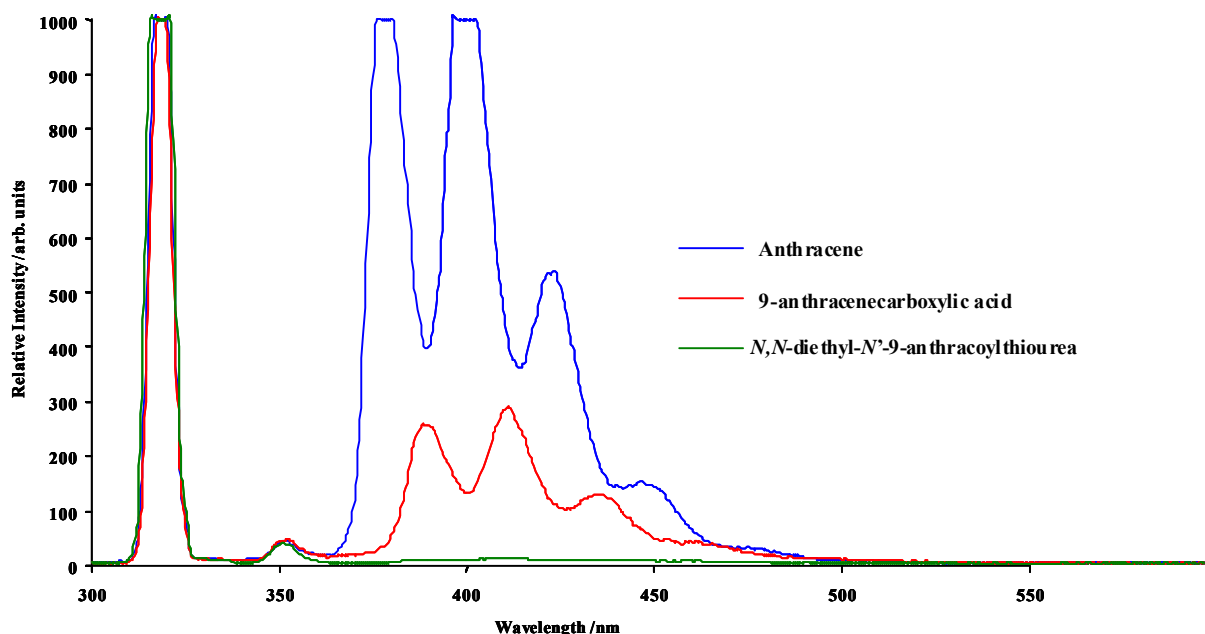


Figure 67 Emission spectra of anthracene, 9-anthracenecarboxylic acid and *N,N*-diethyl-*N'*-9-anthracoylthiourea in ethanol, illustrating quenching. $\lambda_{\text{Ex}} = 320 \text{ nm}$ and conc = $5 \times 10^{-6} \text{ M}$, $1 \times 10^{-5} \text{ M}$ and $1 \times 10^{-5} \text{ M}$ respectively.

The further reduction in emission intensity observed for the acylthiourea derivative may be understood in terms of the various tautomeric equilibria (Figure 68) which are possible with the *N,N*-dialkyl-*N'*-aroylthiourea compounds. The formation of the tautomers in ethanolic solution may provide alternative radiationless pathways and hence increase the probability of radiationless de-excitation of an electron, accounting for the low quantum yield exhibited by the *N,N*-diethyl-*N'*-9-anthracoylthiourea.

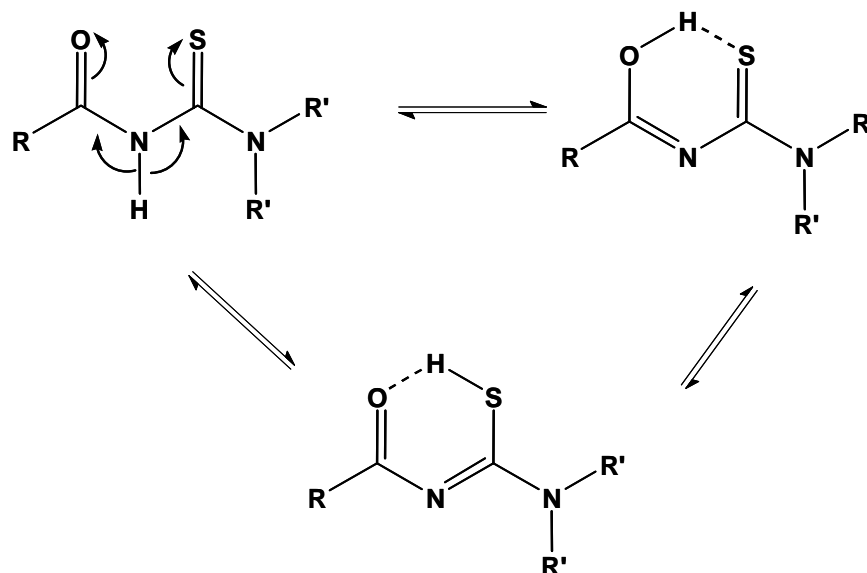


Figure 68 Possible tautomeric forms of *N,N*-dialkyl-*N'*-aroylthiourea in solution.

Unfortunately the complexes *cis*-[Pd(L¹-S,O)₂] and *cis*-[Pt(L¹-S,O)₂] were not sufficiently soluble in ethanol to enable the preparation of stock solutions (conc = $1 \times 10^{-3} \text{ M}$) for further dilution and thus had to be tested in dichloromethane. For comparison *N,N*-diethyl-*N'*-9-anthracoylthiourea was also tested in this

solvent in order to assess the effect of the metal ion on the emission intensity of these compounds. Figure 69 shows the effect of the solvent on the emission intensity of anthracene. The decrease in intensity is expected since solvents containing halide ions are known to reduce the quantum yields of fluorescing compounds.¹ The emission spectra obtained from the *cis*-[Pd(L¹-S,O)₂] and *cis*-[Pt(L¹-S,O)₂] complexes as well as *N,N*-diethyl-*N'*-9-anthracoylthiourea were therefore not expected to be very intense.

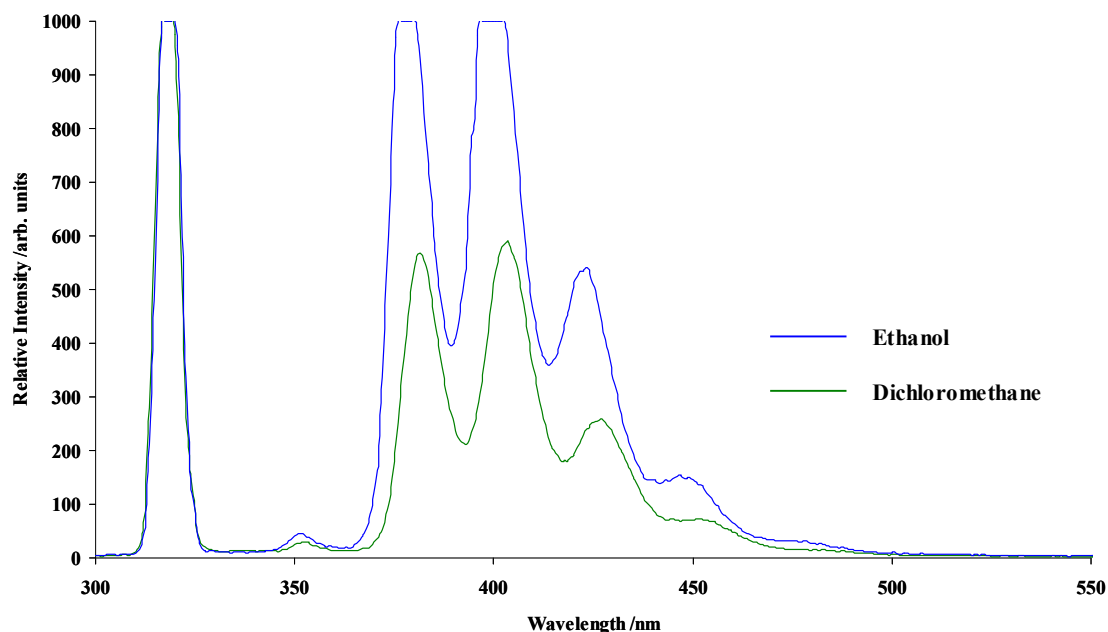


Figure 69 Influence of solvent on emission spectra of anthracene. Conc = 5×10^{-6} M and $\lambda_{\text{EX}} = 320$ nm.

4.4.2.1 Emission spectra of *N,N*-diethyl-*N'*-9-anthracoylthiourea in dichloromethane

The spectra obtained for concentrations of 1×10^{-5} M, 1×10^{-4} M and 1×10^{-3} M of *N,N*-diethyl-*N'*-9-anthracoylthiourea in dichloromethane are shown in Figure 70. The most intense emission of HL¹ was obtained from a 1×10^{-4} M solution and a limited linear correlation between relative fluorescence intensity and concentration is given in Figure 71 where the emission intensity of the peak at 413 nm was plotted as a function of concentration. It is apparent from Figure 71 that at concentrations above 1×10^{-4} M self absorption occurs and a linear relationship between concentration and emission intensity is only maintained in the range 1×10^{-5} M – 1×10^{-4} M. From the UV/Visible spectrum of *N,N*-diethyl-*N'*-9-anthracoylthiourea in dichloromethane (Figure 62), the wavelength of maximum absorption was slightly shifted (330 nm) relative to that of anthracene (320 nm) and the emission spectra of HL¹ were determined at 330 nm rather than at 320 nm to obtain the most intense signal.

As is apparent from the spectra in Figure 70, the smoothness of the curves is severely affected relative to those obtained from anthracene and 9-anthracenecarboxylic acid and this is likely to be due to the low intensity of the signal, resulting in the photomultiplier tube being at maximum gain. Various methods were available to smooth the signal *e.g.* Quadratic Golay-Slavitsky⁵⁴ however employment of these methods did little to improve the quality of the spectra obtained. Despite the poor quality of these emission spectra it can be seen that the wavelength region is similar to that of anthracene and the

transitions involved are therefore largely due to the $\pi^* \leftarrow \pi$ molecular orbitals of the anthracene fluorophore.

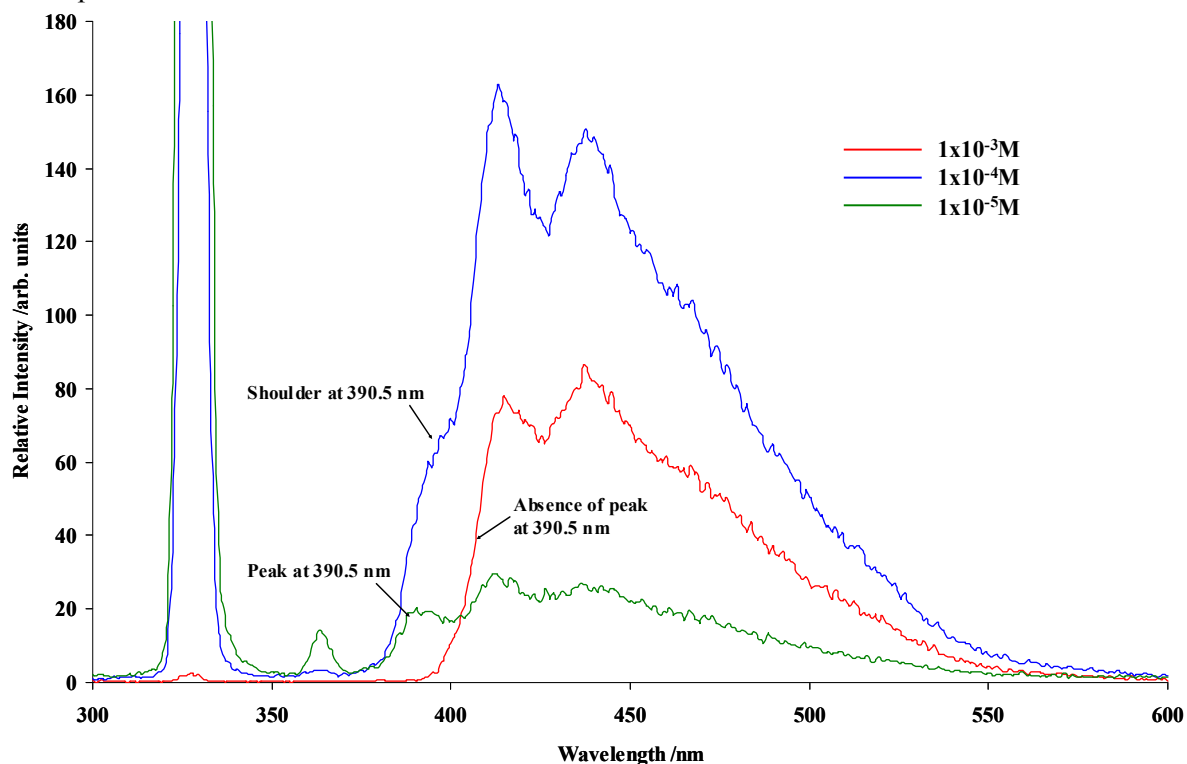


Figure 70 Emission spectra of *N,N*-diethyl-*N'*-9-anthracoylthiourea at various concentrations in dichloromethane. $\lambda_{\text{Ex}} = 330$ nm.

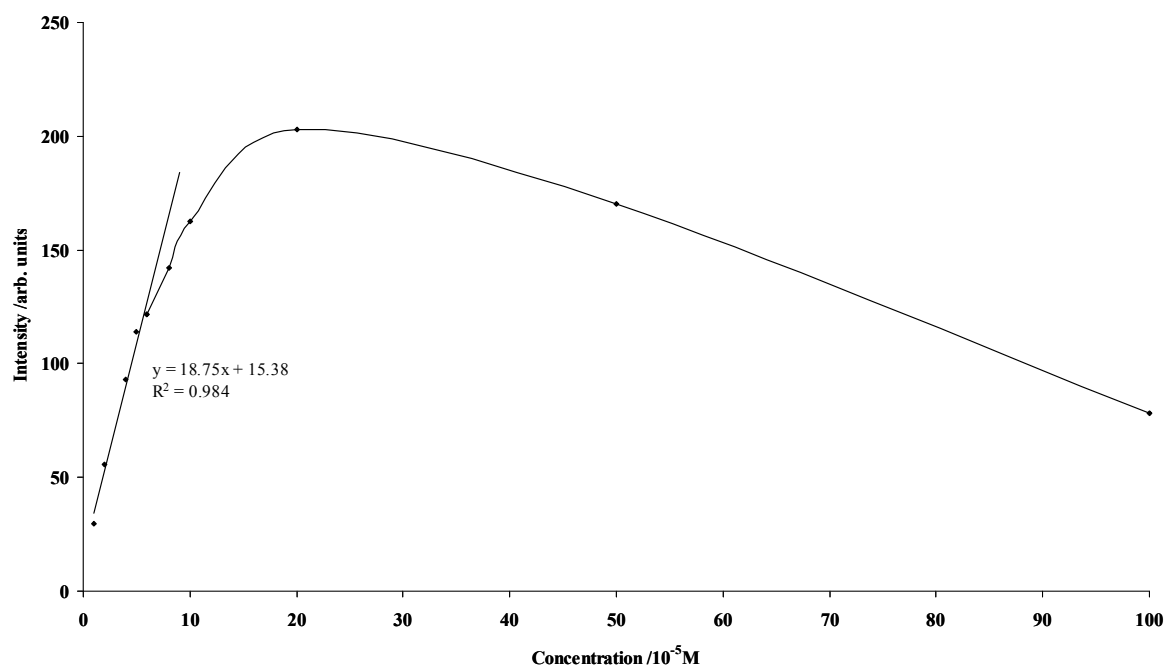


Figure 71 Graph depicting limited linear correlation between fluorescence intensity of emission maxima at 413 nm and concentration of *N,N*-diethyl-*N'*-9-anthracoylthiourea in dichloromethane. $\lambda_{\text{Ex}} = 330$ nm. Best fit equation and R^2 value as indicated.

Careful examination of the emission spectrum obtained from the 1×10^{-5} M solution of *N,N*-diethyl-*N'*-9-anthracoylthiourea shows three partially resolved peaks at 390.5, 412.5 and 436.5 nm. A ten-fold increase

in the concentration (1×10^{-4} M) exhibits only a shoulder in the 390.5 nm region, whilst the peaks at 412.5 and 436.5 nm still remain visible. A further increase in concentration to 1×10^{-3} M results in a decrease in emission and the absence of the 390.5 nm peak. It is well known that the absorption and emission spectra of anthracene overlap, causing self absorption at higher concentrations to be more accentuated than in cases where fluorophores have less spectral overlap. It would appear that a similar phenomenon is present here where the attenuation of the lower wavelength emission is observed as the concentration is increased due to the absorbance of this wavelength of emission by the ligand.⁶⁶

4.4.2.2 Emission spectra of *cis*-[Pd(L¹-S,O)₂] in dichloromethane

The emission spectra of *cis*-[Pd(L¹-S,O)₂] was obtained in dichloromethane and is shown in Figure 72. As with the ligand HL¹, the wavelength of maximum absorption of *cis*-[Pd(L¹-S,O)₂] from the UV/Visible spectrum in dichloromethane (Figure 62) was found to have shifted (330nm) relative to that of anthracene (320 nm). The emission spectra of *cis*-[Pd(L¹-S,O)₂] were therefore determined at 330 nm rather than at 320 nm to obtain the most intense signal.

Introduction of the metal ion in the *cis*-[Pd(L¹-S,O)₂] complex causes an overall reduction in the intensity of emission, however it can be seen that the faint emission present occurs in the same wavelength region as that of the ligand.

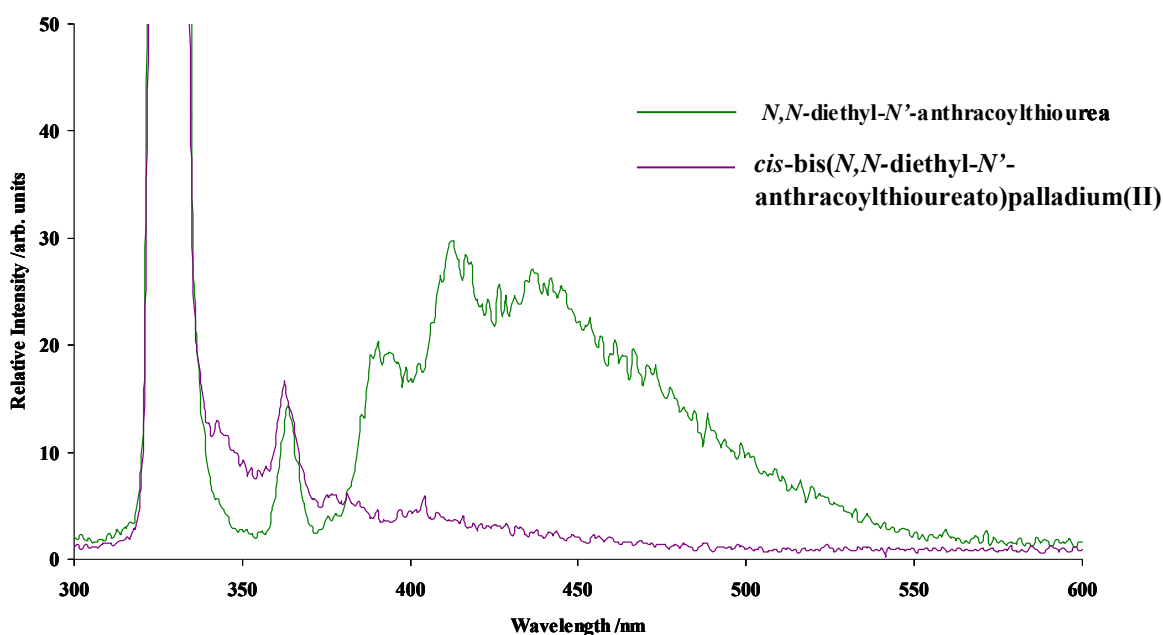


Figure 72 Emission spectra of *N,N*-diethyl-*N'*-9-anthracoylthiourea and *cis*-bis(*N,N*-diethyl-*N'*-9-anthracoylthioureato)palladium(II) in dichloromethane. Conc = 1×10^{-5} M and $\lambda_{\text{Ex}} = 330$ nm.

4.4.3 Discussion of the photophysical properties of the anthracoylthiourea derivatives.

4.4.3.1 Orientation of the carboxyl group

It is well known that anthracene and its derivatives exhibit excimer fluorescence at relatively high concentrations (10^{-2} M). These excimer emissions are at longer wavelengths and generally tend to be less structured relative to the monomer emissions at shorter wavelengths. Work done by Werner and Hercules⁵⁵ shed some new light on the nature of these emissions, particularly at lower concentrations (10^{-5} M). They tested solutions of 9-anthracenecarboxylic acid of similar concentrations to our solutions (10^{-5} M) in ethanol and it was found that the molecular form of 9-anthracenecarboxylic acid exhibited a structureless emission similar to that observed for the emission spectra of 9-anthric acid esters. This was attributed to an alteration in the geometry of the carboxyl group relative to the plane of the anthracene ring, rather than an excimer fluorescence as previously thought. In a solution of anthracene tested in ethanol, the maximum emission was found to occur at 401.6 nm, the emission maximum of 9-anthracenecarboxylic acid in an acidified solution of ethanol (to ensure the presence of the molecular form of the acid) was found to have “red shifted” significantly to 473.9 nm. The emission in this case was also broad and essentially structureless. The difference in the emission spectra of the two compounds was attributed to an excited state rotation of the carboxyl group into the plane of the anthracene ring. This configuration enables significant interaction between the carboxyl group and the anthracene ring and results in the drastic alteration of the emission spectrum observed. Werner and Hercules gave convincing evidence suggesting that the coplanar orientation of the molecular acid is stabilised by the formation of two 6-membered rings *via* hydrogen bonding with the *peri* hydrogens (Figure 73).

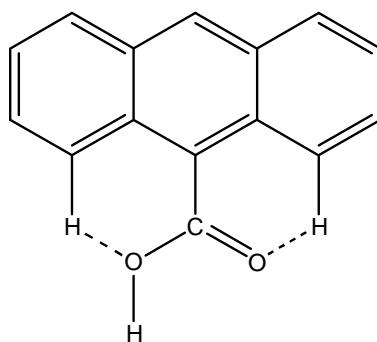


Figure 73 Coplanar orientation of the carboxyl group stabilised *via* hydrogen bonding with the *peri* hydrogen atoms.⁵⁵

As a direct consequence of this excited state stabilisation, an increased resonance interaction can occur between the carboxyl group and the aromatic rings due to greater π overlap. It can therefore be inferred that the emission of the molecular acid (unlike the absorption) is not localised on the anthracene ring, but actually involves a measure of carboxyl group participation through charge-transfer interactions. In the case of the dissociated acid, *i.e.* the ionic form, no longer wavelength emission was observed and the fine structure due to the vibronic bands were very similar to those of anthracene; presumably therefore no charge-transfer interaction between the anthracene ring and electron withdrawing carboxyl group occurs.

The carboxyl group is thought to be on average, in a perpendicular orientation relative to the plane of the anthracene ring due to steric hinderance by the *peri* hydrogens and this leads to a minimal resonance interaction between the carboxyl group and the ring and also minimises the effect that the carboxyl group has on the absorption spectrum. The small red shift observed being attributed to the inductive effect of the carboxyl substituent. Similarly, in the emission spectrum, the ground state geometry is retained and only the inductive effect contributes to the Stokes shift observed.⁵⁵

In the UV/Visible spectra of our compounds (Figure 62) an anthracene-like absorption was observed for all the compounds indicating that in the ground state at least, orthogonality between the carboxyl and aromatic groups is maintained. The 7 nm bathochromic shift of the *N,N*-dialkyl-*N'*-9-anthracoylthiourea derivatives relative to that of unsubstituted anthracene being attributed to the inductive effect of the carboxyl group.

From the emission spectra of HL¹ (Figure 67 and 70) it can be seen that the emission of the uncoordinated ligand is in a similar wavelength region to that of 9-anthracenecarboxylic acid (Figure 67), and that minimal Stoke's shifting has occurred on the addition of the acylthiourea moiety. Whilst the emission spectra of HL¹ are not as well defined as those of 9-anthracenecarboxylic acid, they are not structureless and the peaks of maximum emission are partially resolved (Figure 70). Therefore, based on the observations made by Werner and Hercules it is reasonable to suggest that the excited state orientation of the carboxyl group in HL¹ is perpendicular to the plane of the anthracene ring.

The direct attachment of the carboxyl group to the anthracene moiety in 9-anthracenecarboxylic acid results in a marked decrease in the emission intensity relative to anthracene and the intensity is reduced further by the presence of the nitrogen and sulfur atoms in *N,N*-diethyl-*N'*-9-anthracoylthiourea (Figure 67). This is consistent with work done by Czarnik and Chae.⁵⁶ They investigated the emission of 9-[(Methylamino)thiocarbonyl]anthracene and found it to be 56 times less intense at 413.5 nm than the emission observed for the related *N*-methyl-9-anthracene-carboxamide. The reduction in intensity of the thioamide being attributed to the presence of the sulphur atom, where the weaker C=S bond gives rise to the resonance structure shown in Figure 74. Czarnik *at al.* suggest that due to the ease with which thiolates are oxidized, the thioamide group might be a strong intramolecular quenching entity, the quenching mechanism of both the nitrogen and sulphur atoms being attributed to PET.⁵⁷

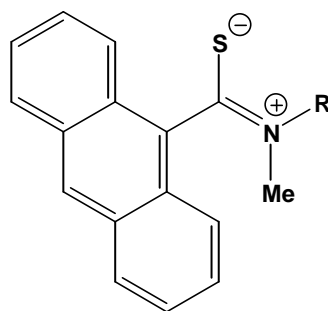


Figure 74 Resonance structure of 9-[(methylamino)thiocarbonyl]anthracene (Adapted from Reference 56).

The weak fluorescence of *N,N*-dialkyl-*N'*-9-anthracoylthiourea is also consistent with observations made by Bricks *et al.*,⁵⁸ on the emission of the closely related *N*-pyrrolidine-*N'*-9-anthracoylthiourea. Sandor *et al.*³⁷ synthesised a similar ligand in which the anthracene moiety was attached as an amine substituent, and the fluorescence quenching due to the attachment of the acylthiourea motif was found to be significantly less in this system, most likely due to the inclusion of a methylene spacer group between the amidic nitrogen atom and the anthracene fluorophore (Figure 75).

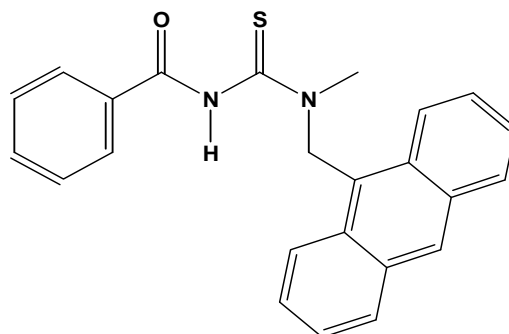


Figure 75 Structure of *N*-methyl-*N*-9-(methylantracene)-*N'*-benzoylthiourea³⁷

The introduction of the metal ion in the *cis*-[Pd(L¹-*S,O*)₂] complex further decreased the emission intensity however not as drastically as expected, (Figure 72). Despite the lower intensity of the emission, it is clear that no longer wavelength emission is present in the spectrum obtained from *cis*-[Pd(L¹-*S,O*)₂] and the orthogonal arrangement of the carboxyl group relative to the anthracene ring, in the excited state, is likely.

According to the design principles of PET systems (see section 4.2) the arrangement of fluorophore to receptor in our anthracoylthiourea derivatives can be classified as either an integral or orthogonal system. In the former, optical excitation leads to ICT and this results in charge shifts within the system and hence of the fluorescence band wavelengths as well. In the latter system, geometrical orthogonality precludes interaction between the molecular orbitals of the fluorophore and receptor and the mechanism of quenching can be thought of as PET with a virtual C_o spacer.

In the ground state, as previously discussed, it is apparent that the orthogonal arrangement of the carboxyl group relative to the anthracene ring prevails in both the ligand and complexes. The excited state geometry is however less apparent. It is possible that the slightly broader emission spectrum of HL¹ would appear to indicate a degree of planarity between the carboxyl group and anthracene rings, this allowing charge shifts between the fluorophore and acylthiourea moieties typical of integral systems. The shift in emission wavelength of HL¹ is however not as large as that reported for the closely related pyrrolidine analogue,⁵⁸ and hence a degree of orthogonality between the carboxyl group and anthracene ring is thought to be retained in the excited state. This would indicate the possibility of the anthracoylthiourea derivatives being an orthogonal system with a virtual C_o spacer. The signalling behaviour of orthogonal systems is generally interpreted as a PET process (ICT being the signalling process in integral systems) although alternative viewpoints do exist.²⁵

Theoretically, metal ion binding should reduce the PET leading to CHEF however we observe a decrease in the emission intensity of *cis*-[Pd(L¹-S,O)₂] relative to HL¹ and hence it can be concluded that in this case the M-F communication is greater than that of the M-R interaction. The form of M-F communication is most likely spin-orbit coupling due to the close proximity of the metal ion to the fluorophore; this leading to intersystem crossing and reducing the emission probability of the complex.⁵⁹ The presence of a M-F interaction is further supported by the presence of the absorption tail above 410 nm in the *cis*-[Pd(L¹-S,O)₂] complex (Figure 62).⁵⁰ It has been stated previously that complete coplanarity between the carboxyl group and the anthracene ring is not essential for a significant resonance interaction to occur⁵⁵ and from the results obtained a degree of carboxyl group participation in the excited state of the ligand and complexes can therefore not be completely excluded.

4.4.4 UV/Visible Spectra of the pyrenebutanoylthiourea derivatives

The UV/Visible absorption spectra of pyrene, *N,N*-diethyl-*N*'-[4-(pyrene-1-yl)butanoyl]thiourea (HL⁷), *cis*-bis(*N,N*-diethyl-*N*'-[4-(pyrene-1-yl)butanoyl]thioureato)platinum(II) *cis*-[Pt(L⁷-S,O)₂], and *cis*-bis(*N,N*-diethyl-*N*'-[4-(pyrene-1-yl)butanoyl]thioureato)palladium(II) *cis*-[Pd(L⁷-S,O)₂], were determined in dichloromethane and are given in Figure 76, the molar absorptivities at selected wavelengths in Table 37. As in the case of the corresponding anthracoylthiourea derivatives, the similarity between the spectrum of the unsubstituted pyrene and the derivatives is clear and the absorbance in the region 220-380 nm is therefore thought to be mainly due to molecular orbitals situated on the aromatic system, (*i.e.* π - π^* transitions). Various studies have been made of the absorption spectra of pyrene^{60,61} notably Becker *et al.* investigated the absorption spectra of a variety of aromatic hydrocarbons and the state assignments, as well as identification of the electronic transitions for pyrene were included.⁶² The introduction of a substituent on the pyrene moiety results in a bathochromic shift, which is not consistent for all the absorption peaks; the difference being very small at shorter wavelengths and increasing to the longer wavelength region with a maximum shift difference of approximately 7 nm at 344 nm. The shift differences between the ligand, *N,N*-diethyl-*N*'-[4-(pyrene-1-yl)butanoyl]thiourea and *cis*-[Pd(L⁷-S,O)₂] and *cis*-[Pt(L⁷-S,O)₂] complexes are negligible. As in the case of the anthracoylthiourea derivatives, *cis*-[Pd(L⁷-S,O)₂] and *cis*-[Pt(L⁷-S,O)₂] exhibit an increased absorbance relative to that of *N,N*-diethyl-*N*'-[4-(pyrene-1-yl)butanoyl]thiourea and this is once again attributed to a charge transfer contribution.

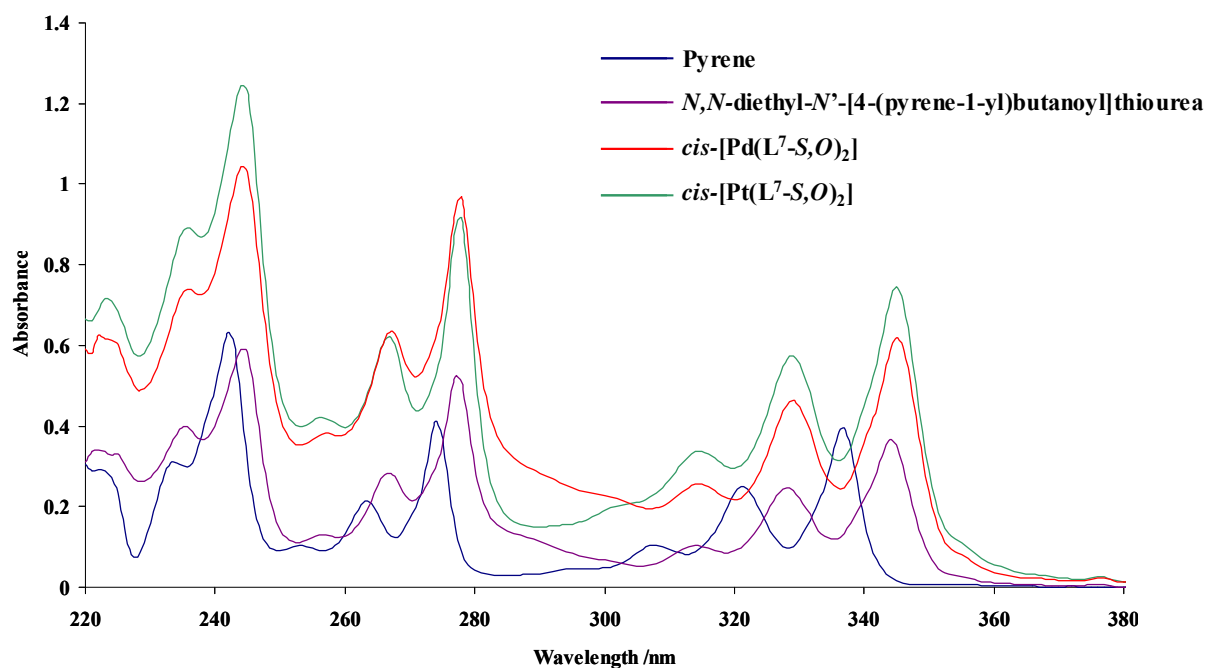


Figure 76 UV/Visible spectra of pyrene, *N,N*-diethyl-*N'*-[4-(pyrene-1-yl)butanoyl]thiourea, *cis*-bis(*N,N*-diethyl-*N'*-[4-(pyrene-1-yl)butanoyl]thioureaato)palladium(II) and *cis*-bis(*N,N*-diethyl-*N'*-[4-(pyrene-1-yl)butanoyl]thioureaato)platinum(II) in dichloromethane at 1×10^{-5} M.

Table 37 Molar absorptivities ($\text{cm} \cdot \text{mol}^{-1} \cdot \text{dm}^3$) of pyrenebutanoylthiourea derivatives at selected wavelengths in dichloromethane.

pyrene		HL^7		<i>cis</i> -[Pd(L^7 -S, O) $_2$]		<i>cis</i> -[Pt(L^7 -S, O) $_2$]	
Wavelength (nm)	log ϵ	Wavelength (nm)	log ϵ	Wavelength (nm)	log ϵ	Wavelength (nm)	log ϵ
234	4.49	235	4.60	236	4.87	236	4.95
242	4.80	244	4.77	244	5.02	244	5.10
253	4.01	257	4.11	257	4.58	256	4.62
263	4.33	267	4.45	267	4.80	267	4.79
274	4.61	277	4.72	278	4.98	278	4.96
308	4.02	314	4.01	315	4.41	315	4.53
321	4.39	328	4.39	329	4.67	329	4.76
337	4.60	344	4.56	345	4.79	345	4.87

From a comparison of data in Table 37 with that of the anthracoylthiourea derivatives (Table 36) it can be seen that the molar absorptivity of pyrene is greater than that of anthracene. The complexes, *cis*-[Pd(L^7 -S, O) $_2$] and *cis*-[Pt(L^7 -S, O) $_2$] both have comparable molar absorptivities, these being somewhat larger than both that of the ligand, HL^7 and the unsubstituted pyrene.

4.4.5 Emission spectra of pyrenebutanoylthiourea derivatives

In the case of the pyrenebutanoylthiourea derivatives, neither the ligand, *N,N*-diethyl-*N'*-[4-(pyrene-1-yl)butanoyl]thiourea, nor the complexes were soluble in ethanol and dichloromethane was therefore used as a solvent, despite its likely quenching effect. In the determination of the linear working range for the pyrenebutanoylthiourea derivatives, all the compounds were irradiated with an excitation wavelength of 340 nm as from the UV/Visible spectra, this frequency lay the closest to an absorption maximum for all the compounds tested. Irradiating all the compounds at their wavelengths of maximum absorption would have given rise to an unquantifiable source of error as the lamp intensity may have varied with the wavelength, the intensity of the irradiating light then not being consistent for each compound. Fortunately there was little variation in the absorption maxima of the compounds. From the UV/Visible spectrum (Figure 76), the strongest absorption is centred around 240 nm and would therefore give rise to the most intense emission signal. In terms of lowering the detection limit of the compounds it would have been advisable to excite the compounds at this wavelength, however the emissions were so intense, for pyrene in particular, that very few concentrations of pyrene were detectable and a more practically useful frequency was established as 340 nm.

The emission spectrum of pyrene was determined at varying concentrations and using different excitation wavelengths. An example of the emission spectrum of pyrene is shown in Figure 77 from which the mirror image relationship between the absorption and emission spectrum so clearly seen for anthracene is not reflected in pyrene. It is however known that the vibronic band intensities in pyrene emissions vary due to sensitivity to solvent effects.⁶³ The intensities of the various bands however agree well with those previously obtained in the literature for ethanolic solutions of pyrene.⁶⁴

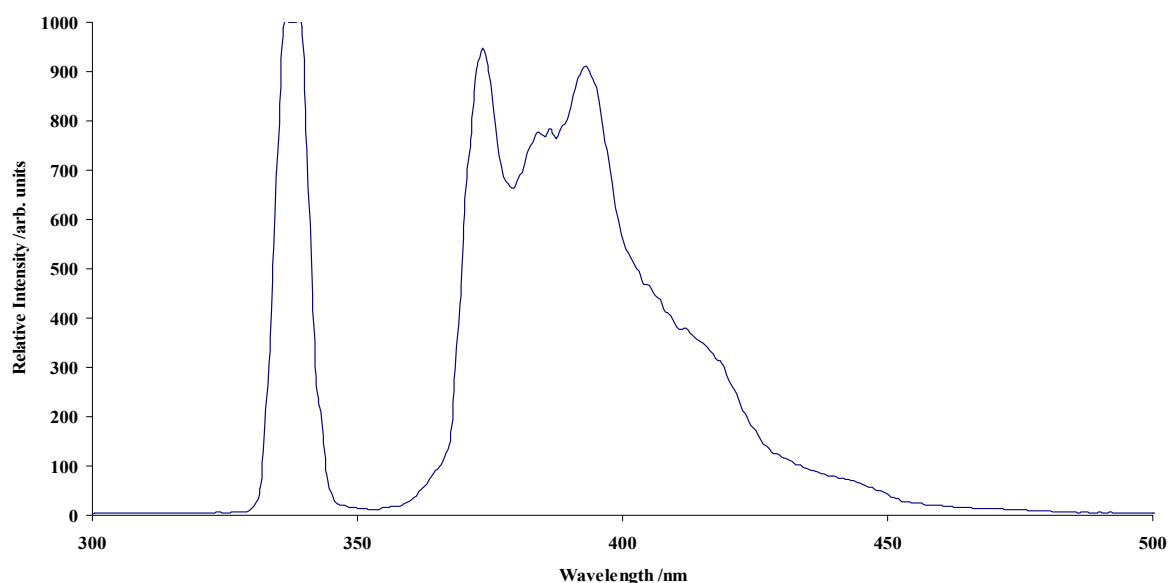


Figure 77 Emission spectrum of pyrene determined in dichloromethane. Conc = 6×10^{-7} M and $\lambda_{\text{Ex}} = 340$ nm.

As in the case for the anthracoylthiourea derivatives, a concentration range needed to be established where all the compounds exhibited a linear correlation between concentration and emission intensity, to

enable accurate comparisons to be made between the spectra obtained from the compounds, as well as for the estimation of the quantum yield. Figure 78 shows the range of concentrations tested for pyrene plotted against the fluorescence intensity of the emission peak at 377 nm. It is apparent that above 1×10^{-6} M the signal was too intense to detect, self absorption at concentrations above 1×10^{-4} M lowering the intensity of the signal and therefore enabling its detection. It is unlikely that the intense emission observed for pyrene at 1×10^{-6} M is due to excimer formation, this usually occurring at concentrations above 1×10^{-3} M (see Section 4.1.2). A linear concentration range was therefore established to be between 1×10^{-7} M and 1×10^{-6} M for pyrene in dichloromethane on the available instrumentation.

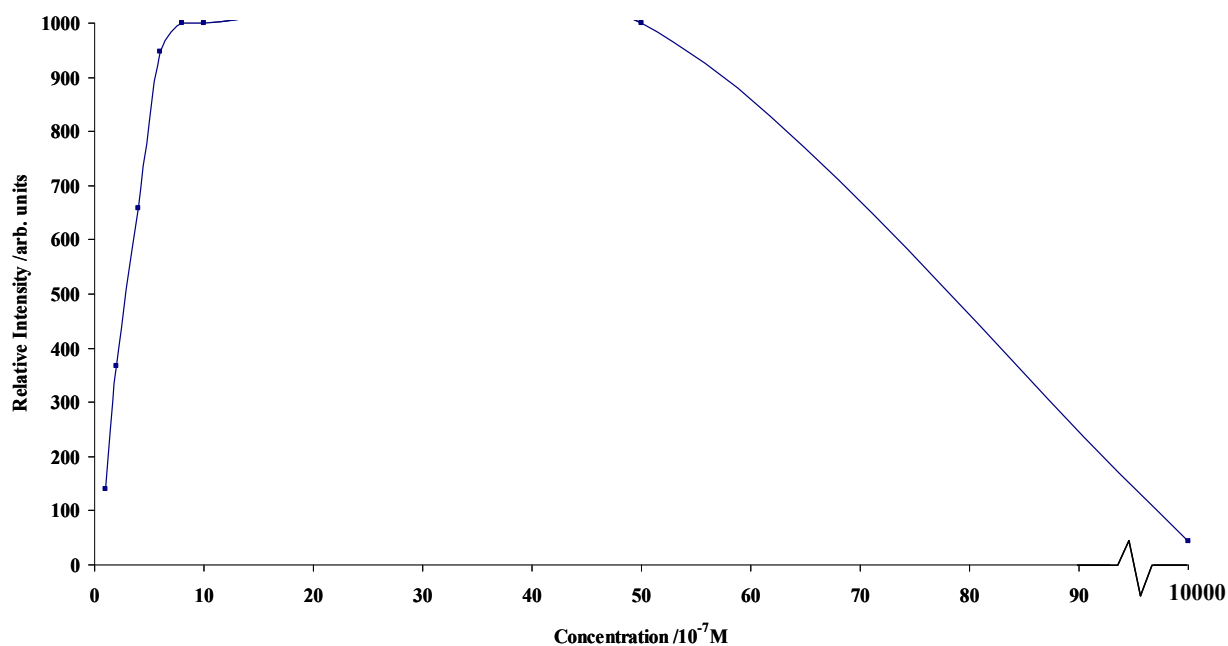


Figure 78 Graph depicting limited linear correlation between fluorescence intensity and concentration for pyrene in dichloromethane. $\lambda_{\text{Ex}} = 340$ nm

The ligand, *N,N*-diethyl-*N'*-[4-(pyrene-1-yl)butanoyl]thiourea was tested under similar conditions and the emission spectrum is given in Figure 79. The linear correlation range between concentration and emission intensity of HL⁷ being shown in Figure 80 where the intensity on the abscissa refers to the emission of the peak centred around 377 nm. Once again self absorption occurred above a concentration of 5×10^{-6} M and the most accurate working range in this case was determined to be between 1×10^{-7} M and 5×10^{-6} M. Emission spectra of HL⁷, *cis*-[Pd(L⁷-S,O)₂] and *cis*-[Pt(L⁷-S,O)₂] are shown in Figure 81 and similarly to HL⁷, linearity between concentration and emission intensity of *cis*-[Pd(L⁷-S,O)₂] and *cis*-[Pt(L⁷-S,O)₂] was only maintained up to a concentration of 1×10^{-6} M before attenuation of the intensity was caused, once again, most likely due to self absorption.

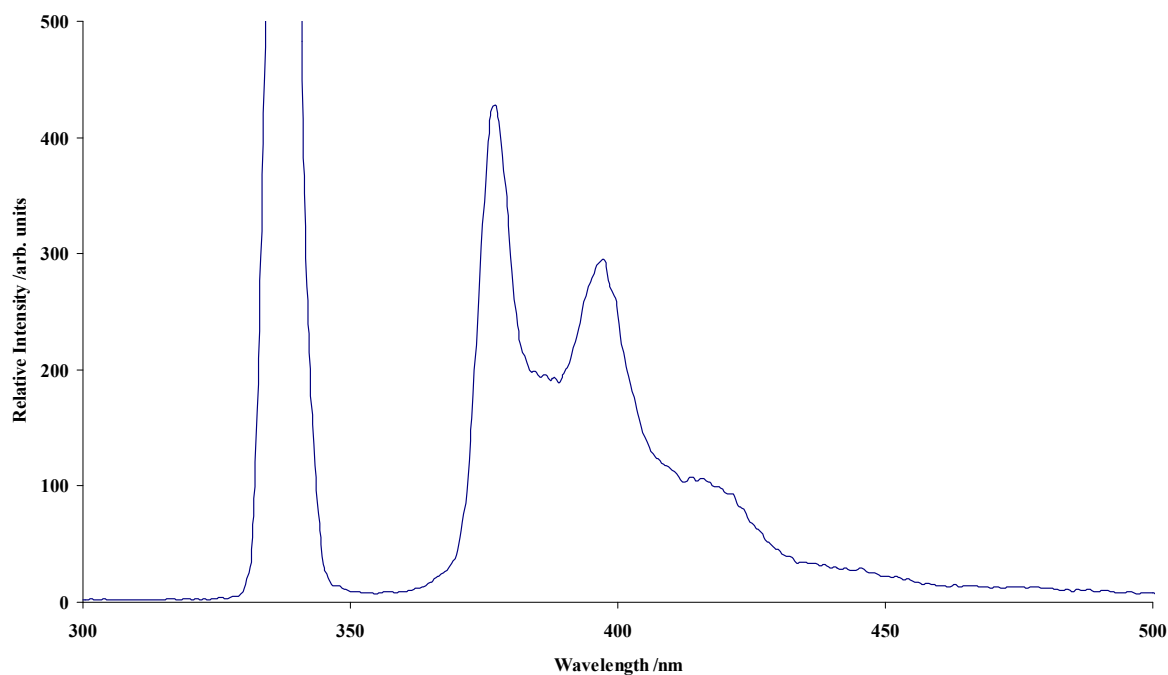


Figure 79 Emission spectrum of *N,N*-diethyl-*N'*-[4-(pyrene-1-yl)butanoyl]thiourea in dichloromethane. Conc = 2.5×10^{-6} M and $\lambda_{\text{Ex}} = 340$ nm.

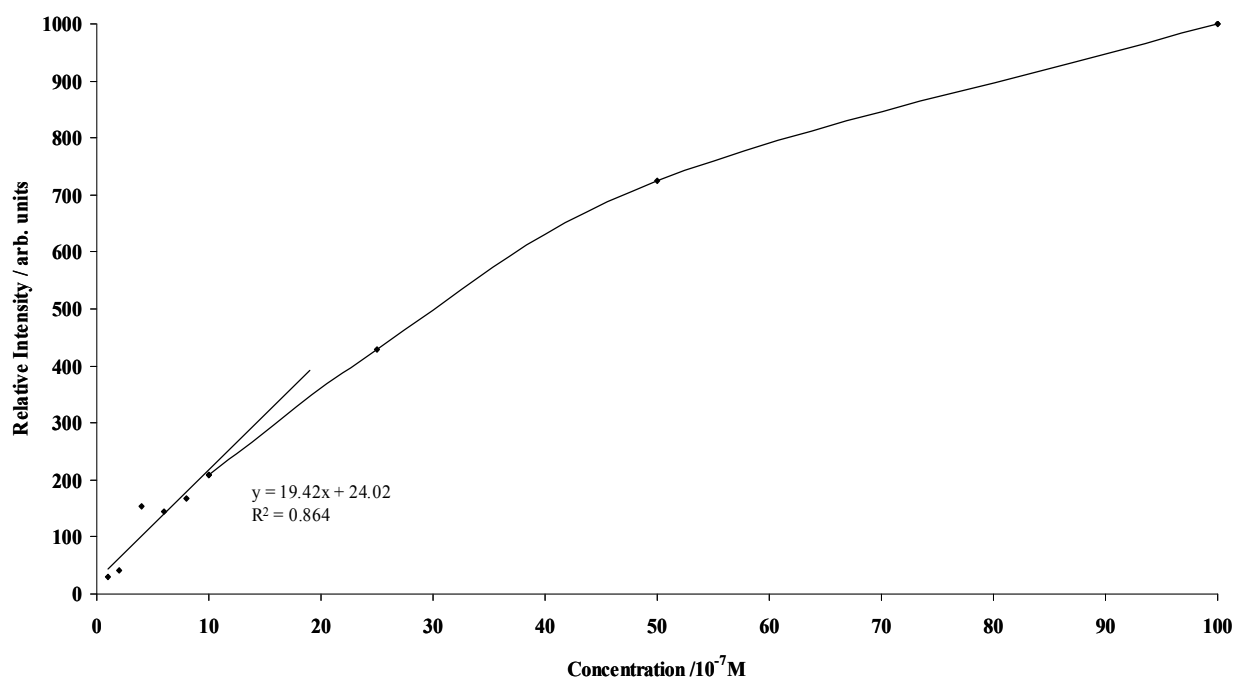


Figure 80 Graph depicting limited linear correlation between fluorescence intensity and concentration of *N,N*-diethyl-*N'*-[4-(pyrene-1-yl)butanoyl]thiourea. $\lambda_{\text{Ex}} = 340$ nm. Best fit equation and R^2 value as indicated. (Relative intensity for 4×10^{-7} M point not included in linear trend line).

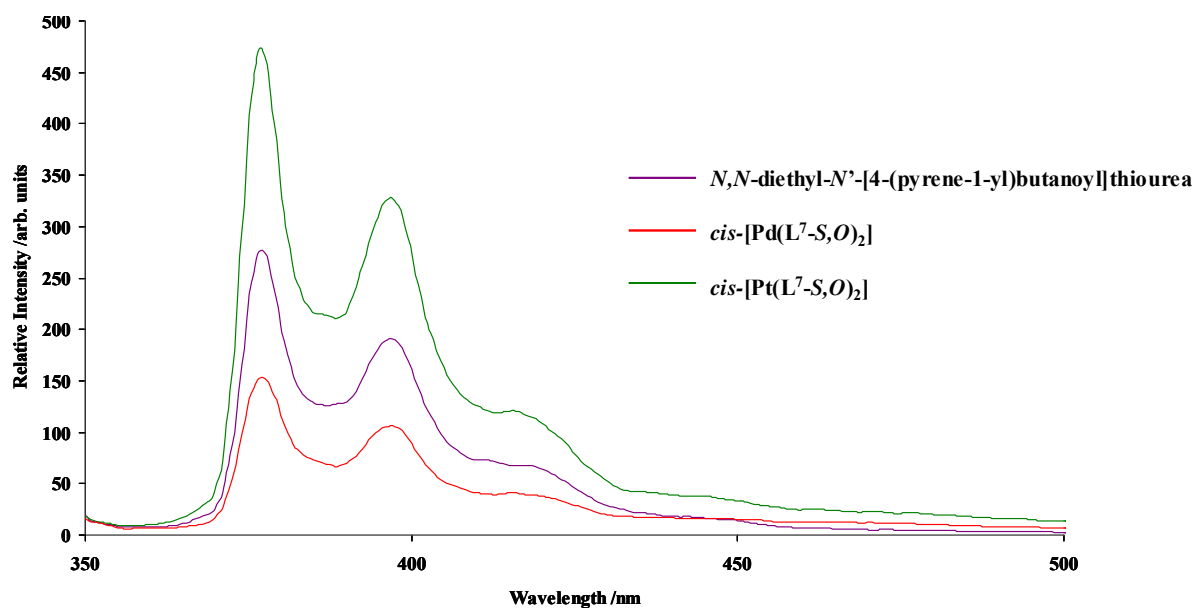


Figure 81 Emission spectrum of *N,N*-diethyl-*N'*-[4-(pyrene-1-yl)butanoyl]thiourea and the platinum and palladium complexes in dichloromethane. Conc = 1.0×10^{-6} M and $\lambda_{\text{Ex}} = 344$ nm.

The emission spectra of HL^7 , $\text{cis-}[\text{Pt}(\text{L}^7\text{-S},\text{O})_2]$ and $\text{cis-}[\text{Pd}(\text{L}^7\text{-S},\text{O})_2]$ (Figure 81) are in contrast to those reported by Schuster *et al.*⁶⁵ for related compounds. Schuster and Unterreitmaier studied chloroform solutions of *N,N*-diethyl-*N'*-[4-(pyrene-1-yl)butanoyl]thiourea (DEPyBuT) (Figure 82), its platinum (II) complex, $\text{Pt}(\text{DEPyBuT})_2$ and *N,N*-diethyl-*N'*-1-pyreneoylthiourea, (DEPyT). Schuster *et al.* reported a reduction of emission intensity upon introduction of the platinum metal ion during complexation. The spectra reported illustrated this, and are shown in Figure 82. The excitation wavelength used was reportedly 345 nm, however the concentration at which these spectra were obtained was not given. In the testing of our compounds similar results to these were obtained when *N,N*-diethyl-*N'*-[4-(pyrene-1-yl)butanoyl]thiourea, $\text{cis-}[\text{Pt}(\text{L}^7\text{-S},\text{O})_2]$ and $\text{cis-}[\text{Pd}(\text{L}^7\text{-S},\text{O})_2]$ were irradiated at 344 nm and at a concentration of 1×10^{-4} M. Figure 83 shows this and a comparison can be made between these spectra and those reported by Shuster. The intensities of $\text{cis-}[\text{Pt}(\text{L}^7\text{-S},\text{O})_2]$ and $\text{cis-}[\text{Pd}(\text{L}^7\text{-S},\text{O})_2]$ were significantly reduced relative to that of HL^7 . By looking at these results, the conclusions made by Schuster *et al.* of quenching due to metal ion introduction resulting in spin-orbit coupling *etc.* are slightly premature. At these concentrations it is clear that no linear relationship between concentration and fluorescence intensity exists (Figure 80). Other factors therefore, such as self absorption play a significant role in the reduction of emission intensity and contrary to Schuster's suggestion, it is most likely external factors such as these, rather than intramolecular spin-orbit coupling, resulting in the decrease in emission intensity of the platinum complex in Figure 82.

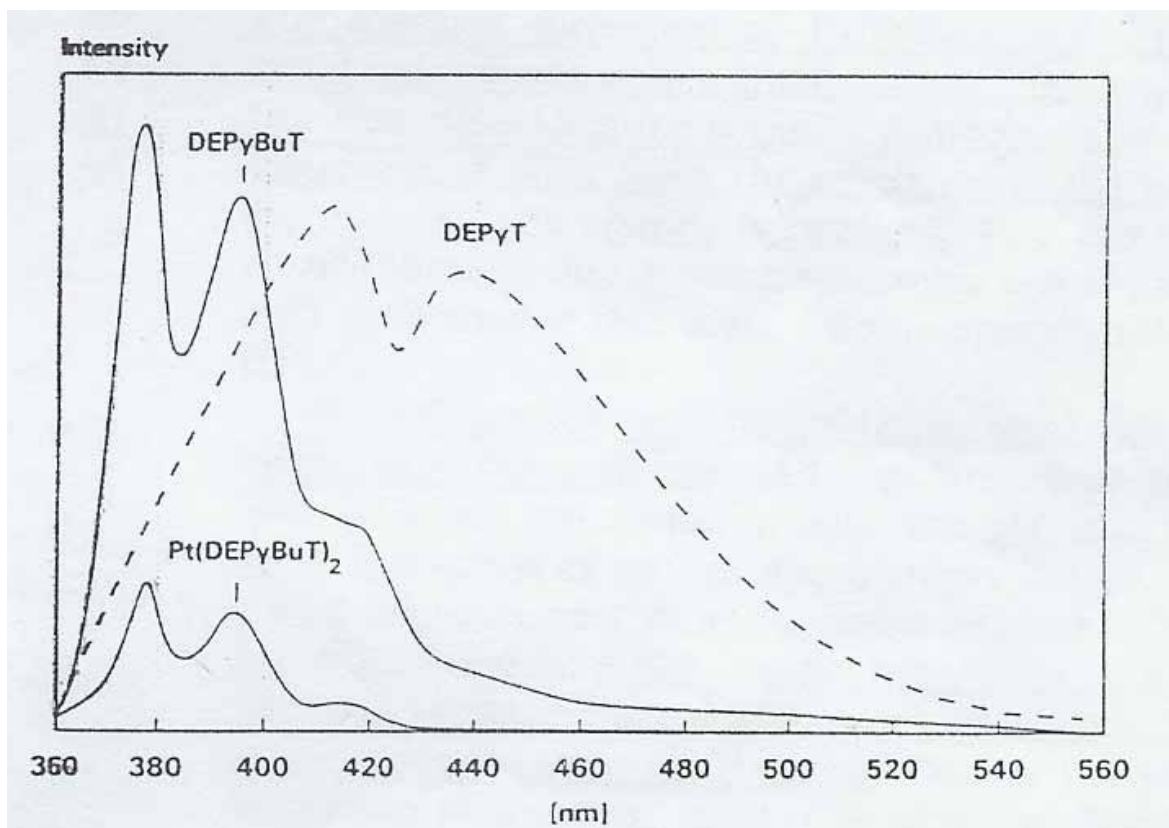


Figure 82 Emission spectra reported by Schuster where DEPyBuT refers to *N,N*-diethyl-*N'*-[4-(pyrene-1-yl)butanoyl]thiourea, DEPyT to *N,N*-diethyl-*N'*-1-pyrenylthiourea and Pt(DEPyBuT)₂ to the platinum complex of *N,N*-diethyl-*N'*-[4-(pyrene-1-yl)butanoyl]thiourea.⁶⁵

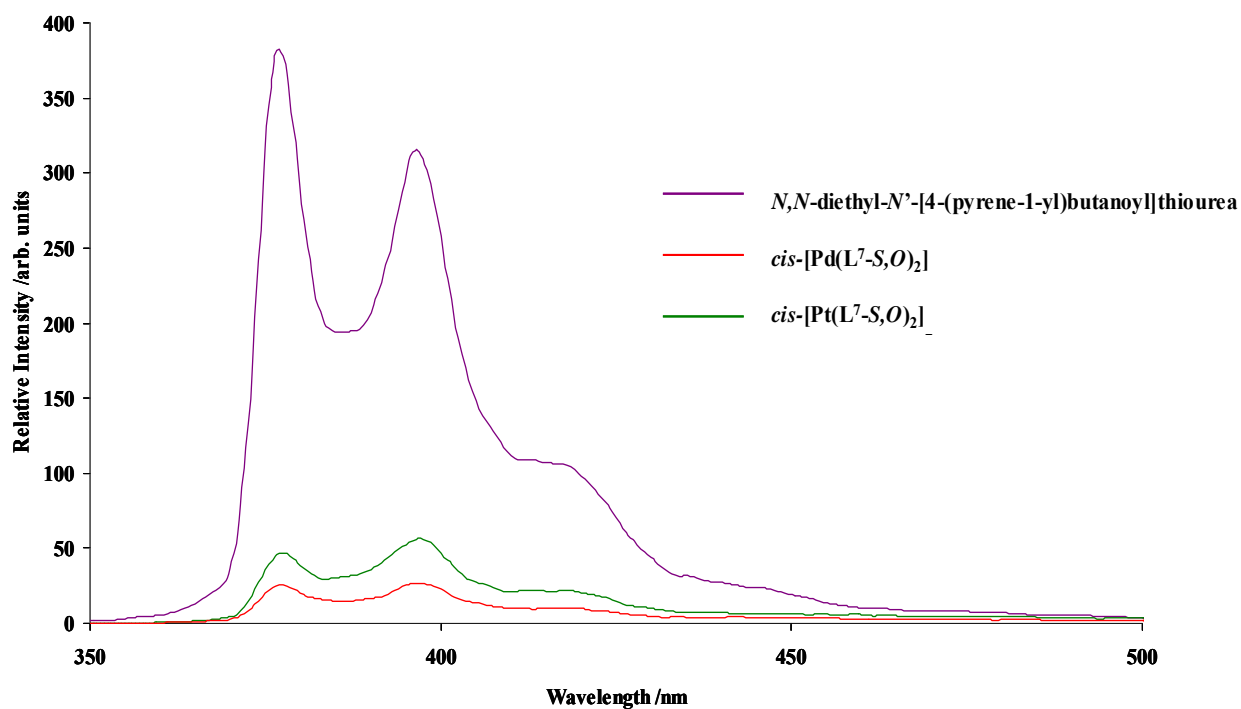


Figure 83 Emission spectra of *N,N*-diethyl-*N'*-[4-(pyrene-1-yl)butanoyl]thiourea, *cis*-[Pt(L⁷-S,O)₂] and *cis*-[Pd(L⁷-S,O)₂] in dichloromethane. Conc = 1 × 10⁻⁴ M and λ_{Ex} = 344 nm.

Lowering the concentration of the pyrenebutanoylthiourea derivatives to within the linear working range (1×10^{-6} M) gives the spectra shown in Figure 81. It is apparent that the difference in emission intensity between HL⁷ and the complexes is much greater at higher concentrations (Figure 83) than at a concentration of 10^{-6} M (Figure 81). It is therefore likely that at a lower concentration, the degree of self-absorption for the ligand and complexes are different, due to the absorbance differences at the excitation wavelength (Table 37). If for a given concentration of HL⁷ vs *cis*-[Pt(L⁷-S,O)₂] or *cis*-[Pd(L⁷-S,O)₂] at an excitation wavelength of 344 nm, the degree of self-absorption for each compound is different. Consequently, as each solution is diluted, truer emission spectra will be observed and hence the difference between Figure 81 and Figure 83 could reflect this. From Figure 81 it would appear that *cis*-[Pt(L⁷-S,O)₂] exhibits a small degree of CHEF and that the *cis*-[Pd(L⁷-S,O)₂] complex, a degree of CHEQ (chelation enhanced quenching). However as previously stated, the complexes are more strongly absorbing than the ligand (Figure 76) and as the quantum yield is the ratio of photons emitted to those absorbed, the emission spectra in this form do not provide sufficient information for photophysical deductions to be made about these compounds, rather, the quantum yield should be used in these inferences.

4.4.6 Quantum yield determination of pyrenebutanoylthiourea derivatives

As previously mentioned, the method for quantum yield determination closely followed that of Russo.⁴⁵ Using this method (Equation 6, Section 4.2.1.) it is assumed that the quantum yield of the known and unknown solutions is determined in the same solvent. The literature value available for the quantum yield of pyrene was determined in ethanol and the determination of the quantum efficiencies of the pyrenebutanoylthiourea derivatives was slightly complicated by this fact as the solubility of these compounds is limited to dichloromethane.

Work done by Hrdlovic, *et al.*⁴⁶ involved the study of multifunctional probes derived from 1-pyrenebutyric acid, both in polymer matrices and in solution. The method used in this work, to establish the quantum yield of the compounds investigated, closely followed those reported previously, however, with the inclusion of two additional terms as given below in Equation 7.

$$\Phi_u = \Phi_s \cdot \frac{\text{Area}_u \cdot (1-10^{-A_s}) \cdot (n^u) \cdot (2-r^s)}{\text{Area}_s \cdot (1-10^{-A_u}) \cdot (n^s) \cdot (2-r^u)} \quad \text{Equation 7}$$

Where all variables are as previously defined and n^u and n^s refer to the refractive indexes for the solvents of the unknown and standard solutions, and r^u and r^s refer to the emission anisotropies. This method could therefore be used to make a comparison between compounds in differing solvents and use of equation 7 in determining the quantum yield of pyrene in dichloromethane would theoretically be possible. As both pyrene solutions were very dilute (ethanol and dichloromethane) and similar concentrations were being used, the anisotropic term was omitted, however the refractive index term was included due to the differing solvents. By determining the quantum yield of pyrene in dichloromethane using this equation,

the quantum yield of the pyrenebutanoylthiourea derivatives could then be calculated in dichloromethane using the method previously described, *i.e.* Equation 6.

Solutions of pyrene in ethanol and dichloromethane were prepared at a concentration of 1×10^{-5} M and the UV/Visible spectra determined. These solutions were diluted ten times and the emission spectra obtained with an excitation wavelength of 313 nm, as this was the wavelength used in the determination of the literature value of pyrene's quantum yield. Excitation at this wavelength had the added advantage of not involving complications due to Rayleigh and Raman scatter peaks, and conformed to the method of Russo⁴⁵ which recommends that the absorbance of the solutions at working concentrations should not exceed 0.4 prior to the dilution. Solutions of the pyrenebutanoylthiourea derivatives were prepared at concentrations of 1×10^{-5} M and the UV/Visible absorption spectra determined followed by 10x dilutions for the determination of the emission spectra.

4.4.6.1 Results and Discussion

Figure 84 shows the UV/Visible absorption spectra of pyrene in ethanol and dichloromethane. It is apparent that the peaks of maximum absorbance are slightly "red shifted" in dichloromethane relative to that of ethanol, however the absorbances are comparable. The emission spectra of pyrene in ethanol and dichloromethane as well as the spectrum of HL⁷ in dichloromethane is shown in Figure 85. It is unusual that the emission intensity of pyrene is greater in dichloromethane than in ethanol as the former is considered a quenching solvent and a lower emission intensity is therefore expected. This is in contrast to the emission spectra of anthracene where the emission intensity of ethanolic anthracene was greater than that of anthracene in dichloromethane. Possible reasons for this will be discussed later in the section.

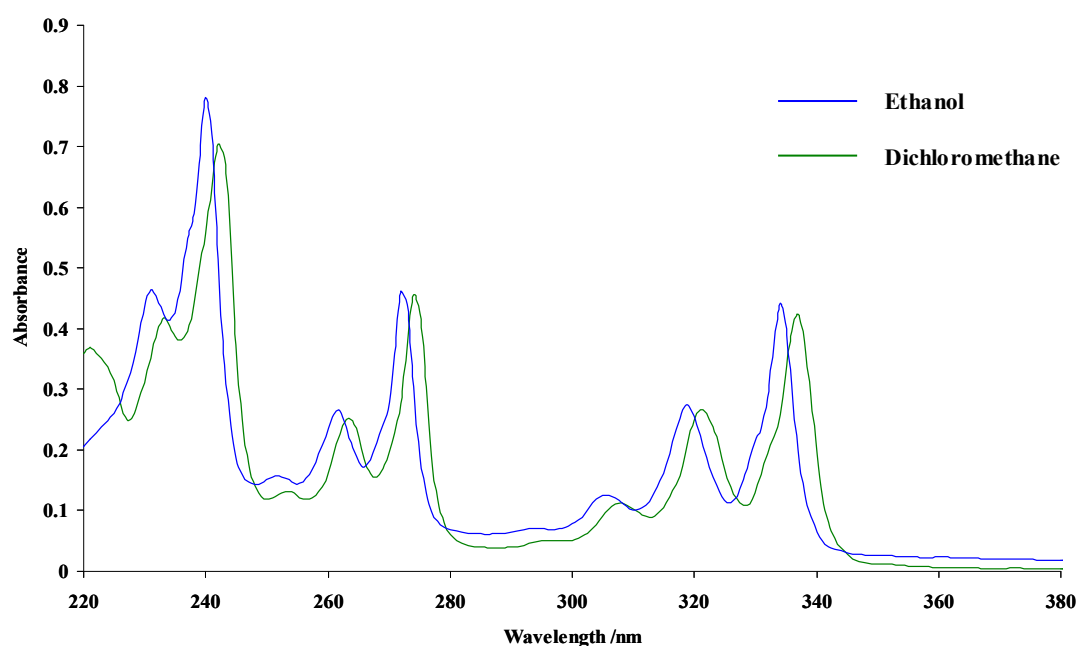


Figure 84 UV/Visible Spectra of pyrene in ethanol and dichloromethane at conc. = 1×10^{-5} M.

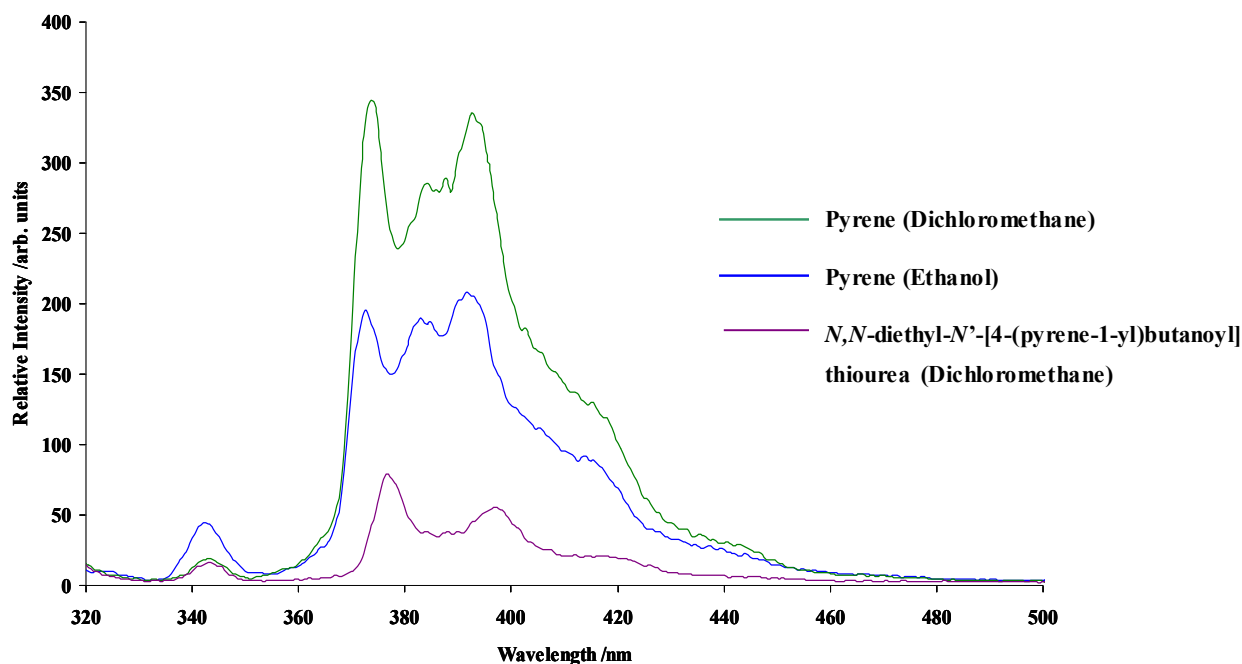


Figure 85 Emission spectra of pyrene in ethanol and dichloromethane and *N,N*-diethyl-*N'*-[4-(pyrene-1-yl)butanoyl]thiourea in dichloromethane. Conc = 1×10^{-6} M and $\lambda_{\text{Ex}} = 313$ nm.

Dawson *et al.*⁶⁶ reported a value of 0.53 for the quantum yield of pyrene in ethanolic solutions ranging in concentration between 10^{-6} M and 10^{-5} M. Using this value and values of 1.359 and 1.424⁶⁷ as the refractive indices of ethanol and dichloromethane respectively gave a value of 1.1 for the quantum yield of pyrene in dichloromethane. This value is clearly anomalous and in order to obtain a more reasonable value, the calculation was repeated, omitting the refractive index term. This was in essence the same as using Equation 6 and gave a value of 0.8 as the quantum yield of pyrene which appeared to be a more realistic value. Both these values were used separately in order to obtain the quantum yields of HL⁷, *cis*-[Pd(L⁷-S,O)₂] and *cis*-[Pt(L⁷-S,O)₂] in dichloromethane using Equation 6 and these are shown in Table 38. Despite the irregular values for the quantum yield of pyrene in dichloromethane, meaningful observations can be made from the relative quantum yields of the pyrenebutanoylthiourea derivatives. Figure 86 shows the emission spectra of *N,N*-diethyl-*N'*-[4-(pyrene-1-yl)butanoyl]thiourea as well as *cis*-[Pd(L⁷-S,O)₂] and *cis*-[Pt(L⁷-S,O)₂] determined in dichloromethane.

Table 38 Quantum yields of pyrenebutanoylthiourea derivatives in dichloromethane.

Pyrene	HL ⁷	<i>cis</i> -[Pd(L ⁷ -S,O) ₂]	<i>cis</i> -[Pt(L ⁷ -S,O) ₂]	Calculation method
1.1	0.2	0.1	0.06	Equation 7
0.8	0.1	0.07	0.04	Equation 6

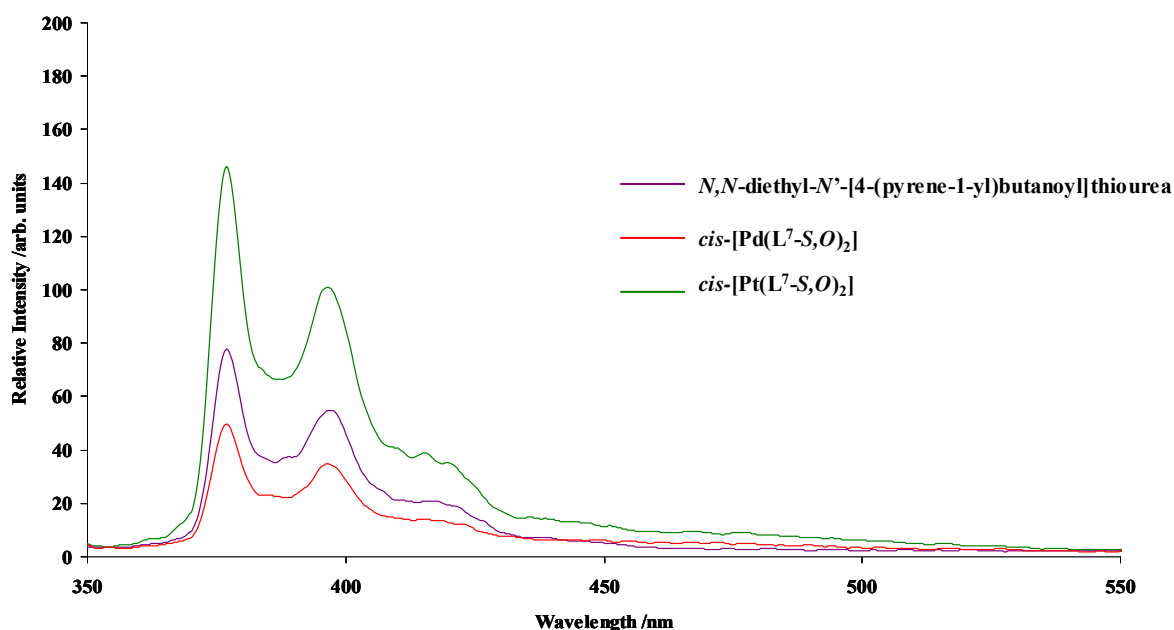


Figure 86 Emission spectra of *N,N*-diethyl-*N'*-[4-(pyrene-1-yl)butanoyl]thiourea, *cis*-bis(*N,N*-diethyl-*N'*-[4-(pyrene-1-yl)butanoyl]thioureaato)palladium(II) and *cis*-bis(*N,N*-diethyl-*N'*-[4-(pyrene-1-yl)butanoyl]thioureaato)platinum(II) in dichloromethane. Conc = 1×10^{-6} M and $\lambda_{\text{Ex}} = 313$ nm.

Before this discussion can be continued however, the anomalous results obtained for the emission spectra of pyrene in ethanol and dichloromethane deserve further attention.

As previously mentioned it is well known that trace amounts of water in solvents used can lead to reduction in the emission intensities. The solvents used were therefore dried according to conventional methods. In the case of ethanol the water content remaining in the solvent, if purified according to the procedure should be less than 0.05%. Whilst these procedures were performed and gave satisfactory results for the emission spectra of the anthracoylthiourea derivatives (Figure 67), this was not reflected in the case of pyrene. A repetition of the drying procedure and subsequent testing of the pyrene solution yielded the same results. No reference to the differing emission intensities in different solvents could be found in the literature. Those reporting spectra obtained in various solvents only referring to the relative intensities of the vibronic bands and not to the intensity of the overall emission.⁶³ Whilst it can be seen that the intensities of the vibronic bands do differ in the solvents, the lower intensity of the emission spectra obtained for the ethanolic solution of pyrene remains an anomaly.

Reference to the quantum yields calculated for the pyrenebutanoylthiourea derivatives (Table 38) provide a more accurate picture of the influence that complexation has on the fluorescent properties of HL⁷. It is apparent that complexation with both platinum and palladium leads to a decrease in the fluorescence efficiency of the fluorophore. The quantum yield of *N,N*-diethyl-*N'*-[4-(pyrene-1-yl)butanoyl]thiourea is only 15.3% relative to that of the unsubstituted pyrene. The *cis*-[Pt(L⁷-S,O)₂] complex being 9.8% that of pyrene and *cis*-[Pd(L⁷-S,O)₂] less than half of this at 4.7% of pyrene. The decrease in fluorescence efficiency upon addition of the acylthiourea moiety is significant and is attributed to PET, the lone pair of

electrons on the nitrogen atom possibly being involved in this mechanism. This is supported by the fluorophore – receptor configuration of the pyrenebutanoylthiourea derivatives leading to their classification as proximal, non-adjacent systems and signalling behaviour in these systems is generally interpreted as being PET. No quantitative comparison with the anthracoylthiourea derivatives is possible; however as the signal of the pyrenebutanoylthiourea derivatives is still readily detectable it would appear that the PET is not as effective in this series of compounds. This is consistent with previous reports where a trimethylene spacer was found to retard PET effects relative to those with a dimethylene spacer and by implication no spacer.⁶⁸ Hence the PET effectivity is reduced in the pyrenebutanoylthiourea derivatives relative to the anthracoylthiourea series where no spacer results in more efficient PET. In cases where PET has been effectively inhibited upon metal ion binding, CHEF by factors of 16^{33} to 70^{69} fold have been reported. Whilst PET is clearly not completely “switched off” upon metal ion complexation, it may be slightly retarded as the lone pair of electrons on the nitrogen atom is delocalised and involved in complexation. No CHEF is observed however, indicating that once again the M-F communication is stronger than the M-R interaction. Similarly to the anthracoylthiourea derivatives the heavy atom effect giving rise to spin-orbit coupling and intersystem crossing is most likely responsible.

Despite the purity of these compounds being ensured by chromatographic separation, it is possible that the unexpectedly high emissions of *cis*-[Pt(L⁷-S,O)₂] and *cis*-[Pd(L⁷-S,O)₂] are due to fluorescent impurities such as an excess of HL⁷. This however could not be the only reason for the increase in intensity. Assuming that the *cis*-[Pt(L⁷-S,O)₂] and *cis*-[Pd(L⁷-S,O)₂] complexes were only for example 90% pure, the remaining 10% being due to HL⁷, the expected quenching would still not be observed as the amount of free ligand (HL⁷) present in the complex would have to be close to 90% to give the observed emission intensities. It is unfortunate in this sense that the emission spectra of *N,N*-diethyl-*N'*-[4-(pyrene-1-yl)butanoyl]thiourea, *cis*-[Pt(L⁷-S,O)₂] and *cis*-[Pd(L⁷-S,O)₂] are at almost identical wavelengths as separation of these signals to determine which is due to free ligand and which is due to the *cis*-[Pt(L⁷-S,O)₂] and *cis*-[Pd(L⁷-S,O)₂] complexes is not possible. One way of ensuring the purity of these compounds and the validity of the data would be through HPLC separation of the compounds and the use of a fluorescence detector. This would have the added advantage of industrial applications.

With this end in mind preliminary RP-HPLC tests were carried out. As previously mentioned the *N,N*-dialkyl-*N'*-acylthioureas have been chromatographically separated in the past, however this work focused on the normal-phase HPLC separation of benzoyl derivatised thioureas⁷⁰ and the use of a reversed-phase system was of interest. The reasons for this have been elaborated on earlier (Chapter 1 section 1.2). The separation of pyrenebutanoylthiourea derivatives was reported by Schuster *et al.*⁶⁵ and it was with interest that HL⁷ and *cis*-[Pt(L⁷-S,O)₂] were injected into our separation system. Due to the compounds having a limited solubility in acetonitrile, dioxane solutions were prepared and injected into the C-18 column, and eluted with varying combinations of mobile phase comprised of acetonitrile, water and sodium acetate buffer. Further experimental details are given in Chapter 5. Regrettably due to the limited time available

in which to complete this work, further tests could not be carried out however limited information could be gained from the chromatograms obtained. Using a mobile phase comprised mostly of acetonitrile and varying the fractions of water added, the elution time of *N,N*-diethyl-*N'*-[4-(pyrene-1-yl)butanoyl]thiourea was between 3 and 7 minutes. The elution time of the *cis*-[Pt(L⁷-*S,O*)₂] was considerably longer varying between 21 and 31 minutes. Separation of HL⁷ and *cis*-[Pt(L⁷-*S,O*)₂] is therefore possible using this system.

4.5 Conclusions

From the UV/Visible absorption spectra obtained for the anthracoylthiourea derivatives, it is apparent that the absorbances of these compounds are largely due to the anthracene moiety; a similar observation being possible for the emission spectra. The introduction of the carboxyl group in close proximity to the anthracene moiety in 9-anthracenecarboxylic acid, leads to a dramatic reduction in emission intensity; a further reduction being seen upon introduction of the acylthiourea moiety in HL¹. The reduction in quantum efficiency of HL¹ is partially due to the many possible tautomeric forms of the *N,N*-dialkyl-*N'*-acylthioureas, these providing alternative radiationless pathways and consequently increasing the possibility of the radiationless de-excitation of an electron. From work done by Werner and Hercules it is evident that in the ground state, the carboxyl group of the anthracoylthiourea derivatives is perpendicularly orientated towards the aromatic moiety, the orthogonal geometry being likely in the excited state as well. Following the attachment of the acylthiourea moiety to the aromatic system, the subsequent reduction in quantum efficiency is most likely due to photoinduced electron transfer. The relative orientation of anthracene and the acylthiourea moiety results in the classification of the anthracoylthiourea derivatives as either integral or orthogonal fluorophore-receptor systems. The absence of a significant shift in the emission wavelengths of the anthracoylthiourea derivatives relative to that of anthracene make it likely that these compounds fall into the latter category with the presence of a C₆ virtual spacer between the receptor and fluorophore, signalling behaviour in these systems being attributed to PET. The introduction of the metal ion in complexation did little to reduce this effect and no chelation enhanced fluorescence was observed indicating that the metal-fluorophore interaction was greater than the metal-receptor interaction. Due to the close proximity of the metal ion to the fluorophore, the mode of interaction between the two is most likely spin-orbit coupling, this leading to intersystem crossing and reducing the emission probability of the complex.

In the pyrenebutanoylthiourea derivatives, introduction of the acylthiourea moiety results in a reduction of quantum efficiency of the fluorophore, however to a lesser degree than in the anthracoylthiourea derivatives. Due to the relative orientation of the pyrene and acylthiourea moieties and the presence of a spacer between the two, the pyrenebutanoylthiourea derivatives can be classified as proximal, non-

adjacent fluorophore-receptor systems, signalling behaviour in these systems generally being attributed to PET. The presence of the trimethylene spacer between the fluorophore and acylthiourea moiety in these derivatives is most likely responsible for the reduction in quantum efficiency, presumably due to photoinduced electron transfer, not being as severe as in the anthracoylthiourea derivatives. The emission spectra obtained in the working concentration range for HL⁷, *cis*-[Pt(L⁷-S,O)₂] and *cis*-[Pd(L⁷-S,O)₂], are in contrast to those reported by Schuster *et al.* for similar compounds. The differing absorbances of the ligand and metal complexes leads to the relative emission intensities being concentration dependant. Introduction of the metal ion as in the anthracoylthiourea derivatives leads to a reduction in the quantum efficiency of the compounds relative to the free ligand, but not as severely as expected – due to the presence of the trimethylene spacer between the fluorophore and metal ion. Due to the absence of chelation enhanced fluorescence being observed upon introduction of the metal ion, the metal-fluorophore interaction is most likely stronger than the metal-receptor interaction and the PET effect is not completely reduced upon complexation. Despite the reduced quantum efficiency upon metal ion introduction, the synthesis of fluorescent complexes has been achieved. Due to the greater emission intensities of the complexes at lower concentrations it is possible that these compounds could be used as a means of fluorescence PGM detection under controlled conditions, despite being imperfect at this time.

References

1. J. Lackowicz, *Principles of Fluorescence Spectroscopy*, **1999**, 2nd Edn, Kluwer, New York.
2. G. Christian, J. O'Reilly, *Instrumental Analysis*, **1978**, 2nd Edn, Allyn & Bacon Inc, Massachusetts, Chpt 9, 247.
3. T. O'Haver, *J. Chem Ed*, **1978**, 55, 7, 423-428 and references therein.
4. P. Atkins, *Physical Chemistry*, **1998**, 6th Edition, Oxford University Press, Oxford, 377.
5. N. Turro, *Modern Molecular Photochemistry*, **1991**, University Science Books, California.
6. J. Birks, *Photophysics of aromatic molecules*, **1970**, Wiley-Interscience, London.
7. G. Christian, *Analytical Chemistry*, **1994**, John Wiley & Sons Inc, New York, 443.
8. Adapted from Holger Spanggard (holger.spanggard@risoe.dk) The Danish Polymer Centre, Risø National Laboratory www.risoe.dk/pol/competence/chemanal/fls920.pdf
9. P. Suppan, "*Chemistry and Light*", **1994**, RSC Cambridge, 54-55.
10. M. Kasha, *J. Chem. Phy.*, **1952**, 20, 71-74.
11. T. Medinger, F. Wilkinson, *Trans. Faraday Soc.*, **1965**, 61, 620-630.
12. L. Hood, J. Winefordner, *Anal. Chem.*, **1966**, 1922-1924.
13. S. Lewin, *J. Chem. Ed*, **1964**, 41, 5, A327-A366.
14. S. Lewin, *J. Chem. Ed*, **1964**, 41, 6, A421-A481.
15. D. Harris, C. Bashford, *Spectrophotometry & spectrofluorimetry - A Practical Approach*, **1987**, IRL Press, Oxford, 17.

-
16. C. Parker, W. Rees, *Analyst*, **1960**, 85, 587-600.
 17. G. Weber, F. Teale, *Trans. Faraday Soc.*, **1957**, 53, 646-655.
 18. W. Dawson, M. Windsor, *J. Phys. Chem.*, **1968**, 72, 3251-3260.
 19. W. Melhuish, *J. Phys. Chem.*, **1961**, 65, 229-235.
 20. W. Melhuish, *J. Phys. Chem.*, **1960**, 64, 762-764.
 21. R. Martinez-Manez, F. Sancenon, *Chem. Rev.*, **2003**, 103, 4419-4476.
 22. K. Koch, T. Grimmacher, C. Sacht, *Polyhedron*, **1998**, 17, 267-274.
 23. B. Valeur, I. Leray, *Coord. Chem. Rev.*, **2000**, 205, 3-40.
 24. A. P. de Silva, H. Gunaratne, T. Gunnlaugsson, A. Huxley, C. McCoy, J. Rademacher, T. Rice, *Chem. Rev.*, **1997**, 97, 1515-1566.
 25. R. Bissell, A. P. de Silva, H. Gunaratne, P. Lynch, G. Maguire, K. Sandanayake, *Chem. Soc. Rev.*, **1992**, 187-195.
 26. A. P. de Silva, R. Rupasinghe, *Chem. Commun.*, **1985**, 1669-1670.
 27. A. P. de Silva, S. de Silva, *Chem. Commun.*, **1986**, 1709-1713.
 28. A. P. de Silva, H. Gunaratne, *Chem. Commun.*, **1990**, 186-188.
 29. M. Beltramello, M. Gatos, F. Mancin, P. Tecilla, U. Tonellato, *Tetrahedron Lett.*, **2001**, 42, 9143-9146.
 30. J. Sclafani, M. Maranto, T. Sisk, S. Van Arman, *Tetrahedron Lett.*, **1996**, 37, 2193-2196.
 31. N. B. Sankaran, S. Banthia, A. Das, A. Samanta, *New Journal of Chemistry*, **2002**, 26, 1529-1531.
 32. I. Aoki, T. Sakaki, S. Shinkai, *Chem. Commun.*, **1992**, 730-732.
 33. A. P. de Silva, H. Gunaratne, T. Gunnlaugsson, M. Niewhouzen, *Chem. Commun.*, **1996**, 1967-1970.
 34. A. P. de Silva, H. Gunaratne, K. Sandanayake, *Tetrahedron Lett.*, **1990**, 31, 5193-5196.
 35. G. Das, P. Bharadwaj, M. Roy, S. Ghosh, *J. Photochem. Photobiol. A*, **2000**, 135, 7-11.
 36. M. Sandor, F. Geistmann, M. Schuster, *Anal. Chim. Acta*, **1999**, 388, 19-26.
 37. E. Unterraitmaier, M. Schuster, *Anal. Chim. Acta*, **1995**, 309, 339-344.
 38. A. Varnes, R. Dodson, E. Wehry, *J. Am. Chem. Soc.*, **1972**, 94, 946-950.
 39. P. Ghosh, P. Baradwaj, *J. Am. Chem. Soc.*, **1996**, 118, 1553-1554.
 40. B. Ramachandram, A. Samanta, *Chem. Commun.*, **1997**, 1037-1038.
 41. K. Rurack, M. Kollmansberger, U. Resch-Genger, J. Daub, *J. Am. Chem. Soc.*, **2000**, 122, 968-969.
 42. B. Bag, P. Bharadwaj, *J. Lumin.*, **2004**, 110, 85-94.
 43. B. Ramachandram, N. B. Sankaran, R. Karmaker, A. Samanta, *Tetrahedron*, **2000**, 56, 7041-7044.
 44. C. Parker, W. Rees, *Analyst*, **1960**, 85, 587.
 45. S. Russo, *J. Chem. Ed.* **1969**, 46, 6.
 46. P. Hrdlovic, S. Chmela, *J. Photochem. Photobiol. A*, **1997**, 105, 83-88.
 47. P. Hrdlovic, S. Chmela, *J. Photochem. Photobiol. A*, **2001**, 143, 59-68.
 48. D. Perrin, W. Armarego, *Purification of laboratory chemicals*, Pergamon Press, Oxford, **1989**.
 49. D. Pavia, G. Landman, G. Kriz, "Introduction to Spectroscopy", **2001**, 3rd edition, Harcourt College, Toronto, 376.
 50. F. Cicogna, M. Colonna, J. Houben, G. Ingrosso, F. Marchetti, *J. Organomet. Chem.*, **2000**, 593-594, 251-566.
 51. Courtesy of A. Westra, *University of Stellenbosch*, South Africa.
 52. T. Matsumoto, M. Sato, S. Hirayama, *Chem. Phys. Lett.*, **1972**, 13, 13-15.

-
53. T. Matsumoto, M. Sato, S. Hirayama, *Chem. Phys. Lett.*, **1973**, 18, 563-566.
 54. Perkin-Elmer, User Guide to software package installed on instrument.
 55. T. Werner, D. Hercules, *J. Phys. Chem.*, **1969**, 73, 2005-2011.
 56. M. Chae, A. Czarnik, *J. Am. Chem. Soc.*, **1992**, 114, 9704-9705.
 57. G. Das, P. Bharadwaj, M. Roy, S. Ghosh, *J. Photochem. Photobiol. A*, **2000**, 135, 7-11.
 58. J. Bricks, K. Rurack, R. Radeaglia, G. Reck, B. Schulz, H. Sonnenschein, U. Resch-Genger, *J. Chem. Soc., Perkin Trans. 2*, **2000**, 1209-1214.
 59. M. Carano, M. Careri, S. Roffie, F. Cicogna, I. D'Ambra, J. Houben, G. Ingrosso, M. Marcaccio, F. Paolucci, C. Pinzino, *Organomet.*, **2001**, 20, 3478-3490.
 60. R. Hochstrasser, *J. Chem. Phys.*, **1960**, 33, 459-463.
 61. A. Bree, V. Vilkos, *J. Chem. Phys.*, **1964**, 40, 3125-3126.
 62. R. Becker, I. Singh, E. Jackson, *J. Chem. Phys.*, **1963**, 38, 2145-2171.
 63. K. Kalyanasundaram, J. Thomas, *J. Am. Chem. Soc.*, **1977**, 99, 2039-2044.
 64. C. Parker, C. Hatchard, *Trans. Faraday Soc.*, **1963**, 59, 284-295.
 65. M. Schuster, E. Unterreitmaier, *Fresenius' J. Anal. Chem.* **1993**, 346, 630-633.
 66. W. Dawson, M. Windsor, *J. Phys. Chem.*, **1968**, 72, 3251.
 67. Aldrich, "*Handbook of Fine Chemical and Laboratory Equipment*", **2003-2004**, South Africa.
 68. J. Callan, A. P. de Silva, J. Ferguson, A. Huxley, A. O'Brien, *Tetrahedron*, **2004**, article in press.
 69. B. Ramachandram, A. Samanta, *Chem. Phys. Lett.*, **1998**, 290, 9-16.
 70. K. Koenig, M. Schuster, B. Steinbrech, G. Schneeweis, R. Schlodder, *Fresenius' J. Anal. Chem.*, **1985**, 321, 457-460.

5.1 Conversion of aroyl acids to their acid chlorides

The synthetic procedures followed for the various conversions are given below. Each method is referred to in turn and where variations of the method were performed only deviations from the original text are mentioned. If no mention is made of reagent quantities or solvent volumes it may be assumed that they were similar to those initially given.

All reagents used were commercially available, and used without further purification except in the case of thionyl chloride which was freshly distilled immediately prior to use. All solvents used were of analytical grade purity and where specified as being anhydrous, were dried according to conventional methods.¹

5.1.1 Conversion of 9-anthracenecarboxylic acid

Method 1.²

A solution of 9-anthracenecarboxylic acid (2.29 mmol) in thionyl chloride (30 ml) was refluxed for 2 ½ hours. The majority of the thionyl chloride was removed *in vacuo* followed by 4 x 10 ml additions of benzene and further distillation *in vacuo* to remove the remaining thionyl chloride.

Variation 1: This method was repeated a second time with a similar quantity of acid, but 50 ml of thionyl chloride and the reaction time was extended to 7 ½ hours.

Variation 2: Oven dried acid was used and the reaction time increased to 40 hours. Unsuccessful monitoring of the conversion using TLC plates was also attempted.

Variation 3: A solution of 9-anthracenecarboxylic acid (11.25 mmol) in thionyl chloride (100 ml) was refluxed for 6 hours. The majority of the thionyl chloride was removed *in vacuo*, after which the solid was washed with 4 x 25 ml volumes of anhydrous benzene.

Method 2.³

Thionyl chloride (2.5 ml) was added to a solution of 9-anthracenecarboxylic acid (2.25 mmol) in anhydrous benzene (50 ml). The mixture was refluxed for an hour and excess thionyl chloride and benzene were removed *in vacuo*.

Variation 1: 9-anthracenecarboxylic acid (2.2 mmol) was dissolved in anhydrous benzene (20 ml). Oxalyl chloride (1 ml) in a solution of anhydrous benzene (10 ml) was added dropwise, and the mixture was refluxed for an hour. The excess solvent was removed *in vacuo*.

Method 3.⁴

A solution of 9-anthracenecarboxylic acid (9 mmol) in thionyl chloride (10 ml) was refluxed for 1 hour. Excess thionyl chloride was removed and the solid obtained was washed with 3 x 15 ml portions of anhydrous toluene.

Method 4.⁵

9-anthracenecarboxylic acid (2.25 mmol) was dissolved in anhydrous diethyl ether (25 ml). Thionyl chloride (1 ml) and pyridine (3 drops) were gradually added. The mixture was stirred at room temperature for 2 hours and filtered. Excess solvent was removed *in vacuo* and the remaining solid washed with 4 x 20 ml portions of diethyl ether. The solid was then dried under vacuum for 1 hour before being analysed.

Variation 1: Thionyl chloride (2 ml) and pyridine (2 drops) were added to a solution of 9-anthracenecarboxylic acid (4.5 mmol) in anhydrous acetone (25 ml). The reaction mixture was stirred at room temperature for 2 hours followed by *in vacuo* removal of the solvent and excess reagent. 3 x 20 ml portions of acetone were used to wash the resulting solid and further removal of thionyl chloride was effected by drying the solid under vacuum for 4 hours.

Variation 2: 9-anthracenecarboxylic acid (4.5 mmol) was dissolved in anhydrous diethyl ether (50 ml). Thionyl chloride (2 ml) was added as well as pyridine (2 drops). The mixture was stirred at room temperature for 2 ½ hours, filtered and excess solvent was removed *in vacuo*. The solid was washed with 3 x 10 ml portions of ether and dried under vacuum overnight.

Method 5.⁶

9-anthracenecarboxylic acid (0.72 mmol) was dissolved in dichloromethane (10 ml). Thionyl chloride (0.5 ml) in dichloromethane (6 ml) was added dropwise and the suspension was stirred overnight. Excess solvent and thionyl chloride were removed *in vacuo*, and the resulting solid dried under vacuum for 4 hours.

Variation 1: Thionyl chloride (1 ml) in anhydrous dichloromethane (15 ml) was added dropwise to a solution of 9-anthracenecarboxylic acid (0.72 mmol) in anhydrous dichloromethane (25 ml). The reaction mixture was refluxed for 5 hours, and then cooled to room temperature where it was stirred for a further hour. *In vacuo* removal of the solvent gave a solid which was dried under vacuum for a further 2 hours.

5.1.2 Conversion of 1-pyrenebutyric acid**Method 1.**

1-pyrenebutyric acid (0.87 mmol) was dissolved in thionyl chloride (30 ml). The resulting mixture was refluxed for 3 hours and excess thionyl chloride was removed *in vacuo*. The resulting solid was washed with 4 x 30 ml volumes of anhydrous benzene.

Method 4.

Thionyl chloride (3.75 ml) and pyridine (2 drops), were added dropwise to a solution of 1-pyrenebutyric acid (8.75 mmol) in diethyl ether (30 ml). The mixture was stirred at room temperature for 90 minutes and then filtered to remove a fine brown residue. Excess solvent was removed *in vacuo* from the filtrate and the solid washed with 3 x 10 ml portions of ether. The resulting acid chloride was dried under vacuum for a further 2 hours before use.

Method 5.

1-pyrenebutyric acid (1.8 mmol) was dissolved in chloroform (25 ml), and a solution of thionyl chloride (1.3 ml) in chloroform (15 ml) was added. The mixture was stirred overnight at room temperature. The excess solvent was removed *in vacuo* and the product recrystallised from hexane.

Variation 1: Thionyl chloride (0.67 ml) and chloroform (7.5 ml) were added dropwise to a solution of 1-pyrenebutyric acid (0.9 mmol) in chloroform (12.5 ml). The mixture was stirred overnight at room temperature and excess solvent removed *in vacuo*. The resulting solid was dried under vacuum for 2 hours prior to analysis.

Method 6.⁷

1-pyrenebutyric acid (0.8 mmol) was dissolved in anhydrous benzene (100 ml). Dropwise addition of thionyl chloride (0.32 ml) was followed by a 7 hour reflux. The solution was allowed to equilibrate to room temperature and then stirred overnight. The solvent was removed and the resulting solid was layered with hexane in an unsuccessful attempt to obtain a pure crystalline product.

Variation 1: Thionyl chloride (0.7 ml) was added to a solution of 1-pyrenebutyric acid (1.7 mmol) in anhydrous benzene (220 ml). The reaction mixture was refluxed for 4 hours and then allowed to cool to room temperature after which it was stirred for 36 hours. The solvent was removed and an unsuccessful recrystallisation from hexane attempted.

5.1.3 Conversion of 1-pyreneacetic acid**Method 4.**

1-pyreneacetic acid (9.6 mmol) was dissolved in anhydrous diethyl ether (25 ml). A solution of thionyl chloride (3.75 ml) and pyridine (2 drops) was gradually added. The mixture was stirred for 90 minutes, and then filtered to remove a dark green suspension. Excess solvent was removed and the solid washed with 4 x 10 ml portions of ether. The resulting chloride was dried under vacuum for 3 hours prior to use.

5.1.4 Characterisation of aroyl chlorides

9-anthracoyl chloride: 95% yield. m.pnt. 74.5-77.0 °C. NMR δ_{H} (600MHz, CDCl₃): 8.54 (1H, s), 8.13 (2H, d), 8.03 (2H, d), 7.62 (2H, t), 7.52 (2H, t), δ_{C} (600MHz, CDCl₃): 170.51, 131.59, 130.63, 130.61, 128.73, 127.90, 126.12, 125.84, 123.87.

1-pyrenebutanoyl chloride: 92% yield. m.pnt. 73.1-75.3 °C. NMR δ_{H} (600MHz, CDCl₃): 8.13 (1H, d), 8.08 (2H, unres d), 8.01 (2H, unres d), 7.94 (2H, d), 7.91 (1H, t), 7.72 (1H, d), 3.27 (2H, t), 2.86 (2H, t), 2.12 (2H, q), δ_{C} (600MHz, CDCl₃): 174.08, 134.59, 131.55, 130.98, 130.56, 128.83, 127.08, 126.09, 123.00, 46.41, 31.71, 26.61.

1-pyreneacetyl chloride: 88% yield. m.pnt. 102.3-107.1 °C. NMR δ_{H} (600MHz, CDCl_3): 8.19 (2H, unres d), 8.14 (2H, unres d), 8.07 (1H, d), 8.06 (1H, d), 8.02 (1H, s), 8.01 (1H, d), 7.88 (1H, d), 4.80 (2H, s), δ_{C} (600MHz, CDCl_3): 171.81, 131.51, 131.15, 130.54, 129.38, 128.60, 128.49, 127.85, 127.21, 126.17, 125.68, 125.50, 124.93, 124.87, 124.86, 124.48, 122.30, 51.04.

5.2 Synthesis of the *N,N*-dialkyl-*N'*-aroylthiourea ligands

5.2.1 Douglass and Dains method for ligand synthesis

Potassium thiocyanate (13.8 mmol) was dissolved in anhydrous acetone (50 ml). An acetone solution (50 ml) of aroyl chloride (13.88 mmol) was added dropwise over a period of 20 minutes. The solution was heated to reflux for an hour and then cooled to room temperature. An acetone solution (50 ml) of amine (13.88 mmol) was added dropwise over 20 minutes. A further reflux of 1 hour was followed by cooling to room temperature and the mixture was then poured onto water (67 ml). The gradual volatisation of acetone afforded the product.

All the pivaloylthiourea derivatives precipitated out as solid products and were then recrystallised from acetone and water mixtures.

All anthracoylthiourea derivatives precipitated out and were recrystallised from a combination of either acetone and water or ethanol and water. These ligands were purified by column chromatography using Silica Gel 60 as stationary phase, (1 g product : 50 g silica gel) and gradient elution systems of acetone and chloroform, or acetone and dichloromethane proved successful in obtaining clean products.

The initial eluent combination was usually 5% acetone : 95% chloroform, by volume, with the acetone percentage gradually increasing to increase the polarity of the system.

All pyrenebutanoylthiourea and pyreneacetylthiourea derivatives usually formed oils and were chromatographed further. In the case of *N,N*-diethyl-*N'*-[4-(pyrene-1-yl)butanoyl]thiourea and *N,N*-diethyl-*N'*-[pyrene-1-ylacetyl]thiourea a gradient elution of acetone and chloroform afforded a clean product.

N-morpholine-*N'*-[4-(pyrene-1-yl)butanoyl]thiourea was eluted with a 5% acetone: 95% diethyl ether elution system that had been cooled to -50°C to prevent cracking of the column caused by the large percentage of ether in the mobile phase.

No suitable elution system was found for *N,N*-di(2-hydroxyethyl)-*N'*-[4-(pyrene-1-yl)butanoyl]thiourea.

5.2.2 “Modified” Douglass and Dains method for ligand synthesis

Aroyl chloride (6.19 mmol) was dissolved in anhydrous acetone (20 ml). An acetone solution (5 ml) of potassium thiocyanate (6.3 mmol) was added dropwise over a period of 10 minutes. The solution was refluxed for 10 minutes and cooled to room temperature. An acetone solution (7 ml) of amine (6.3 mmol) was added dropwise over 15 minutes and the solution refluxed for 10 minutes. Cooling to room temperature the mixture was filtered and 80% of acetone was removed *in vacuo*. The remaining solution was placed in a beaker, 2 drops of 6M HCl was added and the solution was allowed to stand overnight to allow the gradual evaporation of the acetone.

In the case of *N,N*-diethyl-*N'*-[4-(pyrene-1-yl)butanoyl]thiourea a solid precipitate was obtained. Oily by-products were removed by washing with cold isopropyl alcohol and the solid product could be recrystallised from a combination of acetone and water.

N-morpholine-*N'*-[4-(pyrene-1-yl)butanoyl]thiourea formed a mixture of products and was separated on a column using an elution system of 50% ether: 50% chloroform. The column was once again cooled to -50°C to prevent cracking due to the large percentage of ether present in the elution system.

In the case of *N,N*-diethyl-*N'*-[pyrene-1-ylacetyl]thiourea a mixture of products was obtained and no suitable elution system could be found.

5.2.3 Dixon and Taylor method for ligand synthesis.

Step 1: Acid hydrolysis of pivaloylthioureas.

The pivaloylthiourea (0.01 mol) was dissolved in concentrated hydrochloric acid (50 ml). The temperature of the reaction mixture was maintained between 80 -90 °C for 3 ½ hours before being allowed to equilibrate to room temperature.

Careful neutralisation of the mixture was done using a 25% ammonium hydroxide solution (approx 100 ml necessary). The mixture was placed in ice due to the exothermic nature of the neutralisation. The product was separated by successive chloroform extractions (30 x 10 ml). All organic phases were combined and dried over sodium sulphate. Filtration and *in vacuo* removal of the chloroform afforded the product in good yield.

Step 2: Reaction of acyl halide and substituted thiourea.

Aroyl chloride (3.34 mmol) was dissolved in anhydrous acetone (20 ml). A solution of acetone (20 ml), *N*-substituted thiourea (3.34 mmol) and triethylamine (3.8 mmol) was added dropwise over 20 minutes. The solution was refluxed for 45 minutes and allowed to cool to room temperature. The mixture was poured onto water (20 ml) and the acetone allowed to gradually evaporate overnight.

A mixture of products was obtained in all cases and these were separated using column chromatography (1 g product: 50 g silica) and elution systems of between 5 and 10% acetone and either chloroform or dichloromethane.

5.2.4 Characterisation of pivaloylthiourea derivatives

***N,N*-diethyl-*N'*-pivaloylthiourea:** 84% yield. m.pnt. 91.4-92.8 °C. NMR δ_{H} (300MHz, CDCl_3): 7.66 (1H, br s, $>\text{N}'\text{H}$), 3.94 + 3.44 (2H + 2H, br unres q + br unres q, $-\text{N}(\text{CH}_2\text{CH}_3)_2$), 1.24 (15H, br unres t, $(\text{CH}_3)_3\text{CC}(\text{O})-$, $-\text{N}(\text{CH}_2\text{CH}_3)_2$), δ_{C} (300MHz CDCl_3): 179.60, 174.70, 47.98, 47.45, 39.60, 27.02, 13.15, 11.46. IR (KBr pellet, cm^{-1}): 3228.2(s, br), 2970.5 (m, sh), 2932.3 (w-m, sh), 2868.6 (w, sh), 2360.5 (w), 1649.0 (s, sh), 1507.6 (s, sh), 1461.9 (m), 1422.3 (s, sh), 1365.8 (m-w), 1278.6 (m), 1236.6 (s,sh), 1195.2 (m), 1133.9 (m), 1077.7 (w), 944.5 (w), 888.0 (w), 788.5 (w), 617.7 (w, br).

***N*-morpholine-*N'*-pivaloylthiourea:** 75% yield. m.pnt. 134.2-136.2 °C. NMR δ_{H} (300MHz, CDCl_3): 7.89 (1H, br s, $>\text{N}'\text{H}$), 4.15 + 3.79 + 3.50 (2H + 4H + 2H, br unres m + br unres m + br unres m, $-\text{N}(\text{CH}_2\text{CH}_2)_2\text{O}$), 1.25 (9H, br unres t, $(\text{CH}_3)_3\text{CC}(\text{O})-$), δ_{C} (300MHz CDCl_3): 179.49, 174.20, 66.21, 52.47, 51.63, 39.73, 27.04. IR (KBr pellet, cm^{-1}): 3434.5 (m, br), 3295.2 (s, br), 2974.9 (s, sh), 2918.9 (s, sh), 2855.2 (s, sh), 1688.8 (s, sh), 1535.5 (s, sh), 1477.8 (m), 1431.4 (m), 1266.1 (m), 1247.3 (m), 1227.6 (m), 1204.7 (w), 1158.7 (s, sh), 1116.0 (s, sh), 1038.0 (m), 962.9 (w), 892.3 (w), 854.7 (w), 810.9 (w), 709.5 (w, br), 615.4 (w, sh), 572.5 (w), 509.5 (w, sh).

***N,N*-di(2-hydroxyethyl)-*N'*-pivaloylthiourea:** 65% yield. m.pnt. 138.0-141.5 °C. NMR δ_{H} (300MHz, DMSO): 10.1 (1H, br s, $>\text{N}'\text{H}$), 5.70 (1H, br s, $-\text{N}(\text{CH}_2\text{CH}_2\text{OH})$), 4.83 (1H, t, $-\text{N}(\text{CH}_2\text{CH}_2\text{OH})$), 3.92 (2H, t, $-\text{N}(\text{CH}_2\text{CH}_2\text{OH})$), 3.66 (6H, unres m, $-\text{N}(\text{CH}_2\text{CH}_2\text{OH})$ and $-\text{N}(\text{CH}_2\text{CH}_2\text{OH})$), 1.12 (9H, br unres t, $(\text{CH}_3)_3\text{CC}(\text{O})-$), δ_{C} (300MHz DMSO): 181.69, 175.44, 59.13, 57.55, 54.76, 26.50. IR (KBr pellet, cm^{-1}): 3439.8 (s, br), 3312.6 (s, br), 3221.6 (s, br), 2971.5 (m-w, sh), 2917.9 (m-w, sh), 1700.7 (s, sh), 1555.8 (s, sh), 1486.2 (m), 1452.4 (m), 1394.5 (m, sh), 1326.6 (w), 1278.2 (s, sh), 1225.6 (s, sh), 1182.6 (m), 1128.8 (w), 1068.1 (s, sh), 1007.8 (m), 946.0 (w), 919.5 (w), 885.5 (w), 818.0 (w), 745.5 (w), 626.2 (w).

5.2.5 Characterisation of *N*-substituted thioureas.

***N,N*-diethylthiourea:** 92% yield. m.pnt. 101.8-102.9 °C. NMR δ_{H} (300MHz, CDCl_3): 5.819 (2H, br s, $\text{H}_2\text{N}-$), 3.58 (4H, br unres t, $-\text{N}(\text{CH}_2\text{CH}_3)_2$), 1.17 (6H, t, $-\text{N}(\text{CH}_2\text{CH}_3)_2$), δ_{C} (300MHz CDCl_3): 180.85, 45.63, 45.57, 12.15. IR (KBr pellet, cm^{-1}): 3375.4(s, sh), 3297.7 (s, br), 3190.4 (s, sh), 2982.4 (m, sh), 1627.6 (s, sh),

1518.2 (s, sh), 1475.1 (m), 1434.7 (m), 1366.2 (s, sh), 1268.2 (w, br), 1208.2 (w), 1163.9 (w), 1074.9 (m, sh), 992.2 (w), 930.4 (w), 847.5 (m-w), 793.2 (w), 667.2 (w), 639.2 (w), 528.7 (w, br).

***N*-morpholinethiourea:** 81% yield. m.pnt. 175.2-177.1 °C. NMR δ_{H} (300MHz, CDCl_3): 5.78 (2H, br s, H_2N -), 3.77 (4H, br unres t, $-\text{N} < (\text{CH}_2\text{CH}_2)_2 > \text{O}$), 3.72 (4H, br unres t, $-\text{N} < (\text{CH}_2\text{CH}_2)_2 > \text{O}$), δ_{C} (300MHz CDCl_3): 182.92, 65.96, 47.76. IR (KBr pellet, cm^{-1}): 3407.1 (s, br), 3317.8 (s, br), 3213.0 (s, br), 2880.9 (m), 2356.5 (w), 1629.6 (s, sh), 1509.0 (s, sh), 1490.1 (s), 1449.7 (s), 1348.5 (s, sh), 1288.6 (m), 1257.1 (m), 1187.2 (w), 1113.9 (s, sh), 1006.8 (s, sh), 936.3 (m), 875.3 (m), 834.1 (m-s), 691.3 (m, br), 592.2 (m),

5.2.6 Characterisation of anthracoylthiourea derivatives

***N,N*-diethyl-*N'*-9-anthracoylthiourea:** 86.0% yield. m.pnt. 157.5-160.3 °C. NMR δ_{H} (600MHz, CDCl_3): 8.49 (1H, s, H10), 8.12 (3H, d, H1 + H8 + N-H), 7.99 (2H, d, H4+H5), 7.57 (2H, t, H2 + H7), 7.49 (2H, t, H3 + H6), 4.04 (4H, d, br, unres, H13 + H13'), 1.45 (6H, s, H14 + H14'), δ_{C} (300MHz CDCl_3): 178.28, 166.22, 130.87, 129.45, 129.40, 128.68, 128.16, 127.37, 125.61, 124.35, 48.16, 48.15, 13.49, 11.48. Calculated for $\text{C}_{20}\text{H}_{20}\text{O}_1\text{N}_2\text{S}_1$. C, 71.43; H, 5.95; N, 8.33; S, 9.52. Found. C, 71.20; H, 5.89; N, 8.10; S, 9.22. IR (KBr pellet, cm^{-1}): 3174.2 (m, br), 2973.9 (m-w, sh), 2345.4 (w), 1684.1 (s, sh), 1647.9 (s-m), 1540.0 (s, sh), 1534.5 (s), 1438.0 (s, br), 1280.7 (m, sh), 1228.3 (m, sh), 1117.8 (m, sh), 1014.6 (w), 889.4 (w), 847.8 (m, sh), 792.1 (m-w, sh), 728.0 (m, br), 607.9 (w, br).

***N*-morpholine-*N'*-9-anthracoylthiourea:** 79.1% yield. m.pnt. 181.2-183.6 °C. NMR δ_{H} (600MHz, CDCl_3): 8.54 (1H, s, N-H), 8.50 (1H, s, H10), 8.03 (4H, unres dd, H1 + H8 + H4 + H5), 7.57 (2H, t, H2 + H7), 7.49 (2H, t, H3 + H6), 3.90 (8H, br unres d, H13 + H13' + H14 + H14'). δ_{C} (600MHz CDCl_3): 178.62, 165.75, 130.98, 129.87, 129.07, 128.94, 128.27, 127.68, 125.80, 124.31, 66.21, 52.89, 51.73. Calculated for $\text{C}_{20}\text{H}_{18}\text{O}_2\text{N}_2\text{S}_1$. C, 68.55; H, 5.18; N, 7.99; S, 9.15. Found. C, 68.25; H, 5.42; N, 7.93; S, 8.67. IR (KBr pellet, cm^{-1}): 3204.1 (w, br), 3052.4 (w, sh), 2863.0 (w, sh), 1693.3 (s, sh), 1532.6 (s, sh), 1455.5 (s, br), 1423.3 (s), 1354.0 (w, sh), 1272.5 (s, sh), 1246.3 (s, sh), 1196.5 (s, br), 111.9 (s), 1034.0 (m), 956.2 (m-w), 891.4 (m-w), 874.0 (w), 844.2 (w), 796.1 (w), 730.8 (m).

***N,N*-di(2-hydroxyethyl)-*N'*-9-anthracoylthiourea:** 56.0% yield. m.pnt. 152.8-155.0 °C. NMR δ_{H} (600MHz, DMSO): 11.23 (1H, s, N-H), 8.78 (1H, s, H10), 8.19 (4H, unres dd, H1 + H8 + H4 + H5), 7.66 (2H, t, H2 + H7), 7.59 (2H, t, H3 + H6), 5.38 (1H, s, OH(C14')), 4.96 (1H, t, OH(C13')), 4.07 (2H, t, H14'), 3.98 (2H, t, H14), 3.83 (2H, q, H13'), 3.75 (2H, s, H13), δ_{C} (600MHz DMSO): 180.74, 167.25, 131.65, 131.06, 128.99, 128.62, 128.09, 127.36, 126.13, 125.19, 59.26, 57.43, 55.41, 55.27. Calculated for $\text{C}_{20}\text{H}_{20}\text{O}_3\text{N}_2\text{S}_1$. C, 65.20; H, 5.47; N, 7.60; S, 8.70. Found. C, 65.52; H, 5.65; N, 7.71; S, 8.49. IR (KBr pellet, cm^{-1}): 3411.3 (m, br),

3260.0 (m, br), 2958.4 (w, sh), 2345.5 (w), 1708.9 (s, sh), 1647.9 (m-w), 1560.1 (s, sh), 1417.7 (s), 1353.7 (m), 1295.2 (s, sh), 1231.7 (s, br), 1068.4 (m), 1043.1 (m), 896.0 (m-w), 793.5 (m-w), 746.3 (m), 641.9 (w), 565.2 (w).

5.2.7 Characterisation of pyreneacetylthiourea and pyrenebutanoylthiourea derivatives

***N,N*-diethyl-*N'*-[pyrene-1-ylacetyl]thiourea:** 60.0% yield. m.pnt. 141.7-142.5 °C. NMR δ_{H} (600MHz, CDCl₃): 8.19 (1H, d, H3), 8.18 (1H, d, H13), 8.18 (2H, unres d, H8 + H10), 8.11 (1H, d, H12), 8.05 (1H, d, H6), 8.02 (1H, d, H5), 8.01 (1H, t H9), 7.91 (1H, d, H2), 4.38 (2H, s, H17), 3.85 (2H, br unres t, H20/20'), 3.30 (2H, br unres t H20/20'), 1.22 (3H, br unres t, H21/21'), 0.92 (3H, br unres t, H21/21'). δ_{C} (600MHz CDCl₃):178.49, 167.92, 131.39, (2C), 130.83, 129.65, 128.64, 128.57, 127.81, 127.44, 127.27, 126.33, 125.73, 125.55, 125.33, 125.24, 124.68, 122.72, 47.83, 47.23, 42.40, 12.99, 10.99. Calculated for C₂₃H₂₂O₁N₂S₁. C, 73.76; H, 5.92, N,7.48; S, 8.56. Found. C, 74.24; H, 6.26; N, 7.38; S, 7.83. IR (KBr pellet, cm⁻¹): 3439.7 (w, br), 3234.2 (m, br), 2975.4 (w, sh), 2057.2 (w), 1656.7 (s, sh), 1531.6 (s, sh), 1458.9 (m-s), 1429.6 (m-s), 1380.3 (w), 1356.4 (w), 1278.9 (w), 1233.0 (s, sh), 1181.8 (w), 1128.6 (m, sh), 970.1 (w), 848.8 (s, sh), 759.3 (w), 712.1 (m), 681.1 (w), 618.4 (w), 542.1 (w).

***N,N*-diethyl-*N'*-[4-(pyrene-1-yl)butanoyl]thiourea:** 90.0% yield. m.pnt. 142.1-143.5 °C. NMR δ_{H} (600MHz, CDCl₃): 8.27 (1H, d, H13), 8.20 (1H, s, N-H), 8.15 (2H, d, H8 + H10), 8.08 (2H, dd, H3 + H12), 8.01 (2H, s, H5 + H6), 7.98 (1H, t, H9), 7.84 (1H, d, H2), 3.99 (2H, br unres q, H22/22'), 3.48 (2H, br unres q, H22/22'), 3.38 (2H, t, H17), 2.48 (2H, t, H19), 2.20(2H, q, H18), 1.23 (6H, br unres t, H23/23'). δ_{C} (600MHz CDCl₃):178.83, 169.65, 135.36, 131.33, 130.81, 129.94, 128.65, 127.41, 127.40, 127.29, 126.67, 125.78, 125.01, 124.89, 124.86, 124.77, 124.72, 123.21, 47.63 (2C), 36.32, 32.61, 26.72, 13.11, 11.50. Calculated for C₂₅H₂₆O₁N₂S₁·C₃H₆O. C, 73.04; H, 6.96; N, 6.09; S, 7.10 Found. C, 72.80; H, 6.48; N, 6.76; S, 7.50. IR (KBr pellet, cm⁻¹): 3202.3 (m, br), 2973.7 (w, br), 2941.6 (w, br), 1715.8 (s, sh), 1542.7 (s, sh), 1417.4 (s-m), 1432.2 (s-m), 1359.6 (w), 1301.2 (w), 1276.7(m), 1234.2 (s, sh), 1189.6 (s, sh), 1133.5 (s, sh), 1076.3 (w), 940.0 (w), 878.6 (m), 850.7 (m, sh), 786.0 (w), 708.8 (m, sh), 622.3 (w), 509.0(w).

***N*-morpholine-*N'*-[4-(pyrene-1-yl)butanoyl]thiourea:** 22% yield. m.pnt. 161.6-163.0 °C. NMR δ_{H} (600MHz, CDCl₃): 8.26 (1H, d, H13), 8.17 (2H, dd, H8 + H10), 8.12 (2H, dd, H3 + H12), 8.03 (2H, d, H5 + H6), 7.99 (1H, t, H9), 7.98 (1H, s, N-H), 7.84 (1H, d, H2), δ_{C} (600MHz CDCl₃): 178.62, 168.58, 134.99, 131.36, 130.82, 130.09, 128.74, 127.59, 127.41, (2C), 126.86, 125.93, 125.09, 125.04, 124.91, 124.87, 124.82, 123.10, 66.14, 52.50, 36.35, 32.59, 26.46. Calculated for C₂₅H₂₄O₂N₂S₁·½ C₃H₆O. C, 71.46; H, 6.07; N, 6.29; S, 7.19. Found. C, 70.74; H, 6.12; N, 6.58; S, 7.14. IR (KBr pellet, cm⁻¹):3286.6 (m, br), 3037.7 (m, br), 2917.9 (m, br), 1695.8 (s, sh), 1586.7 (w, br), 1540.7 (s, br), 1458.2 (s, sh), 1426.5 (s, br), 1277.5 (s, sh),

1248.6 (s-m, sh), 1204.5 (m, sh), 1163.4 (m, br), 112.7 (m-w, br), 1034.1 (w, br), 841.3 (s, sh), 754.3 (w, sh), 710.9 (w, br).

***N*-morpholine-*N'*-[4-(pyrene-1-yl)butanoyl]amide:** 16% yield. m.pnt. 103.6 – 106.1 °C. NMR δ_{H} (600MHz, CDCl₃): 8.33 (1H, d, H13), 8.17 (2H, dd), 8.11 (2H, d), 8.02 (2H, d, H5 + H6), 7.99 (1H, t, H9), 7.86 (1H, d, H2). 3.65 (4H, unres d t, H21' + H21), 3.54 (2H, t, H20/20'), 3.42 (2H, t, H19), 3.28 (2H, H20/H20'), 2.37 (2H, t, H17), 2.23 (2H, q, H18). δ_{C} (600MHz CDCl₃): 171.27, 135.92, 131.36, 130.85, 129.88, 128.81, 127.41, 127.32, 127.30, 126.67, 125.81, 125.04, 124.93, 124.87, 124.73, 123.37, 66.88, 66.47, 45.75, 41.87, 32.72, 32.11, 26.77. Calculated for C₂₄H₂₃O₂N₁.C, 80.67; H, 6.44; N, 3.92. Found. C, 79.68; H, 6.47; N, 3.87. IR (KBr pellet, cm⁻¹): 3039.0 (m, sh), 2949.8 (m, sh), 2853.8 (m), 1648.6 (s, sh), 1602.0 (m), 1457.6 (m), 1428.3 (s, sh), 1358.1 (m-w), 1300.4 (w), 1277.5 (m), 1242.7 (m), 1217.7 (m, sh), 1193.6 (m-s, sh), 1115.0 (s, sh), 1026.1 (s, sh), 963.8 (w), 847.9 (s, sh), 762.8 (m, sh), 712.5 (m, sh).

5.3 Complex synthesis

5.3.1 Synthesis of Platinum complexes

Synthesis of *cis*-bis(*N,N*-diethyl-*N'*-[4-(pyrene-1-yl)butanoyl]thioureato)platinum(II) *cis*-[Pt(L⁷-S,O)₂]
N,N-diethyl-*N'*-[4-(pyrene-1-yl)butanoyl]thiourea (0.48 mmol) and sodium acetate (0.96 mmol) were dissolved in an acetone (40 ml) and water (10 ml) solvent combination and heated to 50 °C. An aqueous solution (15 ml) of K₂PtCl₄ (0.24 mmol) and acetone (10 ml) was added dropwise to the ligand solution over a period of 20 minutes. The mixture was stirred at an elevated temperature (50 °C) for 90 minutes, followed by cooling to room temperature. The development of a yellow colour was noted. Water (25 ml) was added to aid precipitation of the product, and the mixture cooled to 4 °C overnight. A yellow precipitate and brown oil were extracted with chloroform and the organic phase dried over sodium sulphate. Filtration and recrystallisation from a combination of ethanol and chloroform afforded the product.

Synthesis of *cis*-bis(*N,N*-diethyl-*N'*-[pyrene-1-ylacetyl]thioureato)platinum(II) *cis*-[Pt(L¹⁰-S,O)₂]

This procedure followed that of the *cis*-[Pt(L⁷-S,O)₂] complex, however the addition of ethanol aided the extraction of the product from the aqueous phase to the organic phase.

Synthesis of *cis*-bis(*N,N*-diethyl-*N'*-9-anthracoylthioureato)platinum(II) *cis*-[Pt(L¹-S,O)₂]

This procedure followed that of the *cis*-[Pt(L⁷-S,O)₂] complex, however the more labile Pt[NCPri]₂Cl₂ was used as a starting material and acetonitrile used in place of acetone. The preparative TLC plate was activated for 1 hour at 100 °C and developed using a 10% acetone, 90% toluene solvent combination. Three different fractions could be identified, the product being the most nonpolar – R_f value = 0.857.

5.3.2 Synthesis of Palladium complexes

Synthesis of *cis*-bis(*N,N*-diethyl-*N'*-9-anthracoylthioureato)palladium(II) *cis*-[Pd(L¹-S,O)₂]

N,N-diethyl-*N'*-9-anthracoylthiourea (0.613 mmol) was dissolved in chloroform (25 ml) and shaken together with an aqueous solution (25 ml) of K₂PdCl₄. The lightening in colour of the brown aqueous solution was accompanied by the darkening of the yellow organic layer, to give an orange solution. This was washed with a sodium acetate solution (0.1M, 10 ml), and the organic layer separated and dried overnight over sodium sulphate. Filtration and slow evaporation of the solvent afforded an orange yellow product. This was chromatographed using chloroform as eluting medium.

Synthesis of *cis*-bis(*N*-morpholine-*N'*-9-anthracoylthioureato)palladium(II) *cis*-[Pd(L²-S,O)₂]

This procedure followed that of the *cis*-[Pd(L¹-S,O)₂] complex and afforded a yellow product which was insoluble, hence no chromatographic purification or NMR analysis was possible.

Synthesis of *cis*-bis(*N,N*-diethyl-*N'*-[4-(pyrene-1-yl)butanoyl]thioureato)palladium(II)

cis-[Pd(L⁷-S,O)₂]

This procedure followed that of the *cis*-[Pd(L¹-S,O)₂] complex and afforded a deep orange product.

Synthesis of *cis*-bis(*N,N*-diethyl-*N'*-[pyrene-1-ylacetyl]thioureato)palladium(II) *cis*-[Pd(L¹⁰-S,O)₂]

This procedure generally followed that of the *cis*-[Pd(L¹-S,O)₂] complex, however the volume of chloroform was significantly larger (100 ml). The organic layer containing the dissolved ligand was filtered prior to being mixed with the aqueous metal containing phase, however the formation of a brown emulsion was noted. Careful addition of chloroform enabled its stabilisation and the organic layer could be separated and dried over sodium sulphate. The product was recrystallised from a solvent combination of methanol and chloroform.

5.3.3 Characterisation of platinum complexes

***cis*-[Pt(L¹-S,O)₂]:** 12% yield. m.pnt. 252.0-253.4 °C. NMR δ_{H} (600MHz, CDCl₃): 8.29 (2H, s), 8.19 (4H, m), 7.85 (4H, m), 7.34 (8H, m), 3.83 (4H, q), 3.55 (4H, m), 1.40 (6H, t), 1.05 (6H, t). NMR δ_{C} (600MHz, CDCl₃): 172.56, 166.70, 134.34, 131.17, 128.01, 127.98, 127.16, 126.30, 125.56, 124.90, 46.77, 45.58, 29.69, 13.32, 12.32, δ_{Pt} (600MHz, CDCl₃): -2707.35.

***cis*-[Pt(L⁷-S,O)₂]:** 87% yield. m.pnt. 138.6-140.2 °C. NMR δ_{H} (600MHz, CDCl₃): 8.25 (2H, d, H13), 8.10 (4H, unres dd, H8 + H10), 7.94 (12H, unres m, H3 + H12, H5 + H6, H9, N-H), 7.80 (2H, d, H2), 3.65 (8H, unres m, H22 + H22'), 3.33 (4H, t, H17), 2.51 (4H, t, H19), 2.17 (4H, q, H18), 1.21 (6H, t, H23/H23'), 1.09 (6H, t, H23/H23'). δ_{C} (600MHz CDCl₃): 177.79, 166.54, 136.83, 131.51, 131.03, 129.79, 128.76, 127.60, 127.40, 127.13, 126.50, 125.73, 125.07, 124.81, 124.74, 124.62, 123.72, 46.46, 45.31, 40.14, 32.72, 28.22, 12.66, 12.12, δ_{Pt} (600MHz, CDCl₃): -2734.84. Calculated for C₅₀H₅₀O₂N₄S₂Pt·½CHCl₃·C₂H₅OH. C, 57.12; H, 5.12; N, 5.08. Found. C, 58.92; H, 5.41; N, 5.33.

***cis*-[Pt(L¹⁰-S,O)₂]:** 40% yield. m.pnt. 171.9-172.6 °C. NMR δ_{H} (600MHz, CDCl₃): 8.36 (2H, d, H13), 8.14 (4H, dd, HH8 + H10), 8.10 (2H, d, H3), 8.06 (2H, d, H12), 8.02 (4H, d, H5 + H6), 7.97 (2H, t, H9), 7.93 (2H, d, H2), 4.46 (4H, s, H17), 3.36 (4H, q, H20/H20'), 2.72 (4H, q, H20/H20'), 1.02 (6H, t, H21/H21'), 0.16 (6H, t, H21/H21'). δ_{C} (600MHz CDCl₃): 175.59, 165.99, 131.82, 131.21, 130.79, 130.03, 129.59, 128.62, 127.39, 127.17, 126.61, 125.63, 124.78, 124.71, 124.68, 124.45, 124.41, 46.34, 45.17, 44.61, 11.97, 11.95, δ_{Pt} (600MHz, CDCl₃): -2723.90.

5.3.4 Characterisation of palladium complexes

***cis*-[Pd(L¹-S,O)₂]:** 60% yield. m.pnt. 252.5-253.8 °C. NMR δ_{H} (600MHz, CDCl₃): 8.29 (2H, s), 8.17 (2H), 7.86 (8H), 7.34 (8H), 3.91 (4H, q), 3.61 (4H, q), 1.40 (6H, t), 1.09 (6H, t). δ_{C} (600MHz CDCl₃): 174.66, 170.80, 134.06, 131.21, 128.13, 128.05, 126.96, 126.41, 125.51, 124.91, 47.04, 45.78, 13.35, 12.59. Calculated for C₄₀H₃₈O₂N₄S₂Pd. C, 61.81; H, 4.93; N, 7.21; S, 8.25. Found. C, 61.11; H, 4.50; N, 7.13; S, 7.91. IR (KBr pellet, cm⁻¹): 2970.8 (m, sh), 2930.0 (m), 1490.4 (s, br), 1429.6 (s, sh), 1400.4 (s, sh), 1350.5 (s, sh), 1274.6 (m), 1235.5 (m), 1127.0 (m, sh), 1074.2 (m-w), 1012.3 (w), 890.0 (m, sh), 841.0 (w), 786.2 (w), 730.2 (m), 697.6 (m-w), 602.5 (w).

***cis*-[Pd(L²-S,O)₂]:** 60% yield. m.pnt. 294.9–295.3 °C (decomposition). Calculated for C₄₀H₃₂O₄N₄S₂Pd·½CHCl₃. C, 56.37; H, 3.77; N, 6.49; S, 7.40. Found. C, 55.38; H, 3.80; N, 6.31; S, 7.13. IR

(KBr pellet, cm^{-1}): 2917.8 (w), 2850.0 (w, sh), 1479.4 (s, br), 1429.2 (s, br), 1400.4 (s, sh), 1340.2 (s, sh), 1245.9 (s, sh), 1164.4 (w, sh), 1114.0 (m, sh), 1029.8 (m, sh), 895.7 (m, sh), 781.5 (w, sh), 732.9 (m, sh), 699.8 (m, sh). ESMS: $\text{M}^+\text{H}^+ = 805.42$.

***cis*-[Pd(L⁷-S,O)₂]**: 95% yield. m.pnt. 86.9-88.3 °C. NMR δ_{H} (600MHz, CDCl_3): 8.25 (2H, d, H13), 8.10 (2H, d, H8), 8.09(2H, d, H10), 8.00 (4H, unres dd, H3 + H12), 7.95 (4H, d, H5 + H6), 7.94 (2H, t, H9), 7.82 (2H, d, H2), 3.75 (4H, t, H22/H22'), 3.65 (4H, t, H22/H22'), 3.50 (4H, t, H17), 2.61 (4H, t, H19), 2.20 (4H, q, H18), 1.27 (6H, t, H23/H23'), 1.11 (6H, t, H23/H23'), δ_{C} (600MHz CDCl_3): 179.57, 170.29, 136.72, 131.36, 130.89, 129.64, 128.62, 127.46, 127.27, 126.99, 126.35, 125.59, 124.95, 124.68, 124.60, 124.47, 123.64, 46.86, 45.88, 39.80, 32.99, 28.74, 12.92, 12.60. Calculated for $\text{C}_{50}\text{H}_{50}\text{O}_2\text{N}_4\text{S}_2\text{Pd}\cdot 2\text{H}_2\text{O}\cdot \text{C}$, 63.53; H, 5.72; N, 5.93; S, 6.78. Found. C, 63.40; H, 5.60; N, 5.85; N, 6.53. IR (KBr pellet, cm^{-1}): 2930.0 W, br), 1490.5 (s, sh), 1421.2 (s, sh), 1353.0 (m), 1241.3 (w), 1126.1 (m-w), 1075.5 (w, br), 842.5 (m, sh), 755.1 (w, br), 707.8 (w, br).

***cis*-[Pd(L¹⁰-S,O)₂]**: 51% yield. m.pnt. 196-199 °C (decomposition). NMR δ_{H} (600MHz, CDCl_3):8.37 (2H, d, H13), 8.15 (4H, dd, H8 + H10), 8.10 (2H, d, H3), 8.05 (2H, d, H12), 8.03 (4H, d, H5 + H6), 7.98 (2H, t, H9), 7.94 (2H, d, H2), 4.52 (2H, s, H17), 3.46 (4H, q, H20/H20'), 2.80 (4H, q, H20/H20'), 1.04 (6H, t, H21/H21'), 0.19 (6H, t, H21/H21'), δ_{C} (600MHz CDCl_3):177.70, 170.14, 132.31, 131.30, 130.89, 130.06, 129.63, 128.64, 127.47, 127.17, 126.63, 125.67, 124.73, 124.87, 124.80, 124.70, 124.55, 124.51, 46.68, 45.41, 44.30, 12.25, 12.09. Calculated for $\text{C}_{46}\text{H}_{42}\text{O}_2\text{N}_4\text{S}_2\text{Pd}\cdot 3\text{CH}_3\text{OH}$. C, 61.99; H, 5.69; N, 5.90; S, 6.75. Found. C, 61.40; H, 5.43; N, 5.20; N, 5.40. IR (KBr pellet, cm^{-1}): 1522.4 (s), 1493.2 (s), 1412.3 (s, br), 1353.3 (s, sh), 1261.6 (s), 1181.5 (w), 1092.7 (m, br), 919.9 (w), 842.3 (s, sh), 800.7 (s, br), 749.2 (s, sh), 711.5 (s, sh), 670.6 (m-w).

5.4 Instrumentation

5.4.1 NMR Analysis

¹H and ¹³C NMR spectra were recorded on either a 300 MHz Varian VXR spectrometer equipped with a Varian magnet (7.0 T) operating at 300 MHz for ¹H and 75 MHz for ¹³C, or a 600 MHz Varian Unity Inova spectrometer equipped with an Oxford magnet (14.09 T) operating at 600 MHz for ¹H and 150 MHz for ¹³C. ¹⁹⁵Pt spectra were recorded at 129 MHz on the Varian Unity Inova spectrometer, as were all DEPT and 2-dimensional spectra. Standard pulse sequences were used for all 1-dimensional, DEPT and relayh spectra. HSQC and HMQC spectra were collected with pulse sequences developed by the Darmstadt NMR

application laboratory of Varian GmbH (ghsqc_da and ghmqc_da respectively). HMQC spectra were optimised for $^3J_{H-C}$ couplings.

All samples were measured in deuterated chloroform (unless specified otherwise) at concentrations in the order of 10^{-2} M. Proton chemical shifts are quoted relative to the residual $CHCl_3$ solvent resonance at 7.26 ppm, and ^{13}C chemical shifts relative to the $CHCl_3$ triplet at 77.0 ppm (centre peak). ^{195}Pt spectra were run at 30 °C and externally referenced to 500 mg/cm³ H_2PtCl_6 in 30% (v/v) $D_2O/1M$ HCl. All resonances were assigned by making use of chemical shift values, proton coupling constants where suitable, H-H COSY, and C-H GHSQC and GHMCQ relationships giving single and multiple C-H bond correlations respectively.

5.4.2 X-Ray Analysis

In all cases, data collection was performed on a SMART APEX CCD (Bruker-Nonius), cell refinement and data reduction using SAINT (Bruker-Nonius). Initial structures solution was performed using SHELXS 97⁸ and atomic positions were located from a difference fourier map. The refinement method was full matrix least squares on F^2 using SHELXL 97. Molecular graphics were generated via X-Seed⁹ and using POV-Ray. All hydrogen atoms were placed in geometrically calculated positions (unless specified otherwise) with C-H = 0.99 Å, (for $-CH_2$); 0.98 Å, (for $-CH_3$); 0.95 Å, (for phenyl) and refined using a riding model with $U_{iso}(H) = 1.2 U_{eq}$ (parent), for $-CH_2$ and phenyl or $U_{iso}(H) = 1.5 U_{eq}$ (parent) for $-CH_3$.

5.4.3 Elemental Analysis

Elemental analyses for %C, %H and %N were performed on a Heraeus Universal Combustion Analyser, Model CHN-Micro, by Mr P. Benincasa of the Department of Chemistry, University of Cape Town.

5.4.4 Melting point determination

All melting points were obtained using an Electrothermal digital melting point apparatus. Model Nm IA9300.

5.5.5 Infra-Red Spectroscopy

All IR spectra were obtained using a Perkin-Elmer 1600 series FT-IR Spectrophotometer. KBR pellets were pressed for all samples.

5.5.6 UV/Visible Absorption spectroscopy

Absorption spectra were obtained using an Agilent 8453 UV/Visible spectrometer and quartz cuvettes (1 cm path length) were used.

5.5.7 Fluorescence spectroscopy

All emission spectra were obtained using a Perkin Elmer LS50B Luminescence Spectrometer, with a Xenon discharge lamp giving a signal equivalent to 20 kW for 8 μ s duration the pulse width at $\frac{1}{2}$ peak height being $<10 \mu$ s. The sample detector was a grating photomultiplier with a modified response for operation to 650 nm, and the reference detector was a standard sample detector.

The following instrument settings were maintained throughout the acquisition of all emission spectra.

Emission range monitored: 300-600 nm

Excitation wavelength: As stated in text for each series of compounds.

Excitation slit width : 2.5 nm

Emission slit width: 5 nm

Scan speed: 500 nm/min.

5.5.8 High Performance Liquid Chromatographic separations

Chromatographic analysis were performed on a Varian Polaris system equipped with a 20ml Rheodyne sampling loop, Varian ProStar binary pumps and a Varian ProStar 325 variable wavelength detector. A Zorbax XDB-C18 150 x 4.6 mm, 5 mm, column was used at all times. The mobile phase was made up of 90:10 (%v/v) MeCN:0.1 M acetate buffer (pH \gg 6). An isocratic flow of 1 ml.min⁻¹ was used with photometric detection at 254 nm. Only de-ionized water and HPLC grade organic solvents, filtered through 0.22 μ m and 0.45 μ m filters respectively, were used.

References

-
1. D. Perrin, W. Armarego, *Purification of laboratory chemicals*, Pergamon Press, Oxford, **1989**.
 2. T. Morozumi, T. Anada, H. Nakamura, *J. Phys. Chem. B*, **2001**, 105, 2923-2931.
 3. W. Wiesler, K. Nakanishi, *J. Am. Chem. Soc.*, **1989**, 111, 9205-9213.
 4. E. Ciganek, *J. Org. Chem.*, **1980**, 45, 1407-1505.
 5. M. Schuster, *personal correspondence*, **2003**.
 6. J. Lou, A. Hatton, P. Laibinis, *Anal. Chem.*, **1997**, 69, 1262-1264.
 7. C. Tran, J. Fendler, *J. Am. Chem. Soc.*, **1979**, 102, 2923-2928.
 8. SHELXL 97, G. H. Sheldrick **1997**, *University of Göttingen*, Germany.
 9. X-Seed, L. J. Barbour, *University Stellenbosch*, South Africa.

Conclusions and future recommendations

The *N,N*-dialkyl-*N'*-acyl(aroyl)thiourea ligands are known to undergo selective complexation with heavy metal ions, those of the Platinum Group Metals (PGM's) in particular. Their relatively facile synthesis and the ease with which substituents of varying properties can be attached to the coordinating moiety gives rise to a wealth of practical applications of these ligands. The incorporation of a fluorescent tag such as anthracene or pyrene in these ligands would provide interesting perspectives in the use of these compounds as a means of trace determination of the PGM's by means of fluorescence detection. It was therefore of interest to synthesise both anthracene and pyrene derivatised *N,N*-dialkyl-*N'*-aroylthioureas and to investigate their complexing behaviour and subsequent fluorescent properties.

The synthetic procedures employed in the preparation of the desired *N,N*-dialkyl-*N'*-aroylthioureas called for the use of 9-anthracoyl chloride, 1-pyrenebutanoyl chloride and 1-pyreneacetyl chloride as starting compounds. Since these reagents were not commercially available their synthesis was also necessary. To this end, several procedures for the conversions of 9-anthracenecarboxylic acid, 1-pyrenebutyric acid and 1-pyreneacetic acid to their corresponding chlorides were performed. It was observed that the pyrene derivatised compounds are generally more stable under harsh reaction conditions, including exposure to light and air, than the anthracene containing compounds. However, high yields of all the acid chlorides could be obtained.

The procedure described by Douglass and Dains, for the synthesis of *N,N*-dialkyl-*N'*-aroylthioureas was investigated and a series of *N,N*-dialkyl-*N'*-9-anthracoylthiourea and *N,N*-dialkyl-*N'*-pivaloylthiourea ligands were synthesised in high yield using this method. Crystal structure determinations of the majority of these compounds were carried out and interesting inter- and intramolecular interactions were observed. The presence of an intermolecular hydrogen bond in *N,N*-diethyl-*N'*-9-anthracoylthiourea (HL¹) between the thioamidic proton and the sulphur atom on an adjacent molecule was observed, this giving rise to a form of dimerisation with the aromatic systems in opposite arrangements. The aromatic rings in this compound also exhibited face to edge interactions, and the absence of π - π interactions was noted. Intermolecular hydrogen bonding was also present in *N*-morpholine-*N'*-9-anthracoylthiourea (HL²), this involving the thioamidic proton and the oxygen atom present in the morpholine residue of an adjacent molecule. This was the only ligand in the anthracoylthiourea series to exhibit π - π interactions between the anthracene residues and no face to edge interactions between the aromatic systems were evident, presumably due to these π - π interactions. This resulted in alternating planes of aromatic and heteroatomic nature being evident in the crystalline structure. Both in this compound and in HL¹ it was interesting to note the opposing orientations of the oxygen and sulphur atoms. A crystal structure of *N,N*-di(2-hydroxyethyl)-*N'*-9-anthracoylthiourea (HL³) was determined and the presence of an intramolecular hydrogen bond between the thioamidic proton and oxygen atom in the hydroxyl group of the

hydroxyethylamine fragment was observed. Intermolecular hydrogen bonding was also present between the hydroxyethylamine fragments of adjacent molecules. The absence of π interactions between the anthracene residues was interesting, and the presence of face to edge interactions between the aromatic moieties was noted. These inter- and intramolecular interactions lead to alternating planes of face to edge aromatic contacts and hydrogen bonding being evident in the crystalline structure. The crystal structure of *N,N*-di(2-hydroxyethyl)-*N'*-pivaloylthiourea (HL⁶) was also elucidated and the hydrogen bonding present in this compound closely resembles that previously described for HL³. It is interesting to note that both in this compound and in HL³, the oxygen and sulphur atoms of the acylthiourea moiety assume similar relative orientations, presumably due to the extensive hydrogen bonding present in the solid state.

These compounds were fully characterised by means of NMR spectroscopy and the resonances in the aromatic region could be fully assigned. From the ¹H NMR spectra of HL³ and HL⁶ the inequivalence of the OH resonances in the hydroxy groups on the two pendant arms in the hydroxyethylamine residue was observed, indicating that only the intramolecular hydrogen bond present in these compounds is maintained in solution.

Complex formation of the potentially fluorescent *N,N*-dialkyl-*N'*-9-anthracoylthiourea ligands was investigated with both platinum(II) and palladium(II). *N,N*-diethyl-*N'*-9-anthracoylthiourea reacted readily with palladium(II) to form *cis*-bis(*N,N*-diethyl-*N'*-9-anthracoylthioureato)palladium(II) (*cis*-[Pd(L¹-S,O)₂]). The facile reaction of HL¹ with palladium(II) was not reflected in its complexation with platinum(II), where the ligand exhibited a reticence to react with PtCl₄²⁻ in solution. A more labile starting compound was therefore used, *trans*-Pt(NCPr₁)₂Cl₂, and enabled the preparation of *cis*-bis(*N,N*-diethyl-*N'*-9-anthracoylthioureato)platinum(II) (*cis*-[Pt(L¹-S,O)₂]). The yields of these complexes were disappointingly low however.

Crystal structures of both *cis*-[Pd(L¹-S,O)₂] and *cis*-[Pt(L¹-S,O)₂] could be elucidated, these being to our knowledge, the first of their kind. A buckling in the coordination plane of *cis*-[Pd(L¹-S,O)₂] was observed which is reflected in the inequivalence of the Pd-O' and Pd-O bonds as well as the Pd-S' and Pd-S bonds. This is however not evident in the *cis*-[Pt(L¹-S,O)₂] complex, in which the coordination plane appears to be essentially planar. An offset π overlap between anthracene moieties of adjacent molecules is evident in *cis*-[Pd(L¹-S,O)₂]. The C(S) and C(O) bonds in both *cis*-[Pt(L¹-S,O)₂] and *cis*-[Pd(L¹-S,O)₂] are longer than in the free ligand indicating a reduction in bond order of these bonds upon complexation. The C-N bonds present in the chelate rings of both *cis*-[Pt(L¹-S,O)₂] and *cis*-[Pd(L¹-S,O)₂] are shortened relative to their counterparts in the free ligand indicating a delocalisation of charge in this region upon introduction of a metal ion.

The complexes *cis*-[Pt(L⁷-S,O)₂], *cis*-[Pd(L⁷-S,O)₂] and *cis*-[Pt(L¹⁰-S,O)₂], *cis*-[Pd(L¹⁰-S,O)₂] were also analysed using NMR spectroscopy and several interesting observations could be made. An inequivalence in the ¹H and ¹³C NMR resonances of the pendant arms in the diethylamine residue of these complexes indicates a degree of double bond character between the thiocarbonyl carbon and the nitrogen

atom of the diethylamine residue in these compounds, this serving to reduce the rotation about the bond and giving rise to the separated signals observed. It is apparent from the ^{13}C NMR spectra obtained, that the carbonyl and thiocarbonyl resonances undergo significant shifts upon complexation. Evidence obtained from ^{195}Pt NMR spectra indicated the formation of only the *cis* isomer; this being confirmed by their crystal structures. The increase in the degree of C(O) single bond character upon complexation which is apparent in the crystal structure of *cis*-[Pt(L¹-S,O)₂] and *cis*-[Pd(L¹-S,O)₂] was confirmed by IR evidence where the absence of the carbonyl peak was noted.

The fluorescent properties of the *N,N*-dialkyl-*N'*-9-anthracoylthiourea derivatives were examined. The UV/Visible absorption spectra of HL¹, *cis*-[Pt(L¹-S,O)₂] and *cis*-[Pd(L¹-S,O)₂] are very similar to that of anthracene, indicating that the strongest absorbance of these compounds is largely due to the anthracene moiety. In the investigation of the emission spectra, an accurate working range of concentration was determined for the *N,N*-dialkyl-*N'*-9-anthracoylthiourea derivatives for which a linear correlation between concentration and relative emission intensity could be established. This was necessary to ensure the exclusion of quenching phenomena such as self absorption, present at higher concentrations. Appropriate excitation wavelengths for these compounds were established, where the effects of Raman and Rayleigh scatter were negligible. Introduction of the acylthiourea moiety in HL¹ resulted in a severe reduction in the quantum efficiency of the ligand relative to that of anthracene. Subsequent testing of 9-anthracenecarboxylic acid established that the presence of the carboxyl group in close proximity to the aromatic moiety is most likely responsible for the major reduction in quantum efficiency, the remaining heteroatoms in the acylthiourea moiety being relatively minor contributors. The many tautomeric forms exhibited by the *N,N*-dialkyl-*N'*-aroylthioureas are also thought to contribute to the reduction in quantum efficiency of the ligand by providing radiationless pathways, which increase the probability of the radiationless de-excitation of an electron. The emission spectrum of HL¹ was obtained at varying concentrations and self absorption, resulting in the attenuation of the peak at 390.5 nm at higher concentrations, was apparent. Introduction of the metal ion in *cis*-[Pd(L¹-S,O)₂] unfortunately results in a further reduction of quantum efficiency.

From the UV/Visible absorption spectra of the *N,N*-dialkyl-*N'*-9-anthracoylthiourea derivatives it is suggested that the carboxyl group is perpendicularly orientated relative to the anthracene ring in the ground state, this geometry most likely being maintained in the excited state as well. The perpendicular orientation of the carboxyl group and anthracene ring in the ground state, precludes significant resonance interaction between the two groups and the bathochromic shift in the absorption spectra of the *N,N*-dialkyl-*N'*-9-anthracoylthiourea derivatives relative to that of anthracene is presumably due to the inductive effect of the carboxyl group. The fluorophore (anthracene) – receptor (acylthiourea moiety) configuration of the *N,N*-dialkyl-*N'*-9-anthracoylthiourea derivatives can lead to its classification as either an orthogonal or integral system. The absence of a significant shift in the emission wavelengths of HL¹ relative to those of anthracene, make it likely that these derivatives are orthogonal systems where direct

attachment of the fluorophore to the receptor is through a virtual C_o spacer and photoinduced electron transfer (PET) leads to the observed reduction in quantum efficiency. No chelation enhanced fluorescence (CHEF) was evident upon introduction of the metal ion, suggesting that metal-fluorophore interactions are more significant than metal-receptor interactions in these systems. These metal-fluorophore interactions are most likely spin-orbit coupling, which leads to intersystem crossing and a reduction in the emission probability of the complex.

The Douglass and Dains synthetic procedure whilst being successful for the synthesis of the anthracoylthiourea and pivaloylthiourea derivatives is not suited to the synthesis of the pyrenebutanoylthiourea and pyreneacetylthiourea derivatives, due to the formation of an isothiocyanate intermediate. This intermediate has two electrophilic centres where nucleophilic attack at the carbonyl carbon leads to the formation of an *N*-substituted amide and nucleophilic attack at the thiocarbonyl carbon yields the desired *N,N*-dialkyl-*N'*-acylthiourea. The site of preferential nucleophilic attack is dependant on the steric contributions of both the carbonyl substituent and the nucleophilic amine. Bulky carbonyl substituents and bulky attacking amines lead to the preferential formation of the desired product, as presumably steric congestion at the carbonyl carbon inhibits attack by the amine at this electrophilic centre and consequently nucleophilic attack occurs at the thiocarbonyl carbon. The pyreneacetylthiourea and pyrenebutanoylthiourea derivatives do not provide sufficient steric congestion at the carbonyl carbon to prevent attack by the nucleophilic amine at this site. This leads to the undesired formation of *N*-substituted amides and reduces the isolated yield of *N,N*-dialkyl-*N'*-acylthiourea. An alternative synthetic procedure initially reported by Dixon and Taylor was therefore investigated. This describes the reaction between an acid chloride and an *N*-substituted amide. Initial acylation at the sulphur atom of the *N*-substituted amide and subsequent rearrangement yields an *N,N*-dialkyl-*N'*-acylthiourea. This synthetic procedure efficiently avoids the competing side reaction of *N*-substituted amide formation present in the Douglass and Dains procedure. The *N*-substituted thioureas required in the Dixon and Taylor synthesis were not commercially available and were therefore synthesised in high yield from the acid hydrolysis of *N,N*-dialkyl-*N'*-pivaloylthioureas; these having been previously synthesised using the Douglass and Dains method, for this purpose.

Using the Dixon and Taylor method both pyrenebutanoylthiourea and pyreneacetylthiourea derivatives were synthesised. A crystal structure determination of *N,N*-diethyl-*N'*-[4-(pyrene-1-yl)butanoyl]thiourea (HL⁷) illustrated an intermolecular hydrogen bond between the thioamidic proton and sulphur atom of the adjacent molecule, this being reminiscent of the hydrogen bond displayed in the anthracoylthiourea analogue. The planar pyrene moiety exhibits an offset π overlap with the pyrene moiety on an adjacent molecule. Face to edge aromatic contacts are also present giving rise to the herringbone packing structure exhibited by this compound. Intermolecular hydrogen bonding is also present in *N*-morpholine-*N'*-[4-(pyrene-1-yl)butanoyl]thiourea (HL⁸) and from its crystal structure, it can be seen that this hydrogen bond occurs between the thioamidic proton and carbonyl oxygen atoms, in

contrast to the anthracoylthiourea analogue. Moreover π - π interactions between the planar pyrene residues are apparent although the degree of overlap differs to that exhibited by HL⁷. In both HL⁷ and HL⁸ the opposing orientations of the oxygen and sulphur atoms is evident. In these compounds the length of the C-N bonds present in the acylthiourea moiety is shorter than the average C-N single bond length indicating a degree of electronic delocalisation in this area. Similar observations can be made for the anthracoylthiourea derivatives. The crystals structure determinations of both HL⁷ and HL⁸ are, to our knowledge, the first of their kind.

Detailed high resolution ¹H and ¹³C NMR studies were carried out on both the pyrenebutanoylthiourea and pyreneacetylthiourea derivatives. Use was made of two dimensional techniques including COSY spectra, GHSQC and GHMQC spectra; these showing ¹H-¹H, ¹³C-¹H single bond and ¹³C-¹H multiple bond correlations respectively. These enabled the full assignment of both carbon and proton resonances in the aromatic region of both the pyrenebutanoylthiourea and pyreneacetylthiourea derivatives. It was observed that the methylene carbon between the pyrene and acylthiourea moieties in the pyreneacetylthiourea derivatives exhibited sensitivity to the alteration of the carbonyl substituent, as did the point of attachment on the aromatic moiety. Whilst similar observations could be made in the case of the pyrenebutanoylthiourea derivatives, the influence of the alteration of the carbonyl substituent did not extend as far as the aromatic residue. From these results it could be established that the electronic systems of the pyrene and acylthiourea moieties are separated in the case of the pyrenebutanoylthiourea derivatives, however a degree of “electronic communication” between the two moieties, appears to be present in the pyreneacetylthiourea derivatives.

The complexing behaviour of *N,N*-diethyl-*N'*-[4-(pyrene-1-yl)butanoyl]thiourea and *N,N*-diethyl-*N'*-[pyrene-1-ylacetyl]thiourea (HL¹⁰) was investigated using both platinum(II) and palladium(II). The reticence of the anthracoylthioureas to react with platinum(II) was not reflected in the pyrenebutanoylthiourea and pyreneacetylthiourea derivatives where complexation with both platinum(II) and palladium(II) was relatively facile.

NMR investigations of both the platinum(II) and palladium(II) complexes appeared to confirm the findings of the ligand analyses with regards to the electronic systems of the pyrene and acylthiourea moieties. As in the case of the anthracoylthiourea derivatives it was noted that the ¹³C NMR resonances of the carbonyl and thiocarbonyl carbons in the metal complexes had exchanged positions and moved closer together relative to the corresponding resonances in the free ligand. It was also noted that the shielding of the thiocarbonyl resonance upon complexation was more marked in the case of the platinum(II) complexes; the downfield shift of the carbonyl resonance being more marked in the case of the palladium (II) complexes. From the inversion of the average trend of Δ (Pt(II) complexes) > Δ (Pd (II) complexes) for C(S) and Δ (Pd(II) complexes) > Δ Pt (II) complexes for C(O) (Δ defined as $\delta^{13}\text{C}_{\text{complex}} - \delta^{13}\text{C}_{\text{ligand}}$) and taking into account that coordination occurs through the oxygen and sulphur atoms, it is tempting to

speculate that shift displacements values can reflect the order of HSAB “softness” of the metal centre in the order Pt(II) > Pd(II).

^{195}Pt NMR analyses were also performed and indicated the formation of only *cis*-[Pt(L⁷-S,O)₂] and *cis*-[Pt(L¹⁰-S,O)₂] complexes.

The fluorescent properties of the pyrenebutanoylthiourea derivatives were investigated. The UV/Visible absorption spectra of HL⁷, *cis*-[Pt(L⁷-S,O)₂] and *cis*-[Pd(L⁷-S,O)₂] shows that the absorption exhibited by these compounds is largely due to the pyrene moiety. As in the case of the anthracoylthiourea derivatives, an accurate working range of concentration was determined where a linear correlation between concentration and relative emission intensity was evident. Appropriate excitation wavelengths for these compounds were also established, where the effects of Raman and Rayleigh scatter were minimal. From the emission spectra of pyrene, HL⁷, *cis*-[Pt(L⁷-S,O)₂] and *cis*-[Pd(L⁷-S,O)₂] it is clear that the emission shown by the pyrenebutanoylthiourea derivatives is primarily due to the pyrene moiety. The intensity of the emission spectra of the pyrenebutanoylthiourea derivatives obtained within an accurate working range of concentration are in sharp contrast to those reported by Schuster *et al.* for HL⁷ and *cis*-[Pt(L⁷-S,O)₂]. An estimate of the quantum yield of HL⁷, *cis*-[Pt(L⁷-S,O)₂] and *cis*-[Pd(L⁷-S,O)₂] was determined. Evidently the reduction in quantum efficiency upon the introduction of the acylthiourea moiety is not as significant in HL⁷ as it is in the anthracoylthiourea analogue, most likely due to the presence of the alkyl chain spacer between the pyrene and acylthiourea moieties in HL⁷. The pyrenebutanoylthiourea systems appear to follow a proximal, non-adjacent model where the fluorophore (pyrene) and receptor (acylthiourea moiety) are separated by the presence of a spacer (propyl chain), the signaling behaviour in these systems generally being photo-induced electron transfer. It is evident from the emission spectra that the PET present in HL⁷ is not switched off by the introduction of the metal ion as no chelation enhanced fluorescence is observed. This suggests that the metal-fluorophore interaction is greater than that between the metal and receptor similar to that described for the anthracoylthiourea derivatives. Despite this, at certain concentrations the emission of *cis*-[Pt(L⁷-S,O)₂] and *cis*-[Pd(L⁷-S,O)₂] is observable and therefore the synthesis of fluorescent complexes has been achieved. It is also possible that these compounds could be used for the detection of the PGM's by fluorescence, despite the low quantum yields obtained.

As a continuation of this work it would be particularly interesting to study the attachment of a fluorescent entity with greater water solubility than either anthracene or pyrene, since the synthesis of this type of highly fluorescent *N,N*-dialkyl-*N'*-acylthioureas could have remarkable analytical potential. To this end, other fluorescent tags were briefly examined and preliminary experiments were performed with 9-fluorenylmethoxycarbonyl chloride (Fmoc-Cl) in an attempt to synthesise more water soluble *N,N*-dialkyl-*N'*-acylthioureas. Fmoc-Cl is widely used as a fluorescent tag in the derivatisation of amino acids as well as amino sugars and many of the reported derivatisations take place in aqueous media. Whilst the Douglass and Dains synthetic procedure appeared to be too harsh a method for the synthesis of

these compounds NMR evidence of their formation was clear and the use of a buffer system and room temperature reactions would almost certainly produce *N,N*-dialkyl-*N'*-acylthioureas in high yields. A study of the complexing behaviour of these ligands and subsequent testing of their fluorescent properties as well as those of their metal complexes would be extremely interesting and increase the potential for the analytical application of the remarkable, yet deceptively simple *N,N*-dialkyl-*N'*-acylthioureas.